Improving the Mesodermal Differentiation Potential of Human Embryonic Stem Cells

Paul Wesley Burridge, BSc. (Hons.)

Thesis submitted to the University of Nottingham for the degree of Doctor of Philosophy

September 2007

ABSTRACT

Human embryonic stem cells (hESCs) are thought to have enormous potential for use in regenerative medicine, whilst simultaneously allowing us insights into human embryonic development, disease modelling and drug discovery. Differentiation to mesodermal lineages, such as cardiomyocytes and blood, may allow for improved treatment of cardiac and haematopoietic diseases. hESC-derived immune cell types may also allow the circumnavigation of the immune barrier. This thesis aims to test the hypothesis that formation of hESC derivatives is regulated by the same mechanisms and ontology as *in vivo* embryo development. Therefore, by identifying and facilitating the mechanisms of mesoderm induction, hESC differentiation can be optimised to maximise the production of mesoderm, and, ultimately, mesoderm derivatives.

Using a *Xenopus laevis* animal cap model with simultaneous treatment with activin B or fgf4, together with tal1, lmo2 and gata1 mRNA, resulted in substantial increases in mesodermal, haemangioblast and erythropoietic cell markers. One of the most successful methods for hESC differentiation is by the formation of human embryoid bodies (hEBs). To reduce first the number of variables in current mass culture protocols for hEB formation, such as hEB size, a forced aggregation system was established that produced homogeneous hEBs from defined numbers of cells. This system was then optimised to enhance production beating cardiomyocytes by varying the number of hESCs used for hEB formation and also the number of days in culture. This system was assessed in four hESC lines and demonstrated substantial inter-line variability in cardiomyocyte production ($1.6\pm1.0\%$ to $9.5\pm0.9\%$). Differentiation was also performed using chemically defined media (CDM) with the addition of activin A and FGF2 and resulted in $23.6\pm3.6\%$ of hEBs producing beating cardiomyocytes.

In addition immunohistochemistry was performed to assess the relationship of cells expressing markers for mesoderm, pluripotency, ectoderm, and endoderm to establish a standard spatial and temporal map of hEB differentiation.

DECLARATION

I hereby declare that this thesis has been composed by myself and has not been submitted for any previous degree. Acknowledgement of specific procedures not performed by myself is clearly stated throughout this thesis; otherwise, the described herein is my own.

Paul Burridge

Date: 28th September 2007

PUBLICATIONS

BURRIDGE, P.W., ANDERSON, D., PRIDDLE, H., BARBADILLO MUÑOZ, M.D., CHAMBERLAIN, S., ALLEGRUCCI, C., YOUNG, L.E., & DENNING, C. (2007) Improved human embryonic stem cell embryoid body homogeneity and cardiomyocyte differentiation from a novel V-96 plate aggregation system highlights interline variability. *Stem Cells*, 25, 929-38.

ALLEGRUCCI, C., DENNING, C.N., **BURRIDGE, P.**, STEELE, W., SINCLAIR, K.D. & YOUNG, L.E. (2005) Human embryonic stem cells as a model for nutritional programming: an evaluation. *Reproductive Toxicology*, 20, 353-67.

PRIDDLE, H., JONES, D.R., **BURRIDGE, P.W.** & PATIENT, R. (2005) Hematopoiesis from human embryonic stem cells: overcoming the immune barrier in stem cell therapies. *Stem Cells*, 24, 815-24.

ACKNOWLEDGMENTS

TABLE OF CONTENTS

7

LIST OF FIGURES

18

LIST OF TABLES

ABBREVIATIONS

Abbreviation	Description
ACVR	Activin receptor
AKT1	V-akt murine thymoma viral oncogene homolog 1
BGK	BresaGen Knockout serum replacement medium
BM	Bone marrow
BMP	Bone morphogenetic protein
BMPR	Bone morphogenetic protein receptor
BMT	Bone marrow transplant
BSA	Bovine serum albumin
CDH1	cadherin 1, type 1, E-cadherin (epithelial)
CDM	Chemically defined medium
CDM-BSA	Chemically defined medium with BSA
CDM-PVA	Chemically defined medium with PVA
CM	Conditioned medium
cDNA	Complementary DNA
CTNNB1	β-catenin
DAPI	4',6-diamidino-2-phenylindole
DLP	Dorsal lateral plate
DMEM	Dulbecco's modified Eagle's medium
DMSO	Dimethyl sulfoxide
DNA	Deoxyribonucleic acid
EB	Embryoid body
EC	Embryonal carcinoma
EOMES	Eomesodermin
ERK	Extracellular signal-related kinase
ESC	Embryonic stem cell
FACS	Fluorescent-activated cell sorting
FBS	Foetal bovine serum
FGF2	Fibroblast growth factor
FGFR	Fibroblast growth factor receptor
FITC	fluorescein isothiocyanate

FLI1	Friend leukemia virus integration 1
FOXA2	Forkhead box A2 (HNF3β)
GATA	GATA binding protein
GFP	Green fluorescent protein
GSC	Goosecoid
hEB	Human embryoid body
hESC	Human embryonic stem cell
HNF4A	Hepatocyte nuclear factor 4, alpha
HSC	Haematopoietic stem cell
ICM	Inner cell mass
Id	Inhibitor of differentiation
IHH	Indian hedgehog
IMDM	Iscove's modified Dulbecco's medium
INHBA	Inhibin, beta A
iPSC	Induced pluripotent stem cell
IVF	*In vitro* fertilisation
JAK	Janus kinase
KSR	Knockout serum replacement
LEFTY	Left right determination factor
LIF	Leukemia inhibitory factor
LIFR	Leukemia inhibitory factor receptor
LMO2	LIM-domain only protein 2
MAPK	Mitogen-activated protein kinase
mEB	Mouse embryoid body
MEF	Mouse embryonic fibroblast
mESC	Mouse embryonic stem cell
MIXL1	Mix1 homeobox-like 1
mRNA	Messenger ribonucleic acid
Neu5Gc	*N*-glycolylneuraminic acid
NOG	Noggin
PBS	Phosphate buffered saline
PCR	Polymerase chain reaction
PDGFRA	Platelet-derived growth factor receptor, alpha polypeptide

PGC	Primordial germ cell
PI3K	Phosphatidylinositol 3-kinase
POU5F1	POU domain, class 5, transcription factor 1 (OCT4)
PVA	Polyvinyl alcohol
qPCR	Quantitative real-time polymerase chain reaction
RA	Retinoic acid
RNA	Ribonucleic acid
RT-PCR	Reverse transcription-polymerase chain reaction
SALL4	Sal-like 4 (Drosophila)
SCNT	Somatic cell nuclear transfer
siRNA	Small interfering RNA
SMAD	Mothers against decapentaplegic homolog
SOX	SRY (sex determining region Y)-box
SSEA	Stage specific embryonic antigen
STAT	Signal transducer and activator of transcription
T	Brachyury
TAL1	T-cell acute lymphocytic leukemia 1
TGFB1	Transforming growth factor, beta 1
TGFBR	Transforming growth factor receptor
ULA	Ultra-low attachment
UV	Ultraviolet
VBI	Ventral blood island
VEGF	Vascular endothelial growth factor
VMZ	Ventral marginal zone

Note on gene nomenclature

Due to the lack of clarity regarding gene nomenclature across publications and databases (Fundel and Zimmer, 2006), this thesis uses the recommended notation provided by the respective genome nomenclature committees for each organism.

Human gene and protein names and symbols follow current Human Genome Nomenclature Committee guidelines (http://www.gene.ucl.ac.uk/nomenclature/). To summarise, gene symbols are italicised with all letters in uppercase. Proteins designations are the same as the gene symbol, but not italicised with all letters in uppercase. mRNA and cDNA use the gene symbol and formatting conventions.

Mouse gene and protein names and symbols follow current Mouse Genome Nomenclature Committee guidelines (http://www.informatics.jax.org/mgihome/nomen/). To summarise, gene symbols are italicised with first letter uppercase and the remaining letters in lower case. Proteins designations are the same as the gene symbol, but not italicised with all letters in uppercase. mRNA and cDNA use the gene symbol and formatting conventions.

Xenopus gene and protein names and symbols are in the process of being converted to HGNC nomenclature (http://xlaevis.cpsc.ucalgary.ca/gene/static/geneNomenclature.jsp) as shown in the Xenbase Gene database (http://xlaevis.cpsc.ucalgary.ca/gene/gene.do). To summarise, gene symbols are not italicised with all letters in lowercase. Proteins designations are the same as the gene symbol, but not italicised and all letters in uppercase. mRNA and cDNA use the gene symbol and formatting conventions. Names and symbols of *Xenopus* genes and proteins not yet in the Xenbase Gene database follow nomenclature most frequently used in the literature.

1 INTRODUCTION

1.1 THE POTENTIAL OF HUMAN EMBRYONIC STEM CELLS

Human embryonic stem cells (hESCs) could potentially usher in a new era of cellular regeneration of diseased organs and tissues rather than chronic support with drug therapies (Passier and Mummery, 2003). hESCs can also be used in the field of developmental biology, providing us with novel models for the study of human embryonic and foetal development, including disorders of development such as birth defects or embryonal tumours (Dvash and Benvenisty, 2004). Using hESCs to access human embryonic gene expression ontogeny will also provide us with new tools for the investigation of growth and differentiation factors, which can be used to differentiate hESCs into cell types for use in disease modelling and drug discovery (Ben-Nun and Benvenisty, 2006).

1.1.1 Stem cell potency

A stem cell, by definition, is a cell that can proliferate by a process of self-renewal whilst maintaining the ability to give rise more committed descendents (Reya *et al.*, 2001). In the embryo, cells of the morula have the potential to generate an entire organism and its associated extra-embryonic tissues, termed totipotency (reviewed by Rippon and Bishop, 2004). Subsequently, cellular differentiation results in the formation of the blastocyst which consists of the outer trophectoderm, which will form the trophoblast component of the placenta, and the inner cell mass (ICM), which will develop into the embryo proper and the chorioallantois. The cells of the ICM are described as pluripotent, defined as the ability to form all of the tissues of the developing embryo (Smith, 2005).

1.1.2 Foetal and adult stem cells

Once embryonic and foetal development is complete it is thought that many, if not most, tissues of the human body maintain adult stem cells within their population. These adult stem cells have been proposed to be essential and perhaps the only cells important for lifelong tissue regeneration (Weissman, 2005). Such stem cells are able to self-renew and differentiate into multiple organ specific cell types, termed multipotency (Lakshmipathy and Verfaillie, 2005).

The use of adult stem cells in clinical therapies has existed since 1968 in the form of a bone marrow transplant (BMT) for patients that suffer from congenital blood or immune disorders or have had their own bone marrow damaged by cancer treatment. Haematopoietic stem cells (HSCs) that are transplanted during a BMT are responsible for repairing the patient's capacity to manufacture healthy blood and immune cells (Weissman, 2000). However, in many cases, such as neurodegenerative disorders and type I diabetes, the prospect of transplantation of adult cells is still very poor since they are far less mitotically active than foetal cells and the ability to self-renewal is reserved for a rare population of stem cells (Weissman, 2005).

1.1.2.1 Adult stem cell plasticity

Traditionally organ-specific adult stem cells have been thought to be stringently restricted to making differentiated cell types of the tissue in which they reside (Anderson et al., 2001) and they take on new roles in an orchestrated, unidirectional and irreversible manner (Lemischka, 2001). However, experiments have been performed that have challenged the system of lineage-restriction in organ specific stem cells (Serafini and Verfaillie, 2006). These experiments have been interpreted

as evidence that stem cells from some adult sources, under certain microenvironmental conditions, seem to have that is a wider capacity for renewal, termed 'plasticity' (Lakshmipathy and Verfaillie, 2005).

Whilst the underlying mechanism of the apparent plasticity of adult stem cells is still in debate, it is thought that there are four main possibilities (reviewed by Lakshmipathy and Verfaillie, 2005, Martin-Rendon and Watt, 2003) assuming that results are based on sustained, robust multilineage engraftment and not morphology or the expression of lineage-specific antibodies. Firstly, that the reports are based on infusion of non-pure populations that contain multiple stem cell types. Secondly, the maintenance of more multipotent cells, with higher lineage potential, within a tissue is another option or even the possibility that the entire concept of organ-specific stem cells is wrong and they are essentially pluripotent (Anderson *et al.*, 2001). A third explanation is cell fusion, particularly where stem cells of one lineage are cultured in the microenvironment of another cell type (Ying *et al.*, 2002, Terada *et al.*, 2002, reviewed by Wurmser and Gage, 2002). The final explanation for plasticity, the only one representing true plasticity, is de-differentiation and subsequent re-differentiation, transdetermination or even transdifferentiation (Martin-Rendon and Watt, 2003), perhaps by genomic reprogramming possibly due to the *in vitro* culture.

While clearly useful for some applications such as BMT, autologous adult stem cells are generally difficult to proliferate in culture for extended periods of time and maintain in an 'undifferentiated' state due to an inability to recreate their stem cell niche (Verfaillie *et al.*, 2002). Adult stem cells are also very rare and generally found as tissue-resident cells as well as in the blood and bone marrow, and the prospects of extraction, amplification and transplantation to good manufacturing practice standards on a per patient basis are daunting (Skottman *et al.*, 2006).

1.1.2.2 Mouse and human embryonic carcinoma and PGC derived cells

The first pluripotent cell lines to be established were embryonic carcinoma (EC) cell lines derived from mouse and human germ cell tumours (Stevens and Little, 1954, reviewed by Chambers and Smith, 2004). These cells can be continuously expanded in culture and differentiated into cells of the three germ layers. Mouse EC cells can also be injected into mouse blastocysts and contribute to all of the normal tissues of chimeric mice generated (Illmensee and Mintz, 1976). EC cells being of cancer origin and frequently aneuploid, are not suitable for clinical applications. Similarly, mouse and human embryonic germ cells, which are derived from primordial germ cells (PGCs), are classed a pluripotent and can contribute to all cell lineages in chimeric mice, although they have lower plating efficiencies than ECs (Matsui *et al.*, 1991, Resnick *et al.*, 1992, Shamblott *et al.*, 1998).

1.1.3 Embryonic stem cells

The definition of an embryonic stem cell (ESC) was established in primates by Thomson *et al.* (1998) as (i) derivation from the preimplantation or periimplantation embryo, (ii) prolonged undifferentiated proliferation, and (iii) stable developmental potential to form derivatives of all three embryonic germ layers even after prolonged culture.

Mouse embryonic stem cells (mESCs) were first isolated from day 2.5 post-fertilisation murine blastocysts using techniques based on experience gained from the culture of EC cells (Martin, 1981, Evans and Kaufman, 1981). Only more recently have ESCs from primates been derived (rhesus monkey (Thomson *et al.*, 1995), common marmoset (Thomson *et al.*, 1996), and cynomolgus monkey (Suemori *et al.*, 2001)), along with hESCs in 1998 (Thomson *et al.*, 1998). Similar to ECs, when

injected into mouse blastocysts, mESCs can for chimeras and contribute to all observable tissues and the germ line (Bradley *et al.*, 1984). This ability has lead to the creation of numerous knock-in and knock-out transgenic mice for the investigation of gene expression and regulation *in vivo*.

mESC were initially established on and maintained by co-culture with mitotically inactivated mouse embryonic fibroblast (MEF) feeders. The absence MEFs or MEF conditioned medium results in spontaneous, random differentiation, with heterogeneous populations of differentiated cells appearing throughout the mESC colonies (Martin, 1981, Evans and Kaufman, 1981). Studies identified the cytokine LIF (leukaemia inhibitory factor, Smith and Hooper, 1987, Gearing *et al.*, 1987) as one of the feeder cell-derived molecules that plays a pivotal role in the self-renewal of these cells whilst also inhibiting their differentiation. On gelatine coated plates, in the presence of foetal bovine serum (FBS), recombinant LIF can replace the feeder cell function and maintain the growth of undifferentiated mESCs (Smith *et al.*, 1988, Williams *et al.*, 1988). Although in serum free culture, LIF alone is not able to prevent mESCs from differentiating, the addition of BMP4 (bone morphogenetic protein 4) allows undifferentiated mESC growth (Ying *et al.*, 2003). The combination of these discoveries allows mESC to be grown with defined factors in the absence of serum or feeders.

1.1.4 Signalling pathways involved in maintaining mESC pluripotency

LIF acts by binding to the heterodimeric LIF receptor (LIFR) which consists of two transmembrane proteins, LIFR itself and IL6ST (interleukin 6 signal transducer, previously known as gp130). LIFR activates JAK1 (Janus kinase 1) mediated STAT3 (signal transducer and activator of transcription 3) protein activation (Niwa *et al.*, 1998, Burdon *et al.*, 1999a). A study using a chimeric STAT3 molecule activated by

estradiol suggests that STAT3 signalling alone may be sufficient to block differentiation (Matsuda *et al.*, 1999). The role of the LIF/STAT3 in maintaining pluripotency is thought to be only facultative *in vivo* (Nichols *et al.*, 2001) as *Lif*$^{-/-}$ (Stewart *et al.*, 1992) and *Stat3*$^{-/-}$ (Takeda *et al.*, 1997) mouse embryos can succeed beyond gastrulation. The successful function of LIF/STAT3 signalling in maintaining mESC pluripotency is thought to be a recapitulation of process of diapause. This process occurs naturally when lactating females conceive causing the arrest of embryo development at the late blastocyst stage and the prevention of implantation (Nichols *et al.*, 2001). The binding of LIF to its receptor also initiates signalling pathways that are antagonistic to self-renewal such as the differentiation promoting extra-cellular signal-related kinase mitogen-activated protein kinase (ERK MAPK) pathway, (Burdon *et al.*, 1999b). The balance between these antagonistic pathways plays an important role in regulating self-renewal and determining the fate of undifferentiated mESCs (Burdon *et al.*, 1999a).

The effect of BMP4 on mESC self-renewal involves induction of *Id1* (*inhibitor of DNA binding 1*) expression through SMAD1/5/8 (mothers against decapentaplegic homolog 1, 5 and 8, Ying *et al.*, 2003) and inhibition of the ERK MAPK pathway and the p38 MAPK (response to stress) pathway (Burdon *et al.*, 1999b, Qi *et al.*, 2004). A role for phosphoinositide 3-kinases (PI3K) signalling in enhancing mESC survival and cell cycle progression has also emerged (Burdon *et al.*, 2002).

The maintenance of pluripotency also requires interactions between transcription factors. Three `core` pluripotency factors have been identified: POU5F1 (POU class 5 homeobox 1, previously known as OCT4), which is essential for pluripotency both *in vitro* and *in vivo* (Nichols *et al.*, 1998); SOX2 (SRY (sex determining region Y)-box 2), which is a transcriptional partner for POU5F1 (Avilion *et al.*, 2003, Rodda *et*

al., 2005); and NANOG (Nanog homeobox), which promotes self-renewal and alleviates the requirement for LIF (Mitsui *et al.*, 2003, Chambers *et al.*, 2003), although is not essential for maintaining the pluripotent state (Chambers *et al.*, 2007). These three transcription factors interact in feedback regulatory circuits (Boyer *et al.*, 2005, Loh *et al.*, 2006) and together are thought to act as master regulators of pluripotency (Gokhale and Andrews, 2008). In addition to POU5F1, SOX2 and NANOG, evidence also points to the involvement of a number of other transcription factors in the control of pluripotency (Wang *et al.*, 2006, Zhou *et al.*, 2007, Kim *et al.*, 2008). An overview of the factors that control mESC pluripotency is shown in Figure 1-1.
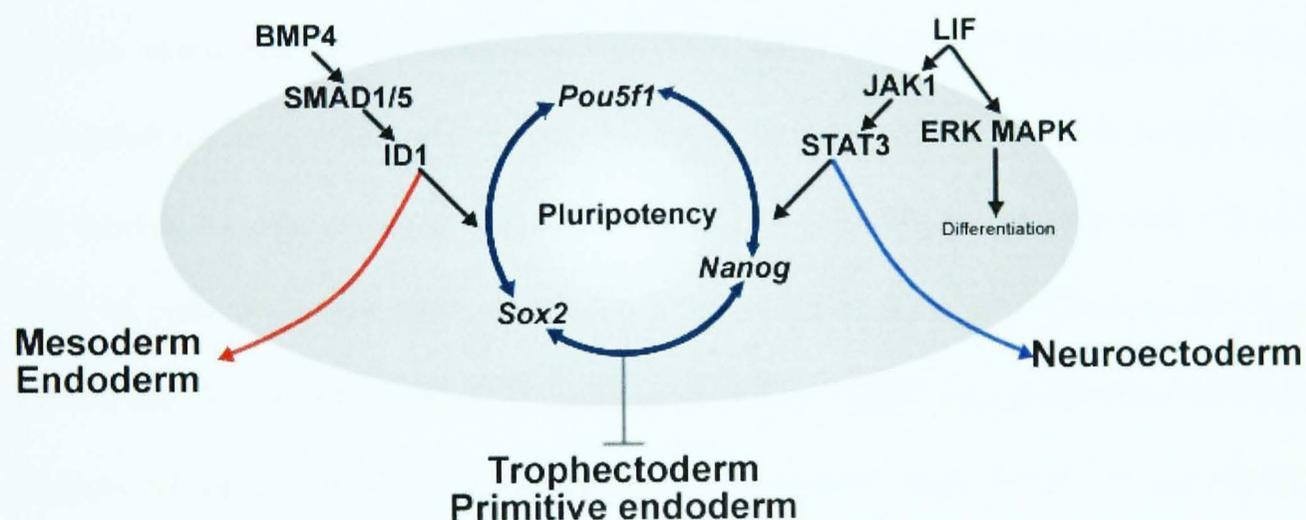
Figure 1-1: Signalling pathways regulating mESC pluripotency

LIF signalling (through the JAK1/STAT3) and BMP4 signalling (through SMAD1/5 and ID1) maintain pluripotency, however, when added individually, BMP4 and LIF induce mesodermal/endodermal and neuroectodermal differentiation of mESC cultures respectively (Ying *et al.*, 2003, Rao, 2004). POU5F1, SOX2, and NANOG act in concert to promote pluripotency. LIF can also signal the ERK MAPK pathway that can induce differentiation. Diagram adapted from Hyslop *et al.*, (2005b).

1.1.5   Human embryonic stem cells

hESCs have been derived from fresh or frozen, blastocyst stage embryos generated through assisted reproduction procedures, fertilised either by *in vitro* fertilisation (IVF) or intracytoplasmic sperm injection (ICSI). These embryos are donated for

research with informed consent after being selected for disposal either because they are excess to patients needs or because they are of insufficient quality for embryo transfer (Mitalipova et al., 2003). Alternatively embryos can be created in vitro, with informed consent, specifically for the purpose of deriving hESCs lines (Lanzendorf et al., 2001) although in most countries this is considered ethically inappropriate. Other methods of producing hESCs such as parthenogenesis as performed with non-human primates (Cibelli et al., 2002, Vrana et al., 2003) have recently proven feasible in humans (Revazova et al., 2007, Kim et al., 2007a).

As with mESCs, the derivation process for hESCs involves culturing embryos to the blastocyst stage and isolating the ICM. hESC lines have also been derived from morula stage embryos (Strelchenko et al., 2004). The cell population is then expanded on feeder cells and serially passaged to form a hESC line. Most cell lines are derived from between d6 and d8 blastocysts which provide approximately 30 and 50 ICM cells respectively (Stojkovic et al., 2004b). Under the appropriate conditions, hESCs are able to self-renew and maintain undifferentiated phenotype over extended periods of time, possibly indefinitely. hESCs express high levels of telomerase (Thomson et al., 1998), a ribonuclearprotein that adds telomere repeats to chromosome ends, thereby maintaining their length, which is highly correlated with immortality in human cell lines (Kim et al., 1994).

The very first study that describes the separation of human ICM cells and their continued culture, although only for two passages, was performed in 1994 by manually isolating the ICM (Bongso et al., 1994). This method was superseded, with few exceptions (Amit and Itskovitz-Eldor, 2002), by immunosurgery (Thomson et al., 1998, Solter and Knowles, 1975), a process in which the zona pellucida is first removed by digestion with pronase followed by selectively removal of the

trophectoderm layer of the blastocyst using specific antibodies such as rabbit anti-human whole serum (Reubinoff *et al.*, 2000). This method resulted in the first successful derivation of hESCs by Thomson *et al.* (1998) with the H1, H7, H9, H13 and H14 lines. These cells were grown on MEFs in a medium containing FBS. These lines have formed the basis of the vast majority of hESCs experiments that have been performed to date (Goh *et al.*, 2005, Allegrucci *et al.*, 2005). Derivations of hESCs all result in the isolation of a pluripotent population from several ICM cells. The cell line H9 was the first to undergo single cell cloning (Amit *et al.*, 2000) to form two clonal lines H9.1 and H9.2, demonstrating that individual hESCs are in fact pluripotent. Similar experiments have since been performed with the H1, H13, I3 and I6 lines (Amit and Itskovitz-Eldor, 2002). It has also been demonstrated that zygotes with chromosomal abnormalities can be used as a source for derivation of hESCs (Suss-Toby *et al.*, 2004) and hESCs can be derived from single blastomeres (Klimanskaya *et al.*, 2006).

Numerous hESCs lines have now been established (Table 1-1) using a variety of media, feeders and enzymatic (collagenase/trypsin), non enzymatic (cell dissociation buffer) or mechanical passage methods (reviewed by Allegrucci and Young, 2007).

Table 1-1: Main hESC lines derived to date

hESC line	Reference
H1, H7, H9, H13, H14	(Thomson *et al.*, 1998)
HES-1 to 4	(Reubinoff *et al.*, 2000, Richards *et al.*, 2002)
ES-76, ES-78-1, ES-78-2	(Lanzendorf *et al.*, 2001)
I-3, I-4, I-6, I-9	(Amit and Itskovitz-Eldor, 2002, Suss-Toby *et al.*, 2004)
BG01 to 4	(Mitalipova *et al.*, 2003)
Miz-hES	(Park *et al.*, 2003, Lee *et al.*, 2005)
WT3	(Pickering *et al.*, 2003)
HS181	(Hovatta *et al.*, 2003)
HSF-1, HSF-6	(Abeyta *et al.*, 2004)
Royan H1, H2, H6	(Baharvand *et al.*, 2004, Baharvand *et al.*, 2006a)
Maria Biotech MB	(Park *et al.*, 2004b)
Sahlgrenska 1 to 3	(Heins *et al.*, 2004)
hES-NCL1	(Stojkovic *et al.*, 2004a)
HUES-1 to 17	(Cowan *et al.*, 2004)
ACT-14	(Klimanskaya *et al.*, 2005)
SNUhES1 to 3	(Oh *et al.*, 2005)
UCSF-1	(Genbacev *et al.*, 2005)
HS293, HS306	(Inzunza *et al.*, 2005)
VAL-1, VAL-2	(Simon *et al.*, 2005)
PKU1, PKU2	(Hong-mei and Gui-an, 2006)
H15, H16	(Ludwig *et al.*, 2006b)
ReliCell hES1	(Mandal *et al.*, 2006)
MA01, MA09	(Klimanskaya *et al.*, 2006)
VUB01 to 5	(Mateizel *et al.*, 2006)
NOTT1, NOTT2	(Burridge *et al.*, 2007)
NTU1 to 3	(Chen *et al.*, 2007)

1.1.6 Surface markers of hESCs and mESCs

hESC lines derived from different laboratories show similar expression profiles of surface markers including: 1) the globoseries glycolipid stage specific embryonic antigens, SSEA3 and SSEA4; 2) the keratan sulphate antigens, TRA-1-60, TRA-1-81, GCTM2 and GCTM343 and 3) the liver alkaline phosphatase antigens, TRA-2-49 and TRA-2-54 (Adewumi *et al.*, 2007). Mouse ICM and mESCs also express SSEA1 but do not express SSEA3, SSEA4, TRA-1-60 or TRA-1-81 (Carpenter *et al.*, 2003). Despite these differences, 191 proteins have been detected as expressed in both mESCs and hESCs but not in their differentiated derivatives (Van Hoof *et al.*, 2006).

1.1.7 Maintaining hESC pluripotency

1.1.7.1 Serum and serum replacement

The first hESCs lines were originally derived in medium containing FBS (Thomson et al., 1998). FBS is serum harvested from bovine foetuses and consists of a complex mix of proteins of unknown composition that exhibits substantial batch variation. FBS can contain compounds both beneficial and detrimental to hESC culture (Amit et al., 2000). The use of FBS raises the concern of the introduction of viruses, prions or xenobiotic pathogens from cow to human (Cobo et al., 2005).

Knockout® Serum Replacement (KSR) from Invitrogen (Price et al., 1998) and VitroLife (Chen et al., 2007) has been used in an attempt to remove the FBS from hESC experiments, although these still contains animal proteins. Evidence exists that H1 hESCs lines can incorporate immunogenic nonhuman sialic acid, N-glycolylneuraminic (Neu5Gc), from the mouse feeder layer and/or KSR they are cultured with (Martin et al., 2005). Many humans have circulating antibodies to Neu5Gc, though not necessarily at a high titre (Cerdan et al., 2006), which could result in complement mediated cell death of cells bearing this molecule (Nguyen et al., 2005). The use of xenogenic FBS or KSR in these culture media makes them unsuitable for transplantation therapy and a substitute needs to be found such as a serum/serum replacement containing only human proteins or serum-free media formulations. Human serum is used in human IVF procedures (Wang and Sun, 2005), therefore exposure to human materials maybe possible. Human serum has been demonstrated to be able to replace FBS in hESC culture (Richards et al., 2002).

1.1.7.2 Murine and human feeders

The fibroblast feeder layer remains the most poorly defined component of the hESC culture (Amit *et al.*, 2000). These fibroblasts secrete multiple growth factors, including fibroblast growth factors (FGFs), transforming growth factor β (TGFB1), activin A, WNTs and antagonists of BMP signalling (Levenstein *et al.*, 2006). Therapeutic treatment using cell lines which have been cultured on these nonhuman cells may not be possible. Human marrow stromal cells (Cheng *et al.*, 2003), foreskin cells (Hovatta *et al.*, 2003, Choo *et al.*, 2004), uterine endometrial cells (Lee *et al.*, 2005) and foetal muscle and skin cells derived from aborted foetuses (Richards *et al.*, 2003), and fibroblasts derived from the hESCs themselves (Wang *et al.*, 2005d) have all been tested for their potential to support undifferentiated growth. With the addition of human serum, human feeders have demonstrated the capacity to support undifferentiated growth in a completely xeno-free system (Richards *et al.*, 2002).

1.1.7.3 Artificial matrices for feeder-free culture

The presence of feeders both slows passaging and complicates studies of hESC undifferentiated growth; therefore attempts have been made to use alternative matrices for feeder-free culture. It has been demonstrated that hESCs can be cultured in a feeder-free environment using KSR containing MEF conditioned medium on a basement membrane matrix called Matrigel. This matrix was shown to be equal or superior to laminin, fibronectin or collagen IV matrices (Xu *et al.*, 2001). Matrigel is derived from mouse Engelbreth Holm-swarm sarcoma, a tumour rich in extra-cellular matrix proteins. Its major component is laminin, followed by collagen IV, heparan sulfate proteoglycans, and entactin (Xu *et al.*, 2001). Using Matrigel with MEF-conditioned medium the hESCs have no direct contact with the MEFs so any feeder cell contact-related factors which may be aiding hESCs pluripotency can be

eliminated. However, Matrigel is still produced from animal products. To avoid this, human laminin has also been used as a matrix (Stojkovic *et al.*, 2005). Recently a entirely synthetic semi-interpenetrating polymer network, a polymer hydrogel, has been used as artificial matrix for support of HSF-6, but this was only demonstrated to support growth for up to 5 days (Li *et al.*, 2006b). Progress in avoiding the use of using FBS and MEF-conditioned medium to maintain undifferentiated hESCs has been made by combining KSR containing medium with high concentrations of FGF2 (100 ng ml^{-1}) without conditioning the medium with growth on Matrigel (Levenstein *et al.*, 2006).

1.1.7.4 Chemically defined media

Further progress has been made using Matrigel along with semi-chemically defined medium, avoiding the use of FBS or KSR. As well as improving the potential for clinical use, more defined media greatly simplifies studies of developmental mechanisms. Some of the more successful media have included Iscove's Modified Dulbecco's Medium/F-12 Nutrient Mixture (IMDM/F-12) supplemented with activin A or NODAL and FGF2 (Vallier *et al.*, 2005), Dulbecco's Modified Eagle's Medium/F-12 Nutrient Mixture (DMEM/F-12) supplemented with N2/B27 and high concentrations of FGF2 (Liu *et al.*, 2006b, Yao *et al.*, 2006), HESCO (hESC cocktail) supplemented with WNT3A and FGF2 (Lu *et al.*, 2006), or TeSR1 or modified TesR1 supplemented with FGF2 (Ludwig *et al.*, 2006a, Ludwig *et al.*, 2006b). None of these media can be classed as full chemically defined as they each are supplemented with bovine serum albumin (BSA). Ultimately, development of a fully defined culture system suitable for supporting hESC derivation, growth and differentiation without feeders, serum or serum replacement (human or otherwise) and using a medium of a known protein composition will allow us to minimise the

variability that affects the reproducibility and robustness of hESC cultures and allow the initiation of differentiation in a fully controlled manner.

1.1.8 Signalling pathways involved in maintaining hESC pluripotency

Unlike mESCs, which can be maintained in a undifferentiated state by LIF, the addition of LIF does not sustain the culture of hESCs in the absence of feeder layers (Thomson *et al.*, 1998) and it is not fundamental to hESC pluripotency (Humphrey *et al.*, 2004, Daheron *et al.*, 2004), despite the expression of both LIF and LIFR in hESCs (Aghajanova *et al.*, 2006). The signalling pathways involved in maintaining hESC pluripotency have been well characterised and are reviewed below and shown in Figure 1-2.
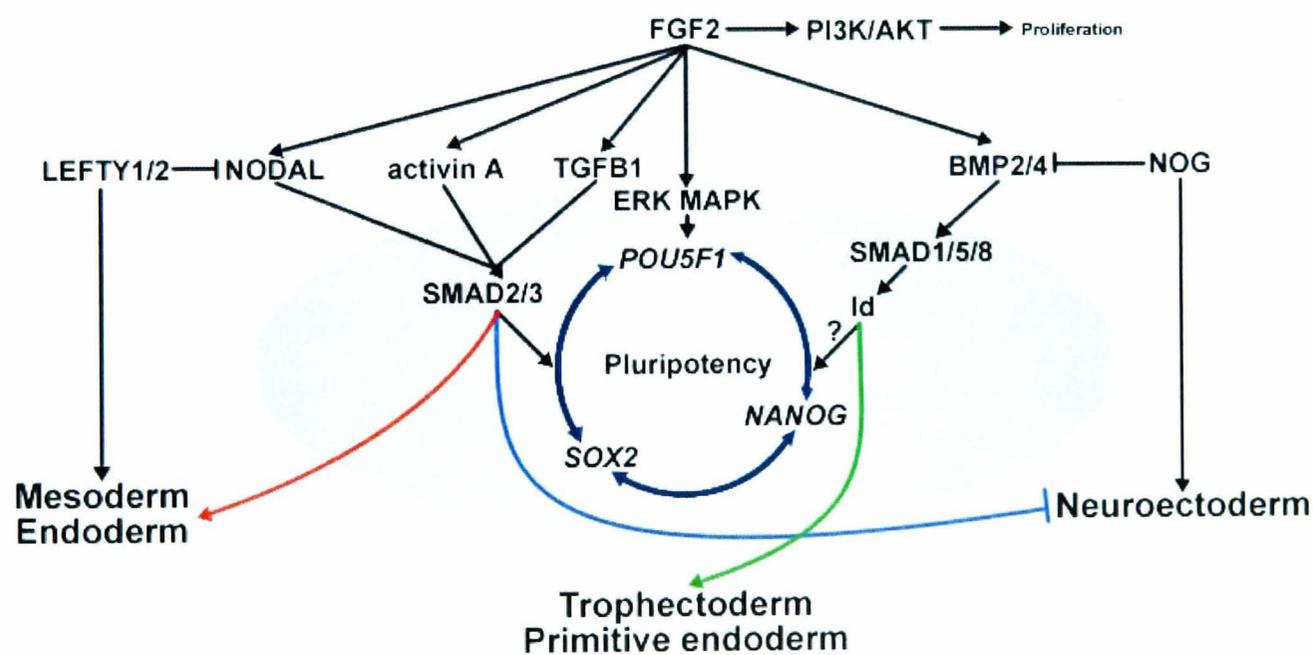
Figure 1-2: Signalling pathways regulating hESC pluripotency

TGFB1/activin A/NODAL pathway activation and BMP pathway repression by NOG (noggin) are required to maintain hESC pluripotency whilst FGF2 signalling through PI3K/AKT is required to maintain cellular proliferation. Diagram adapted from Hyslop *et al.*, (2005b).

1.1.8.1 FGF signalling

Although it remains unclear what direct role FGF signalling has on hESCs, the requirement for FGF2 to maintain pluripotency in the absence of feeders (Vallier *et al.*, 2005, Xu *et al.*, 2005b) and the presence of FGF2, FGF11, FGF13 as well as

FGF receptor 1 (FGFR1), FGFR2, FGFR3 and FGFR4 transcripts in hESCs indicates that FGF signalling is active in undifferentiated hESCs (Sato *et al.*, 2003, Sperger *et al.*, 2003, Dvash *et al.*, 2004, Ginis *et al.*, 2004, Rao *et al.*, 2004, Dvorak and Hampl, 2005). Of the 22 members of the FGF family, FGF2 has the most well defined role in contributing to hESC pluripotency (Xu *et al.*, 2005a, Xu *et al.*, 2005b). FGF2 signalling is initiated by the binding of FGF2, along with the co-ligand heparan sulphate, to any of the four FGFRs. The resulting dimerisation results in the phosphorylation of the docking protein FRS2 (fibroblast growth factor receptor substrate 2), followed by the recruitment of several GRB2 (growth factor receptor-bound protein 2) molecules. Activated GRB2 molecules then recruit the nucleotide exchange factor SOS1 (son of sevenless homolog 1, Dvorak and Hampl, 2005). The formation of the FRS2-GRB2-SOS complex results in activation of the ERK MAPK and PI3K/anaplastic lymphoma kinase (AKT) pathways that are suggested to have roles in self-renewal/differentiation and cell proliferation, respectively, in hESCs (Kang *et al.*, 2005, Armstrong *et al.*, 2006, Li *et al.*, 2007). In addition, FGF2 has been demonstrated to up-regulate activin A, TGFB1, and BMP4 in hESCs (Greber *et al.*, 2007).

1.1.8.2 BMP signalling

BMPs are members of the TGFβ superfamily. Of the 20 BMPs, the roles of BMP2 and BMP4 have been most intensely studied in hESCs. The four BMP receptors, activin receptor 1 (ACVR1), BMP receptor 1A (BMPR1A), BMPR1B and BMPR2 can form a variety of dimer combinations at the cell surface, each generating different signalling effects and responses (Stewart *et al.*, 2006). The canonical BMP signalling pathway is initiated by the binding of BMP to a heterodimer of BMPR1A and BMPR2 (Ying *et al.*, 2003). This leads to activation of SMAD1, SMAD5 and

SMAD8, which forms a heteromeric complex with SMAD4 (Miyazawa *et al.*, 2002). This complex then binds to SMAD responsive elements in *ID1* promoters and activates transcription (Ruzinova and Benezra, 2003).

In hESCs, the undifferentiated state is characterised by low levels of phosphorylated SMAD1/5/8 suggesting that suppression of BMP signalling is necessary for the maintenance of pluripotency (James *et al.*, 2005, Xu *et al.*, 2005b). In addition, BMP antagonists such as NOG (noggin), have been demonstrated to aid the maintenance of pluripotency in hESCs (Xu *et al.*, 2005b, Wang *et al.*, 2005a), although it is suggested that some level of BMP signalling may be required to maintain the undifferentiated state (Xu *et al.*, 2005b). BMP signalling also promotes differentiation to extra-embryonic lineages (Xu *et al.*, 2002b, Pera *et al.*, 2004) whilst NOG can promote differentiation to neuroectoderm (Pera *et al.*, 2004).

1.1.8.3 TGFB1, activin A and NODAL signalling

TGFB1, NODAL and activin A form disulphide-linked homodimers (in the case of activin A formed from two inhibin βA (INHBA) subunits) that all function through a similar mechanism by binding a type II receptor (ACVR2 or ACVR2B) which recruits and trans-phosphorylates a type I receptor (ACVR1, ACVR1B, ACVR1C or TGFBR1, Ebner *et al.*, 1993). The type I receptor then recruits and phosphorylates SMAD2 and SMAD3 (Lebrun *et al.*, 1999). SMAD3 then translocates to the nucleus and interacts with SMAD4 through multimerisation, resulting in their modulation as transcription factor complexes responsible for the expression of a large variety of genes (Chen *et al.*, 2002). Non-SMAD pathways, such as the ERK, p38 and JNK MAPK and PI3K/AKT pathways, have also been associated with TGFB1/activin A/NODAL signal transduction (reviewed by Chen *et al.*, 2006b). Binding of NODAL to the type II receptor requires the co-receptor TDGF1 (teratocarcinoma-

derived growth factor 1, previously known as Cripto, Gritsman *et al.*, 1999) and is inhibited by LEFTY1 and LEFTY2 (left-right determination factor 1 and 2) and CER1 (Cerberus 1, Schier and Shen, 2000). TDGF1 also acts as an inhibitor of activin A along with FST (follistatin) and FSTL3 (follistatin-like 3, Chen *et al.*, 2006b).

In hESCs, SMAD2 and SMAD3 have been shown to be necessary in maintaining the undifferentiated state, although these are not necessary for maintaining mESCs pluripotency (James *et al.*, 2005). Individually, TGFB1 (Amit *et al.*, 2004) or activin A (Beattie *et al.*, 2005) can maintain the pluripotent state, although proliferation is reduced. The combination of activin A or TGFB1 and FGF2 can maintain pluripotency and proliferation (Amit *et al.*, 2004, Vallier *et al.*, 2005). Additionally, it has been demonstrated that activin A regulates FGF, WNT and BMP pathways in hESCs (Xiao *et al.*, 2006). NODAL initiates the expression of NODAL antagonists LEFTY1 and LEFTY2 which are suggested to have a role in mesoderm induction (Dvash *et al.*, 2006). NODAL also prevents differentiation along the neuroectoderm pathway (Vallier *et al.*, 2004a) and can bind extra-cellular BMP leading to inhibition of the effects mediated by both NODAL and BMP (Yeo and Whitman, 2001).

1.1.9 Maintenance of karyotype

Karyotypic stability is an important consideration when hESCs for developmental studies. The first report of karyotypic abnormality in hESCs was observed in the H9 cell line after 7 months of culture (Amit *et al.*, 2000). This was followed by reports of the use of feeder free systems promoting genomic instability of hESCs after prolonged *in vitro* culture, such as aneuploidy (Carpenter *et al.*, 2004), gain of chromosome 17q and 12 when using KSR (Draper *et al.*, 2004) and aberrant X chromosome expression (Inzunza *et al.*, 2004). In addition, attempts to adapt the

HS181 cell line to grow without an extra-cellular matrix resulted in a karyotype change to 47,XX,del(7)(q11.2),+i(12)(p10) along with decreased pluripotency (Imreh *et al.*, 2006).

1.1.10 Differences between hESC lines and transcriptome profiles

The transcriptome profile of hESCs has been studied using a wide variety of methods to attempt to identify potential markers and regulators of self-renewal and differentiation. The use of hierarchical clustering of microarray data has been used in the past to identify if adult and embryonic stem cells have a common 'stemness' molecular profile (Ramalho-Santos *et al.*, 2002, Ivanova *et al.*, 2002). A number of groups have used microarrays to asses the gene expression profiles of undifferentiated hESC lines (Boyer *et al.*, 2005, Enver *et al.*, 2005, Skottman *et al.*, 2005, Golan-Mashiach *et al.*, 2005, Rao *et al.*, 2004, Bhattacharya *et al.*, 2004, Abeyta *et al.*, 2004, Carpenter *et al.*, 2004, Zeng *et al.*, 2004b, Sperger *et al.*, 2003). Along with microarrays, properties of hESCs have also been compared by RT-PCR, quantitative real-time PCR (Noaksson *et al.*, 2005), *in situ* hybridisation (Itskovitz-Eldor *et al.*, 2000), expressed sequence tag scan (Brandenberger *et al.*, 2004b), serial analysis of gene expression (Richards *et al.*, 2004) and massively parallel signature sequencing (Wei *et al.*, 2005, Brandenberger *et al.*, 2004a, Miura *et al.*, 2004).

Although data produced by microarray studies is of constantly improving quality, a concern is the apparent little agreement between different studies. Meta-analysis of the data from microarray studies only manages to achieve the resolution to suggest that markers present in hESCs but absent in other cell populations exist and one review of three independent studies found the expression of just 7 genes commonly agreed to be significant (Suarez-Farinas *et al.*, 2005). This problem has undermined confidence in microarray technology (Marshall, 2004, Allegrucci and Young, 2007).

To compare hESCs lines in a rigorous manner requires them to be cultured under identical culture conditions (Denning *et al.*, 2006), when studied in this manner substantial differences in growth efficiency, cloning efficiency and stable transfection rates have been noted (Richards *et al.*, 2002, Ware *et al.*, 2006). These differences between lines have been suggested to be due to the legacy of inherited epigenetic effects from early culture conditions (Allegrucci *et al.*, 2007).

1.1.11 Legal and ethical issues of hESC research

The legal position of different countries on hESC research varies across the globe depending on religious, moral, historical or socio-economic grounds (McLaren, 2001). The main ethical issue surrounding hESC research involves the determination of when does the embryo become a human being and if the blastocyst stage human embryo classifies as 'life', is a basic human rights being disrespected by destroying the embryo (Tsai, 2005). The creation of hESC lines, which is generally from surplus human embryos created during an IVF course, is more frequently seen as acceptable as these embryos would normally be disposed as they are either not longer required or not capable of forming an embryo. (Lo *et al.*, 2005). The creation of human embryos explicitly for the derivation of hESCs, or through therapeutic cloning methods such as somatic cell nuclear transfer (SCNT), is currently allowed in only a very limited number of countries (Daley *et al.*, 2007).

1.1.12 Applications of human embryonic stem cells

1.1.12.1 Use as a model for early human development

As a result of their ability to differentiate into many different cell types, hESCs open up exciting new opportunities to model human embryonic development and study the mechanisms underlying lineage specification *in vitro* (Dvash and Benvenisty, 2004).

Early human development is relatively inaccessible to experimental analysis due to logistical and moral considerations, and the majority of current information on the development of human embryos has been obtained from sectioning terminated foetuses (Daley, 2002). Since hESCs can recapitulate embryogenesis by expressing developmentally regulated genes and by activating signalling pathways as they occur *in vivo*, they can be used to analyse the effect of specific mutations on particular developmental events (Dvash *et al.*, 2006).

1.1.12.2 Drug discovery and toxicology screening

Functional assays are used at various stages of drug development such as target identification and validation, library screening for early hits and leads, and for pharmacological analysis of lead optimisation and drug candidate selection (Friel *et al.*, 2005). Many drug discovery programs have failed because targets validated in animal models prove to be of less significance in humans (Pouton and Haynes, 2005). The ability of hESCs to differentiate to a variety of adult cells types provides a platform to improve cell culture models used for drug discovery and development by replacing animal- or tumour-derived cell lines or lines immortalised by genetic modification (Pouton and Haynes, 2005).

1.1.12.3 Cellular model for human disorders

Human genetic disorders are caused by gain of or loss of function mutations. Gain of function mutations can be modelled in hESC-derived cells by introducing a gene harbouring at mutation using techniques such as transfection. However, most inherited genetic defects involve loss of function mutations which can be introduced into hESCs using techniques such as homologous recombination, lentiviral transfection or RNA interference (Ben-Nun and Benvenisty, 2006). Additionally,

hESC lines can be created using techniques such as SCNT using somatic cells from patients with the disease of interest (Alberio *et al.*, 2006) or by deriving hESCs from embryos diagnosed with the disease of interest by preimplantation genetic diagnosis (Pickering *et al.*, 2005).

1.1.12.4 Source of cells for cell therapy and regenerative medicine

Diseases caused by the loss of a specialised organ-specific cell type, such as Parkinson's disease in which dopamine producing neuronal cells are destroyed (Lerou and Daley, 2005) or heart disease due to a loss of function of cardiomyocytes (Nir *et al.*, 2003), are prime candidates for hESC-derived cell therapy (Ringe *et al.*, 2002). Other diseases, such as those caused by self-reactivity of the immune system including: multiple sclerosis, rheumatoid arthritis, lupus, type 1 diabetes and inflammatory bowel disease (Weissman, 2005) may also be potential candidates for treatment with hESC-derived HSCs.

1.1.13 Overcoming tissue incompatibility in hESC-derived transplants

Transplantation of heterologous hESC-derived cells or tissues could potentially raise the same possibility for graft rejection that currently hampers traditional solid-organ transplantation (Drukker and Benvenisty, 2004), although it has been demonstrated that hESCs and hESC-derived cells do possess some immune-privileged properties (Li *et al.*, 2004b).. The transplantation of HSCs, derived from hESCs, into foetal sheep has been shown lead to successful, albeit with only low level and limited, engraftment (Narayan *et al.*, 2006). It has been suggested that cells derived from HSCs, the precursor of blood and the immune system, may be able to induce donor-specific tolerance by mixed haematopoietic chimerism (Bradley *et al.*, 2002, Sykes, 2001). This raises the hope that transfer of hESC-derived HSCs into a patient could

lead to the stable long-term coexistence of multilineage haematopoietic cells of both the patient and the hESC line (Kaufman *et al.*, 2001). This could then lead to immunological tolerance to the alloantigens expressed by any other cell types derived from the same hESC line (Priddle *et al.*, 2006).

Another route to evading the immune system, which would avoid the potential ethical concerns of hESCs, has recently been demonstrated by the production of induced pluripotency (iPS) cells. This system involved the reprogramming of mouse fibroblasts by retroviral introduction of *Pou5f1*, *Sox2*, *Myc* and *Klf4* and selection for *Fbxo15* expression to produce cells of mESC-like character (Takahashi and Yamanaka, 2006). This process has been further enhanced by selection for *Nanog* expression (Okita *et al.*, 2007, Wernig *et al.*, 2007, Maherali *et al.*, 2007). If this work could be repeated using human fibroblasts it would potentially provide a route for providing patient specific pluripotent stem cells (Yamanaka, 2007).

1.2 APPROACHES TO DIRECTED HUMAN EMBRYONIC STEM CELL DIFFERENTIATION

When removed from the factors that maintain pluripotency, hESCs spontaneously differentiate through symmetric cell division (Zwaka and Thomson, 2005), lose their near-homogenous phenotype, begin to differentiate and then form basic primitive structures in a chaotic manner (Thomson *et al.*, 1998, Itskovitz-Eldor *et al.*, 2000). Theoretically, hESCs are capable of differentiating to all of the 200 or more somatic and germ cell types in the adult human body (Reubinoff *et al.*, 2000). Culture conditions and protocols have been developed to improve upon this random differentiation and numerous terminal cell types have been derived as shown in Table 1-2.

Table 1-2: Cell types produced by *in vitro* differentiation of hESCs

Cell type	hESC line	Reference
Endoderm		
insulin producing cells	H9, H9.2, H13, I6	(Assady *et al.*, 2001, Segev *et al.*, 2004, Jiang *et al.*, 2007)
hepatocyte-like cells	H1, H9, Sahlgrenska 1	(Rambhatla *et al.*, 2003, Lavon *et al.*, 2004, Shirahashi *et al.*, 2004, Baharvand *et al.*, 2006b, Soderdahl *et al.*, 2007)
pancreatic cells	H9	(Lavon *et al.*, 2006)
lung alveolar epithelium	H9.2	(Wang *et al.*, 2007a)
Mesoderm		
haematopoietic cells	H1, H9, HES2, HSF6, BG01, BG02, BG03, SNUhES3	(Kaufman *et al.*, 2001, Chadwick *et al.*, 2003, Cerdan *et al.*, 2004, Lu *et al.*, 2004, Zhan *et al.*, 2004, Tian *et al.*, 2004, Wang *et al.*, 2004, Wang *et al.*, 2005b, Vodyanik *et al.*, 2005, Wang *et al.*, 2005c, Menendez *et al.*, 2004, Zambidis *et al.*, 2005, Ng *et al.*, 2005b, Kim *et al.*, 2005, Qiu *et al.*, 2005, Woll *et al.*, 2005, Bowles *et al.*, 2006, Slukvin *et al.*, 2006, Anderson *et al.*, 2006, Chang *et al.*, 2006, Vodyanik *et al.*, 2006, Galic *et al.*, 2006, Srivastava *et al.*, 2007)
vascular endothelial cells	H1, H9, H9.2, H13, I6	(Wang *et al.*, 2004, Levenberg *et al.*, 2002, Gerecht-Nir *et al.*, 2003, Gerecht-Nir *et al.*, 2004c, Gerecht-Nir *et al.*, 2005, Wang *et al.*, 2007b)
cardiomyocytes	H1, H7, H9, H9.1, H9.2, H14, HES-2, HUES-7, NOTT1, NOTT2, BG01, ReliCell1	(Kehat *et al.*, 2001, Xu *et al.*, 2002a, Mummery *et al.*, 2002, Kehat *et al.*, 2002, Mummery *et al.*, 2003, He *et al.*, 2003, Snir *et al.*, 2003, Satin *et al.*, 2004, Kehat *et al.*, 2004, Reppel *et al.*, 2004, Xue *et al.*, 2005, Huber *et al.*, 2007, Pal and Khanna, 2007, Burridge *et al.*, 2007)
osteoblasts	H1, H9, TNG15	(Sottile *et al.*, 2003, Bielby *et al.*, 2004, Lerou and Daley, 2005)
germ cells	H9, HSF1, HSF6	(Clark *et al.*, 2004)
mesenchymal stem cells	HUES9, H1, H9	(Barberi *et al.*, 2005, Lian *et al.*, 2007)
adipocytes	H9	(Xiong *et al.*, 2005)
skeletal myoblasts	H9	(Barberi *et al.*, 2005)
Ectoderm		
neurons/ neural progenitors	H1, H7, H9, H9.2, HES-1, HES-2, HES-3 BG01, BG02	(Reubinoff *et al.*, 2001, Schuldiner *et al.*, 2001, Carpenter *et al.*, 2001, Zhang *et al.*, 2001, Schulz *et al.*, 2003, Pera *et al.*, 2004, Ben-Hur *et al.*, 2004, Nasonkin and Koliatsos, 2006, Johnson *et al.*, 2007, Pankratz *et al.*, 2007, Nat *et al.*, 2007)
dopaminergic neurons	H1, H9, HES-3, BG01, BG02, BG03, MB03, HSF-1, SNU-hES-3, M	(Schulz *et al.*, 2004, Perrier *et al.*, 2004, Zeng *et al.*, 2004a, Park *et al.*, 2004a, Buytaert-Hoefen *et al.*, 2004)
motorneurons	H1, H9	(Li *et al.*, 2005)
oligodendrocytes	H7	(Nistor *et al.*, 2005)
keratinocytes	H9	(Green *et al.*, 2003)
retinal	H1, H7, H9	(Klimanskaya *et al.*, 2004, Ahmad *et al.*, 2007)
Extra-embryonic		
trophoblast	H1, H7, H9, H14	(Xu *et al.*, 2002b, Gerami-Naini *et al.*, 2004)
yolk sac visceral endoderm	HES-2	(Conley *et al.*, 2004a)

A variety of different techniques have been applied to direct the differentiation of hESCs and the main approaches are reviewed below.

1.2.1 Co-culture

To direct differentiation to a particular lineage, co-culture systems using stromal cell types characteristic of the same lineage or 'niche' location have been used. For blood differentiation, co-culture of undifferentiated hESCs with the murine bone marrow cell lines, S17 and OP9, or the yolk sac endothelial line, C166, have proven successful (Kaufman *et al.*, 2001, Vodyanik *et al.*, 2005). For cardiomyocyte differentiation, mouse visceral-endoderm-like END-2 cells have proven successful (Mummery *et al.*, 2002). This type of experiment, although useful to prove the possibility of deriving a cell type, allow us only limited insights into the regulators of differentiation to a particular lineage (Weitzer, 2006).

1.2.2 Monolayer and adherent colony differentiation

Several lineages have been formed when hESC colonies have been plated as monolayers on Matrigel-, fibronectin- or gelatine-coated plates. Neuroectoderm formation has been reported using NOG to block BMP signalling (Gerrard *et al.*, 2005, Nasonkin and Koliatsos, 2006), smooth muscle cells formation has been reported using all-trans retinoic acid (Huang *et al.*, 2006), oseteogenic cell and mesenchymal stem cells formation has been reported using enzymatic dissociation of partially differentiated aggregates in dexamethasone, ascorbic acid-2-phosphate and β-glycerolphosphate (Karp *et al.*, 2006, Olivier *et al.*, 2006); chondrocyte formation has been reported using BMP2 (Toh *et al.*, 2007), and endothelial cell formation has been reported without supplementation (Wang *et al.*, 2007b). Successful haematopoietic differentiation in monolayer cultures has been achieved in primate

ESCs using OP9 (bone-marrow derived stromal cells) conditioned medium (Zhang *et al.*, 2006). However, adherence of dissected mESC colonies to gelatinised surfaces produced almost no haematopoietic colony forming units (Nishikawa *et al.*, 1998, Dang *et al.*, 2002). The potential for monolayer-based directed differentiation of hESCs colonies to neural, definitive endoderm/pancreatic and early cardiac muscle cells in CDM supplemented with growth factors has also been reported (Yao *et al.*, 2006). As yet the differentiation of hESCs as true monolayers (i.e. allowing single cell hESCs to attach to a matrix rather than colonies of hESCs, which would facilitate scale-up to clinically relevant levels) has not been described.

1.2.3   Three-dimensional differentiation on polymer scaffolds

Polymer scaffolds are an ideal system for inducing three-dimensional tissue formation as they can be tailored to modulate cell attachment, growth and differentiation, by varying scaffold polymer and fabrication technique, and can be biodegradable (Zoldan and Levenberg, 2006). hESCs have been differentiated on polymeric scaffolds coated with Matrigel or fibronectin supplemented with growth factors and were observed to form structures of neural tissues, cartilage and liver as well as a network of blood vessels (Levenberg *et al.*, 2003).

1.2.4   Genetic modification

Delivery of defined factors to promote directed differentiation can be problematic. Genetic modification can be used to direct hESC differentiation by over-expression or ablation of regulatory genes (reviewed by Drukker and Benvenisty, 2004, Yates and Daley, 2006). In order to monitor differentiation, tissue specific promoters can drive a visible marker gene product such as green fluorescent protein (GFP), or a selectable marker, such as an antibiotic resistance gene (Eiges *et al.*, 2001). Cell

sorting can be used to select relevant cells if the desired cell type expresses a unique pattern of cell surface antigens, such as CD34$^+$ CD38$^-$ for the isolation of haematopoietic progenitors (Kaufman *et al.*, 2001).

In hESCs various methods for ectopic gene expression have been explored so far (reviewed by Wobus and Boheler, 2005, Menendez *et al.*, 2005). These include transient or stable transfection (Eiges *et al.*, 2001, Lakshmipathy *et al.*, 2004, Vallier *et al.*, 2004b), stable lentiviral transduction (Ma *et al.*, 2003, Gropp *et al.*, 2003, Smith-Arica *et al.*, 2003), retroviral-based vector transduction (Menendez *et al.*, 2004, Wang *et al.*, 2005c), and conditional gene expression using an inducible recombinase (Nolden *et al.*, 2006, Vallier *et al.*, 2007). Loss-of-function studies using small interfering (siRNAs) have been shown to be effective at knocking down gene expression (Hay *et al.*, 2004, Matin *et al.*, 2004, Vallier *et al.*, 2004b, Zaehres *et al.*, 2005, Hyslop *et al.*, 2005a). Homologous recombination, which allows for gene targeting, has also been reported in hESCs (Zwaka and Thomson, 2003, Urbach *et al.*, 2004).

1.2.5 Embryoid bodies

Thus far the most widely used strategy for successful directed *in vitro* differentiation of hESCs has employed an initial aggregation step to form human embryoid bodies (hEBs) that promote germ layer formation before specialised cell types. Embryoid bodies (EBs) are 3-D, spherical multi-cellular aggregates that differentiate in a spontaneous manner (reviewed by Weitzer, 2006). Mouse EBs (mEBs) can, to a limited extent, recapitulate early post implantation embryonic development and mimic the ontogeny of gene expression patterns that appear during embryogenesis (Doetschman *et al.*, 1985, Keller, 1995). The first *in vitro* studies were performed in the 1970's on EBs generated from teratoma and teratocarcinoma cells (Levine *et al.*,

1974, Martin *et al.*, 1977). In the 1980's mEBs formed from mESCs (Evans and Kaufman, 1981, Martin, 1981) demonstrated the capacity of ESCs to form all three germ layers. After the initial isolation of hESCs (Thomson *et al.*, 1998) hEBs were quickly demonstrated to have a potential comparable to mEBs (Itskovitz-Eldor *et al.*, 2000, Schuldiner *et al.*, 2000).

1.2.6 Gastrulation-like development in mouse embryoid bodies

Gastrulation-like processes are known to take place in mEBs (reviewed by Weitzer, 2006), but the regulation of germ layer specification remains poorly understood (reviewed by Murray and Edgar, 2004, Spagnoli and Hemmati-Brivanlou, 2006). The early stages of mEB development have been best characterised in mEBs formed in suspension cultures and can be separated into seven distinct stages; (1) aggregation, (2) primitive endoderm formation, (3) basement membrane assembly (4) primitive ectoderm epithelium formation, (5) cavitation, (6) visceral and parietal endoderm formation and (7) germ layer induction. These stages are summarised in Figure 1-3.
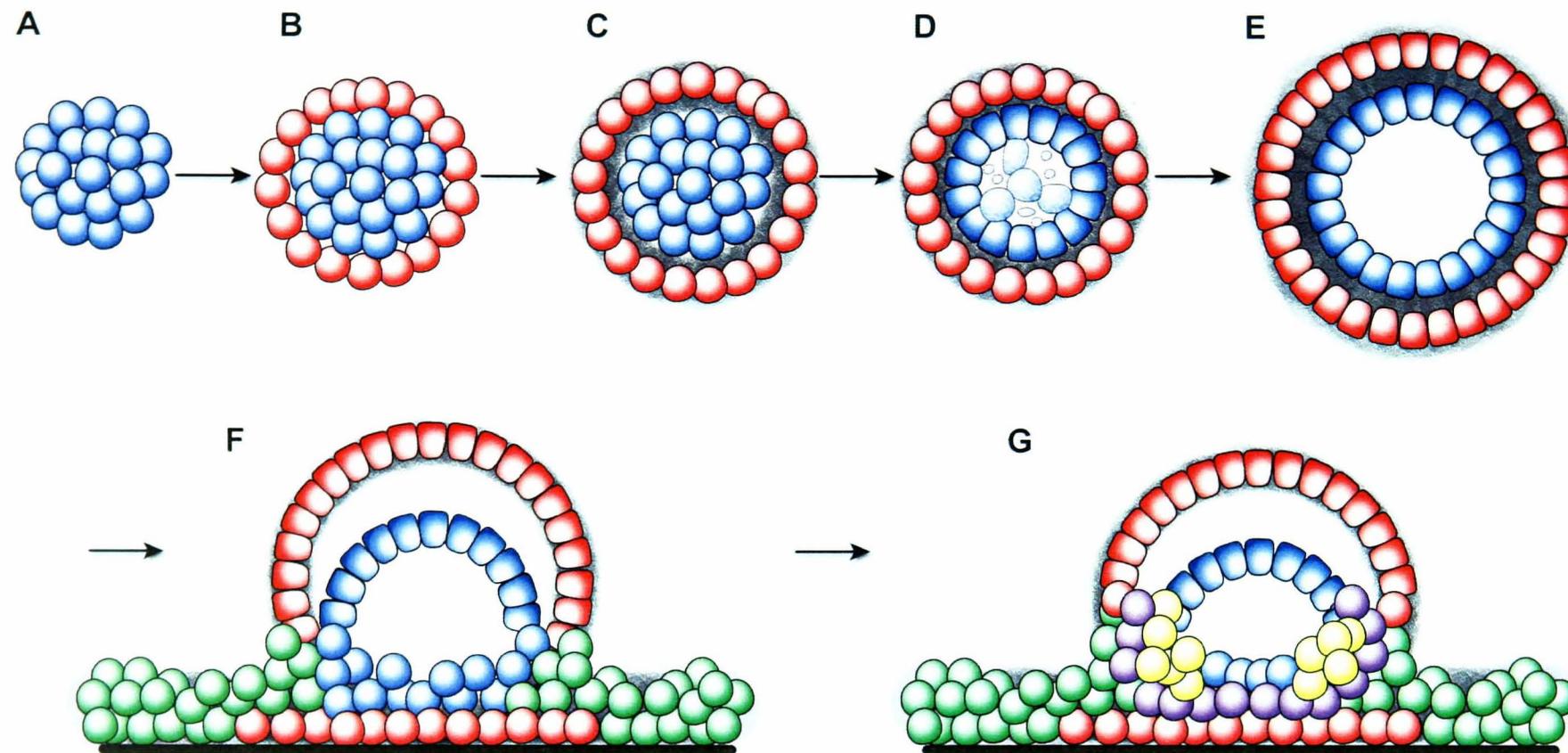
Figure 1-3: Diagrammatic representation of early mEB differentiation

A) d1, CDH1 mediated mESC compaction (blue cells). B) d2-4, primitive endoderm formation on the exterior of the mEB (red cells). C) d3-5, basement membrane assembly (grey). D) d4-5, primitive ectoderm epithelium formation and programmed cell death of epiblast-like cells not in contact with basement membrane. E) d5-6, continued development of primitive ectoderm epithelium, visceral ectoderm development and of cavitation completion. F) d7, mEB attachment to a plate or collagen matrix (black line) via primitive endoderm (red cells underneath the centre of the mEB) which spreads away from the mEB to form parietal endoderm (green cells). Visceral endoderm forms epithelial cysts on top of the central cell mass of the mEBs (red cells above centre of mEB). G) Primitive ectoderm epithelium (blue cells) differentiate to mesodermal cells (yellow) and definitive endoderm (purple). The culture medium substitutes for the blastocoel, and the central cyst (inside primitive ectoderm epithelium) is analogous to the pro-amniotic cavity in the embryo (diagram adapted from Weitzer, 2006, Li *et al.*, 2003, Rodda *et al.*, 2002).

1.2.6.1 Aggregation

On d1 following suspension mESCs form an irregularly shaped aggregate of cells that are morphologically indistinguishable from one another (reviewed by Murray and Edgar, 2004). An essential factor in this process is CDH1 (E-cadherin). *Cdh1*$^{-/-}$ mESCs fail to aggregate or undergo differentiation (Larue *et al.*, 1994). CDH1 stimulates the phosphorylation of the multiple docking protein, GAB1 (Shinohara *et al.*, 2001), thereby regulating FGF1 activation of the anti-apoptotic PI3K/AKT pathway (Lamothe *et al.*, 2004) and preventing cell death. In addition, CDH1-dependent mESC aggregation may be a prerequisite for the restriction of FGF signalling to the outer cells of the developing mEB and primitive endoderm formation discussed below.

1.2.6.2 Primitive endoderm formation

After d1 mEBs begin to expand then, at d2-4, bubbles of cells can be seen on the surface of the mEB (Li *et al.*, 2002, Murray and Edgar, 2000). These outer cells form a monolayer that covers the entire surface of the mEB (Bader *et al.*, 2001, Ikeda *et al.*, 1999), which then elongate (Murray and Edgar, 2001b) to form hypoblast-like, extra-embryonic primitive endoderm (Smyth *et al.*, 1999), see Figure 1-3B. Primitive endoderm is characterised by the expression of *Afp* (α-fetoprotein, Abe *et al.*, 1996), Dolichos bioflorus agglutinin (Bader *et al.*, 2001), *Nrtf1* (COUP-TF1, Murray and Edgar, 2001b) and KRT8 (cytokeratin 8), recognised by TROMA-1 antibody, and an absence of expression of the pluripotency markers *Pou5f1* (Mountford *et al.*, 1998) and *Nanog* (Hamazaki *et al.*, 2004).

Primitive endoderm differentiation is dependent on FGF signalling, as demonstrated by the targeted disruption of *Fgf4* (Wilder *et al.*, 1997). FGF4 is expressed in the

ICM and contributes to the maintenance of the endoderm (Goldin and Papaioannou, 2003). The majority of FGF dependent signals go through FRS2, a docking protein (Lax *et al.*, 2002), that communicates with the adaptor molecule GRB2 (Cheng *et al.*, 1998). Previously it was thought that FGF4 signalled endoderm induction through the ERK MAPK pathway, activation of which has been shown to induce endoderm differentiation in F9 embryonal carcinoma cells (Verheijen *et al.*, 1999). However, while *Fgf4*$^{-/-}$ (Feldman *et al.*, 1995) or *Grb2*$^{-/-}$ (Cheng *et al.*, 1998) mouse embryos die with defective endoderm formation, *Frs2*$^{-/-}$ embryos survive until advanced gastrulation (Hadari *et al.*, 2001). Subsequent analysis of signal transduction in mEBs formed from mESCs with a dominant negative *Fgf2r* mutation which aggregate but do not form primitive endoderm (Chen *et al.*, 2000, Li *et al.*, 2001a) revealed that PI3K/AKT pathway rather than ERK MAPK signalling is affected by FGF activity (Chen *et al.*, 2000, Li *et al.*, 2001b). Downstream of this FGF4, GRB2, PI3K/AKT cascade are GATA6 and GATA4 (Li *et al.*, 2004a). mESCs can be induced directly to an endodermal-like phenotype by forced *Gata4* or *Gata6* expression (Fujikura *et al.*, 2002). *Gata4*$^{-/-}$ embryos die between E8.0 and E9.0 during heart morphogenesis (Kuo *et al.*, 1997, Molkentin *et al.*, 1997) whereas *Gata6*$^{-/-}$ embryos die at E5.5-7.5 because of defects in visceral endoderm formation (Morrisey *et al.*, 1998). Ectopic *Gata6* expression can induce *Gata4* expression and loss of *Gata6* expression results in the loss of *Gata4*, whereas loss of *Gata4* results in the up-regulation of *Gata6* (Kuo *et al.*, 1997, Morrisey *et al.*, 1998). Taken together these results suggests that *Gata6* is upstream of *Gata4* and behaves as the master gene for endoderm regulation (Fujikura *et al.*, 2002). GATA4/GATA6 up-regulate the expression of the transcription factors *Nr2f1* and *Nr2f2* (COUP-TF2, Murray and

Edgar, 2001b) which in turn induce laminin 1 subunit expression, such as *Lamc1* and *Lamb1* (Li *et al.*, 2004a).

Initially it was perceived that this primitive endodermal cell fate is determined by intercellular interactions resulting from the cell's position on the surface of the aggregate, rather than from heterogeneous cells that migrate to the surface (Becker *et al.*, 1992, Mountford *et al.*, 1998). In F9 human embryonal carcinoma cell-derived EBs, the primitive endoderm cells on the EB surface have been suggested to provide a barrier that prevents factors in the medium from modulating differentiation of internal cells (Miki, 1999). Recently it was demonstrated that the ICM of E3.5 mouse embryo is already heterogeneous, with NANOG and GATA6 expressed in a 'salt and pepper' pattern. This expression pattern was shown not to be based on blastomere history or position the ICM (Chazaud *et al.*, 2006).

1.2.6.3 *Basement membrane assembly and primitive ectoderm epithelium formation*

Once formed, this outer layer of primitive endodermal cells expresses large amounts of basement membrane components, largely consisting of laminins (reviewed by Li *et al.*, 2003). Contact with the basement membrane induces undifferentiated mESCs in the centre of the mEB to become epiblast-like (Li *et al.*, 2004a, Murray and Edgar, 2000), see Figure 1-3C. This is associated with up-regulation of *Fgf5* (Haub and Goldfarb, 1991) and down-regulation of *Bmp4* (Coucouvanis and Martin, 1995), although no obvious morphological changes occur (Rathjen *et al.*, 1999). Once the basement membrane is formed epiblast-like cells that are contact become polarised to form primitive ectodermal epithelium (Coucouvanis and Martin, 1995, Ikeda *et al.*, 1999), see Figure 1-3D. This is suggested to be in response to BMP and IHH

signalling from the primitive endoderm (Coucouvanis and Martin, 1999, Maye *et al.*, 2000).

1.2.6.4 Cavitation

The combination of primitive endoderm, basement membrane and columnar epiblast epithelium initiates programmed cell death (PCD) in the majority of remaining epiblast cells that are not in contact with the basement membrane. This promotes cavitation at the centre of the mEB (Li *et al.*, 2004a, reviewed by Murray and Edgar, 2004). mEBs formed from mESC lines with double knockout of *Lamc1*, that encodes the laminin γ1 subunit, do not form a basement membrane or columnar ectodermal epithelium and do not cavitate (Smyth *et al.*, 1999, Murray and Edgar, 2000, Murray and Edgar, 2001c). Apoptosis and autophagy are the two dominant methods of PCD. In mEBs two autophagy related genes, *Atg5* and *Beclin1*, are essential for cavitation (Qu *et al.*, 2007).

1.2.6.5 Visceral and parietal endoderm formation

Simultaneously to cavitation the outer surface primitive endoderm differentiates to visceral endoderm (see Figure 1-3F). This has a characteristic columnar epithelial morphology and expresses markers such as *Hnf4a (Hepatic nuclear factor 4, alpha)*, *Foxa2, Sox17, Afp, Evx1, Ttr (transthyretin)* and *Krt8* (Coucouvanis and Martin, 1999, Dufort *et al.*, 1998, Spyropoulos and Capecchi, 1994, Conley *et al.*, 2007). BMP4 has been implicated in cavitation and visceral endoderm formation and inhibition of BMP signalling using a dominant negative *Bmpr1b* prevents *Hnf4a* expression, cavitation and visceral endoderm formation. Using mEBs formed from a *Bmp4⁻* mESC line that do not cavitate, it has been demonstrated that media supplementation with of any one of BMP2, BMP4 or BMP7 can rescue *Hnf4a*

expression, cavitation and visceral endoderm formation (Coucouvanis and Martin, 1999). Indian hedgehog (IHH) signalling also has a role in visceral endoderm formation, since the IHH signalling can be inhibited downstream of the signalling receptor by stimulating PKA activity with cAMP and forskolin (Maye *et al.*, 2000). Thus promotes the outer primitive endoderm to form parietal endoderm instead of visceral endoderm.

If transferred onto tissue culture plates, the basement membrane allows mEB attachment and the surface of the tissue culture plate fulfils a role similar to Reichert's membrane (Weitzer, 2006). The remaining primitive endoderm in contact with the dish is induced to from a spreading sheet of parietal endoderm (Grabel and Casanova, 1986) which migrates away from the mEB and then undergoes an epithelial to mesenchymal transition (Bader *et al.*, 2001). This is characterised by denoted by the up-regulation of *Plat* (tissue plasminogen activator or t-PA, Bader *et al.*, 2001) and KRT19 (cytokeratin 19), recognised by TROMA-3 antibody (Sauer *et al.*, 1998, Murray and Edgar, 2001c), and down-regulation of *Afp* (Stary *et al.*, 2005). After attachment, visceral endoderm is maintained as an epithelial bubble on top of the cell mass (Bader *et al.*, 2001, Murray and Edgar, 2001a).

1.2.6.6 Definitive germ layer formation

Once mEBs have attached to culture plates the primitive ectoderm epithelium inside the ring of visceral and parietal endoderm begins to undergo differentiation towards the three definitive germ layers, endoderm, mesoderm and ectoderm see (Figure 1-3G). mEBs germ layer formation is suggested involve recapitulation of some of the signalling pathways experienced *in vivo* and mEBs are thought to express most if not all of the growth factors, signal mediators and transcription factors necessary for the regulation of embryogenesis *in vivo* (Weitzer, 2006). In mEBs the parietal endoderm

has been shown to influence the primitive ectoderm epithelium to differentiate towards mesodermal lineages, as demonstrated by the detection of a proliferating horseshoe shaped area of mesoderm, that expresses *T*, inside the ring of parietal endoderm which goes onto form erythrocytes and cardiomyocytes (Bader *et al.*, 2001).

1.2.6.7 Chaotic differentiation in mEBs due to lack of polarity

The chaotic nature of germ layer differentiation in mEB is most likely due to the lack of polarity and related asymmetry of gene expression (Weitzer, 2006). The lack of polarity is due to a combination of mEB cell aggregation, rather than embryo-type clonal differentiation, and the lack of trophoblast and subsequent extra-embryonic ectoderm. Polarity has yet to be studied in free floating EBs (Weitzer, 2006).

1.2.7   Primitive endoderm formation and cavitation in human and primate embryoid bodies

Similar processes to those that occur in mEBs, including radial differentiation, apoptosis, central cavitation and expression of primitive endoderm associated markers have been reported in hEBs.

Ikskovitz-Eldor *et al.*, (2000) described H9 hEBs as composed of densely packed cells at d3 before becoming cavitated at d4, accumulating fluid and becoming cystic at d14 (with between 20-90% of hEBs cystic at d20). Conley *et al.*, (2007) described HES-2 hEBs as containing fluid-filled cysts from d7 onwards and observed the presence of apoptotic cells at d3, 5 and 7. Cavity formation in hEBs was suggested to be less extensive as than in mEBs (Conley *et al.*, 2007). Apoptosis in hEBs also occurs before the formation of a visceral endoderm layer, suggesting that the visceral endoderm may not be required for the initiation of cavitation in the hEB system

(Conley *et al.*, 2007). In addition, in FES22 and FES30 hESCs, only limited proportions of hEBs formed cavities at d7 (Mikkola *et al.*, 2006).

The presence of primitive endoderm has been described in HES-2 hEBs by the detection of AFP, KRT8, and GATA6 expression throughout d3 and d5 (Conley *et al.*, 2007). At d7 expression of these markers, as well as TTR, was detected in a thin layer of cells at the hEB periphery, suggesting differentiation of primitive endoderm to visceral endoderm (Conley *et al.*, 2007). Primitive endoderm marker expression in an outer epithelial layer has also been described in d8 H1 hEBs by the detection of KRT8 (Gerami-Naini *et al.*, 2004) and in d13 HSF6 hEBs by the detection of AFP (Poon *et al.*, 2006).

hEBs formed from H9 or HSF6 hESCs differentiated in CDM without additional growth factors grew as homogenous spheres with no apparent tissue organisation at d10 and neuroectoderm-like differentiation at d11-d14 (Vallier *et al.*, 2004a). In contrast, when using the same culture conditions, the transgenic over-expression of *NODAL* induced 75-95% of hEBs to form three distinct cell layers at d10. AFP was expressed in the outside layer and POU5F1 was expressed in the inner layers, although no definitive germ layer differentiation was detected (Vallier *et al.*, 2004a). Comparison of these properties between lines and differentiation methods has not been made.

1.2.8 Differences between human and mouse development and their implications for EB formation and differentiation

There are significant differences between mouse and human development that may be reflected in EB differentiation. In humans, the first 10 days of embryonic differentiation are almost exclusively devoted to the formation of the extra-

embryonic membranes whereas the mouse has already reached midgestation by this point (Dvash and Benvenisty, 2004). This suggests that *in vitro* hEB differentiation will be substantially slower than mEB differentiation. Also of particular relevance to hEB differentiation are the differences in the arrangement of the germ layers. Human embryos form a planar bilaminar disc, whereas mouse embryos form a more compact egg cylinder that undergoes germ layer-inversion (Eakin and Behringer, 2004). It has been suggested that mouse gastrulation, which is substantially more three-dimensional than human gastrulation may have unique features compared to gastrulation in other mammals (Tam and Behringer, 1997, Beddington and Robertson, 1998). Also in the human embryo, extra-embryonic mesoderm is thought to be derived from the extra-embryonic endoderm before the appearance of the primitive streak (Bianchi *et al.*, 1993).

Although mEBs only partially mimic the formation process of the embryo, striking patterning processes have been reported in common marmoset EBs with the formation of chaotic structures resembling yolk sac, amnion and embryonic disc with a primitive streak-like structure (Thomson *et al.*, 1996). These complex structures were not reported in rhesus monkey EBs (Thomson *et al.*, 1995), although the formation of a bilaminar disc in colonies with the lower layer undergoing a epithelial-mesenchymal transition was observed (Behr *et al.*, 2005).

1.3 MAMMALIAN GASTRULATION

To differentiate hESCs to mesoderm by mimicking *in vivo* ontology, an in-depth knowledge of the process of gastrulation is required. Very little data on germ layer induction and the signalling pathways involved human gastrulation are available, and only recently has it been possible to perform large scale gene expression studies on the human blastocyst (Adjaye *et al.*, 2005). In contrast, the mouse embryo is a well studied example of mammalian gastrulation and the processes involved are now well understood (reviewed by Tam and Loebel, 2007).

1.3.1 Lineage choice in the mouse embryo

At the morula stage, when the mouse embryo consists of a ball of about 16 cells, the outer cells express *Cdx2* and develop epithelial characteristics (Strumpf *et al.*, 2005), these cells become the trophectoderm. This trophectoderm forms numerous extra-embryonic tissues in later in development including the extra-embryonic ectoderm and the ectoplacental cone (Downs and Davies, 1993). The inner cells of the embryo form the ICM which gives rise to all embryonic and some extra-embryonic tissues (Smith, 2005).

At around E4.0 to E4.25 the outer layer of the ICM facing the blastocoelic cavity differentiates to from the primitive endoderm which contributes cells to form the parietal endoderm. These cells migrate over the blastocoelic surface and, together with the trophoblast will, later in differentiation, form the parietal yolk sac which secretes a basement membrane to form Reichert's membrane (Salamat *et al.*, 1995).

At E5.0 the ICM forms epiblast which maintains expression of genes that are characteristic of pluripotent cells such as *Pou5f1*, *Sox2*, *Nanog* and *Sall4*. At the same time, the polar trophectoderm cells differentiate to extra-embryonic ectoderm

and remaining primitive endoderm differentiates to form visceral endoderm which surrounds the embryo and will eventually provide contribute to the visceral endoderm lining of the extra-embryonic yolk sac (Lawson and Pedersen, 1987).

At E5.5 the remaining polar trophectoderm forms the ectoplacental cone and the familiar 'egg cylinder' shape is formed. The egg cylinder consists of the extra-embryonic ectoderm formed from the trophectoderm surrounded by extra-embryonic visceral endoderm at the proximal end (top) of the egg cylinder and the embryo proper at the distal end (bottom) as shown in Figure 1-4A. The embryo proper acquires the shape of a cup made of two layers, an outer layer of visceral endoderm and an inner layer of epiblast. Both the extra-embryonic ectoderm and epiblast surround the proamniotic cavity (Tam and Behringer, 1997). At this time-point the proximal-distal patterning of the epiblast occurs (Beddington and Robertson, 1999, Lu et al., 2001). At E.6.0, anterior-posterior patterning of the embryo occurs (Perea-Gomez et al., 2004), as shown in Figure 1-4B. At E6.5, gastrulation commences with the formation of the primitive streak on the posterior side of the embryo. The epiblast cells then undergo an epithelial to mesenchymal transition, ingress via morphogenetic cell movements and migrate along the outer surface towards the anterior pole to form mesoderm and endoderm (Figure 1-4C). At E7.5 mesodermal cell types become patterned to their respective fates and endoderm and the node are formed (Figure 1-4D). These two tissues and the ectoderm, the descendents of epiblast cells that do not pass through the primitive streak, constitute the three primary germ layers that contain progenitors of all embryonic tissues as well as the extra-embryonic mesoderm of the yolk sac, the allantois and the amnion (Tam and Behringer, 1997, Loebel et al., 2003, Tam and Loebel, 2007, Ang and Constam,

2004). A diagram of the relationships between cell types in mouse development is

provided in Figure 1-5.
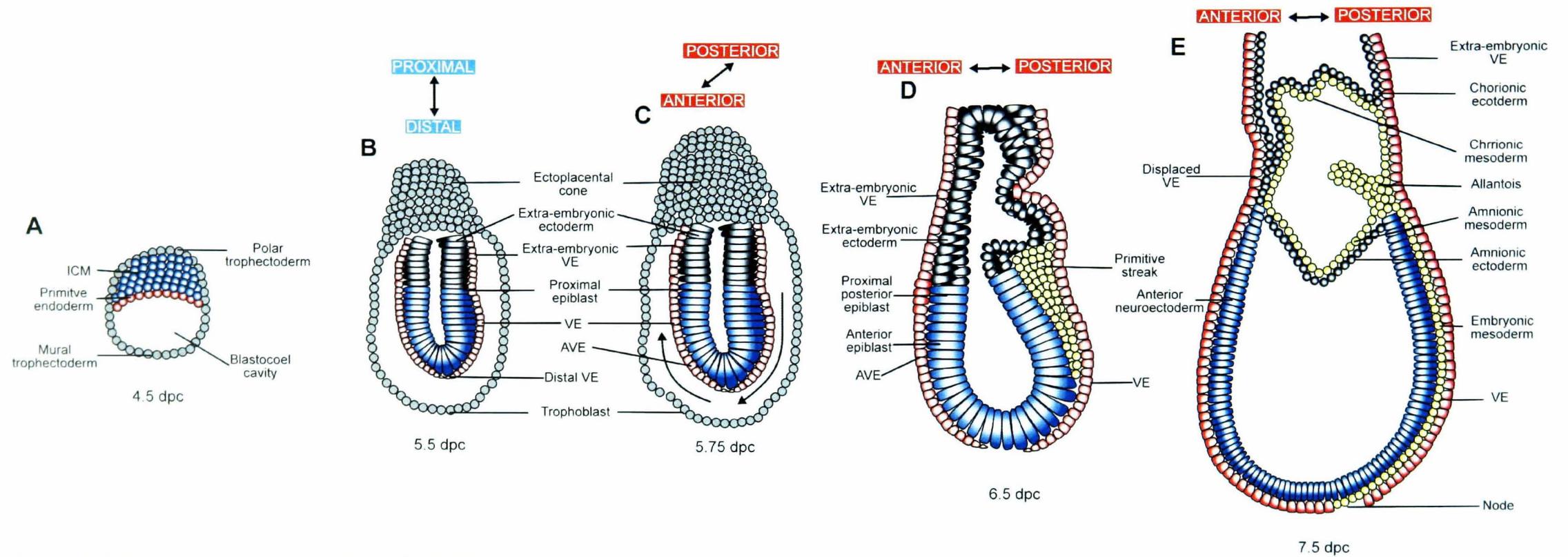
Figure 1-4: Lineage formation within the E4.5-E7.5 mouse embryos

A) E5.5, ICM (blue cells) and primitive endoderm formation (red cells). B) E5.5, visceral endoderm, extra-embryonic ectoderm (black cells) and epiblast formation (blue cells). C) E5.75, movement of the visceral endoderm. D) E6.5, primitive streak formation. E) E7.5, continued development of the primitive streak and embryonic and extra-embryonic mesoderm formation. ICM, inner cells mass; VE, visceral endoderm; AVE, anterior visceral endoderm. Diagram adapted from Lu *et al.*, (2001).

65
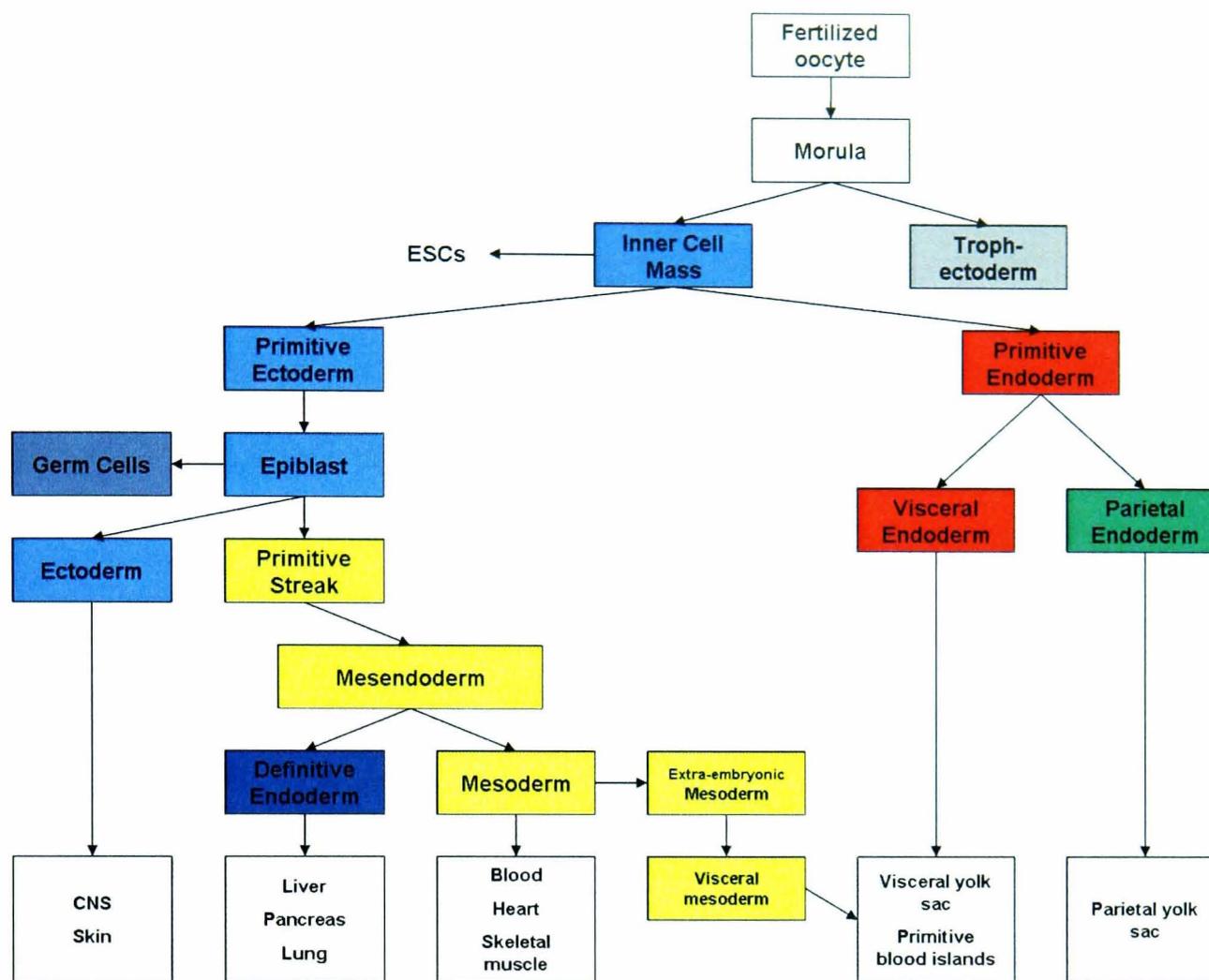
Figure 1-5: Relationships between cell lineages during mouse development

1.3.2 Signalling in gastrulation

To generate the primitive streak on one side of the embryo, the embryo must have established proximal-distal and anterior-posterior axis prior to gastrulation (reviewed by Lu *et al.*, 2001). The processes that establish these asymmetries are now understood well enough for a gene network of the interactions involved to be formed (Ang and Constam, 2004, Tam and Loebel, 2007) and are reviewed below.

1.3.2.1 *Nodal establishes the proximal-distal axis*

NODAL signalling from the epiblast are responsible for the establishment of the proximal-distal axis (Brennan *et al.*, 2001). *Nodal* is expressed throughout the epiblast and visceral endoderm at early post-implantation stages (Varlet *et al.*, 1997). *Nodal*$^{-/-}$ embryos arrest shortly before gastrulation and fail to establish a primitive

streak (Conlon *et al.*, 1994). NODAL is first detected in the ICM and primitive endoderm at E4.5. Up to E5.5 NODAL has a role in maintaining the expression of pluripotency markers *Pou5f1* and *Nanog* as well as *Tdgf1* (previously known as *Cripto*) and *Foxd3* in the ICM/Epiblast (Mesnard *et al.*, 2006).

At E4.5-5.5 NODAL also has as role in patterning the embryonic and the extra-embryonic visceral endoderm. At E4.5, *Furin*, a convertase enzyme that cleaves the NODAL precursor to form mature NODAL, is also expressed along with NODAL in the primitive endoderm. At E5.0, the distal primitive endoderm has become the embryonic visceral endoderm and the cleaved mature NODAL induces the up-regulation of *Lhx1*, *Fgf5*, *Fgf8*, *Otx2* and *FoxA2*. At E5.5 NODAL signals from the epiblast maintain the expression of *Gata4*, *Hnf4a*, *Ttr* and in extra-embryonic visceral endoderm whilst they and *Furin* are down-regulated in the embryonic visceral endoderm (Mesnard *et al.*, 2006), see Figure 1-6A.

NODAL precursor acts in the extra-embryonic ectoderm via ACRV1A and ACRV2A to activate the transcription of *Furin* along with an additional convertase enzyme, *Pcsk6* (Beck *et al.*, 2002, Ben-Haim *et al.*, 2006). The extra-embryonic ectoderm then secretes these convertase enzymes into the epiblast then which cleave the NODAL precursor to form mature NODAL (Beck *et al.*, 2002). NODAL then amplifies the expression of the co-ligand, TDGF1 (Yan *et al.*, 2002, Beck *et al.*, 2002). An additional transforming growth factor family member, GDF1, is also expressed in the epiblast and signals through a similar pathway to NODAL (Chen *et al.*, 2006a). The NODAL signalling through SMAD2/SMAD3 also activates an autoinductive feedback loop mediated by the transcription co-activator, FOXH1 (Dunn *et al.*, 2004), see Figure 1-6B.

At E5.5, a subset of visceral endoderm at the distal tip of the embryo responds to NODAL-SMAD2 signalling by expressing a specific repertoire of genes (Mesnard *et al.*, 2006, Brennan *et al.*, 2001) including *Hhex* (Thomas *et al.*, 1998) and the NODAL antagonists, *Lefty1* (Perea-Gomez *et al.*, 1999) and *Cer1* (Belo *et al.*, 1997).

TGFB1/activin/NODAL receptors ACRV1B (activin receptor A receptor, type 1B) and ACRV2A (activin receptor A receptor, type 2A) are essential for egg cylinder organisation and *Acrv1b$^{-/-}$* or *Acrv2a$^{-/-}$* embryos show a developmental arrest before gastrulation (Gu *et al.*, 1998, Song *et al.*, 1999) despite the demonstration that activin A and activin B are both dispensable for gastrulation and embryos develop to term with no gross defects in mesoderm formation or patterning (Matzuk *et al.*, 1995).

The combination of a proximally localised source of the NODAL activating *Furin* and *Pcsk6* from the extra-embryonic ectoderm (Beck *et al.*, 2002) and expression *Lefty1* and *Cer1* at the distal/anterior end of the embryo (Perea-Gomez *et al.*, 2002) result in a proximal-distal gradient of NODAL signalling with highest expression at the extra-embryonic/epiblast boundary (Lu and Robertson, 2004), see Figure 1-6C.
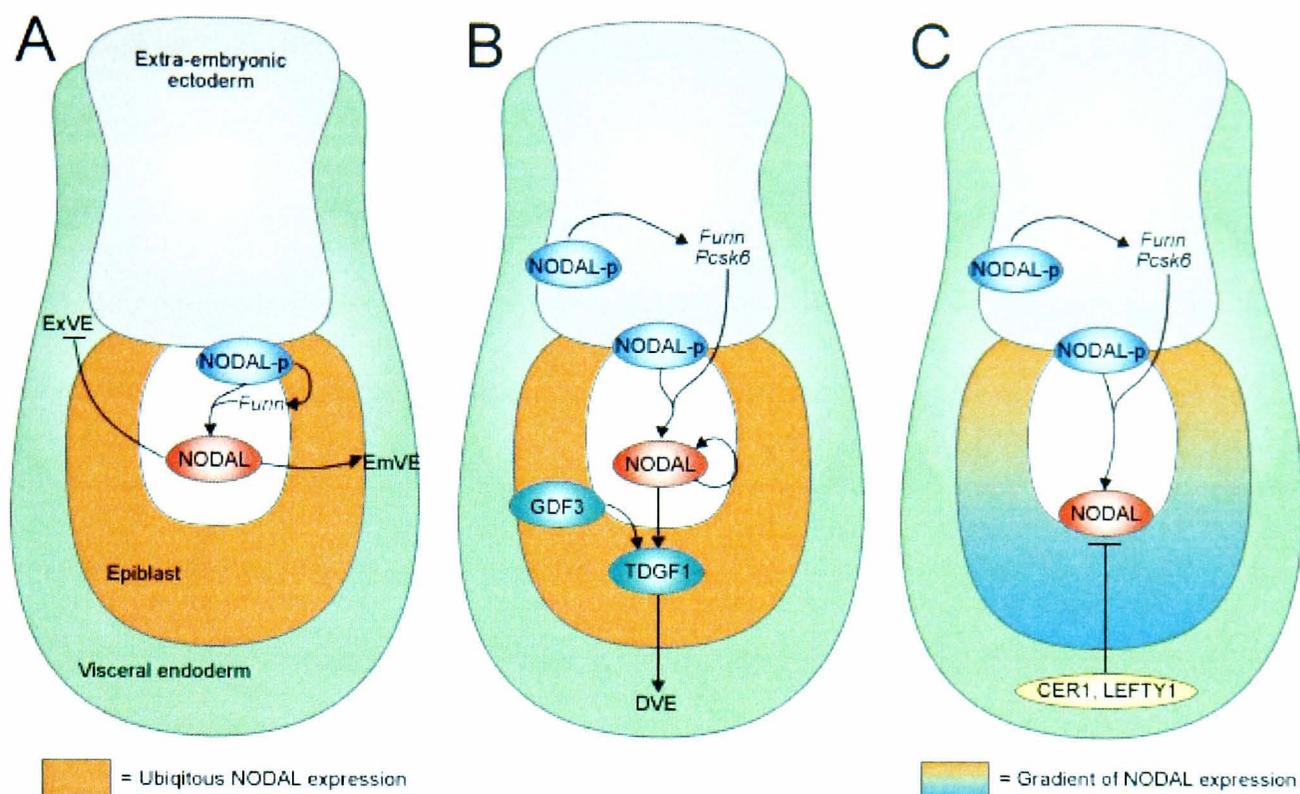
Figure 1-6: Establishment of the proximal-distal gradient by NODAL during E5.0 to E5.5

A) E5.0, NODAL precursor protein activates the transcription of *Furin* which cleaves the NODAL precursor protein to produce the processed form of NODAL. NODAL signals from the epiblast repress the expression of genes such as *Hnf4a*, *Gata4*, *Ttr* (*transthyretin*) and *Furin* in the extra-embryonic visceral endoderm (ExVE). Simultaneously, in the embryonic visceral endoderm (EmVE) NODAL signals up-regulate the expression of *Lhx1*, *Fgf5*, *Fgf8*, *Bmp2*, *Otx2* and *FoxA2*.

B) E5.25, NODAL precursor protein from the epiblast acts in the extra-embryonic ectoderm to activate the transcription of *Furin* and *Pcsk6*, by signalling activin receptors 1B and 2A (ACRV1B and ACRV2A). NODAL and GDF3, working with a co-receptor TDGF1, specifies the distal visceral endoderm (DVE).

C). E5.5, The graded signalling of processed NODAL from the epiblast/extra-embryonic boundary is additionally antagonised by LEFTY1 and CER1 from the DVE to create the proximal-distal gradient. Diagram adapted from Tam *et al.*, (2007).

1.3.2.2   *BMP4 and inductive signals from the extra-embryonic ectoderm*

Along with roles in epiblast patterning, NODAL also patterns the extra-embryonic ectoderm through SMAD2 independent pathways (Brennan *et al.*, 2001). NODAL precursor maintains *Bmp4* expression in extra-embryonic ectoderm adjacent to the epiblast (Brennan *et al.*, 2001, Ben-Haim *et al.*, 2006), see Figure 1-7A. *Bmp4⁻* embryos fail to gastrulate and have severe deficiencies of mesoderm (Winnier *et al.*,

1995). Loss of BMPR1 and BMPR2 function also results in reduced epiblast proliferation and no formation of mesoderm (Mishina *et al.*, 1995, Beppu *et al.*, 2000).. BMP4 signalling induces *Wnt3* which amplifies mesoderm expression in the epiblast and mediates the induction of mesoderm (Liu *et al.*, 1999). *Wnt3* is expressed at the proximal epiblast and the adjacent proximal visceral endoderm at E5.0 and subsequently becomes restricted to the posterior epiblast and posterior visceral endoderm (Liu *et al.*, 1999, Rivera-Perez and Magnuson, 2005). *Wnt3*^{-/-} embryos develop a normal egg cylinder but do not form a primitive streak (Liu *et al.*, 1999). Embryos lacking the WNT co-receptors LRP5 and LRP6 also fail to establish a primitive streak (Kelly *et al.*, 2004). The expression of WNT target genes is regulated by nuclear β-catenin that is bound to transcription factors of the LEF/TCF family activation of β-catenin (Morkel *et al.*, 2003). Non-phosphorylated β-catenin is expressed in the extra-embryonic visceral endoderm and subsequently the anterior/proximal epiblast and primitive streak (Mohamed *et al.*, 2004). *Catnb*^{-/-} (which encodes β-catenin) embryos have a lack of node formation, axis truncation and diversion of definitive endoderm to mesodermal fate (Lickert *et al.*, 2002). Similar to NODAL, one downstream target of BMP4/WNT/β-catenin is *Tdgf1* (Beck *et al.*, 2002, Morkel *et al.*, 2003). This forms a positive feedback loop as WNT3 is necessary to maintain normal expression of NODAL (Liu *et al.*, 1999).

FGF4 expression is also dependent on NODAL signalling (Ang and Constam, 2004). FGF4 is expressed in the epiblast and subsequently the prospective primitive streak (Niswander and Martin, 1992). FGF4 acting through FGFR2 and ERK2 sustains the proliferation of undifferentiated trophoblast stem cells that express *Eomes* and *Bmp4* (Ang and Constam, 2004). FGF4 also maintains *Hnf4a* expression in the visceral endoderm maintaining its identity (Goldin and Papaioannou, 2003).

1.3.2.3   Anterior visceral endoderm and anterior-posterior patterning

Around E5.5, the distal visceral endoderm (DVE) cells migrate up the anterior portion of the embryo to from the AVE (Thomas and Beddington, 1996), see Figure 1-7B. Recently, *Lefty1* has been demonstrated to be expressed asymmetrically as early as E4.25. *Lefty1* expressing cells are located closer to one pole of the long axis of the blastocyst and this asymmetric expression pattern is induced by transient NODAL signalling and does not rely on any embryo-uterus interaction (Takaoka *et al.*, 2006). NODAL signalling is symmetric along the anterior–posterior axis at E5.5 and E5.7, the latter being the time when DVE cells begin to migrate to the AVE (Yamamoto *et al.*, 2004), therefore the asymmetric expression of *Lefty1* may be the first step towards the anterior-posterior patterning of the embryo (Takaoka *et al.*, 2007). A role for WNT signalling has also been described in distal visceral endoderm (DVE) formation and embryos that lack *Ctnnb1* (as above) or APC (adenomatous polyposis coli protein, which modulates canonical WNT signalling) result in impaired DVE formation owing to defective proximal-distal regionalisation of the visceral endoderm (Huelsken *et al.*, 2000, Chazaud and Rossant, 2006).

AVE precursors cells actively migrate by continuously changing shape and projecting filopodial processes in their direction of motion (Srinivas *et al.*, 2004). AVE precursors also migrate towards the site of elevated *Cer1* and *Lefty1* expression and away from the site of ectopic NODAL activity (Mesnard *et al.*, 2006). It is proposed that the inhibition of NODAL signals reduce cell proliferation on one side of the embryo, leading to an asymmetric accretion of cells that may also provide a propulsive force on the DVE population (Yamamoto *et al.*, 2004). The AVE expresses genes such as *Gsc* (Filosa *et al.*, 1997), *Otx2* (Ang *et al.*, 1994), *Hex* (Thomas *et al.*, 1998), *Lhx1* (Perea-Gomez *et al.*, 1999), *Fox.12* (Filosa *et al.*, 1997),

Cer1 (Belo *et al.*, 1997), *Dkk1* (Glinka *et al.*, 1998), *Nodal* and *Lefty* (Mesnard *et al.*, 2006). *Otx2* has been demonstrate to have a role in the movement of the DVE to the AVE and in *Otx2⁻/⁻* embryos a proliferation of visceral endoderm is not affected but the morphogenetic movement of the visceral endoderm and the expression of *Lefty1* and *Dkk1* are ablated (Perea-Gomez *et al.*, 2001).

Cer1, *Lefty1*, *Dkk1*, *Srfp1*, *Srfp2* act to restrict NODAL and WNT signalling to the posterior of the embryo (Kimura *et al.*, 2000, Perea-Gomez *et al.*, 2002, Yamamoto *et al.*, 2004, Kemp *et al.*, 2005) and maintain the competence of the anterior epiblast to react to neural inducing signals (Rossant *et al.*, 2003, Tam and Steiner, 1999). Formation of the AVE requires *Smad2* (Brennan *et al.*, 2001) or both *FoxA2* and *Lhx1* (Perea-Gomez *et al.*, 1999) in the visceral endoderm. AVE migration is abolished in embryos lacking *Tdgf1* (Lu *et al.*, 2001).

In addition to signals from within the visceral endoderm, signals from the prospective posterior part of the extra-embryonic ectoderm have been shown to be responsible restricting the size of the AVE. Removal of the extra-embryonic ectoderm results in an expansion of the *Cer1* expression domain which can be counteracted by posterior extra-embryonic cells transplanted to the vicinity of the AVE precursors (Richardson *et al.*, 2006).
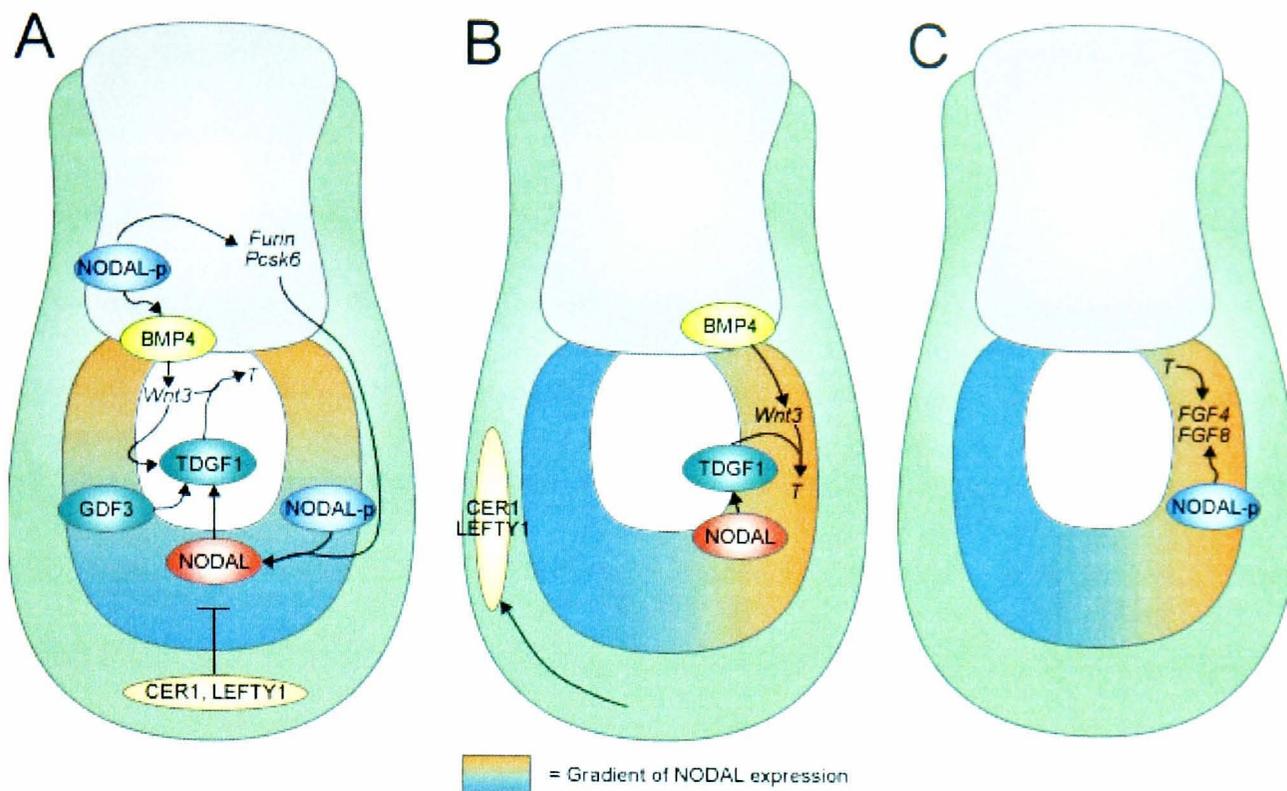
Figure 1-7: BMP4 and FGF signalling in the mouse embryo during E6.0 to E6.5

A) E6.0, BMP4 signalling from the extra-embryonic ectoderm activates a regulatory pathway involving WNT3 which activates *T* expression initially near the epiblast/extra-embryonic ectoderm boundary.

B) E6.25, Movement of the *Cer1* and *Lefty1*-expressing AVE to the anterior side of the embryo establishes an anterior/posterior gradient and the primitive streak forms on the posterior side of the embryo.

C) E6.5, Expression of *Fgf4* and *Fgf8*, which is downstream of T and is enhanced by the activity of the NODAL precursor protein, maintains the mesoderm and cells move through the primitive streak. Diagram adapted from Tam *et al.*, (2007).

1.3.2.4 FGF4, FGF8 and epithelial to mesenchymal transition

At the same time as the DVE moves to the AVE on the anterior side of the embryo, on the opposite side, expression of markers such as *Nodal* and *Wnt3* progress down the posterior side (Lu *et al.*, 2001) see Figure 1-7C. The expression of numerous genes is restricted to the posterior epiblast prior to gastrulation in addition to *Nodal* and *Wnt3* including *T* (Wilkinson *et al.*, 1990), *Mixl1* (Pearce and Evans, 1999), *Eomes* (Ciruna and Rossant, 1999) and *Gsc* (Blum *et al.*, 1992). Subsequently, genes such as *Evx1* (Dush and Martin, 1992), *Fgf4* (Niswander and Martin, 1992), and *Fgf8*

(Sun *et al.*, 1999) are expressed in the developing primitive streak. In chimeric embryos containing *Nodal*$^{-/-}$ mESCs, the *Nodal*-deficient cells preferentially populate the anterior compartment of the epiblast, suggesting that cell mixing in the epiblast is not random and NODAL signalling mediates a cell-sorting process within the epiblast before gastrulation (Lu and Robertson, 2004). Clonal analysis shows that epiblast cells are not restricted to their lineage potency prior to recruitment and ingression (Lawson and Pedersen, 1992). NODAL signalling through SMAD2/SMAD3 pattern the middle primitive streak derivatives (Dunn *et al.*, 2004) and selective loss of *Smad2* in the epiblast results in a failure to specify the anterior mesoderm and endoderm (Vincent *et al.*, 2003). NODAL can directly up-regulate some genes such as *Mixl1* which is strongly responsive through SMAD2/SMAD4 or SMAD3/SMAD4 and FOXH1 (Hart *et al.*, 2005). The positive feedback loop with WNT/β-catenin also up-regulates targets including *T, Tdgf1, Evx1* and *Fgf8* (Morkel *et al.*, 2003). *Eomes* is required for the expression of *T, Fgf8, Wnt3* and other proximal-posterior genes (Russ *et al.*, 2000). In addition maintenance of *T* expression in the primitive streak is required for paraxial mesoderm formation *and* in *Wnt3a*$^{-/-}$ embryos *T* expression is completely absent from the anterior half of the primitive streak suggesting expression of WNT3A is required for maintenance of *T* expression (Yamaguchi *et al.*, 1999, Arnold *et al.*, 2000).

FGFs control the specification of and maintenance of mesoderm rather than primary mesoderm induction (Burdsal *et al.*, 1998, Ciruna and Rossant, 2001). Mutational analysis of the known *Fgf* genes have demonstrated that only *Fgf4* and *Fgf8* are required for early embryonic development (Niswander and Martin, 1992, Crossley and Martin, 1995, Ciruna and Rossant, 2001). *Fgf8*$^{-/-}$ embryos fail to express *Fgf4* in the primitive streak and in the albescence of both FGF8 and FGF4 epiblast cells

move into the primitive streak and undergo a epithelial to mesenchymal transition but then fail to move away from the primitive streak (Sun *et al.*, 1999) FGFR1 is expressed throughout the epiblast prior to gastrulation and becomes restricted to the posterior/primitive streak as gastrulation proceeds (Yamaguchi *et al.*, 1992). FGFR1 has a role in mesoderm cell fate and is required for *T* and *Tbx6*, a marker of paraxial mesoderm (Chapman *et al.*, 2003), expression in the primitive streak. FGFR1 orchestrates the epithelial to mesenchymal transition at the primitive streak by up-regulating *Snail* which functions to repress *Cdh1*. FGFR1 also functions indirectly in mesoderm/endoderm cell fate specification, since down-regulation of *Cdh1* (which has a potent ability to sequester β-catenin) allows the WNT/β-catenin pathway to positively regulate *T* and *Tbx6* expression (Ciruna and Rossant, 2001).

1.3.2.5 Mesendodermal cell types

Mesendoderm (also sometimes referred to as endomesoderm) is a bipotent precursor cell of both the mesodermal and definitive endodermal lineages (Rodaway and Patient, 2001). Not all mesoderm is derived from the mesendoderm; non-mesendodermal mesoderm cells are predominantly fated to form somitic tissue/body muscle, whilst mesendodermal mesoderm is fated to become lineages such as blood and heart (Warga and Nusslein-Volhard, 1999). The presence of mesendoderm in zebrafish has been demonstrated lineage tracing (Warga and Nusslein-Volhard, 1999) and by the co-expression of the zebrafish mesendoderm marker, *t*, and the endoderm marker, *gata5* (Rodaway *et al.*, 1999). The presence of mesendoderm in *Xenopus* has similarly been demonstrated lineage tracing (Nieuwkoop, 1997) and by the co-expression of the *Xenopus* mesoderm marker, t, and the mesendoderm marker, mix1 (Lemaire *et al.*, 1998). Characterisation of mesendoderm in the mouse embryo is still unclear (Tada *et al.*, 2005) but the close proximity of mesoderm and endoderm

formation in the primitive streak supports the concept established in the other model systems that these lineages are generated from a bipotent population (Kimelman and Griffin, 2000).

The presence of mESC-derived mesendoderm has been identified by the production of endodermal cell types from T^+ cell populations that also display mesoderm potential (Kubo *et al.*, 2004) and, more specifically, by the isolation of a $GSC^+CDH1^+PDGFRA^+$ expressing population (markers for mesendoderm, mesoderm and endoderm respectively) that subsequently diverges to $GSC^+CDH1^+PDGFRA^-$ and $GSC^+CDH1^-PDGFRA^+$ intermediates that eventually differentiate to endoderm and mesoderm lineages respectively (Tada *et al.*, 2005). As yet the presence of mesendoderm in humans or from hESCs has not been verified.

1.3.2.6   Patterning of the primitive streak

Fate mapping studies demonstrate in the mouse embryo that the order of and the site of progenitor cell ingression through the primitive streak will determine the fate of the mesendodermal cell types (Tam and Beddington, 1987, Kinder *et al.*, 1999). Once the primitive steak is formed over the next 12-24 hr the streak elongates from the rim of the cup to its distal tip. Here at the anterior end of the primitive streak specialised organiser structures form progressively, known as the early gastrula organiser (EGO), mid gastrula organiser (MGO) and the node (Kinder *et al.*, 2001). The EGO and the MGO generate the axial mesendoderm, which comprises of the mesoderm which will populate the midline of the embryo (prechordal plate and notochord) and the definitive endoderm (which forms the gut tube, lungs and organs including the liver, pancreas and thyroid). Until the node forms (and hence the definitive gut endoderm) the embryo is encased in visceral endoderm. The posterior end of the streak gives rise to the extra-embryonic mesoderm (which forms the yolk

sac vasculature and blood), while the lateral plate mesoderm (which forms the circulatory system and the gut wall) and paraxial mesoderm (which forms the somites, the vertebral column and the skeletal muscle) emerge from the intervening levels of the streak (Kinder *et al.*, 1999, Beddington and Robertson, 1999, Tam *et al.*, 2007).

The formation of different populations of mesoderm and endoderm depends on the expression intensity, duration and locations of NODAL and WNT signalling activity in the primitive streak (Ben-Haim *et al.*, 2006). Loss of NODAL signalling leads to the absence of anterior primitive streak derivatives such as the axial and paraxial mesoderm and the definitive endoderm (Hoodless *et al.*, 2001, Beck *et al.*, 2002, Yamamoto *et al.*, 2004). Elevation of NODAL signalling (due to the loss of the transcription of a co-repressor or expression of a NODAL antagonist) results in the over-expression of mesodermal markers (Meno *et al.*, 1999, Perea-Gomez *et al.*, 2002). Whether the gradient of NODAL activity exists in the primitive streak is still not known (Tam and Loebel, 2007).

1.3.3 Summary

hESCs, when given the necessary cues, can be induced to differentiate as a population towards a specified lineage, although current methods for hESC differentiation result in poor yields of the desired lineages. hEB formation is currently one of the most successful methods for hEB differentiation and, although the process of differentiation is poorly understood in hEBs, it is well understood in mEBs. Given that hESCs represent early embryonic cells, the same mechanisms that regulate differentiation in the embryo should also regulate differentiation in hESCs. Using the mouse and *Xenopus* embryos as models for human development, factors that induce mesoderm formation *in vivo* may prove useful to improve the differentiation of hESCs to mesoderm and therefore provide the greatest population of cells capable of differentiating towards terminally differentiated mesodermal cell types.

1.3.4 Thesis aims and objectives

The specific aims and objectives of this thesis are:

- To identify methods for mesoderm induction in *Xenopus laevis* and apply them to hESCs.

- To devise a system to standardise the initiation of differentiation of hESCs by controlling hEB formation suitable for use in a high throughput manner.

- To develop methods for increasing the proportion of mesoderm lineage cells differentiated from hESCs using simple, optimised treatments.

- To assess the effectiveness of this system in four hESC lines and identify any inter-line variation.

- To develop a standard spatial and temporal map of hEB differentiation and compare to hEBs treated with growth factors.

2 IDENTIFYING PUTATATIVE MECHANISMS OF MESODERM INDUCTION AND BLOOD DEVELOPMENT IN *XENOPUS LAEVIS*

2.1 INTRODUCTION

To improve the efficiency of mesoderm induction and blood development from hESCs, by mimicking the *in vivo* development of these lineages, we must understand the network of factors that direct this differentiation. Mesoderm induction and blood development have been intensely studied in the African clawed frog *Xenopus laevis* (Kofron *et al.*, 1999). Despite differences in morphology between mammalian and non-mammalian species, the major growth factor signalling pathways and transcription factor networks in development are largely conserved (reviewed by Kimelman, 2006) and therefore a valid cross-species comparison can be made. In addition, *Xenopus* embryos are externally fertilised and comparatively large which makes them particularly suited for micromanipulation. That they are also able translate synthetic, injected mRNA has considerably facilitated higher throughput gene function studies than is possible in mammals (Harland and Misher, 1988).

2.1.1 Mesoderm induction in *Xenopus*

Similar to mesoderm induction in the mouse embryo, families of signalling molecules regulate the various stages *Xenopus* mesoderm induction. The NODAL family is involved in mesoderm initiation, FGFs and WNTs are involved in maintaining the mesoderm state and BMPs are involved in patterning the mesoderm. However, numerous experimental models have demonstrated that ectopically expressed FGFs, WNTs and BMPs are capable of promoting mesodermal differentiation (reviewed by Kimelman, 2006).

The *Xenopus* oocyte is visibly divided into two parts; a lower lightly pigmented vegetal hemisphere and an upper darkly pigmented animal hemisphere (Figure 2-1A).
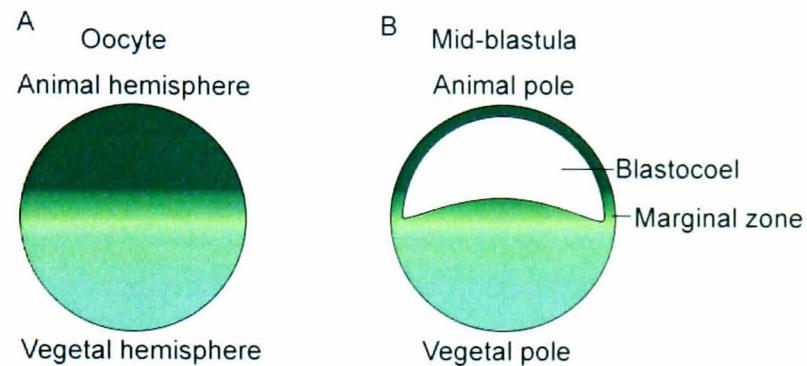
Figure 2-1: *Xenopus* oocyte and mid-blastula embryo

At fertilisation the T-box transcription factor VEGT (also known as BRAT) diffuses upwards from but is restricted to the vegetal hemisphere by the third, equatorial, cleavage plane and inherited equally by all vegetal cells (reviewed by Heasman, 2006). As development proceeds VEGT activates the expression of nodal5, nodal6 (previous known as Xnr5 and Xnr6) and gdf3a (previously known as derrière) in a pathway that requires β-catenin/TCF3 signalling (Rex *et al.*, 2002). In turn nodal 1, nodal2 and nodal4 (previously known as Xnr1, Xnr2 and Xnr4) are activated (Clements *et al.*, 1999, Takahashi *et al.*, 2000, Onuma *et al.*, 2002). This NODAL signalling from the vegetal blastomeres induces a broad band of cells in the region midway between the animal and vegetal poles (the equatorial marginal zone) to adopt a mesodermal fate (reviewed by Kimelman, 2006).

2.1.2 Mesoderm induction in the animal cap assay

After fertilisation eleven rapid cell divisions follow that divide the embryo into a ball of 4096 cells, called the mid-blastula. The mid-blastula has a large fluid filled cavity (the blastocoel) in the animal hemisphere (Figure 2-1B). Mid-blastula cells have been shown to be pluripotent, demonstrated by the implantation of labelled cells

from vegetal pole into the blastocoel and subsequent contribution to all three germ layers (Heasman *et al.*, 1984). Without additional signalling dissected explants from the animal pole (known as the animal cap) form ectodermal derivatives in culture, explants from the equatorial region form mesoderm and explants from the vegetal pole form endoderm (reviewed by Heasman, 2006). The addition of exogenous factors to the pluripotent *Xenopus* animal cap explants can direct the differentiation to each of the three germ layers (reviewed by Okabayashi and Asashima, 2003), making this system an useful, well characterised model for the differentiation of hESCs.

As with the mouse embryo, the *Xenopus* embryos has two mesodermal populations that contribute to haematopoiesis: dorsal mesoderm (analogous to the embryonic mesoderm in the mouse) that gives rise to the dorsal lateral plate (DLP) mesoderm (analogous to the P-Sp/AGM in the mouse) and definitive haematopoiesis; and the ventral mesoderm (analogous to extra-embryonic mesoderm in the mouse) that gives rise to the ventral blood island (VBI, analogous to the extra-embryonic blood islands in the mouse) and primitive haematopoiesis (Kau and Turpen, 1983, Ciau-Uitz *et al.*, 2000) as shown in Figure 2-2.
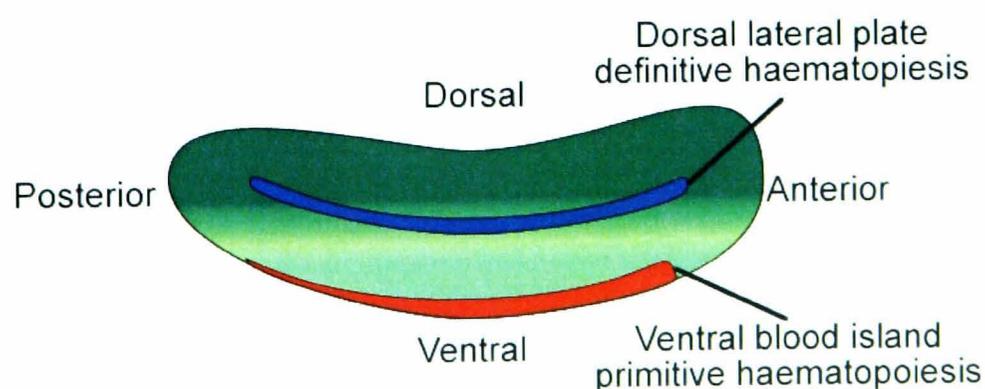
Figure 2-2: Axis of the *Xenopus* embryo and positioning of the dorsal lateral plate and ventral blood island

Numerous factors have been demonstrated to have the potential to induce *Xenopus* animal caps to differentiate towards mesoderm and mesodermal lineages including: BMP4 (Dale *et al.*, 1992); FGF4 (previously known as eFGF, Slack, 1994); and activin A (Ariizumi *et al.*, 1991).

Animal caps from mid-blastula embryos micro-injected with high concentrations of bmp4 mRNA at the 1-cell stage differentiate to ventral mesoderm, and can express globin mRNA suggesting that BMP4 signalling can directly induce pluripotent cells to differentiate to mesoderm and subsequently erythrocytes (Dale *et al.*, 1992). Ectopic expression of bmp4 mRNA in the developing *Xenopus* embryo results in ventralisation, that is characterised by a lack of a notochord, decreased muscle formation, and increased blood formation (Dale *et al.*, 1992, Jones *et al.*, 1992). Ectopic expression of bmp4 in the embryo is thought not to effect the initial steps of mesoderm induction, either dorsal or ventral, but instead causes ventralisation during gastrulation to promote ventral mesoderm and attenuate dorsalising signals (Jones *et al.*, 1996). Interference of BMP4 signalling with either a dominant negative BMP receptor (mRNA that encodes a truncated BMP receptor that blocks the BMP signalling pathway) or using antagonists, such as NOG (noggin) or CHRD (chordin), results in dorsalisation of the embryo with decreased blood formation (Maeno *et al.*, 1994, Piccolo *et al.*, 1996).

fgf4 mRNA is expressed maternally and is known to be present at the stage of mesoderm induction (Isaacs *et al.*, 1992). FGF4 is involved in the establishment and maintenance of mesoderm through a positive feed back loop with T (brachyury, Isaacs *et al.*, 1994, Casey *et al.*, 1998). Inhibition of FGF4 signalling in whole embryos by a dominant negative FGF receptor results in disruption of the movements of gastrulation (Isaacs *et al.*, 1994). In animal caps, ectopic expression of

fgf4 mRNA results in the formation of ventral mesoderm and FGF4 has been demonstrated to be a substantially more potent inducer of mesoderm than FGF2. (Isaacs *et al.*, 1994).

Activin mRNAs and proteins are uniformly distributed throughout the embryo until after mesoderm induction (Dohrmann *et al.*, 1993) and, although this uniform distribution could be transformed into an activity gradient by positive or negative regulators, there is no evidence of such (McDowell and Gurdon, 1999). Therefore activin is not thought to induce mesoderm *in vivo*. However, animals caps cultured in the presence of activin been demonstrated to respond in a concentration dependent manner with lower concentrations of activin (0.1-1 ng ml^{-1}) promoting the differentiation to ventral mesoderm and higher concentrations (5+ ng ml^{-1}) resulting in more dorsal types of mesoderm (reviewed by Okabayashi and Asashima, 2003).

2.1.3 Transcription factor complexes in haematopoietic development

One transcription factor known to play an important role in haematopoiesis is T-cell acute lymphocytic leukemia 1 (TAL1, previously known as SCL). TAL1 is a basic helix-loop-helix transcription factor identified via chromosome translocation of chromosome 1p32 of in T-cell acute lymphoblastic leukaemia (Begley *et al.*, 1989, Aplan *et al.*, 1990, Begley *et al.*, 1991, Visvader and Begley, 1991). In *Xenopus* embryos, tal1 is expressed in the VBI and DLP (Mead *et al.*, 1998, Walmsley *et al.*, 2002), and gene targeting in the mouse experiments have demonstrated an essential role in both primitive and definitive haematopoiesis as well as vasculogenesis (Shivdasani *et al.*, 1995, Robb *et al.*, 1995, Porcher *et al.*, 1996, Visvader *et al.*, 1998). *Tal1*$^{-/-}$ mouse embryos die at E9.5 due to the complete lack of primitive and definitive haematopoiesis (Robb *et al.*, 1995, Shivdasani *et al.*, 1995). *Tal1*$^{-/-}$ mESCs

do not contribute to either primitive or definitive haematopoiesis in chimeric mice (Porcher *et al.*, 1996).

Using a mouse erythroleukaemia cells it has been demonstrated that TAL1 can form complexes with other transcription factors such as LIM-only protein-2 (LMO2, previously known as RBTN2, Osada *et al.*, 1995). LMO2 is a member of the LIM only class of LIM zinc finger proteins and was identified via chromosome translocation of chromosome 11p13 of in T-cell acute lymphoblastic leukaemia (Boehm *et al.*, 1991, Royer-Pokora *et al.*, 1991). In the *Xenopus* embryo, lmo2 is expressed in the VBI and DLP (Mead *et al.*, 2001). As with $Tal1^{-/-}$ mouse embryos, $Lmo2^{-/-}$ mouse embryos die at E9.5 due to the complete lack of primitive and definitive haematopoiesis and $Lmo2^{-/-}$ mESCs do not contribute to either primitive or definitive haematopoiesis in chimeric mice (Yamada *et al.*, 1998).

In mouse erythroleukaemia cells LMO2 can form a bridging complex between TAL1 and GATA1 (Osada *et al.*, 1995). The GATA family all have two zinc finger domains and bind the DNA sequence GATA (Weiss and Orkin, 1995). In *Xenopus* embryos gata1 is expressed in the VBI (Kelley *et al.*, 1994). $Gata1^{-/-}$ mouse embryos die at E11.5 due to anaemia caused by the complete lack of mature erythrocytes (Weiss *et al.*, 1994). In chimeric mice $Gata1^{-/-}$ mESCs do give rise definitive erythroid progenitors but $Gata1^{-/-}$ erythroid cells arrest at the proerythroblast stage (Pevny *et al.*, 1991, Weiss *et al.*, 1994).

Along with the LIM binding protein, LDB1, that binds LMO2 (Agulnick *et al.*, 1996, Jurata *et al.*, 1996) and the ubiquitously-expressed E protein bHLH transcription factors encoded by tcfe2a (Wadman *et al.*, 1997), TAL1, LMO2 and GATA1 can form the transcription factor complex shown below (Figure 2-3).
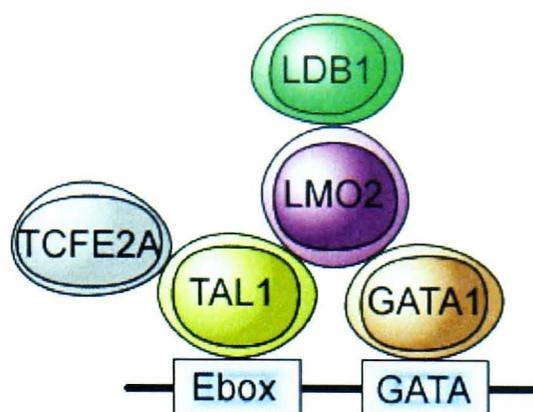
Figure 2-3: TAL1, GATA1 and LMO2 containing transcription factor complex

Relative locations binding locations of the TAL1, LMO2 and GATA1 transcription factor complex constituents. Adapted from Wadman *et al.* (1997).

This transcription factor complex recognises the E-box motif (CAGGTG) that lies 9-12 base pairs upstream of a GATA site and promotes erythropoiesis (Wadman *et al.*, 1997). In mouse erythroleukaemia cells, over-expression *Ldb1* inhibits E-box-GATA DNA binding activity and inhibits erythroid differentiation (Xu *et al.*, 2003). One target of this transcription factor complex is the gene that encodes erythrocyte protein band 4.2 (currently referred to as *Epb4.2*) the protein of which is an important component of the red blood cell membrane (Xu *et al.*, 2003).

The transcription factors involved in haematopoiesis can form a variety of different complexes with different constituents. As haematopoiesis progresses, these transcription factor complexes change in composition and define differentiation to different lineages as shown in Figure 2-4 (reviewed by Sieweke and Graf, 1998, Lecuyer and Hoang, 2004).
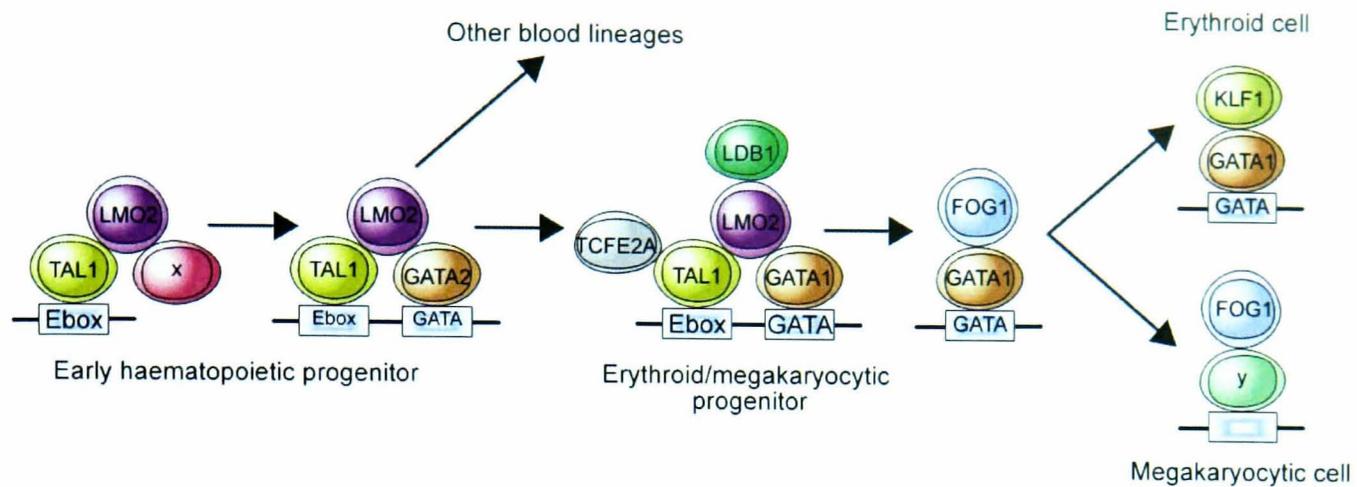
Figure 2-4: Transcription factor complexes during erythroid/megakaryocytic development

Changes in transcription factor complex constituents during erythroid and megakaryocytic differentiation in the mouse. Adapted from Sieweke and Graf (1998).

2.1.3.1   Ectopic expression of transcription factor complex constituents

It has been established that the injection of mRNA encoding the key elements of the erythroid transcriptional complex, tal1, gata1 and lmo2 into the one cell *Xenopus* embryo results in increased primitive haematopoiesis (Mead *et al.*, 2001). This was demonstrated by an increase in the size of the VBI, detected by the expression of the primitive erythroid marker, αT4 globin (Banville and Williams, 1985), currently assigned as hypothetical protein MGC64611. This simultaneous ectopic expression of tal1, gata1 and lmo2 also results in hyperventralised embryos with virtually no dorsal-anterior structures and expression of αT4 globin throughout the body axis (Mead *et al.*, 2001). Ectopic expression of tal1 and lmo2 simultaneously results in a ventralised and truncated body and an enlarged VBI. However, ectopic expression of either tal1, gata1 and lmo2 individually results in normal blood island formation (Mead *et al.*, 2001).

Animal cap explants from mid-blastula *Xenopus* embryos co-injected with tal1, lmo2 and gata1 at the 1-cell stage cultured the presence of mesoderm inducing activin or FGF2 also resulted in a massive increase in the proportion of erythroid cells

produced (Mead *et al.*, 2001). In the same experiment Mead *et al.*, (2001) analysed the effect of injection of these transcription factors individually, which resulted in a small increase in the number of erythrocytes, and in pairs, which resulted larger increase number of erythrocytes than individually injected transcription factors but still substantially less than the three transcription factors injected together. These data suggests that tal1, lmo2 and gata1 synergise in nascent mesoderm to promote primitive haematopoiesis, although it was not established if this process involves an increase in the population of haemangioblasts or HSCs.

2.1.4 Aims

The addition of signalling molecules transcription factors has been shown to augment erythrocyte differentiation in the *Xenopus* animal cap assay (Mead *et al.*, 2001), a system analogous to hESCs. This chapter aimed to utilise the *Xenopus* animal cap system to further investigate mesoderm and blood inducing factors that could then be applied to hESCs.

The specific aims of this chapter were:

- To confirm previous observations that the injection of key constituents of the blood inducing transcription factor complex, tal1, lmo2 and gata1, in to *Xenopus* zygote animal pole is capable of increasing the proportion of αT4 globin-expressing erythrocytes.

- To investigate the time-course over which tal1, lmo2 and gata1 injected into the zygote animal pole induce αT4 globin expression.

- To investigate whether an increased in erythrocyte production by the above transcription factors involves the induction of bmp4 expression.

- To determine if increased proportions of αT4 globin-expressing erythrocytes is due to an increased population of haemangioblasts.

- To determine if all three transcription factors are required for exogenous blood induction.

- To determine whether the mesoderm inducers activin B and FGF4 act synergistically with TAL1, LMO2 and GATA1 in inducing haematopoiesis in the *Xenopus* animal cap explant.

2.2 METHODS

2.2.1 Animals

Animal husbandry was performed by the University of Nottingham Biomedical Sciences Unit. Mature female *X. laevis* were purchased from Nasco and males from Blades Biological. Offspring of these animals were bred in-house. Maintenance was performed on a 12-hour light cycle at 19 °C in a slow-flowing water system that results in two water changes per hour. *X. laevis* were fed two to three times a week, one being of liver and the remainder pellet food.

2.2.2 Production of mRNA for *Xenopus* embryo injections

2.2.2.1 Determination of nucleic acid concentrations

DNA and RNA concentrations were assessed using a spectrophotometer (Spectronic 10, Thermo) to monitor UV absorption at 260 nm. Purity of samples was assessed by the ration of absorption at 260 nm:280 nm.

2.2.2.2 Plasmids

Pre-constructed pβUT2-HA plasmids were used to generate the following mRNAs:

- *tal1* (*scl*); cloned from *Danio rerio*, courtesy of M. Gering, (Gering *et al.*, 1998).

- *gata1*; cloned from *Danio rerio*, courtesy of M. Gering (Gering *et al.*, 2003).

- *Lmo2*; cloned from *Mus musculus*, courtesy of M. Gering (Gering *et al.*, 2003).

- inhbb (forms activin B homodimer); cloned from *Xenopus laevis*, courtesy of B. Afouda (unpublished).

- fgf4 (efgf); cloned from *Xenopus laevis*, courtesy of H. Issacs (Isaacs *et al.*, 1994).

2.2.2.3 *Restriction enzyme digestion*

Plasmids were linearised using *Eco*RI (Invitrogen) according to the manufacturer's instructions. Confirmation of digestion by running 1 µl of the reaction on an agarose/TAE gel and comparison with the undigested plasmid.

2.2.2.4 *Agarose gel electrophoresis*

Agarose gel electrophoresis was performed as described by Sambrook and Russell (2001). 1% agarose (Invitrogen) gels were prepared in 0.5 x TAE (50 x TAE: 2 M Tris-acetate; 50 mM EDTA). Ethidium bromide (Sigma) was added to the molten agarose to a final concentration of 0.5 µg ml^{-1}. Samples were supplemented with 2 µl Gel Loading Buffer (Sigma) run in comparison to 500 ng of Lambda DNA/*Eco*RI + *Hin*d III Markers (Promega). Gels were run in 0.5 x TAE at 100v for 30 min then visualised using a UV transilluminator and photographed using a UVIdoc gel documentation system (UVItec).

2.2.2.5 *Purification of plasmid DNA*

Phenol/chloroform protein removal was performed as described in Sambrook and Russell (2001). One volume of phenol:chloroform:isoamylalcohol (25:24:1) was added to each sample and the tubes were vortexed thoroughly before centrifugation at 13,000 *g* for 3 min at RT in a bench top microfuge. The lower organic protein containing phase was then removed along with any interface. The upper aqueous phase was then re-extracted to remove any phenol with an equal volume of chloroform:isoamylalcohol (24:1) with vortexing and centrifugation as before.

2.2.2.6 Concentration of plasmid DNA

Ethanol precipitation was performed as described in Sambrook and Russell (2001). Sodium acetate was added to each tube to a final concentration of 0.3 M. 2 volumes of 100% ethanol at -20 °C were then added and the samples were mixed by pipetting and incubated at -20 °C for 1 hr. The tubes were then centrifuged at 13,000 g for 20 min at 4 °C. The supernatant was then removed and the pellet was washed with 70% ethanol and centrifuged at 13,000 g for 3 min at RT. Pellets were air-dried on the bench for 10 min and re-suspended in ddH$_2$0. Concentrations were established as in 2.2.2.1.

2.2.2.7 In vitro transcription of mRNA for zygote injections

mRNA for embryo injections was transcribed using mMessage mMachine® (Ambion) kit following manufacturers instructions. To remove plasmid DNA 2U of DNase 1 (Roche) was added to each sample after transcription and incubated at 37°C for 15 min. Samples were then purified (2.2.2.5) and concentrated (2.2.2.6 but replacing the 100% ethanol with isopropanol) and analysed on an RNase-free agarose/TAE gel by comparison to pre-DNase I treated samples as in 2.2.2.4. mRNA concentrations were established (2.2.2.1) and cocktails of the following mRNAs were injected: tal1 (2.5-100 pg); lmo2 (2.5-100 pg); gata1 (2.5-100 pg); inhbb (activin B, 200 fg); and fgf4 (2 pg). Concentrations of transcription factor mRNA used were established by serial dilution down from the concentrations used by Mead *et al.* (2001). Concentrations of growth factor mRNA used were as those previously demonstrated to successfully induce mesoderm within the Patient Lab (unpublished). Concentrations referred to hereafter in experiments where more than 1 mRNA was injected, indicate the concentration of each mRNA used.

2.2.3 *Xenopus* embryo production, manipulation and injection

2.2.3.1 Embryo production and manipulation

To obtain embryos adult female *X. laevis* were injected in to the dorsal lymph sac with 600U of human chorionic gonadotrophin (Chorulon, Intervet) and kept at 19 °C overnight. Testes were removed from male *X. laevis* and maintained at 4 °C in 70% Liebowitz medium (Flow) supplemented with penicillin/streptomycin (10 μg ml⁻¹) and kept for up to 1 week. Oocytes were squeezed from the female and fertilised immediately with macerated testis in 0.1 x MBS (88 mM NaCl; 1 mM KCL; 2.4 mM NaHCO3; 15 mM HEPES.NaOH or Tris.HCL (pH 7.6); 0.3 mM $CaNO_3.4H_2O$; 0.41 mM $CaCl_2.6H_2O$; 0.82 mM $MgSO_4.7H_2O$; 10 μg ml⁻¹ penicillin/streptomycin (Invitrogen). After 5 min the sperm was washed off with 0.1 x MBS. After a further 25 min the zygote's gel coat was then removed using 2% cystene in MBS (pH 8), before washing four times in 1 x MBS.

2.2.3.2 Zygote injection

Embryos were then transferred to 1 x MBS supplemented with 3% Ficoll (Type 400-DL, Sigma) and arranged on injection grids. Embryos were injected directly into the centre of the animal pole with 4 nl of the relevant mRNA preparation using injection apparatus (PL1-100, Medical Systems Corps.) that had first been calibrated by adjusting the injection time to produce a bubble of the correct diameter corresponding to 4 nl. Control embryos were injected with the same dH_2O used for mRNA dilution. After 1 hour embryos were transferred into 0.1 x MBS. The rate of embryo development was partially controlled by varying temperature between 14 and 21 °C (14 hr at 14°C or 6 hr at 22°C). Embryos were staged according to Nieuwkoop and Faber (1967), see Figure 2-5.

2.2.4 Animal cap dissection

For each experimental variable approximately 30 embryos were incubated to stage 8.5 and dissected. The vitelline membrane was removed using steel forceps whilst embryos were in Petri dishes containing a layer of 1% agarose and 1 x MBS supplemented with 1% Gentamycin (Sigma). Dissected animal caps were then cultured in 1 x MBS on 1% agarose, ~15 animal caps were developed to the equivalent of stage 17 and ~15 to stage 30. Staging was assessed in comparison to undissected whole embryos as shown in Figure 2-5.

Stage 1
1-cell

Stage 8.5

Stage 17

Stage 30

mRNA injected into
animal pole

animal cap
dissection
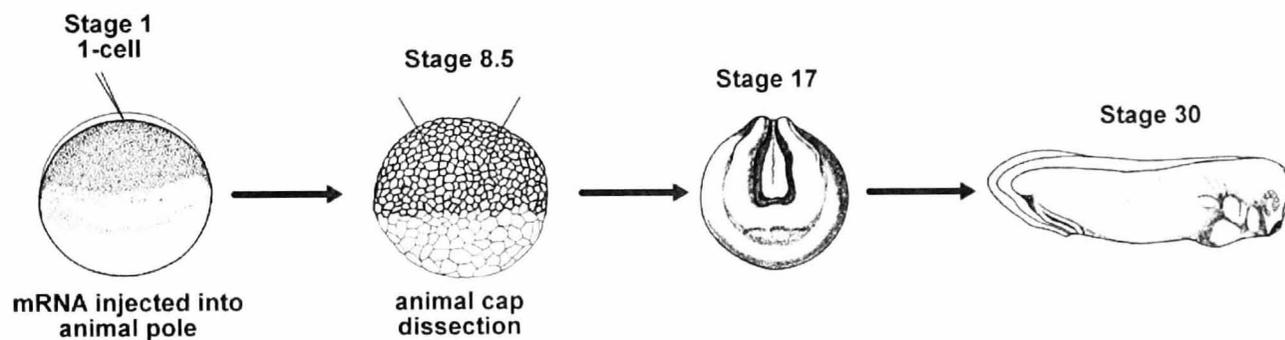
Figure 2-5: *Xenopus* **embryo stages used**

2.2.5 Whole mount *in situ* hybridisation

2.2.5.1 *Preparation for whole mount* in situ *hybridisation*

At stage 17 or 30 embryos were transferred to 1.5 ml Eppendorf tubes (having released stage 30 embryos from their vitelline membranes first). Embryos were fixed in MEMFA (0.1 M 3-[N-Morpholino] propanesulfonic acid, pH 7.4; 2 mM EGTA; 1mM $MgSO_4$; 3.7% formaldehyde) for one hour at room temperature. MEMFA was then replaced with methanol twice and the tubes left to stand at room temperature for 30 min. Methanol was then replaced with a fresh aliquot and the tubes were stored at -20 °C at least overnight.

2.2.5.2 *Whole mount* in situ *hybridisation*

Whole mount *in situ* hybridisation was performed as described by Harland (1991) with minor modifications. All steps were carried out using 1 ml volumes in 1.5 ml Eppendorf tubes at room temperature unless otherwise stated. 10-20 intact embryos stored in methanol were selected and rehydrated with 75%, 50% and 25% methanol in PBS/Tween (PBS: 150 mM phosphate buffer, pH 7.2; 0.85% NaCl containing 0.1% TWEEN 20 (Sigma)) for 5 minutes each wash, then washed in PBS/Tween for 5 minutes. PBS/Tween was replaced by bleaching solution (5% deionised formamide (Sigma); 0.5 x SSC (20 x SSC: 3 M NaCl; 0.3 M sodium citrate, pH 7.0; 10% H_2O_2) and tubes were placed on a light box for 5-10 minutes or until the pigment could no longer be seen. Embryos were then washed three times in 1 ml PBS/Tween for 5 minutes then acetylated in 0.1 M Triethanolamine for 5 min then 0.1M Triethanolamine with 2.5 µl acetic anhydride twice. Embryos were then washed in PBS/Tween for 5 min twice. The PBS/Tween was then replaced twice with 0.5 ml Hybridisation mix (50% deionised formamide (Sigma); 5 x SSC; 1 mg ml^{-1} tRNA, MRE600 (Sigma); 100 µg ml^{-1} Heparin (Sigma); 1 x Denhardt's; 0.1% Tween 20 (Sigma); 5 mM EDTA) in 0.5 ml volume, and prehybridised for at least 6 hours at 60 °C. The hybridisation mix was then removed and replaced with hybridisation mix containing 200 ng-1 µg ml^{-1} DIG labelled probe (2.2.5.3) and hybridised at 60 °C overnight.

The hybridisation mix was removed and stored at -20°C (as it can be used three times). Embryos were washed for 10 min at 60 °C in 50% formamide/5xSSC, 25% formamide/2xSSC, 2.5% formamide/2xSSC, 2 X SSC,0.1% Tween, 0.2 X SSC. Embryos were then washed in 0.1% Tween at 60°C for 30 min followed by PBS/Tween at room temp for 5 min three times and in Maleic Acid Buffer (MAB,

100 mM Maleic acid; 150 mM NaCl; pH 7.5) at room temp for 10 min. Following this embryos were blocked in MAB + 2% Boehringer Block at room temp for 4-5 hr. Antibody staining was performed using 1/2000 dilution of Anti-Digoxygenin-AP, Fab fragments (Roche) conjugated to alkaline phosphatase in MAB + 2% Boehringer Block at room temp with gentle rocking overnight.

Excess antibody was then washed away with 5 x 1 hr washes in MAB. Embryos were then equilibrated with a 10 min wash in AP buffer (0.1 M Tris, pH 9.0, 50 mM MgCl$_2$, 0.1 M NaCl, 0.1% Tween) with gentle rocking then colour development was performed by incubating embryos at room temperature in AP buffer:BM Purple AP Substrate, precipitating (Roche) (3:1) at room temp in the dark until the colour had developed (this was moved to 4°C if overnight) as observed under a light microscope. Once the colour reaction had developed sufficiently, embryos were washed twice in PBS/Tween for 5 min at room temperature and fixed in MEMFA for 1 hr then washed for 5 min 3 times in methanol before storage at -20°C. Embryos were then photographed under bright field optics on a blue background.

2.2.5.3 In vitro *transcription of whole-mount* in situ *hybridisation probes*

DIG labelled probes for whole-mount *in situ* hybridisation were prepared as described by Harland (1991). Digestion was performed using stated restriction enzymes (Table 2-1) according to the manufacturer's instructions. Samples were then purified (2.2.2.5) concentrated (2.2.2.6) and analysed on an agarose/TAE gel by comparison to undigested samples as in 2.2.2.4. Concentrations were established as in 2.2.2.1. Transcription was performed using SP6, T3 or T7 kits (Promega) and DIG UTP mix (Roche) for 2 hr at 37 °C. Template was then removed with DNaseI (Roche) and the reaction stopped with EDTA to a final concentration of 2 mM. The

probe was then concentrated (2.2.2.6) and pellets were re-suspended in hybridisation mix. A portion of the sample was analysed on an agarose/TAE gel by comparison to pre-DNase I samples as in 2.2.2.4.

Table 2-1: Digestion enzymes and transcription kits used in the construct *in situ* hybridisation probes

Probe	Linearisation	Transcription	Reference
αT4 globin	EcoRI (Promega)	SP6	(Walmsley et al., 1994)
fli1	Sma I (NEB)	T3	(Meyer et al., 1995)
runx1	Sal I (Invitrogen)	T7	(Tracey et al., 1998)
bmp4	EcoRI (Promega)	SP6	M. Jones, unpublished

2.2.6 Real-time PCR

2.2.6.1 RNA extraction

For each sample ~15 animal caps (at either stage 17 or 30) or whole embryos were snap frozen in dry ice for 15 min, before storage at -80°C. Samples were then suspended in embryo homogenisation buffer (50 mM NaCl; 50 mM Tris, ph 7.5; 5 mM EDTA, pH 8.0; 0.5% SDS; 1/100 volume Proteinase K). For caps, embryo homogenisation buffer was supplemented with 10 μg glycogen. Embryos/caps were disaggregated using a pipette tip, vortexed and incubated for 1 hr at 37°C with occasional inversion. Samples were then purified (2.2.2.5), concentrated (2.2.2.6) and pellets were re-suspended in RNase free water. Concentrations were established as in 2.2.2.1.

2.2.6.2 Reverse transcription

Reverse transcription was performed using M-MLV Reverse Transcriptase Kit (Invitrogen) and random primers (10mer, Sigma) at 42°C for 90 min. Optical densities were established using a spectrophotometer.

2.2.6.3 Real-Time PCR

Semi-quantitative Real-Time PCR was performed using an Applied Biosystems Prism 7700 Sequence Detector (Applied Biosystems) using Taqman probes. qPCR Mastermix Plus (Eurogentec) was used according to the manufacturer's instructions in a 25 µl volume containing 1 µl of cDNA, 5 pmol of forward and reverse primers and 5 pmol of probe. Primer and probe sequences (designed within the Patient Lab) are included in Table 2-2. All samples were run in triplicate and normalised to ornithine decarboxylase (odc) expression, known to remain constant in *Xenopus* development (Isaacs *et al.*, 1992), using the comparative CT method. Assay conditions were as follows: 50 °C for 2 min; 95 °C for 10 min; 40 cycles of 95 °C for 15 sec and 60 °C for 1 min.

Table 2-2: Primers and probes used for Real-Time PCR

Primer/probe	Sequence
αT4 globin (forward primer)	TCTGAATCTGCTACTTGCTG
αT4 globin (reverse primer)	TCTCCGATCGTCATTCTGCC
αT4 globin (probe)	CACACAGGCTGCTTGGGACAAATTCCT
fli1 (forward primer)	CTGCAGCCTCGACATTCAATGGATTC
fli1 (reverse primer)	CTGGCTTGTCCCGATCTGAA
fli1 (probe)	TGTCCCTTCACACCCATCCTCTATGCC
runx1 (forward primer)	TGTTGCTGTCTCCCAGTCCT
runx1 (reverse primer)	AAAAGTCTCAAAGTTCTCCT
runx1 (probe)	CAAATCCCATGCCCAACCCACG
odc (forward primer)	AGATCGGCAGCCTTTCACAGAAA
odc (reverse primer)	ACACCGTGTCATCAGAAAAGGGC
odc (probe)	CTGCAGCCTCGACATTCAATGGATTC

All primer pairs and probes were validated by comparing the reaction efficiency with that of odc when using a serial dilution of cDNA. A log of the serial dilution of cDNA was plotted against the difference in threshold cycle value (ΔCt) between the

two primer/probe sets. A gradient value <0.1 and a correlation coefficient of 0.95-1

were deemed suitable validation of reaction and detection efficiency.

2.3 RESULTS

2.3.1 Effect of transcription factor injection into the animal pole on embryo development and blood marker expression

In order to ascertain the effect of various combinations of tal1, lmo2, and gata1 mRNAs on blood development, mRNAs were injected as a cocktail into the animal pole of a 1-cell *Xenopus* embryo and embryos were developed to between stages 17 and 30 (Figure 2-6). Whole embryos were then *in situ* hybridised using probes for: αT4 globin, a primitive erythrocyte marker (Banville and Williams, 1985); bmp4, a growth factor involved in mesoderm patterning (Dale *et al.*, 1992), fli1, an early endothelial marker (Meyer *et al.*, 1995); and runx1, an early blood marker (Tracey *et al.*, 1998). All pictures show the typical result for each experiment represented by at least 75% of embryos.

mRNA injected into animal pole   **fli1 and runx1 expression**   **αT4 globin expression**

Stage 1 1-cell   **Stage 17**   **Stage 30**
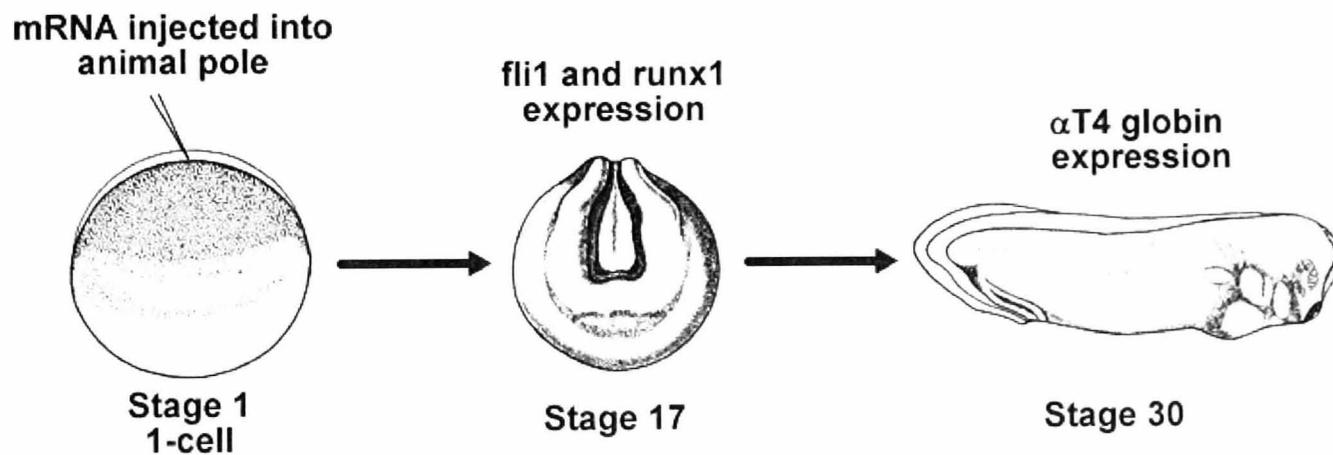
Figure 2-6: Transcription factor mRNA co-injection and effect measurement time-points

2.3.1.1 Effect of co- injecting of a combination of tal1, gata1 and lmo2 on αT4 globin expression

To confirm the effect of the addition of blood development related transcription factors on primitive haematopoiesis in the whole embryo as seen by Mead *et al.*, (2001), equal amounts of tal1, gata1 and lmo2 mRNA were co-injected as above and

in situ hybridisation was performed using an αT4 globin probe. To minimise the ventralised phenotype seen by Mead *et al.*, (2001) with co-injection of 1 ng of each of tal1, gata1 and lmo2, a dilution gradient was established. Embryos co-injected with 10, 20, 40, and 80 pg of tal1, gata1 and lmo2 mRNA were developed to stage 24 as these doses were judged to be embryonic lethal beyond this stage (Figure 2-7). Embryos co-injected with 2.5, 5, 10, and 15 pg of tal1, gata1 and lmo2 mRNA were developed to stage 30.

In general a dose/response relationship was observed between the levels of αT4 globin expression and increasing doses of tal1, gata1 and lmo2 mRNA. In embryos exposed to higher concentrations of tal1, lmo2 and gata1 mRNA (≥10 pg), αT4 globin expression was no longer restricted to the ventral surface of the embryo but was extended laterally up the side of the embryo. These embryos were hyperventralised and the body axes were severely truncated.

In embryos exposed to 2.5 and 5 pg of tal1, gata1 and lmo2 mRNA the VBI was expanded without overt ventralisation and the doses were used in all subsequent experiments.
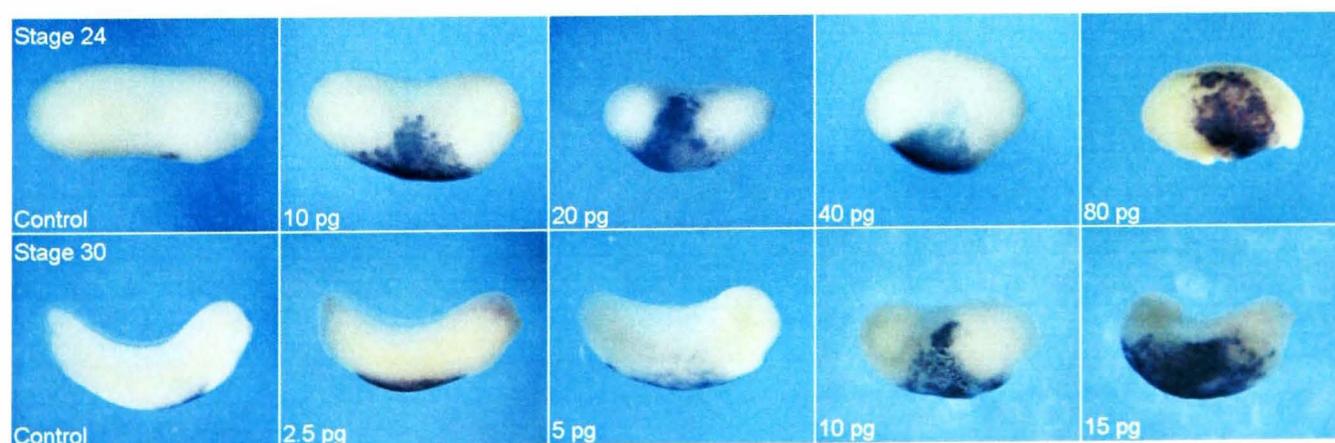
Figure 2-7: Expression of αT4 globin at stages 24 and 30 after the co-injection of tal1, gata1 and lmo2 mRNA at varying concentrations

Embryos were co-injected at the 1-cell stage with between 2.5 pg and 80 pg of tal1, gata1 and lmo2 mRNA and expression of αT4 globin at stage 24 or 30was detected by *in situ* hybridisation.

2.3.1.2 Time-course of the effect of the co-injection of tal1, gata1 and lmo2 mRNA on αT4 globin expression

To assess if the introduction of these exogenous blood development transcription factors to the zygote animal cap was having an effect on the timing of blood induction a time-course was performed, developing embryos to stages 17, 19, 21, 24, and 30 (Figure 2-8). In sham-injected, Control embryos αT4 globin expression was first detected at stage 24. The of area of expression of αT4 globin was observed visually to be increased relative to the Control embryos at stages 24 and 30 in embryos co-injected with 2.5 pg of tal1, gata1 and lmo2 mRNA and even earlier at stages 19 and 21 in embryos injected with 5 pg of tal1, gata1 and lmo2 mRNA. Slight ventralisation was also noted in embryos co-injected with 5 pg of tal1, gata1 and lmo2 mRNA at both stage 24 and 30.
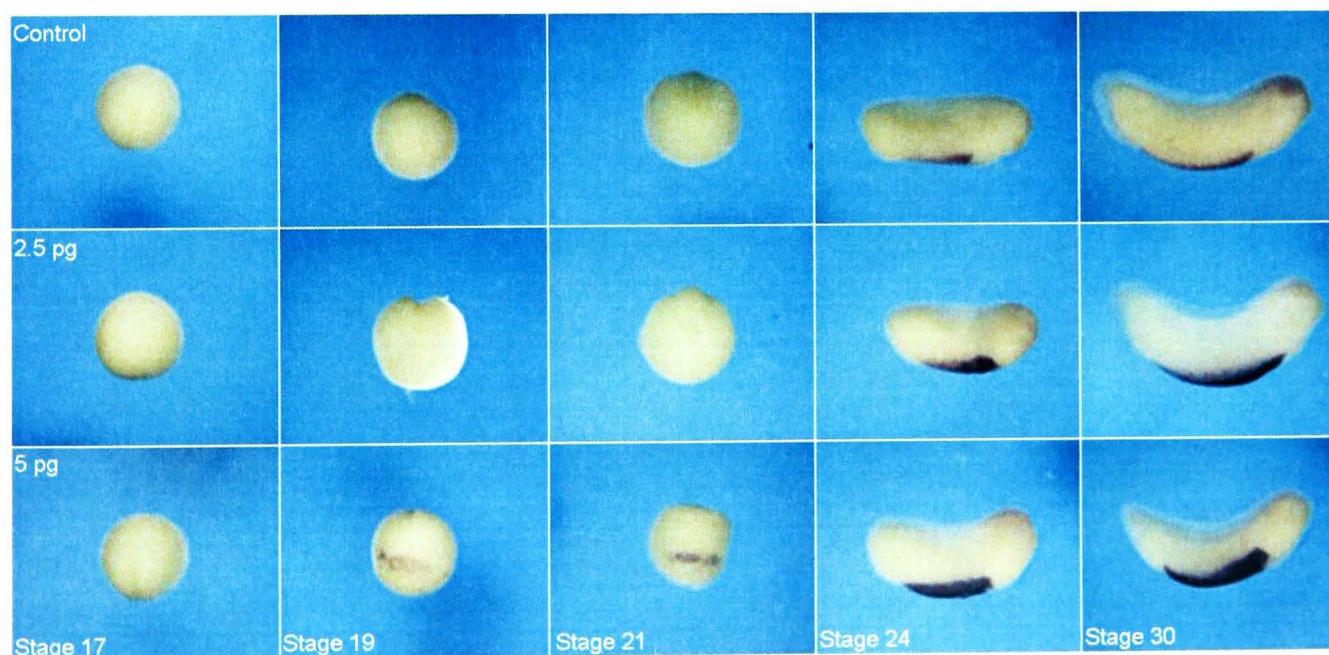
Figure 2-8: Expression of αT4 globin between stages 17 and 30 after the co-injection tal1, gata1 and lmo2 mRNA

Embryos were co-injected at the 1-cell stage with 2.5 pg and 5 pg of tal1, gata1 and lmo2 mRNA and expression of αT4 globin at stages 17, 19, 21, 24, 30 was detected by *in situ* hybridisation.

2.3.1.3 Effect of co-injection of tal1, gata1 and lmo2 mRNA on bmp4 expression

Since the ventralised phenotype observed after injection of high concentrations of the tal1, lmo2 and gata1 mRNA cocktail was reminiscent of the phenotype previous reported when injecting bmp4 mRNA into the animal pole (Jones *et al.*, 1996). Embryos co-injected with tal1, lmo2 and gata1 were *in situ* hybridised using a bmp4 probe to assess if these three transcription factors induce bmp4 expression (Figure 2-9). Expression of bmp4 was similar to the Control in embryos co-injected with 2.5 pg of tal1, lmo2 and gata1 mRNA. In embryos co-injected with 5 pg, elevated bmp4 expression was detected at stages 17-24, with a particularly enlarged area of bmp4 expression on the ventral side of the embryo at stage 19 (indicated by arrow).

Figure 2-9: Expression of bmp4 between stages 17 and 30 after the co-injection tal1, gata1 and lmo2 mRNA

Embryos were co-injected at the 1-cell stage with 2.5 pg or 5 pg of tal1, gata1 and lmo2 mRNA and expression of bmp4 at stages 17, 19, 21, 24, 30 was detected by *in situ* hybridisation.

2.3.1.4 Effect of co-injection of tal1, gata1 and lmo2 mRNA on fli1 and runx1 expression

The effect of co-injection of tal1, gata1 and lmo2 in to the animal pole on early endothelial (fli1; Figure 2-10) and early blood (runx1, Figure 2-11) marker

expression at stages 17 and 28 was examined. An increase in the area of marker expression was observed for both markers relative to the Controls. At stage 17 the areas of both fli1 and runx1 expression was increased on the prospective ventral side of the embryo in a dose/response manner (indicated with arrows on runx1 images, Figure 2-11). At stage 28 wider fli1 expression was detected in the DLP and anterior VBI (Figure 2-11) and wider runx1 expression was detected in the VBI in embryos exposed to 2.5 pg of tal1, lmo2 and gata1 and which was expanded laterally in embryos exposed to 5 pg (Figure 2-11).
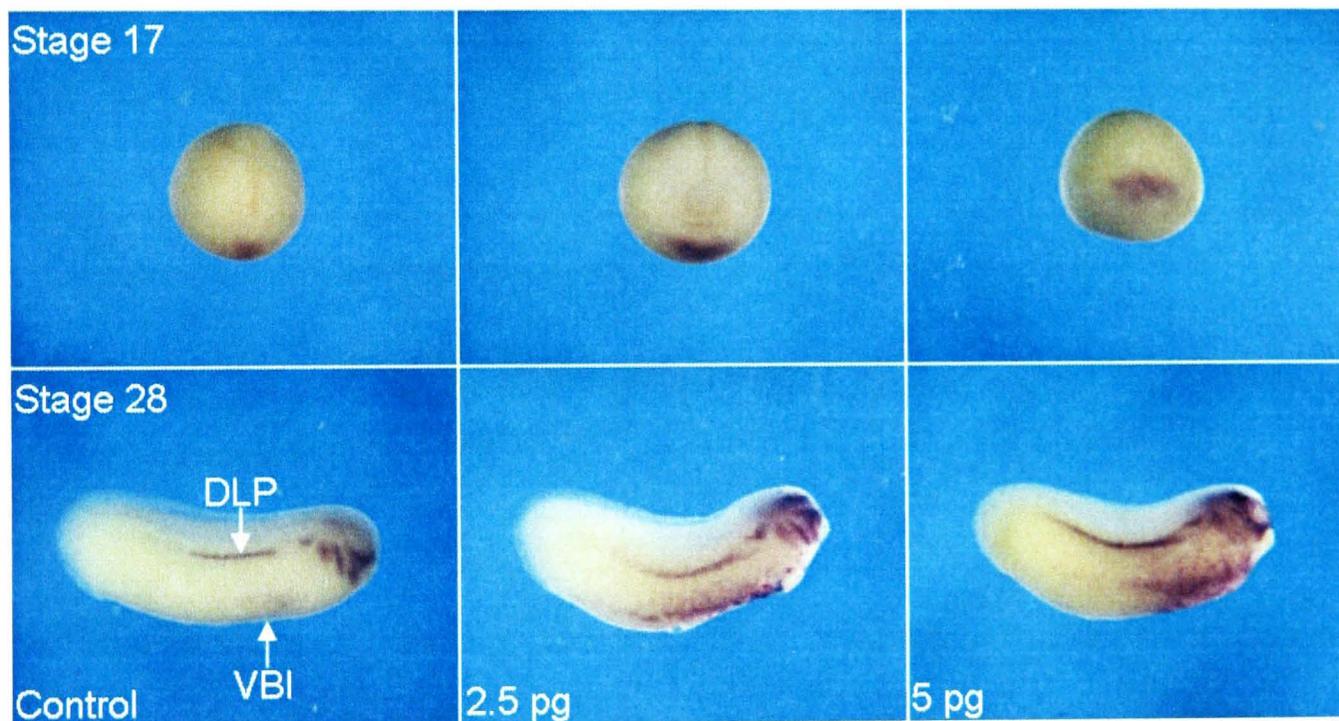
Figure 2-10: Expression of fli1 at stages 17 and 28 after the co-injection tal1, gata1 and lmo2 mRNA

Embryos were co-injected at the 1-cell stage with 2.5 pg or 5 pg of tal1, gata1 and lmo2 mRNA and expression of fli1 at stages 17 and 28 was detected by *in situ* hybridisation.
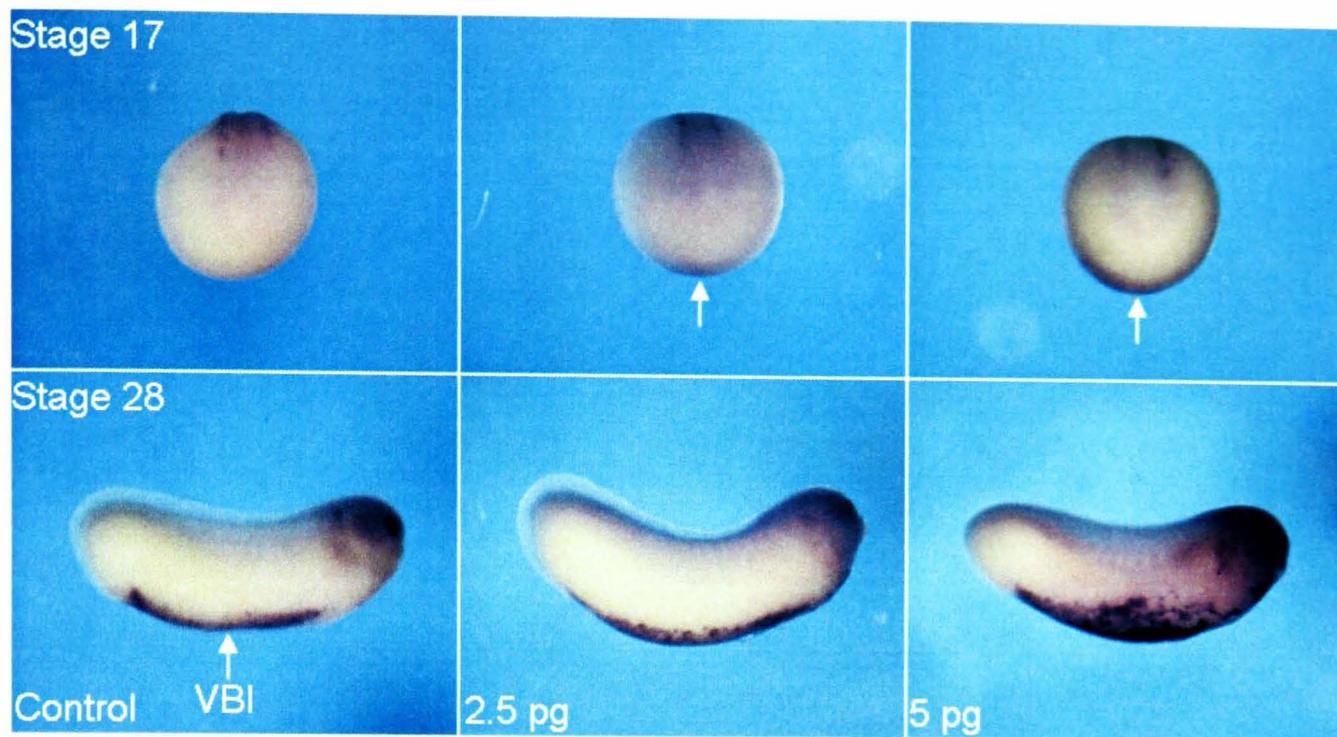
Figure 2-11: Expression of runx1 at stages 17 and 28 after the co-injection tal1, gata1 and lmo2 mRNA

Embryos were co-injected at the 1-cell stage with 2.5 pg or 5 pg of tal1, gata1 and lmo2 mRNA and expression of runx1 at stages 17 and 28 was detected by *in situ* hybridisation.

2.3.1.5 *Effect of individual injection of tal1, lmo2 or gata1 mRNA on αT4 globin expression at stage 17*

In order to ascertain whether individual injection of the three haematopoietic inducing transcription complex members could result in increased erythrocyte induction, stage 17 embryos injected with 5, 25 or 100 pg of each were examined for αT4 globin expression. Higher quantities of the individual mRNAs were used as experiments in *Danio rerio* have demonstrated that substantially higher quantities of transcription factors (100 pg) are required to induce globin expression when injected individually (Gering *et al.,* 2003). At stage 17 no expression of αT4 globin was detected after injection with either tal1, lmo2 or gata1 mRNA at concentrations of 5, 25 or 100 pg. (Figure 2-12).
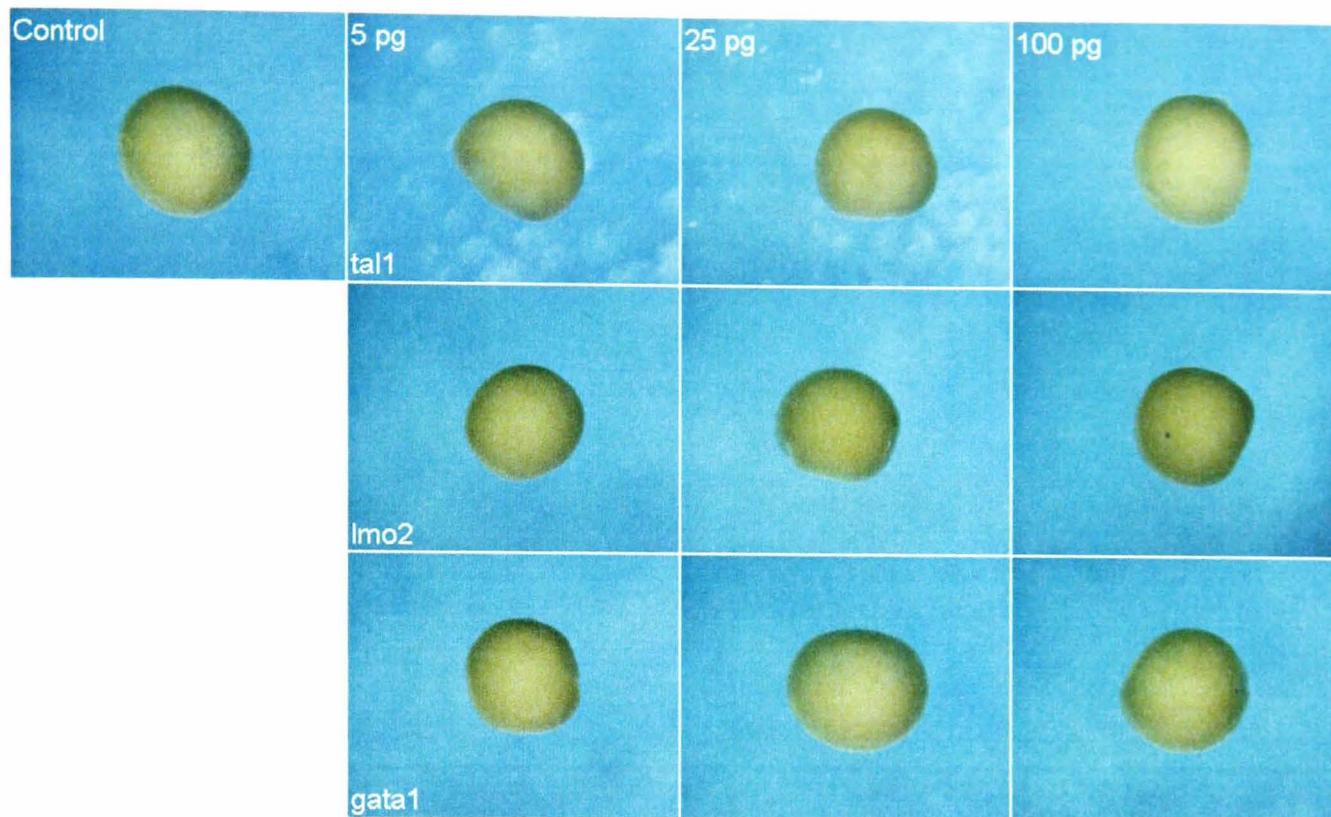
Figure 2-12: Expression of αT4 globin at stage 17 after the injection tal1, lmo2 or gata1 individually

Embryos were injected at the 1-cell stage with 2.5 pg, 5 pg or 100 pg of either tal1, gata1 or lmo2 mRNA and the expression of αT4 globin at stage 17 was detected by *in situ* hybridisation.

2.3.1.6 *Effect of individual injection of tal1, lmo2 or gata1 mRNA on αT4 globin expression at stage 30*

Expression of αT4 globin at stage 30 after injection of individual mRNAs was also examined (Figure 2-13). In embryos injected with 25 pg of tal1, lmo2 or gata1 mRNA the VBI was slightly enlarged compared to Control embryos whereas in embryos injected with 5 pg of mRNA there was no detectable effect. In embryos injected with 100 pg of tal1 or lmo2 mRNA the VBI was of similar size to those injected with 25 pg. For embryos injected with 100 pg of gata1 mRNA the VBI was substantially increased in size and the embryos were distinctly ventralised.
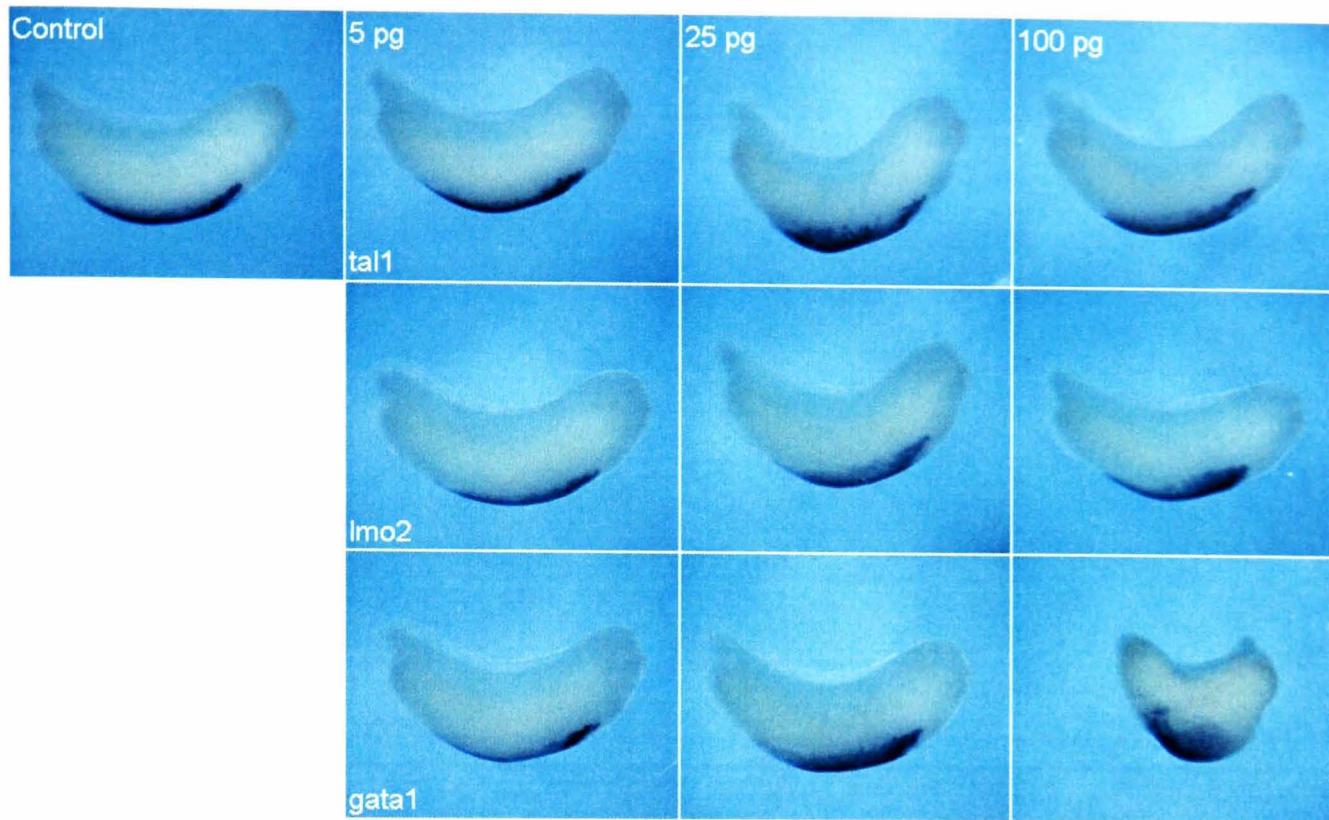
Figure 2-13: Expression of αT4 globin at stage 30 after the injection of tal1, lmo2 or gata1 individually

Embryos were injected at the 1-cell stage with 2.5 pg and 5 pg of either tal1, gata1 or lmo2 mRNA and expression of αT4 globin at stage 30 was detected by *in situ* hybridisation.

2.3.1.7 Effect of injection of tal1, lmo2 and gata1 mRNA in pairs on αT4 globin expression at stage 17

Transcription factor mRNA was also injected in pair combinations: tal1 and lmo2; tal1 and gata1; gata1 and lmo2 (Figure 2-14). In embryos allowed to develop to stage 17, αT4 globin expression was detected in all embryos injected with 5 pg of the pairs of mRNAs, whereas none was detected in the Control embryos. In particular the combination of tal1 & gata1 induced the largest and most scattered area αT4 globin expression. In embryos injected with 25 pg of the pairs of mRNAs the combinations of tal1 & gata1 and gata1 & lmo2 produced similar enlarged and scattered populations of αT4 globin positive cells whereas tal1 & lmo2 induced a population of similar size to that induced by 5 pg of tal1 & lmo2. In the embryos injected with

100 pg of both mRNAs the αT4 globin expression showed a marked decrease compared to the 5 pg and 25 pg injected embryos.
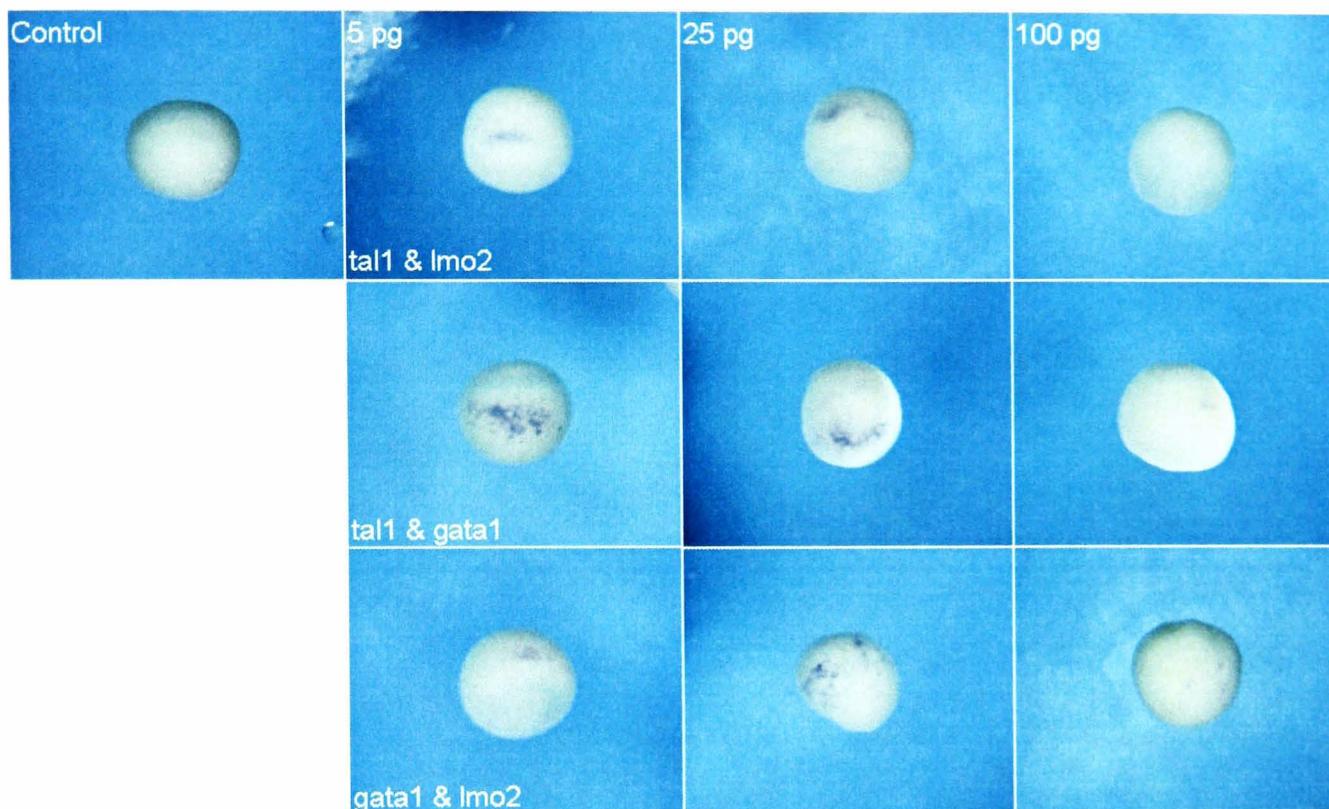
Figure 2-14: Expression of αT4 globin at stage 17 after the injection tal1, lmo2 and gata1 mRNA in pairs

Embryos were injected at the 1-cell stage with 2.5 pg, 5 pg or 100 pg of either: tal1 & lmo2, tal1 & gata1, or gata1 & lmo2 mRNA and the expression αT4 globin at stage 17 was detected by *in situ* hybridisation.

2.3.1.8 *Effect of injection of tal1, lmo2 and gata1 in pairs on αT4 globin expression at stage 30*

As above transcription factors were injected in embryos pair combinations and the embryos were allowed to develop to stage 30 (Figure 2-15). Injecting 5 pg of mRNA for each of the combinations resulted in a no or very little increase in the area of αT4 globin expression. Injection of 25 pg of gata1 & lmo2 mRNA resulted in a more substantial increase in the area αT4 globin expression. In embryos injected with 25 pg of tal1 & lmo2 or tal1 & gata1 mRNA, an enlarged VBI was observed, although tal1 & gata1 injected embryos were partially ventralised. In embryos injected with 25

pg of gata1 & lmo2 mRNA a very large area of αT4 globin expression was detected along with substantial ventralisation. Injection of 100 pg of tal1 & lmo2 mRNA resulted in a further enlarged VBI although with slight ventralisation. 100 pg of tal1 & gata1 mRNA resulted in more extreme ventralisation without any further increase in the size of the VBI. Embryos injected with 100 pg of gata1 and lmo2 were fully ventralised and truncated with little expression of αT4 globin detectable.
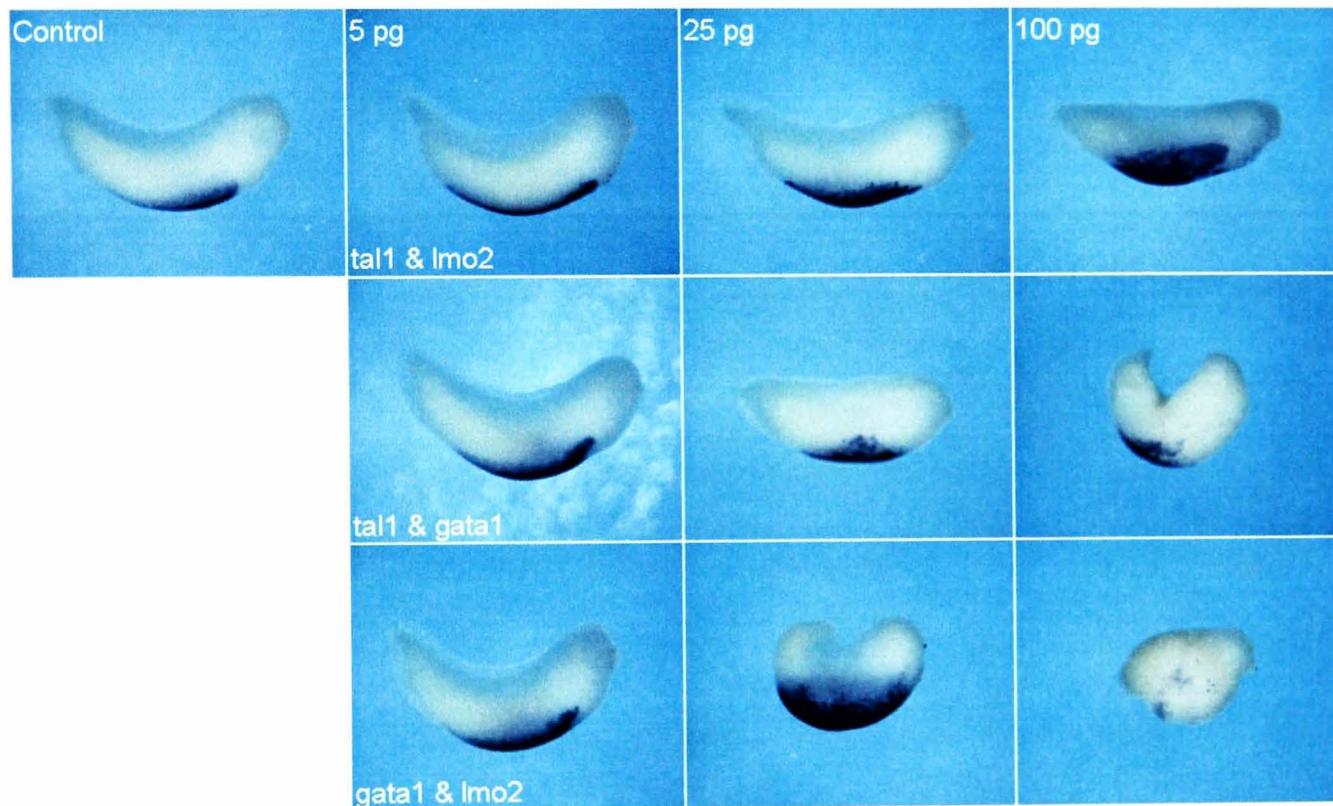
Figure 2-15: Expression of αT4 globin at stage 30 after the injection tal1, lmo2 and gata1 in pairs

Embryos were injected at the 1-cell stage with 2.5 pg and 5 pg of either: tal1 and lmo2, tal1 and gata1 or gata1 and lmo2 mRNA and the expression of αT4 globin at stage 30 was detected by *in situ* hybridisation.

2.3.2 Effect of co-injecting activin B or fgf4 with tal1, lmo2 and gata1 mRNA into zygote animal poles on haemangioblast and primitive erythrocyte gene expression in the animal cap explant

Once it was established that co-injection of tal1, gata1 and lmo2 mRNA into the animal pole of the zygote can induce an increase in the haemangioblast and

erythrocyte populations in the whole embryo, the animal cap explant assay was used to quantitate how this system performs in an *in vitro* setting. mRNA encoding a mesoderm inducer (either activin B or fgf4, see 2.1.2) was also included to direct the pluripotent animal cap to mesoderm whereupon tal1, gata1 and lmo2 can direct differentiation to haemangioblasts and primitive erythrocytes. Similar experiments by Mead *et al.*, (2001), using 1ng of tal1, lmo2 and gata1 mRNA and culturing animal caps in the presence of 100 pM activin resulted in a ~1200 fold increase in the number of erythroid cells.

Real time PCR was used to quantify changes in gene expression associated with exogenous mRNA co-injection into the animal pole. Embryos were co-injected at the 1-cell stage with a cocktail of 2.5 pg or 5 pg of tal1, lmo2 and gata1 mRNA along with either activin B (200 fg) or fgf4 (2 pg) mRNA. Other embryos were injected only with activin B or fgf4 mRNA. The animal cap of each embryo (30 per sample) was then removed at stage 8.5 and half were cultured to the equivalent of stage 17 (by comparative staging to a whole embryo) and the remaining cultured to the equivalent of stage 30 (Figure 2-16). Taqman real time PCR was then performed on both stages for markers of haemangioblast (fli1 and runx1) and primitive erythroid cell gene expression (αT4 globin).
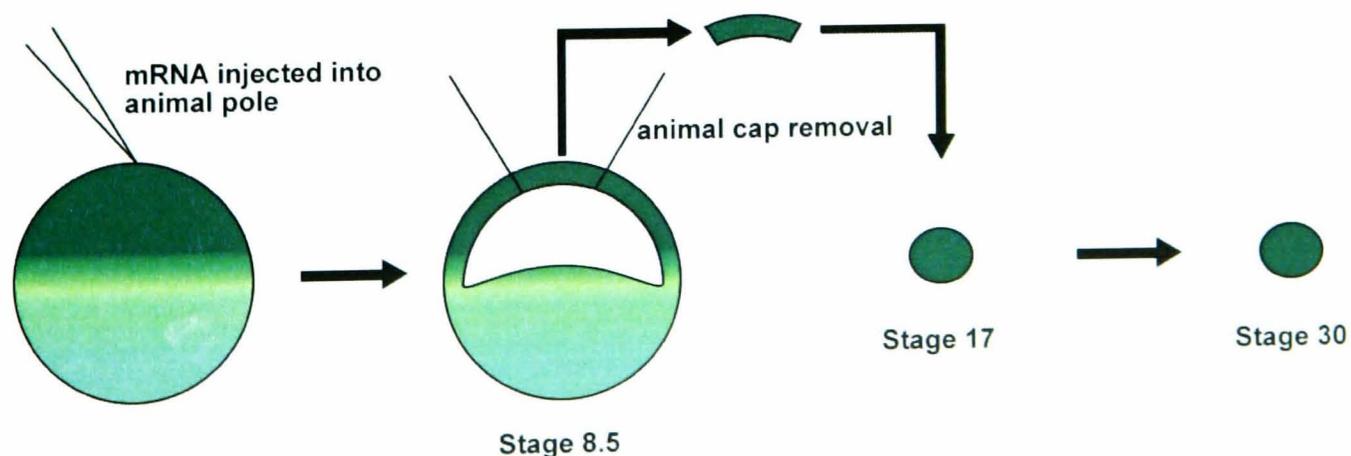
Figure 2-16: mRNA injection and animal pole explant procedure

2.3.2.1 Expression of *fli1* and *runx1* in animal caps cultured to stage 17 after co-injection of *tal1, lmo2, gata1* and *activin B or fgf4*

Expression of both fli1 and runx1 in stage 17 animal caps co-injected with tal1, lmo2 and gata1 mRNA without a mesoderm inducer was similar or lower that that of the sham-injected Control (Figure 2-17).

Where activin B mRNA was used as the mesoderm inducer, no increase in fli1 expression was detected when activin B mRNA was injected alone or with the addition of tal1, lmo2 and gata1 mRNA. A 2.2 fold increase in runx1 expression was induced by injection of activin B mRNA alone which was further augmented by 2.5 pg (4.5 fold increase) and 5 pg (10.8 fold increase) of tal1, lmo2 and gata1 mRNA.

When using injection of fgf4 mRNA as the mesoderm inducer only in combination with 5 pg tal1, lmo2 and gata1 was an increase in fli1 expression detected (9.0 fold). A small increase runx1 expression was induced by injection of fgf4 mRNA alone (1.5 fold) which was augmented by 2.5 pg (6.6 fold increase) and 5 pg (20.9 fold increase) of tal1, lmo2 and gata1 mRNA.
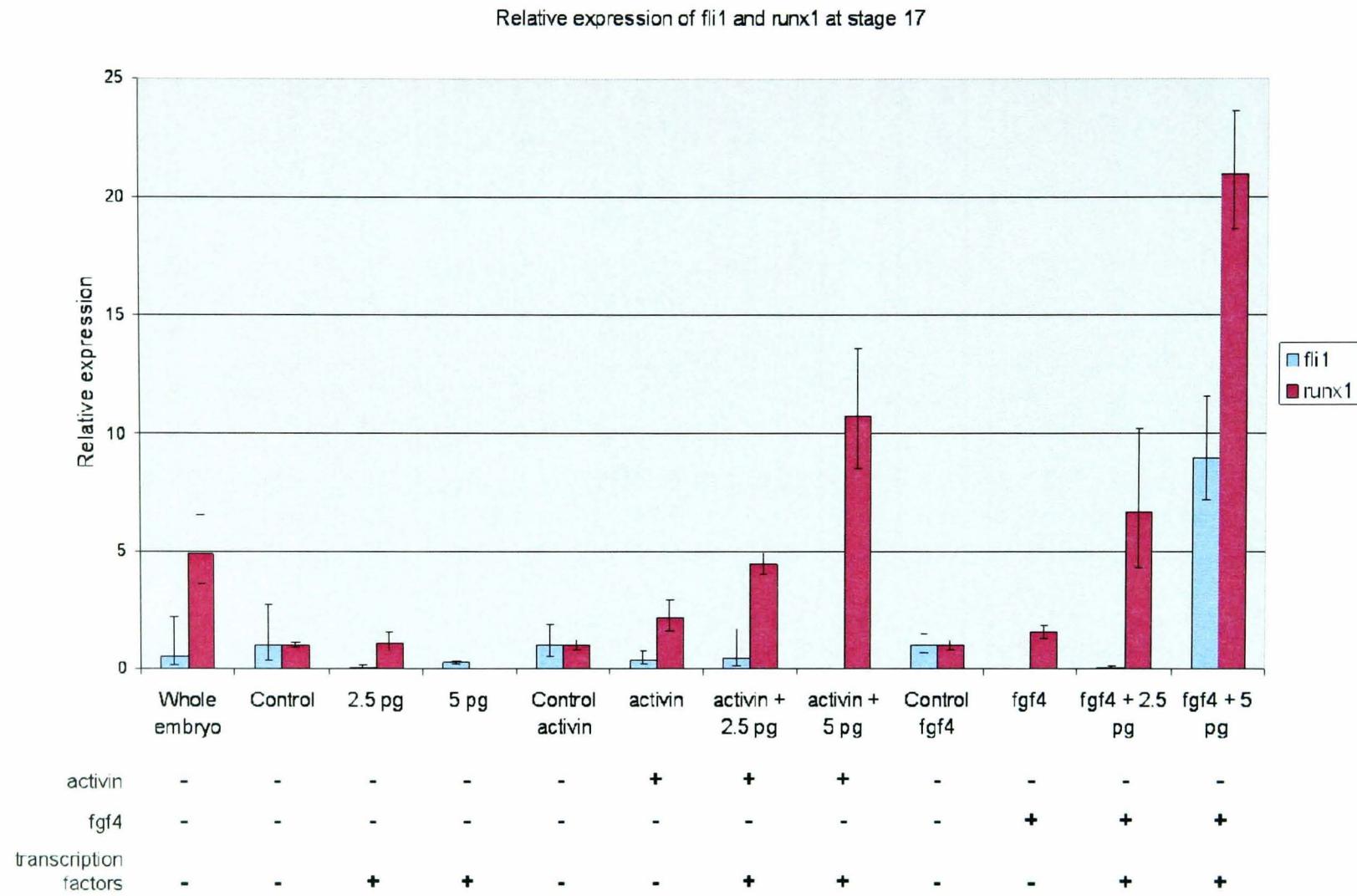
Figure 2-17: Expression of fli1 and runx1 in stage 17 animal caps detected by real time PCR

Expression of fli1 and runx1 in animal caps developed to equivalent of stage 17 was assessed by real time PCR. Experiments were performed co-injecting 2.5 and 5 pg of tal1, lmo2 and gata1 either: without a mesoderm inducer; using activin as the mesoderm inducer; or using fgf4 as the mesoderm inducer. Relative expression was established by comparison to Control (relative expression = 1), sham-injected animal caps. Each data point represents average (±SEM) of 2 independent experiments.

2.3.2.2 Expression of fli1 and runx1 in animal caps cultured to stage 30 after co-injection of tal1, lmo2, gata1 and activin B or fgf4

Expression of both fli1 and runx1 in stage 30 animal caps co-injected with tal1, lmo2 and gata1 mRNA without a mesoderm inducer was lower that that of the sham-injected Control (Figure 2-18).

Where activin B mRNA was used as the mesoderm inducer, a small increase in fli1 expression (1.3 fold) was detected when activin B mRNA was injected alone. This effect was abrogated by co-injection of tal1, lmo2 and gata1 along with activin B mRNA. Expression of runx1 was not increased by injection of activin B alone but a small increase in expression was detected after co-injection of activin B and 2.5 pg (1.7 fold increase) and 5 pg (2.0 fold increase) of tal1, lmo2 and gata1 mRNA.

When using injection of fgf4 mRNA as the mesoderm inducer a decrease in fli1 expression was detected either with or without tal1, lmo2 and gata1 co-injection. A similar decrease in runx1 expression was detected in animal caps injected with only fgf4 mRNA. Conversely co-injection of fgf4 plus 2.5 or 5 pg of tal1, lmo2 and gata1 mRNA resulted in a substantial increase in runx1 expression (7.6 and 4.7 fold respectively).

Relative expression of fli1 and runx1 at stage 30

	Whole embryo	Control	2.5 pg	5 pg	Control activin	activin	activin + 2.5 pg	activin + 5 pg	Control fgf4	fgf4	fgf4 + 2.5 pg	fgf4 + 5 pg
activin	-	-	-	-	-	+	+	+	-	-	-	-
fgf4	-	-	-	-	-	-	-	-	-	+	+	+
transcription factors	-	-	+	+	-	-	+	+	-	-	+	+
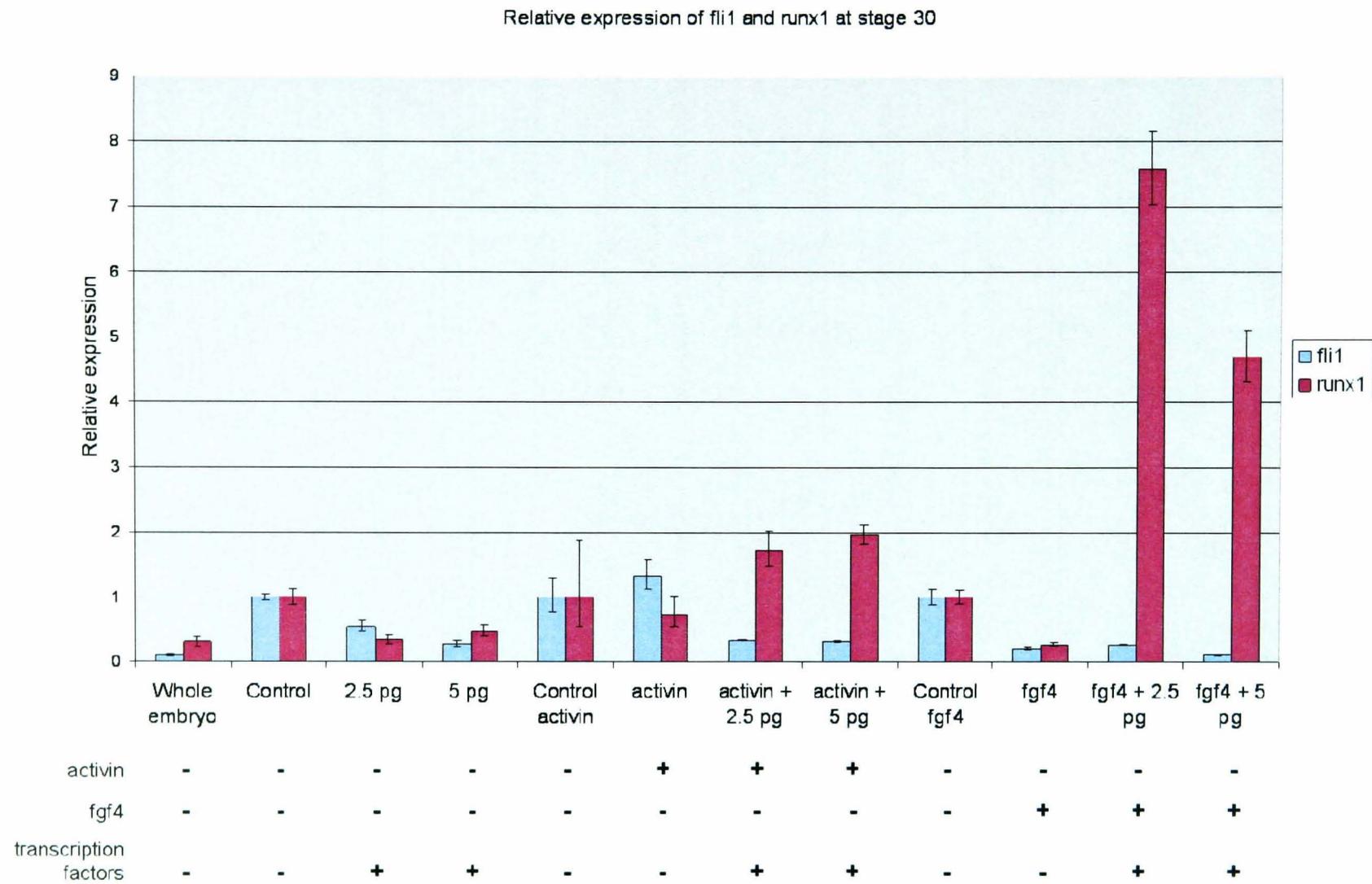
Figure 2-18: Expression of fli1 and runx1 in stage 30 animal caps detected by real time PCR

Expression of fli1 and runx1 in animal caps developed to equivalent of stage 30 was assessed by real time PCR. Experiments were performed co-injecting 2.5 and 5 pg of tal1, lmo2 and gata1 either: without a mesoderm inducer; using activin as the mesoderm inducer; or using fgf4 as the mesoderm inducer. Relative expression was established by comparison to Control (relative expression = 1), sham-injected animal caps. Each data point represents average (±SEM) of 2 independent experiments.

114

2.3.2.3 Expression of αT4 globin in animal caps cultured to stage 30 after co-injection of tal1, lmo2, gata1 and activin B or fgf4

Expression of αT4 globin was detected in stage 30 animals co-injected with tal1, lmo2 and gata1 with and without activin B mRNA. This experiment was repeated twice (two real time PCR experiments performed on the same animal cap cDNA samples) due to unexpected negative effect of a combination of activin B and tal1, lmo2 and gata1 on αT4 expression (see below). In both replicates (Globin 1, blue bars and Globin 2, red bars; Figure 2-19) injection of tal1, lmo2 and gata1 mRNA without a mesoderm inducer did not induced αT4 globin expression.

In replicate 1 (Globin 1) injection of activin B mRNA alone was sufficient to induce an 1130 fold increase in αT4 globin expression. This effect was reduced when 2.5 pg of tal1, lmo2 and gata1 mRNA was added to the activin mRNA (111 fold increase) and no increase in αT4 globin expression was detected when 5 pg of tal1, lmo2 and gata1 mRNA along with activin B mRNA was co-injected. This result was not seen in replicate 2 (Globin 2).

In both replicate 1 and 2, injection of fgf4 alone induced an increase in αT4 globin expression (1425 and 317 fold respectively) which was augmented by in the addition of 2.5 pg of tal1, gata1 and lmo2 mRNA (1825 and 357 fold respectively) and even further augmented by the addition of 5 pg of tal1, gata1 and lmo2 mRNA (2215 and 633 fold respectively).

Relative expression of αT4 globin at stage 30

2500

2000

Relative expression

1500

1000

500

0

Globin 1
Globin 2

	Whole embryo	Control	2.5 pg	5 pg	Control activin	activin	activin + 2.5 pg	activin + 5 pg	Control fgf4	fgf4	fgf4 + 2.5 pg	fgf4 + 5 pg
activin	-	-	-	-	-	+	+	+	-	-	-	-
fgf4	-	-	-	-	-	-	-	-	-	+	+	+
transcription factors	-	-	+	+	-	-	+	+	-	-	+	+
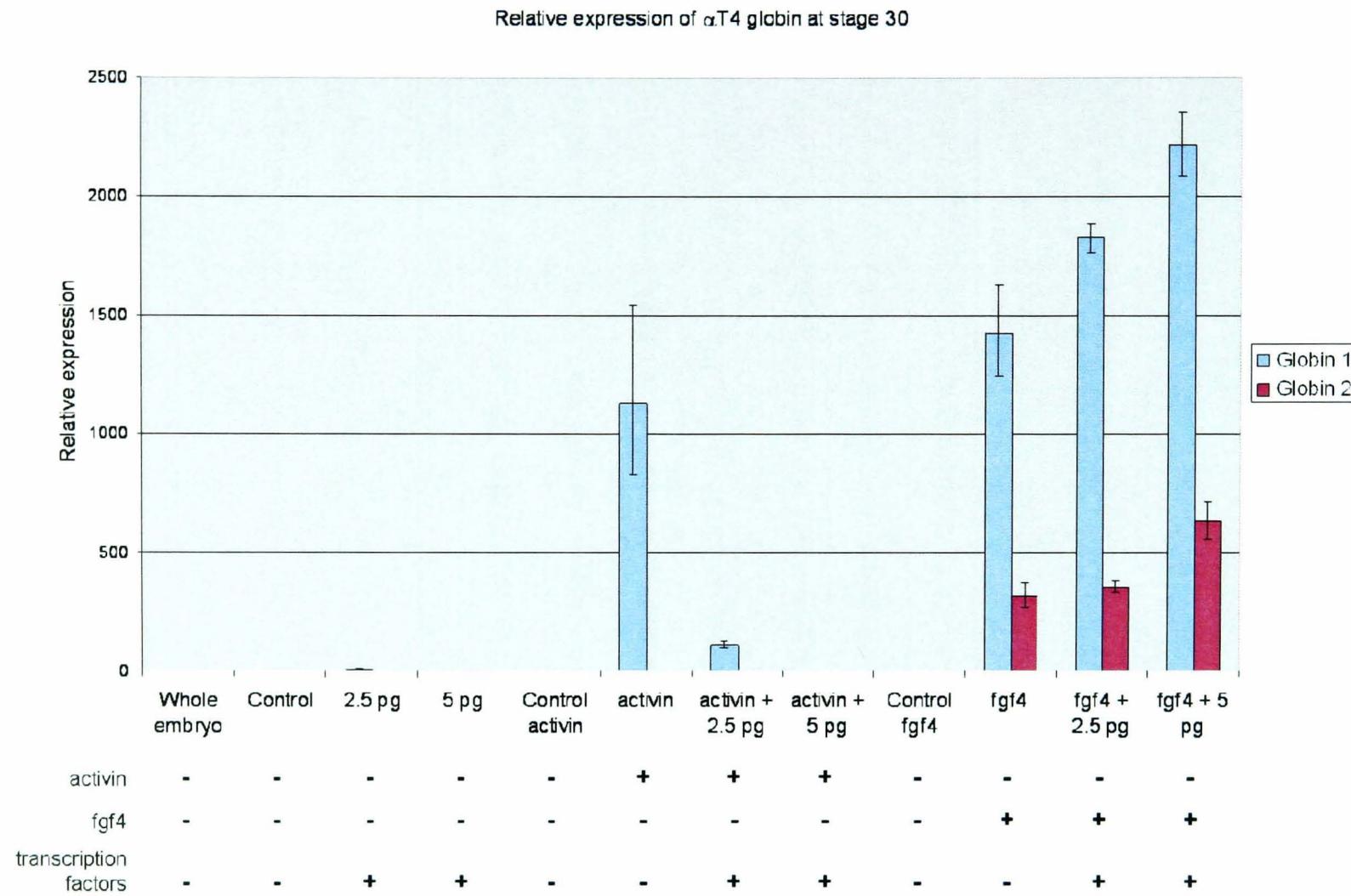
Figure 2-19: Expression of αT4 globin in stage 30 animal caps detected by real time PCR

Expression of αT4 globin in animal caps developed to equivalent of stage 30 was assessed by real time PCR. Experiments were performed co-injecting 2.5 and 5 pg of tal1, lmo2 and gata1 either: without a mesoderm inducer; using activin as the mesoderm inducer; or using fgf4 as the mesoderm inducer. Relative expression was established by comparison to Control (relative expression = 1), sham-injected animal caps. Globin 1 and Globin 2 are two real-time replicates performed on the same cDNA samples. Each data point represents average (±SEM) between real time PCR triplicates.

116

2.4 DISCUSSION

The objective of this study was to evaluate whether factors known in *Xenopus* development to be mesoderm (activin B and FGF4) and blood inducers (TAL1, LMO2, GATA1) could successfully increase globin expression in *Xenopus* animal caps and assess if this improvement occurs through the normal process of haematopoiesis.

2.4.1 Increased and earlier expression of αT4 globin is induced by co-injection of tal1, gata1 and lmo2 into the zygote animal pole

Previous experiments using *Xenopus* embryos have demonstrated that the expression of αT4 globin can be increased by co-injecting a combination of tal1, lmo2 and gata1 (1 ng of each) although acute ventralisation of the embryo was also seen (Mead *et al.*, 2001). By titrating down the concentrations of the combination of tal1, lmo2 and gata1 co-injected into the embryos it was possible establish a level which induced increased αT4 globin expression without overtly ventralising/posteriorising the embryo (Figure 2-7), as previously demonstrated in zebrafish (Gering *et al.*, 2003). Co-injection of 2.5 pg of tal1, lmo2 and gata1 increased the size of the αT4 globin expressing area at stages 24 and 30 in comparison to the sham-injected Control embryos (Figure 2-8), whereas in embryos co-injected with 5 pg of tal1, lmo2 and gata1, αT4 globin expression could be detected earlier (at stage 19 and 21) along the future ventral side of the embryo. In addition, at stages 24 and 30 the area of expression of αT4 globin was larger in these 5 pg injected embryos relative to 2.5 pg injected embryos; although slight ventralisation was detectable. Interestingly, high concentrations of the mRNA cocktail (above 20 pg of each transcription factor) were embryonic lethal beyond stage 28, although it was not established if this lethality was

due to hyperventralisation of the embryo or mRNA toxicity. One method of testing mRNA toxicity would be to inject a scrambled mRNA sequence at the same concentration as the transcription factor mRNAs. Scrambled mRNA sequence would also provide a more appropriate Control for *Xenopus* embryo injection experiments than injecting water.

Together these results demonstrate that ectopic expression of tal1, lmo2 and gata1 are capable of increasing erythropoiesis and may provide a useful method for control of haematopoiesis in hESCs, although careful attention will need to be paid to transcription factor dose.

2.4.2 Pairs of transcription factors, but not individual transcription factors, are sufficient to induce on αT4 globin expression

When injected alone neither tal1, gata1 or lmo2 induced αT4 globin expression at stage 17 (Figure 2-12). At stage 30, a small increase αT4 globin expression was observed in embryos injected with higher concentrations of individual transcription factors. In particular, injection of gata1 appeared to ventralise the embryo and induce a larger population of αT4 expressing cells at a concentration of 100 pg than either tal1 or lmo2 (Figure 2-13). These results are consistent with those from both whole embryo and animal cap experiments performed by Mead *et al.*, (2001), who demonstrated a small increase in the number of erythroid cells when injecting single transcription factor mRNA into the zygote animal pole, but much less than the three transcription factors together. When pairs of transcription factors were co-injected all combinations were capable of inducing αT4 globin expression in the presumptive ventral region of the embryo at stage 17 although this effect seemed to lessen as doses were increased (Figure 2-14). At stage 30 all combinations of pairs of transcription factors induced an increase αT4 globin expression in a dose-dependent

manner over 5-25 pg (Figure 2-15). Of interest, when gata1 was injected either on its own at 100 pg, or with tal1 or lmo2 at either 25 or 100 pg, the embryos became ventralised. This suggests than gata1 or gata1-containing complexes may have a more prominent role in the induction of factors that increase ventralisation, and may be responsible for the hyperventralisation seen in embryos injected with high doses of the three transcription factors together. The lower increase in erythropoiesis in embryos injected with single transcription factors and lack of induction at stage 17 suggests that, although single transcription factors are able to up-regulate other transcription factor complex constituents (e.g. lmo2 up-regulation of tal1, Mead *et al.*, 2001), this is not substantial enough to induce increased αT4 globin expression. In addition of 25 pg and 100 pg of tal1 and lmo2 induced the largest area of αT4 globin expression with the lowest level of ventralisation when compared to combinations of tal1 and gata1 or gata1 and lmo2. This combination of tal1 and lmo2 has been demonstrated to be sufficient to induce haemangioblasts in non-axial mesoderm in zebrafish embryos although, without the addition of gata1, these haemangioblasts differentiate to endothelial cells (Gering *et al.*, 2003). This suggests that although a combination of tal1 and lmo2 may have the least effects on additional pathways (i.e. those involved in ventralisation), the combination of tal1, lmo2 and gata1 will be most suitable for future experimentation in the hESC system.

2.4.3 tal1, gata1 and lmo2 co-injection induce bmp4 expression

The similarities of the ventralisation phenotype of tal1, gata1 and lmo2 co-injected embryos (Mead *et al.*, 2001) with the phenotype of bmp4-injected embryos (Jones *et al.*, 1996), lead Mead *et al.*, (2001) to postulate that the combination of tal1, gata1 and lmo2 may be able to induce bmp4 expression. Ectopic bmp4 alone is able to induce erythropoiesis in animal cap explants after injection into the zygote animal

pole (Dale *et al.*, 1992). Thus, the current study was aimed to test whether co-injection of tal1, lmo2 and gata1 directly induced erythrocyte differentiation or whether these transcription factors induced bmp4 expression which then subsequently induced erythrocyte differentiation. No substantial increase in bmp4 expression over the Control embryos was detected in embryos injected with 2.5 pg of tal1, lmo2 and gata1 (Figure 2-9), although this dose did expanded the area of αT4 globin (Figure 2-8). However, co-injection of 5 pg of tal1, lmo2 and gata1 had a more dramatic result with ectopic expression of bmp4 with at stages 17-24, particularly at stage 19. Once induced, this ectopic bmp4 may be able to form a positive feedback loop with tal1, lmo2 and gata1 as bmp4 is known to induce the expression of these three transcription factors (Zhang and Evans, 1996, Mead *et al.*, 1998, Mead *et al.*, 2001, Sanada *et al.*, 2003). The bmp4 promoter contains multiple E-box and GATA binding sites (Kim *et al.*, 1998) and therefore can be induced by the transcription factor complex that includes tal1, lmo2 and gata1. In addition bmp4 can also form a self-inducing auto-activational loop and increase its own expression (Metz *et al.*, 1998). Therefore, although increased erythropoiesis is can be induced without ectopic bmp4 expression, as in the case of 2.5 pg injected embryos, this positive feedback loop may be responsible for the further increased erythropoiesis detected in 5 pg injected embryos. This result is substantially different to that seen in zebrafish embryos where the injection of 25 pg of each of tal1, lmo2 and gata1 mRNA neither activated ectopic bmp4 expression nor ventralised the embryo yet was sufficient to cause anterior erythropoiesis (Gering *et al.*, 2003). Injection of 100 pg of each mRNA did result in increased bmp4 expression in half of the embryos although these embryos were not ventralised/posteriorised (Gering *et al.*, 2003). To establish if this is a true inter-species difference these *Xenopus* experiments could be furthered

by the use of a dominant-negative BMP receptor which would clarify if tal1, gata1 and lmo2 are able to induce erythropoiesis without the assistance of bmp4. In hESCs, induction of this positive feedback loop between bmp4 and tal1, lmo2 and gata1 may be beneficial for the production of erythrocytes but could also limit the production of definitive haematopoietic lineages.

2.4.4   Increased αT4 globin expression occurs through the normal route of haematopoiesis

To assess if the increased, premature αT4 globin expression was a result of the normal route of haematopoiesis *in vivo*, i.e. through mesoderm to haemangioblast to HSC to erythrocyte, a potential increase in the haemangioblast population (Walmsley *et al.*, 2002) was investigated using the haemangioblast/endothelial marker, fli1 (Ciau-Uitz *et al.*, 2000) and the haemangioblast/haematopoietic progenitor marker runx1 (Tracey *et al.*, 1998). At stage 17, the co-injection of tal1, gata1 and lmo2 induced an increase in area of both fli1 and runx1 expression, in comparison to the Control embryos, on the prospective ventral side of the embryo (Figure 2-10 and Figure 2-11). At stage 28 the area of fli1 expression was increased in both the DLP and VBI in comparison to the Control embryos (Figure 2-10). The area of runx1 expression was increased in the VBI (Figure 2-11) in a similar pattern to that seen for the expression of αT4 globin (Figure 2-8), with the area of expression increased laterally in embryos co-injected with 5 pg of tal1, lmo2 and gata1. Taken together these results suggest that the increase in αT4 globin expression is preceded and accompanied by an increase in the haemangioblast population and therefore tal1, lmo2 and gata1 co-injection induces αT4 globin expression by the normal route of haematopoiesis as reported in the zebrafish (Gering *et al.*, 2003). This result is particularly relevant to hESCs as it demonstrates that these three transcription factors

promote the increased differentiation of mesoderm to haemangioblasts, rather than merely encouraging differentiation of HSCs to erythrocytes.

2.4.5 Induction of haemangioblast marker and αT4 globin expression in animal cap explants

The induction of substantial number of erythroid cells from animal caps by the co-injection of tal1, lmo2 and gata1 mRNA into the animal pole of the zygote, and culture in the presence of either activin or fgf2 has been demonstrated by Mead *et al.*, (2001). To further the understanding of this process and to assess if, as in the whole embryo, αT4 globin expression is preceded by and increase in the expression of haemangioblast markers, real time PCR was performed on animal caps at stage 17 and 30. In animal cap experiments a mesoderm inducer is required to direct the animal cap cells to mesoderm and without a mesoderm inducer animal cap cells will form atypical epidermis (Okabayashi and Asashima, 2003). In these experiments activin B and fgf4 were chosen as the mesoderm inducers. Activin B has been reinstated as a mesoderm inducer in the whole embryo (Piepenburg *et al.*, 2004) and FGF4 is known to be a more potent inducer of mesoderm than FGF2 (Isaacs *et al.*, 1994). FGFs synergise with many haematopoietic cytokines to stimulate the proliferation of haematopoietic progenitors (Huber *et al.*, 1998, Miyanaga *et al.*, 1999) although FGF4 has also been demonstrated to inhibit BMP4-induced erythropoiesis (Xu *et al.*, 1999).

A key difference between experiments performed here and those performed by Mead *et al.*, (2001) is that in these experiments mRNA encoding the mesoderm inducers, was co-injected into the animal pole of the zygote (stage 1) along with tal1, lmo2 and gata1 mRNA rather than culturing the animal caps (stage 8.5) in soluble growth factor protein.

At stage 30 the co-injection of fgf4, tal1, lmo2 and gata1 mRNA induced a massive increase in the expression of αT4 globin (Figure 2-19). A less dramatic increase in αT4 globin expression was also detected with the use of fgf4 alone. This suggests that although cells induced to form mesoderm (using just fgf4) can form erythrocytes; this process is greatly improved when cells are also further directed to the blood lineage using the haematopoietic transcription factors. Also no increase in αT4 globin expression was detected when using the combination of transcription factors alone without either of the mesoderm inducers therefore directed differentiation to mesoderm is an obligatory step required for haematopoiesis. Although globin expression is a well established marker of erythrocytes, these experiments could have been further enhanced by isolating cells from the stage 30 animal cap samples, adhering them to a slide and performing Wright-Giemsa stain to allow the visual identification of primitive erythrocytes.

At stage 17 high levels of both fli1 and runx1 expression were detected in animal caps from embryos co-injected with fgf4, tal1, lmo2 and gata1 (Figure 2-17). Co-injection of activin B, tal1, lmo2 and gata1 had a lesser effect on runx1 expression and no effect on fli1 expression. In animal caps embryos from embryos co-injected with fgf4, tal1, lmo2 and gata1 and developed to stage 30, runx1 expression was substantially lower than that detected at stage 17 and little fli1 expression was detected (Figure 2-18). Together these results suggest that, as with the whole embryo, tal1, lmo2 and gata1-induced erythropoiesis occurs through the normal route of haematopoiesis.

Taken together this work demonstrates that tal1, lmo2 and gata1 do act synergistically in a multi-protein complex to promote primitive erythrocyte formation. At higher concentrations this combination of transcription factors also

induces bmp4. bmp4 may then form a positive feedback loop by forming and auto-inductional loop with itself whilst also increasing the expression of the transcription factor complex constituents which in turn increase bmp4 expression. At lower concentrations tal1, lmo2 and gata1 induce an increase in αT4 globin expression without ventralisation or ectopic expression of bmp4. Also demonstrated is that this increase in αT4 globin expression is preceded by an increase in haemangioblast markers which indicates that tal1, lmo2 and gata1 act to increase the haemangioblast population rather than simply specifying erythrocyte differentiation.

2.4.6 Potential for use of this system in hESCs

A key difference between the animal cap assay and hESCs is that although animal cap cells are pluripotent, when allowed to differentiate without the addition of growth factors they form atypical epidermis whereas hESCs will form cells of the three germ layers suggesting that animal cap cells are from a later stage of development. In addition injection of mRNAs in the animal pole of the single cell zygote and removal of the animal cap at stage 8.5 in *Xenopus* does not have an analogous human system as injection would have to be made into the human zygote and a hESC line derived from the blastocyst. Therefore to adapt this mRNA injection system to hESCs a different delivery route will be required such as transfection although as yet, the introduction three separate genes into human cells, as would be required for tal1, lmo2 and gata1, has not been demonstrated. This work does provide proof of principle of a system that can successfully induce erythropoiesis through the normal route of haematopoiesis and therefore provide the first step towards creating a similar system in hESCs.

3 OPTIMISING AN EMBRYOID BODY SYSTEM FOR EVALUATING DIFFERENTIATION STRATEGIES IN HUMAN EMBRYONIC STEM CELLS

3.1 INTRODUCTION

Methods for differentiation of hESCs to the mesodermal lineage from are still in their infancy and optimised differentiation protocols that are efficient and work across a range of hESC lines have yet to be established. One of the most frequently used methods for controlling haematopoietic and cardiac differentiation is via hEBs. hEB lineage induction relies on the innate propensity of hESCs to randomly differentiate to the three germ layers when cultured as three dimensional aggregates, usually in the presence of undefined FBS and the absence of pluripotency-maintaining growth factors. Once formed, to direct differentiation to a particular cell type, hEBs are treated with lineage-specific growth factors, then enriched by selected according to relevant blood and cardiac surface/intracellular markers. The common 'mass culture' method for hEB formation results in highly heterogeneous hEBs with potential contamination with MEFs. This heterogeneity results in a population of hEBs that that differentiates asynchronously, complicating the identification of factors that direct differentiation towards a particular lineage.

This chapter details the establishment of a forced aggregation system to promote hESC differentiation in a more homogeneous and therefore reproducible manner. This system was then used to identify and evaluate differentiation in CDM, with and without the addition of growth factors, to assess hEB formation in a serum free environment. This system will allow clearer future insight into the factors that effect hESC differentiation and aims to provide a platform for first increasing

differentiation to mesoderm in a controlled manner and thus producing a progenitor greater population that is capable of haematopoietic and cardiac differentiation. Inter-line variability of differentiation in this system across four hESC lines has also been examined to establish the generic applicability of the technique.

3.1.1 Methods of mouse embryoid body formation

3.1.1.1 *Mass culture*

Numerous methods have been devised for the formation of mEBs (reviewed by Desbaillets *et al.*, 2000, Dang *et al.*, 2002). Static suspension in mass culture is the most widely used for forming mEBs and involves partial disaggregation of the colonies from the MEF feeder layer before either seeding onto culture gelatine-coated bacteriological Petri dishes for 1-4 days in culture medium with or without the addition of LIF (Williams *et al.*, 1988) then/or transferring to untreated dishes allowed to form aggregates in a medium containing 15-20% FBS without LIF (Doetschman *et al.*, 1985). Spinner flasks have also been demonstrate for successful mEB cultivation (Wobus *et al.*, 1991).

3.1.1.2 *Induced aggregation*

The 'hanging drop' methods is commonly used for mEB formation and involves the suspension of 400-1000 mESCs from the lid of a Petri dish, after 2 days of incubation mEBs are harvested and subsequently cultivated in suspension (Wartenberg *et al.*, 1998). It has also been established that there is a optimum number of mESC cells formed in hanging drop mEBs that gives rise to the highest number of cardiomyocytes (Bader *et al.*, 2001), therefore mEB size may have a crucial role in directing differentiation towards a particular lineage. Although the hanging drop method has been used to form hEBs from clumps of hESCs (Yoon *et*

al., 2006, Baharvand *et al.*, 2006c) it has not yet been demonstrated that fully disaggregated hESCs will form hEBs in this manner (Reubinoff *et al.*, 2000).

More recent methods for mEB formation have involved using 96-well U bottom plates coated with the polymer 2-methacryloyloxyethyl phosphorylcholine to reduce the adhesion of cells and successfully form mEBs without the need for centrifugation with mEB size correlating to seeding cell number (Konno *et al.*, 2005). Also an attempt has been made to 'engineer' mEBs by aggregating mESCs using biotinylation and avidin cross-linking which proved successful for improving bone nodule formation (De Bank *et al.*, 2007).

3.1.1.3 *Semi-solid methylcellulose*

Suspension of single cells in semi-solid methylcellulose and subsequent growth allows the formation of clonal mEBs (Keller *et al.*, 1993). It is suggested that mEB size may be self-regulated, perhaps resulting from the lack of some developmental cue(s), demonstrated by experiments demonstrating that mEBs whether generated from 1 cell or 1000 cells are equivalent by d12 (Dang *et al.*, 2002). hEBs have yet to be demonstrated initiate from single cells (Daley, 2003) therefore formation in semi-solid methylcellulose medium is unlikely possibly due to hESCs poor survivability at clonal levels (Amit *et al.*, 2000).

3.1.2 Methods of human embryoid body formation

The three main methods for successful hEB formation: static suspension culture; bioreactors, spinner flasks and stirred culture vessels; and forced aggregation are reviewed below.

3.1.2.1.1 *Static suspension in mass culture*

The standard method for hEB formation involves culture of hESCs on MEFs followed by dissociation from the feeder layer in to small clumps of cells. These clumps can be formed by either manual dissection into approximately 200 µm pieces (Khoo et al., 2005), or a combination of dissection/scraping, pipette tip dissociation and enzymatic treatment (Gerecht-Nir et al., 2005). For enzymatic dissociation, clumps of different cells numbers have proven optimum for hEB formation: 3-20 cells with collagenase IV (Kehat et al., 2001); ~100 or more cells with collagenase IV (Mummery et al., 2002); 500 to 800 cells with dispase (He et al., 2003). Partial disaggregation with trypsin has also been used although yields a hEBs of heterogeneous sizes (Sottile et al., 2003). Clumps are then suspended in a medium containing 20% FBS without FGF2 in non-treated Petri dishes for 4 to 10 days (Kehat et al., 2001, Cui et al., 2007, Mummery et al., 2002)

3.1.2.1.2 Bioreactors, spinner flasks and stirred culture vessels

The use of bioreactors or spinner flasks, horizontally rotating fluid-filled culture vessels, is particularly amenable to scale-up of the process to produce clinically significant numbers of cells (Cameron et al., 2006) although one problem might be the expense of defined media on a large scale. Bioreactors have been demonstrated to enhance the efficiency of hEB formation (Gerecht-Nir et al., 2004a) and stirred culture vessels have improved hEB proliferation (Cameron et al., 2006). Agglomeration between two mEBs has been demonstrated as the major process limiting cell proliferation and differentiation, a process which is accelerated in stirred culture (Dang et al., 2002) although it is suggested that this can be avoided by using bulb-shaped impellers rather than paddle-type impellers (Schroeder et al., 2005). The encapsulation of mESCs in size-specific support matrices combined with culture in

stirred suspension bioreactors have proved successful for producing large quantities of haematopoietic progenitor cells (Dang *et al.*, 2004).

3.1.2.1.3 Forced aggregation

To improve the heterogeneity of hEB size a forced aggregation has been used (Ng *et al.*, 2005b). This system involves depositing a know number of hESCs grown on MEFs in round-bottom ultra low attachment 96-well plates then aggregating the cell into hEBs by centrifugation After 8-12 days, these hEBs were transferred to tissue-culture treated plates to differentiate further and demonstrated superior haematopoietic precursor frequencies than have previously been reported in serum-free cultures (Tian *et al.*, 2004). Also noted was the effect of initial numbers of hESCs on propensity to differentiate to the haematopoietic lineage with 3000 cells per well producing the highest percentage of hEBs forming blood.

Of all of the methods for hEB formation forced aggregation provides the greatest control over hEB size and cell-cell interaction.

3.1.2.2 Embryoid body adhesion

Once hEBs have formed and developed they become adherent. mEB formation followed by plating of cells on gelatine (reviewed by Conley *et al.*, 2004b) or fibronectin coated plates (Carpenter *et al.*, 2001) is frequently used to continue differentiation. Typically hEBs have been cultured in suspension for 4 or more days before plating on specific matrix components for further differentiation (reviewed by Carpenter *et al.*, 2003). Dang *et al.* (2002) noted no difference in the kinetics or frequency of haematopoietic development between suspension culture, semi-solid methylcellulose medium or hanging drop techniques although, importantly, they demonstrated that attachment prior to d4 impairs haematopoietic development of

mEBs as the mEBs quickly flatten out and loose 3-D structure. Collagen 3D scaffolds have been demonstrated to be useful in the differentiation of hepatocytes from hEBs, and this strategy is suggested to more closely resemble *in vivo* environment than standard hEB culture (Gerecht-Nir *et al.*, 2004b, Baharvand *et al.*, 2006b).

An overview of the variables in steps that can be used in hEB formation and development is shown in Table 3-1.

Table 3-1: Summary of strategies used for hEB formation and differentiation

Summary of the strategies used for hEB formation, including methods of standard culture, methods for culture just prior to hEB formation (Preparation), enzymatic and non-enzymatic dissociation methods, methods for hEB aggregation, hEB growth/development and finally surfaces used for hEB adhesion. TC, tissue culture; CDM, chemically defined medium; FBS, foetal bovine serum.

Culture	Preparation	Dissociation	Aggregation	Development	Adhesion
MEFs	MEFs	Dispase	Suspension culture	Conditioned medium	Gelatin-coated TC dish
	Low density MEFs	Collagenase	96-well forced aggregation	15-20% FBS	
	Collagen TC Flasks	Trypsin	Stirred vessel	Growth factors	TC dish
Matrigel	Matrigel	Scraping	Bioractor	CDM	96-well flat bottom

3.1.3   Factors affecting hEB formation and development

The pattern and efficiency of differentiation are affected by parameters like hESC cell density, media components and amino acids, growth factors and extra-cellular matrix proteins, pH and osmolarity and the particular batch of FBS (Weitzer, 2006).

3.1.3.1   Chemically defined media

The use of CDM removes numerous variables facilitates greater understanding of the factors involved in differentiation. CDM has been successfully used for neuronal differentiation of hESCs (Zhang *et al.*, 2001, Li *et al.*, 2005, Nasonkin and Koliatsos, 2006) and for haematopoietic differentiation, albeit with the addition of a number of

growth factors (Ng *et al.*, 2005b). The most commonly used CDM is that first used for mEB differentiation by Johansson and Wiles (1995), although the same authors also suggest that mesodermal differentiation is inhibited in strictly serum-free conditions (Wiles and Johansson, 1999).

3.1.3.2   *Effects of growth factors on differentiation*

Controlling the growth factor environment that hESCs are exposed to allows us to study how these factors influence cellular differentiation. As detailed in Chapter 1 (1.3) and Chapter 2 (2.1.1), mouse and *Xenopus* studies have implicated the TGFβ, FGF and WNT families in mesoderm induction.

Activin A has been demonstrated to increase the expression of markers of mesoderm in d4 and d5 mEBs such as *T, Mixl1* and *Gsc*, (Ng *et al.*, 2005a, Johansson and Wiles, 1995, Tada *et al.*, 2005). Activin A has been demonstrated to restrict differentiation of hEBs to the mesodermal lineage (Schuldiner *et al.*, 2000). The addition of activin A to hESCs has also been shown to induce differentiation to endodermal rather than mesodermal lineages (Levenberg *et al.*, 2003, D'Amour *et al.*, 2005). This was suggested to only occur when PI3K signalling through insulin/IGF is suppressed (McLean *et al.*, 2007). This apparent paradox in activin A effect is likely explained by the a dose effect, as seen in *Xenopus* animal caps, where lower concentrations promote mesodermal lineage and higher concentrations promoting endodermal lineages (Okabayashi and Asashima, 2003).

NODAL has been demonstrated to maintain pluripotency whilst reducing differentiation to the neuroectodermal linage (Vallier *et al.*, 2004a) Inhibition of NODAL decreases the expression of LEFTY1 and LEFTY2 as well as T and

increases expression of ectodermal markers, suggesting that NODAL has a role in promoting differentiation to the mesodermal lineage (Dvash *et al.*, 2007).

BMP4 has been suggested to be a more potent mesoderm inducer than activin A (Johansson and Wiles, 1995, Ng *et al.*, 2005a) but induces it mesoderm markers (such as *T*) only transiently, suggesting that that BMP4 induces extra-embryonic mesoderm and primitive haematopoiesis (Wilkinson *et al.*, 1990, Johansson and Wiles, 1995) rather than embryonic mesoderm which produces cardiomyocytes and definitive haematopoiesis.

FGF2 has a well established role in maintaining hESC pluripotency (see Introduction, 1.1.7) however treatment of hEBs from d0 onwards with the FGF receptor inhibitor SU5402 demonstrated a significant reduction of expansion by d4 and <1% cell survival by d8 (Joannides *et al.*, 2006). In mEBs, a dominant negative FGFR2 abrogated the formation of the primitive ectoderm layer, by affecting basement membrane formation and mEBs became necrotic after 6-8 days (Li *et al.*, 2001a). These results suggest that FGF2 signalling is essential for hEB growth and development. FGF2 has also been demonstrated to alter the fate of mouse epiblast cells to mesoderm *in vitro* (Burdsal *et al.*, 1998) and be essential for mEB differentiation via signalling through PI3K (Chen *et al.*, 2000). In *Xenopus*, FGF4 has been demonstrated to have a role in mesoderm induction (Isaacs *et al.*, 1994), but in the mouse and in mESCs, FGF4 has been suggested to have a role in maintaining trophectoderm (Feldman *et al.*, 1995, Goldin and Papaioannou, 2003, Guzman-Ayala *et al.*, 2004)

Growth factors that have been used to direct hESC differentiation are reviewed in Table 3-2.

3.1.4 Low molecular weight differentiating agents

It is possible that small molecules can drive differentiation by driving up- or down-regulation of transcription factors. Steroids are likely candidates given that they can directly activate nuclear receptors (Pouton and Haynes, 2005).

All-trans retinoic acid (RA), is essential for mouse normal embryonic development and plays key roles in cell differentiation, proliferation and apoptosis in a concentration dependant manner (reviewed by Ross *et al.*, 2000). Undifferentiated hESCs express retinoid receptors (Huang *et al.*, 2006). In hESCs high concentrations of RA have been shown to induce smooth muscle (Huang *et al.*, 2006) and neurons (Carpenter *et al.*, 2001, Li *et al.*, 2005) but not to be inductive for cardiomyocytes (Xu *et al.*, 2002a). DMSO has also failed to induce hESCs to cardiomyocytes (Kehat *et al.*, 2001, Xu *et al.*, 2002a). 5-aza-2'-deoxycytidine, a demethylating agent, has been demonstrated to successfully improve the differentiation hEBs to cardiomyocytes (Mummery *et al.*, 2002, Xu *et al.*, 2002a, Yoon *et al.*, 2006, Cui *et al.*, 2007), as has ascorbic acid (Passier *et al.*, 2006). A combination of dexamethasone, ascorbic acid-2-phosphate and β-glycerolphosphate has been demonstrated to promote both mesenchymal stem cell and osetogenic differentiation (Olivier *et al.*, 2006, Sottile *et al.*, 2003, Bielby *et al.*, 2004).

Low molecular weight differentiating agents that have been used to direct hESCs differentiation are reviewed in Table 3-2.

Table 3-2: Directed differentiation of hESCs using growth factors and low molecular weight differentiating agents

Table of growth factors and low molecular weight differentiating agents that have been used to direct hESC differentiation. Adapted from Trounson (2006).

Lineage	Primary inducers	Tissue type	Reference
Trophectoderm	FGF2, BMP4	Trophectoderm	(Xu *et al.*, 2002b)
Extraembryonic endoderm	BMP2	Yolk sac	(Pera *et al.*, 2004)
Ectoderm	EGF, FGF2, PDGF-AA, IGF1	Neurons	(Carpenter *et al.*, 2001)
	RA, NGFB	Neurons	(Schuldiner *et al.*, 2001)
	NOG	Neural progenitors	(Pera *et al.*, 2004)
	FGF2, RA, BDNF, TGF-α	Dopaminergic neurons	(Park *et al.*, 2004a)
	NOG	Neural progenitors	(Gerrard *et al.*, 2005)
	FGF2, FGF8, SHH	Forebrain and midbrain TH+ neurons	(Yan *et al.*, 2005)
	FGF2	Transplantable neural progenitors	(Zhang *et al.*, 2001)
	FGF2, EGF, RA, DMSO	Oligodendrocytes	(Nistor *et al.*, 2005)
	FGF2, RA, SHH, BDNF, GDNF, IGF1	Motor neurons	(Li *et al.*, 2005)
	NOG, DKK1, IGF1	Retinal progenitor cells	(Lamba *et al.*, 2006)
	WNT3A, END3, SCF,	Melanocytes	(Fang *et al.*, 2006)
Mesoderm	Dexamethasone, ascorbic acid-2-phosphate, β-glycerolphosphate	Mesenchymal stem cells	(Olivier *et al.*, 2006)
	Dexamethasone, ascorbic acid-2-phosphate, β-glycerolphosphate	Osteogenic cells	(Sottile *et al.*, 2003)
	BMP2	Chondrogenic cells	(Toh *et al.*, 2007)
	5-aza-2'-deoxycytidine	Cardiomyocytes	(Mummery *et al.*, 2002)
	BMP2	Cardiomyocytes	(Mandal *et al.*, 2006)
	BMP4, SCF, FLT3L, IL3, IL6, GCSF	Blood	(Murdoch *et al.*, 2002)
	SCF, TPO, FLT3L	Blood	(Tian *et al.*, 2004)
	VEGF, BMP4	Blood	(Cerdan *et al.*, 2004)
	SCF, FLT3L, TPO, IL3, IL6, GCSF	Blood	(Zhan *et al.*, 2004)
	BMP4, VEGF, SCF, FLT3L, IL6, IGF2	Blood	(Ng *et al.*, 2005b)
Endoderm	Sodium butyrate, DMSO	Hepatocytes	(Rambhatla *et al.*, 2003)
	FGF2, nicotinamide	Pancreatic and Beta-cells	(Segev *et al.*, 2004)
	activin A and low FBS	Definitive Endoderm	(D'Amour *et al.*, 2005)
	activin A and PI3K suppression	Definitive Endoderm	(McLean *et al.*, 2007)

3.1.5 Aims

Substantial heterogeneity exists in hEBs formed from using the mass culture technique. This heterogeneity hinders the analysis of conditions that improve directed lineage differentiation. Using a forced aggregation methodology along with CDM and growth factors that maintain cell viability and promote mesoderm induction, it will be possible to devise a system optimised for mesodermal lineage differentiation. This system will also be tested in multiple hESCs lines to confirm transferability.

The specific aims of this chapter are:

- To assess mass culture heterogeneity.

- To devise a system for controlled hEB formation that improves hEB homogeneity and allows robust differentiation towards the mesodermal lineage.

- To analyse the effect of the system on multiple hESCs lines to confirm transferability and assess inter-line variation.

- To quantify improvements of differentiation to mesoderm derivatives.

3.2 METHODS

3.2.1 hESC culture

The following manually passaged hESC cell lines were used: HUES-7 (p11), kindly gifted by Harvard University (Cowan *et al.*, 2004); BG01 (p24) purchased from BresaGen (Mitalipova *et al.*, 2003) and NOTT1 (p22) and NOTT2 (p18) derived at The University of Nottingham (Burridge *et al.*, 2007). After progression from manual passage on MEFs, continued culture was maintained by enzymatic trypsin passaging on MEFs (CD1 strain, E13.5) and feeder-free culture with trypsin passaging on Matrigel. Briefly, for co-culture MEF feeders were first maintained in 75 cm^2 tissue culture flasks (Falcon, BD Biosciences) with MEF medium which consists of DMEM high glucose (Invitrogen) supplemented with 10% foetal bovine serum (FBS; EU Approved, Invitrogen), 2 mM Glutamine (Sigma) and 1% Non-Essential Amino Acids (Sigma) and passaged by exposure to a minimal volume of 0.05% Trypsin-EDTA (Invitrogen) for 1 min at 37 °C, followed by tapping of the flasks to liberate single cells. At p2 MEFs were mitotically inactivated for 2.5 hours with 10 μg ml^{-1} mitomycin C, trypsin passaged and seeded at 6 x 10^4 cm^{-2} onto 35, 65 or 90 mm tissue culture dishes or 8-well chamber slides (NUNC) and used 24-48 hours later. For creation of conditioned medium for hESC feeder-free culture mitomycin C treated p2 MEFs were plated into T75 flasks as before. Standard culture medium, referred to as BGK in Denning *et al.*, (2006), which consists of DMEM-F12 (Invitrogen) supplemented with 15% Knockout serum replacement (Invitrogen), 2 mM Glutamine (Sigma) and 1% Non-Essential Amino Acids, 100 μM 2-Mercaptoethanol (Sigma) and 4 ng ml^{-1} FGF2 (Peprotech) was conditioned for 22-26 hours on mitomycin C treated MEFs, pooled and supplemented with an additional 4 ng ml^{-1} FGF2 (referred to as conditioned medium). Medium was conditioned for 5

consecutive days and unused aliquots were frozen for use at a later date. Feeder-free

hESC cultures were maintained on 25-75 cm² tissue culture flasks (Falcon, BD

Biosciences) coated with Matrigel (Matrix Growth Factor Reduced, BD Biosciences)

in conditioned medium and passaged with trypsin (Denning *et al.*, 2006, Xu *et al.*,

2001). All culture was carried out at 37 °C in a humidified atmosphere containing

5% CO_2. Medium was changed daily for hESC culture. All lines were shown to be

karyotypically normal before use and expressed high levels of the stem cell markers

SSEA4, TRA-1-60 and TRA-1-81 and were negative for SSEA1 expression.

3.2.2   hEB formation and size assessment

hEBs were formed by either of two methods referred to as mass culture or forced

aggregation. The mass culture method, described previously (Denning *et al.*, 2006),

involved culture of hESCs on MEFs to confluence in a 90 mm dish, as detailed

above, followed by treatment with Collagenase IV (Sigma) for 15 min at 37 °C then

scraping with a cell scraper (Orange Scientific). The clumps formed by this process

were then suspended in conditioned medium, further disaggregated by vigorously

pipetting with a 10 ml pipette and centrifuged at 100 *g* for 4 min before transfer into

fresh conditioned medium and a 90 mm bacteriological Petri dish. The forced

aggregation method is based a protocol devised by Ng *et al.*, (2005b) with

improvements to allow the use of hESCs cultured on Matrigel, (see Figure 3-1).

Briefly, hESCs were grown in 25 cm² flasks to standard confluence (1.8×10^5 cells

cm^{-2}) on Matrigel in conditioned medium, trypsin passaged as above and re-

suspended at either 1×10^4 cells ml^{-1}, 3×10^4 cells ml^{-1} or 1×10^5 cells ml^{-1} in either:

conditioned medium; differentiation medium, which consists of DMEM high glucose

(Invitrogen) supplemented with 20% fetal bovine serum (FBS; EU Approved,

Invitrogen), 2 mM Glutamine (Sigma) and 1% Non-Essential Amino Acids and 100

μM 2-Mercaptoethanol (Sigma); or CDM with BSA (Vallier *et al.*, 2005) which consists of 50% F-12 Nutrient Mixture (Ham's, Invitrogen), 50% Iscove's Modified Dulbecco's Medium (Invitrogen), 5 mg ml^{-1} bovine serum albumin fraction V (BSA), 1 x Chemically Defined Lipid Concentrate (Invitrogen), 450 μM 1-Thioglycerol (Sigma), transferrin (Sigma) and insulin (Roche). Differentiation medium was also tested with 10% serum instead of 20% and CDM was tested replacing BSA with 1 mg ml^{-1} polyvinyl alcohol (PVA, Sigma). A summary of mediums used in this study is included in Table 3-3. Cells were then pipetted into U-bottom (U-96), V-bottom (V-96), or U-bottom ultra low attachment (ULA U-96) 96-well plates and centrifuged at 950 *g* for 5 min. hEBs were kept in suspension by pipetting every other day. Samples were collected every 2 days between days 2-12 and the medium was changed every 3 days. hEB sizes were assessed both in the wells and after transfer to dishes to remove optical distortion created by U and V bottom plates using a Nikon TE2000 microscope.

Figure 3-1: Schematic of the 96-well forced aggregation procedure

A) All hESC lines were cultured on Matrigel in conditioned medium (BGK CM) with trypsin passaging. B) On d0 hEB formation was initiated by seeding into 96-well plates and centrifuging at 950 g for 5 min at room temperature. For media and plate combination testing hEBs were matained at this stage upto d12. C) For cardiomyocyte and blood differentiation hEBs cells were maintained in V-96 plates (step B) for 2, 4 or 6 days before transferr into untreated 90 mm Petri dishes containing D-FBS20 for 6 days (cardiomyocytes) or 12 days (blood). D) For the final stage of cardiomyocyte differentiation hEBs were individually re-plated into untreated U-bottomed 96-well plates and maintained upto d24.

Table 3-3: List of media assessed for hEB formation and maintenance efficiency

Highlighted media are those also used for maintaining hESC pluripotency.

Media	Acronym	Base	Serum	Growth factors	Additional ingredients
Standard Culture Medium	BGK	DMEM:F12	15% KSR	4 ng ml⁻¹ FGF2	glutamine, NEAA, 2-mercaptoethanol
Conditioned Medium	BGK CM	DMEM:F12	15% KSR	4 ng ml⁻¹ FGF2	glutamine, NEAA, 2-mercaptoethanol. 24 h on MEFs, refreshed 4 ng ml⁻¹ FGF2
Differentiation Medium with 20% FBS	D-FBS20	DMEM	20% FBS	None	glutamine, NEAA, 2-mercaptoethanol
Differentiation Medium with 10% FBS	D-FBS10	DMEM	10% FBS	None	glutamine, NEAA, 2-mercaptoethanol
Chemically Defined Medium with BSA	CDM-BSA	IMDM:F12	None	None	BSA, lipid concentrate, 1-thioglycerol, transferrin and insulin (Vallier *et al.*, 2004)
Chemically Defined Medium with PVA	CDM-PVA	IMDM:F12	None	None	PVA, lipid concentrate, 1-thioglycerol, transferrin and insulin
Chemically Defined Medium with PVA supplemented with FGF2 and activin A	CDM-PVA+	IMDM:F12	None	12 ng ml⁻¹ FGF2, 10 ng ml⁻¹ activin A	PVA, lipid concentrate, 1-thioglycerol, transferrin and insulin

3.2.3 Tissue processing and haematoxylin-eosin staining

hEBs were washed in twice in D-PBS (Invitrogen), fixed in 4% paraformaldehyde (PFA, Sigma) in D-PBS for 15 min then washed twice in D-PBS again. hEBs were then set into 1% agarose (Invitrogen) in distilled H_2O and processed over-night using Shandon Excelsior tissue processor (Thermo). Processed agarose blocks were then embedded in paraffin wax (Tissue-Tek) using a Tissue-Tek III thermal / dispensing / cryo-consol and sectioned using a microtome at 5 μm and affixed to SuperFrost Plus slides (Menzel-Glaser). Slides/sections were dewaxed using xylene (VWR), rehydrated through a Ethanol/H_2O gradient, stained with Harris' Haematoxylin (VWR) and Eosin Yellowish (VWR) then dehydrated and mounted using DePeX mounting medium (VWR) before visualisation using a Leica DMRB upright microscope and Improvision OpenLab 4.0.2 and Velocity 4 software.

3.2.4 Cardiomyocyte formation assay

To assess cardiomyocyte formation hEBs were formed from 1000, 3000 or 10000 HUES-7, BG01, NOTT1 or NOTT2 hESCs in V-96 plates in either BGK-CM, CDM-PVA or CDM-PVA supplemented with 12 ng ml^{-1} activin A and 10 ng ml^{-1} FGF2 (CDM-PVA+). After either 2, 4 or 6 days hEBs were transferred into 90 mm Petri dishes containing D-FBS20 for 6 days. hEBs were kept in suspension by pipetting every other day. hEBs were then transferred into U-96 well plates (1 hEB per well) containing D-FBS20 and cultured upto day 24. At each stage medium was changed every 3 days. At d24 the number of wells per plate with beating areas was assessed using a Nikon TE2000 microscope.

3.2.5 Haematopoietic colony-forming assay

To assess haematopoietic potential hEBs were cultured as above (3.2.4) but maintained until d16 in the 90 mm Petri dishes in D-FBS20. At d16 the hEBs were disaggregated with trypsin and cells were counted and suspended in MethoCult growth factor enriched methylcellulose (HF4434, Stem Cell Technologies) which contains BSA, FBS, Stem Cell Factor (KITLG), GM-CSF (CSF2), IL3 and Erythropoietin (EPO). Cell suspensions were then transferred to 35 mm dishes and cultured for up to 30 days. Colonies of haematopoietic appearance were isolated; cytospun onto SuperFrost Plus slides (Menzel-Glaser), fixed in methanol and stained with Wright-Giemsa (BDH) before visualisation using a Leica DMRB upright microscope and Improvision OpenLab 4.0.2 and Velocity 4 software.

3.2.6 Non-author contributions to results

The modification and adaptation of forced aggregation of hEBs from defined numbers of hESCs in ultra low-attachment U-bottom plates as described by Ng *et al.*, (2005b) to V-bottom plates was done jointly by P. Burridge and C. Denning. The use of V-96 plates was suggested by C. Denning, while selection of conditioned medium and chemically defined medium for hEB formation was jointly discussed and formulated by P. Burridge and C. Denning. The additional media types used were selected by P. Burridge, who also developed and optimised all Bond-max histology protocols. Haematopoietic differentiation protocols were jointly developed by P. Burridge and H. Priddle. The experiments to assess inter-line variability were devised by C. Denning and L. Young and performed jointly by C. Denning, P. Burridge, D. Anderson and H. Priddle.

3.3 RESULTS

3.3.1 Size variability in mass culture hEBs

To assess traditional methods of hEBs formation, HUES-7 and BG01 hESCs cultured on MEFs or Matrigel were harvested by treatment with either collagenase IV or trypsin. Cells were place in suspension in mass culture in conditioned medium (BGK CM) to allow hEBs to form for 6 days at which in time hEB size was assessed. BGK CM was used for hEB formation as previous experiments within our lab had demonstrated that when directly transferring disaggregated hESCs produced via the scraping method to a differentiation medium (D-FBS20) hEB formation was unsuccessful (Denning *et al.*, 2006). Measurements were taken in two directions, at 90° to each other (See Table 3-4). These results demonstrated a substantial heterogeneity in the size of hEBs produced, particularly with the commonly used collagenase IV treatment of hESCs on MEFs with hEB diameters ranging from 100-850 μm and 175-1100 μm for HUES-7 and BG01 respectively. Treatment of HUES-7 cells grown on Matrigel with trypsin produced the most homogenous hEBs with diameters ranging from 137-288 μm although the number of hEBs was poor. No hEBs formed when using these conditions with BG01 cells. Figure 3-2 contains example images of the heterogeneity of hEBs formed by traditional mass culture method. Incubation of hanging drop cultures seeded with between 300 and 10000 HUES-7 or BG01 cells for up to 6 days in BGK CM failed to produce hEBs (Burridge *et al.*, 2007) as noted by others (Reubinoff *et al.*, 2000).

Table 3-4: Formation of hEBs from HUES-7 and BG01 by mass culture

hESC lines HUES-7 and BG01 were cultured using one of three methods and induced to form hEBs. Coll IV, collagenase IV; SE, standard error. Data courtesy of C. Denning (Burridge *et al.*, 2007).

hESC line	Passage	Matrix	Enzyme	hEB #	Ave. Diameter	SE	Diameter range (μm)
HUES-7	p25	MEFs	Coll IV	40	166	26	100-850
HUES-7	p28	Matrigel	Coll IV	40	211	12	75-400
HUES-7	p28	Matrigel	Trypsin	40	187	6	137-288
BG01	p51	MEFs	Coll IV	40	333	27	175-1100
BG01	p52	Matrigel	Coll IV	40	178	9	100-450
BG01	p52	Matrigel	Trypsin	40	0	0	0-0
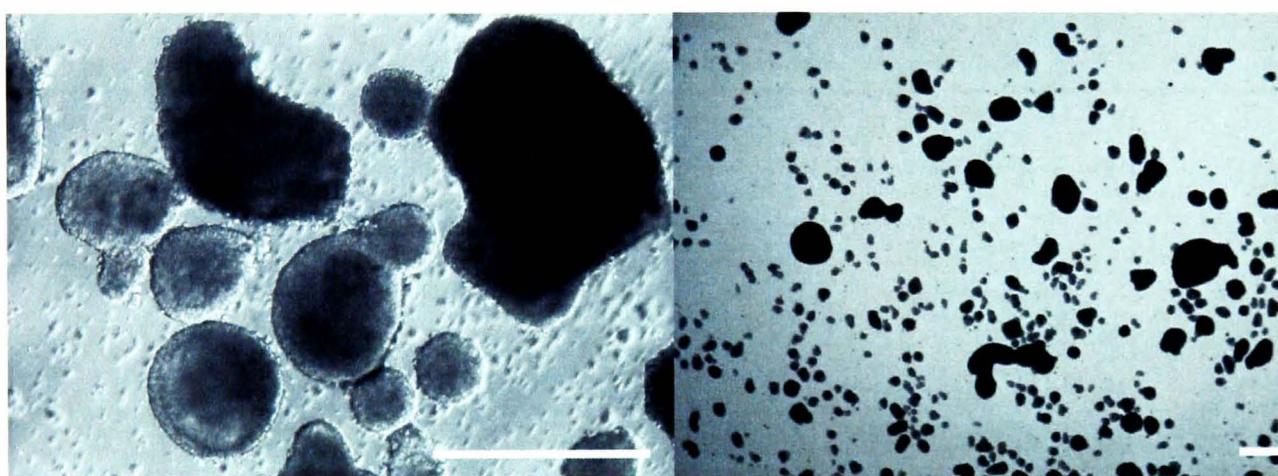
Figure 3-2: Image of hEBs formed by suspension culture

Representative image of d6 hEBs formed in BGK CM in suspension culture by collagenase IV treatment and scraping of HUES-7 cells grown on MEF feeders. Scale bar= 500 μm (images courtesy of D. Anderson (Burridge *et al.*, 2007)).

3.3.2 Comparison of 96-well plate formats and cell seeding density on forced aggregation hEBs

These observations (3.3.1) prompted the evaluation of methods to generate hEBs directly from trypsin passaged hESCs cultured on Matrigel. The forced aggregation system devised by Ng *et al.*, (2005b) was evaluated and potential improvements were tested. The combination of this system with hESCs maintained feeder-free conditions would enable the formation of hEBs from a defined number of cells and therefore potentially reduce variability in hEB size. Ultra-low attachment plates (ULA U-96)

plates used by Ng *et al.*, (2005b) were prohibitively expensive for large scale experiments so comparisons were made using standard uncoated U-bottom and V-bottom plates alongside ULA plates. Trypsin dissociated HUES-7 hESCs were re-suspended in BGK CM at plated in 100 µl volumes into 96-well plates at 1000, 3000 and 10000 cells per well and centrifuged. Medium was changed in the wells every three days up to day 12. Comparisons were made between the number of hEBs per well (Figure 3-4) and the number of single or multiple hEBs per well (Figure 3-5).

hEB formation was also visually assessed. If hEBs were present ~5 hEBs from each seeding density and plate type were removed from the 96-well plate to a 35mm flat bottomed tissue culture dish to remove any effect the shape of the well may have on perceived hEB size and remove any free floating hESCs that obscured the hEB. Pictures were taken every 2 days of representative wells from each cell number/plate combination and hEBs discarded (Figure 3-6).

Centrifugation of HUES-7 cells in untreated U-bottom plates resulted in erratic and/or poor hEB formation (Figure 3-5). In contrast V-bottom plates produced hEBs at a similar efficiency to ULA U-96 plates of >90% hEB formation per well. The presence of a single hEB or a number of hEBs in each well was also observed (Figure 3-5) and demonstrated that wells seeded with 3000 cells produced a higher proportion or multiple hEBs per well. hEBs formed in ULA U-96 plates showed higher levels of agglomeration than those formed in V-96 plates. When using these conditions without centrifugation no hEB formation was observed (observation C. Denning (Burridge *et al.*, 2007)).

Visual analysis of hEB formation and development was also observed with HUES-7 hESCs (Figure 3-6). In U-bottom plates hESCs formed no hEBs with 1000 or 3000 cells and numerous small hEBs in each well from 10000 cells. ULA U-96 plates

formed no hEBs with 1000 cells, small hEBs with 3000 cells and hEBs comparable to those made in V-bottom plates with 10000 cells. V-bottom wells provided a single consistent hEBs in each well at all cell numbers.

Together these experiments demonstrated that hEBs can be efficiently formed from either 3000 or 10000 HUES-7 hESCs and uncoated V-bottom plates to be most advantageous for producing single hEBs per well. A visual comparison between hEBs produced by mass culture and the optimised forced aggregation system is provided in Figure 3-3 and demonstrates the proportional increase in hEB formation and homogeneity provided by this system.
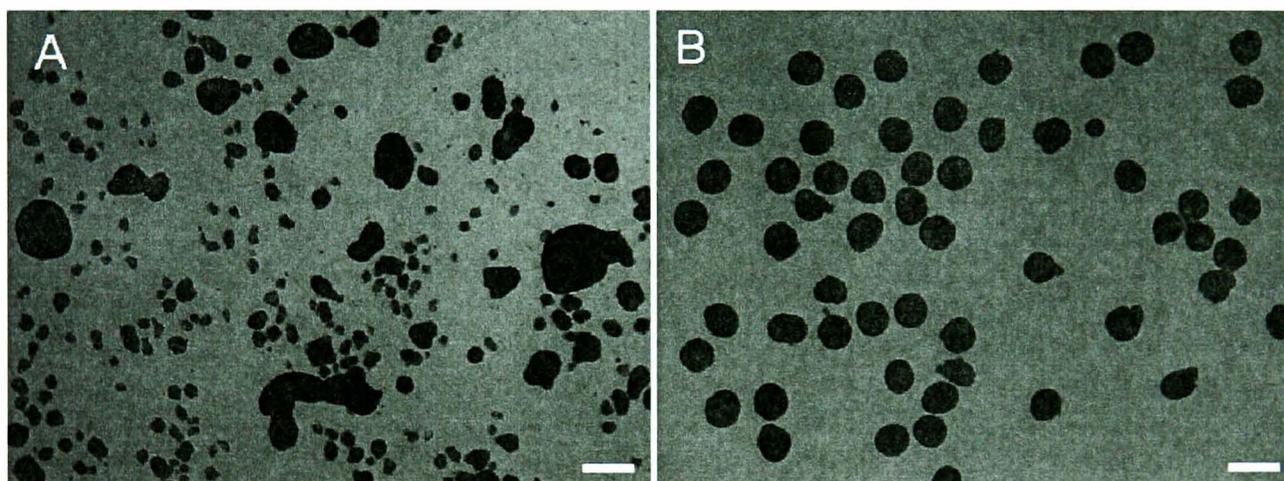
Figure 3-3: Visual comparison of hEBs produced by the mass culture and forced aggregation systems

Representative image of d6 hEBs A) formed in BGK CM in suspension culture by collagenase IV treatment and scraping of HUES-7 cells grown on MEF feeders and B) hEBs formed in BGK CM from 10000 HUES-7 cells per well grown on Matrigel. Scale bar= 500 μm (images courtesy of D. Anderson).
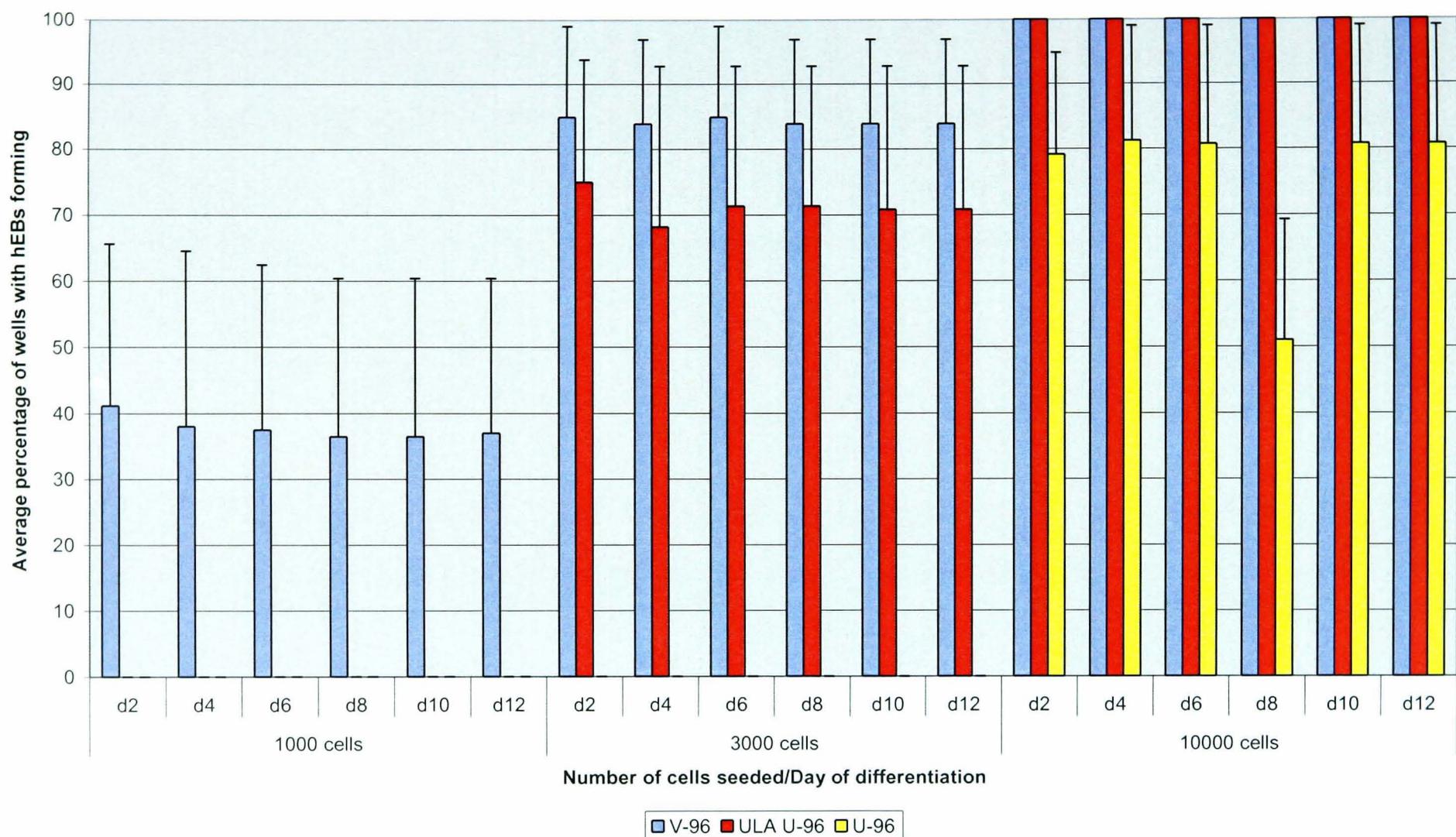
Figure 3-4: Effect of cell seeding density and 96-well plate format on the number of hEBs formed per well

HUES-7 hEBs were formed in BGK CM from 1000 (left), 3000 (centre) or 10000 (right) cells per well in either uncoated V-bottom (V-96, blue bar); ultra low attachment coated U-bottom (ULA U-96, red bar) or uncoated U-bottom 96-well plates (U-96, yellow bar). hEBs were maintained in the wells and medium was changed every 3 days. Numbers of wells with 1 or more hEBs present were recorded every 2 days over 12 days of differentiation. Each data point represents the average percentage of wells (±SEM) of 2 independent experiments (192 wells in total). In total 3456 wells were counted in these experiments.
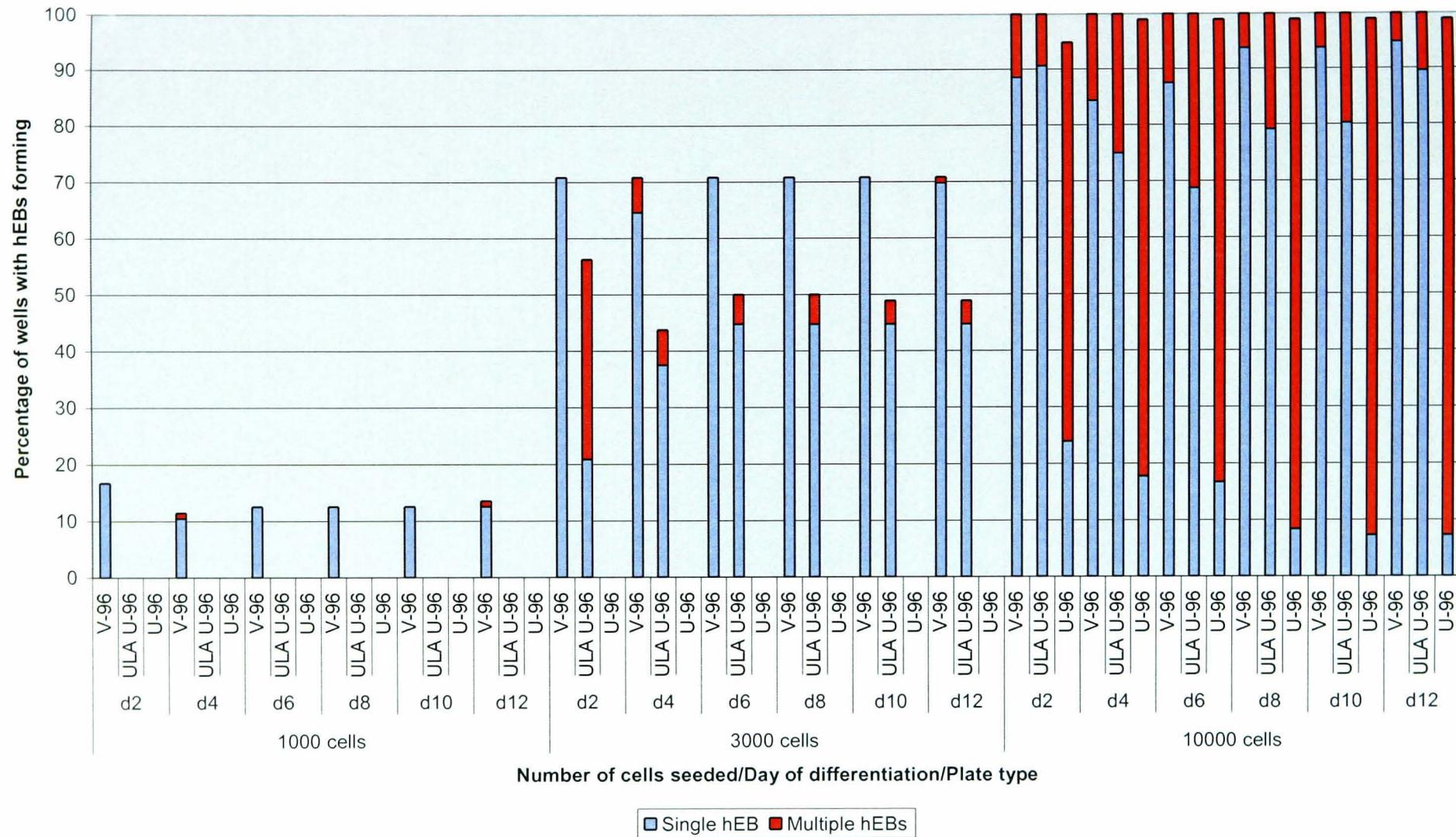
Figure 3-5: Effect of cell seeding density and 96-well plate format on the number of single or multiple hEBs formed per well

HUES-7 hEBs were formed in BGK CM from 1000 (left), 3000 (centre) or 10000 (right) cells per well in either uncoated V-bottom (V-96); ultra low attachment coated U-bottom (ULA U-96) or uncoated U-bottom 96-well plates (U-96). hEBs were maintained in the wells and medium was changed every 3 days. Numbers of wells with 1 hEB (blue bar) or more 1 hEB (red bar) present were recorded every 2 days over 12 days of differentiation. Each data point represents the percentage of wells one experimental replicate (96 wells in total). In total 1725 wells were counted in this experiment.
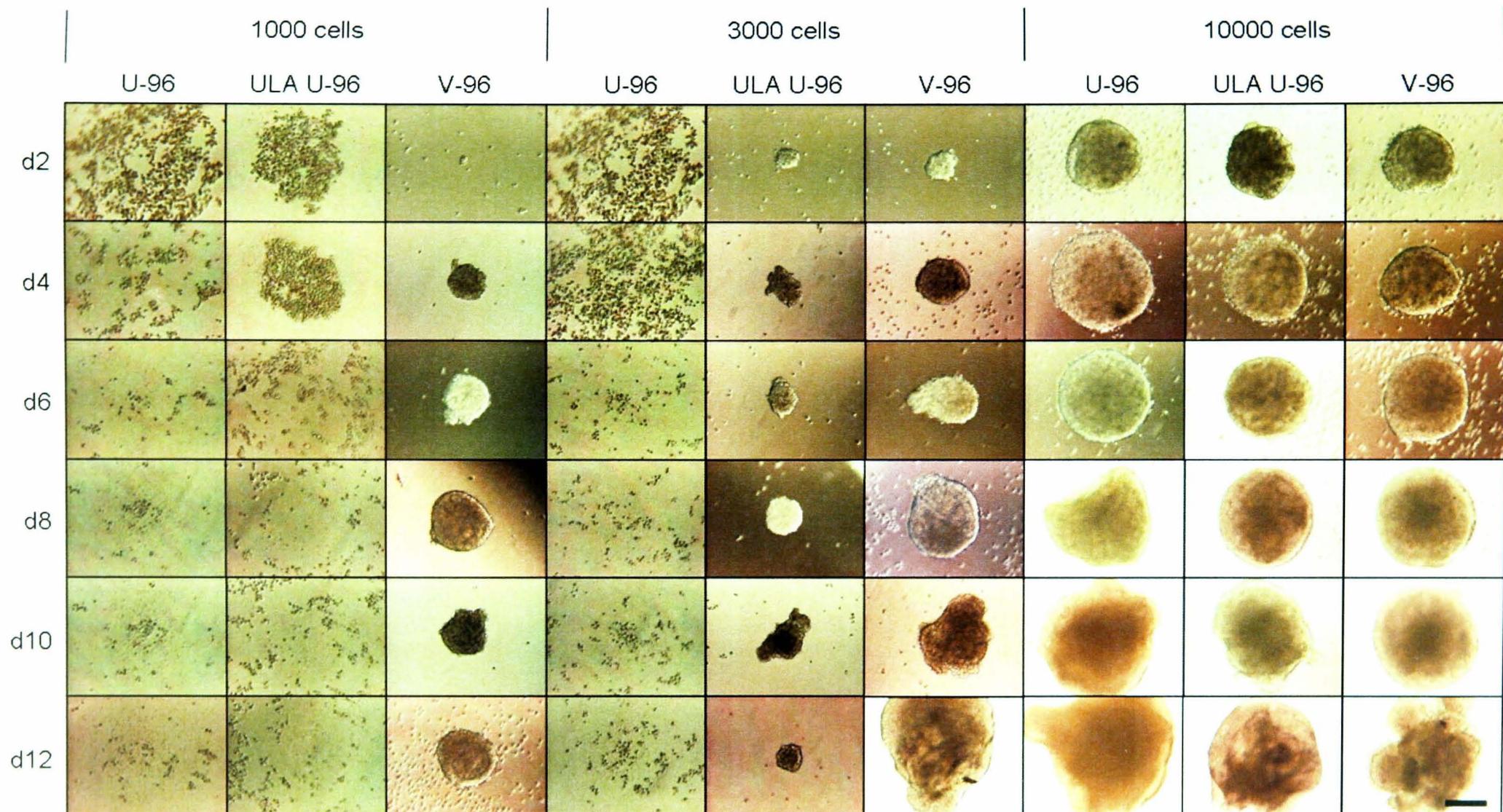
Figure 3-6: Visual analysis of the effect of 96-well plate formats and cell seeding density on forced aggregation HUES-7 hEB formation and maintenance

HUES-7 hEBs were formed in BGK CM from 1000 (left), 3000 (centre) or 10000 (right) cells per well in either uncoated U-bottom 96-well (U-96), ultra low attachment coated U-bottom (ULA-96) or uncoated V-bottom (V-96) plates. hEBs were maintained in the wells and medium was changed every 3 days. hEBs were removed from plates every 2 days and photographed. Data collected from two experimental replicates. Scale bar = 100 µl.

3.3.3 Visual analysis of the effect of media and cell number on forced aggregation hEB formation and maintenance

A variety of media were tested to determine capacity for supporting hEB formation. The media tested were unconditioned medium (BGK), differentiation medium with 10% serum (D-FBS10), differentiation medium with 20% serum (D-FBS20), and conditioned medium (BGK CM) to be used as a control. A semi-chemically defined medium (CDM-BSA, Johansson and Wiles, 1995, Vallier *et al.*, 2005) was also trialled along with a fully chemically defined medium as CDM-BSA but replacing BSA with the chemically defined PVA (CDM-PVA, personal communication Ludovic Vallier, University of Cambridge). In addition CDM-PVA supplemented with 10 ng ml^{-1} activin A and 12 ng ml^{-1} FGF2 was also trailed (CDM-PVA+). Activin A is a well established mesoderm inducer allowing for an increase in the population of mesodermal cells before further differentiation, FGF2 was included to maintain cell proliferation in, what is, a limiting medium. Trypsin dissociated HUES-7 hESCs were re-suspended in the 7 different media at plated in 100 μl volumes into 96-well V-bottom plates either 3000 or 10000 cells per well and centrifuged (Figure 3-7). hEBs were removed from the well to photograph as above. Medium was changed in the wells every three days up to day 12. Analysis of percentage hEB formation in different media is provided in Figure 3-8. Consistent with the above, data high efficiency of formation and maintenance (100%) up to d12 was noted with BGK CM. High efficiency was also observed in CDM-PVA and CDM-PVA+. hEB formation in less efficient CDM-BSA (77-90%), unconditioned medium (BGK, 66-82%) and standard differentiation mediums (D-FBS10 or D-FBS20, 0%). Therefore subsequent differentiation experiments focussed on formation, growth and

differentiation from hEBs formed in V-96 plates using BGK CM, CDM-PVA and CDM-PVA+.
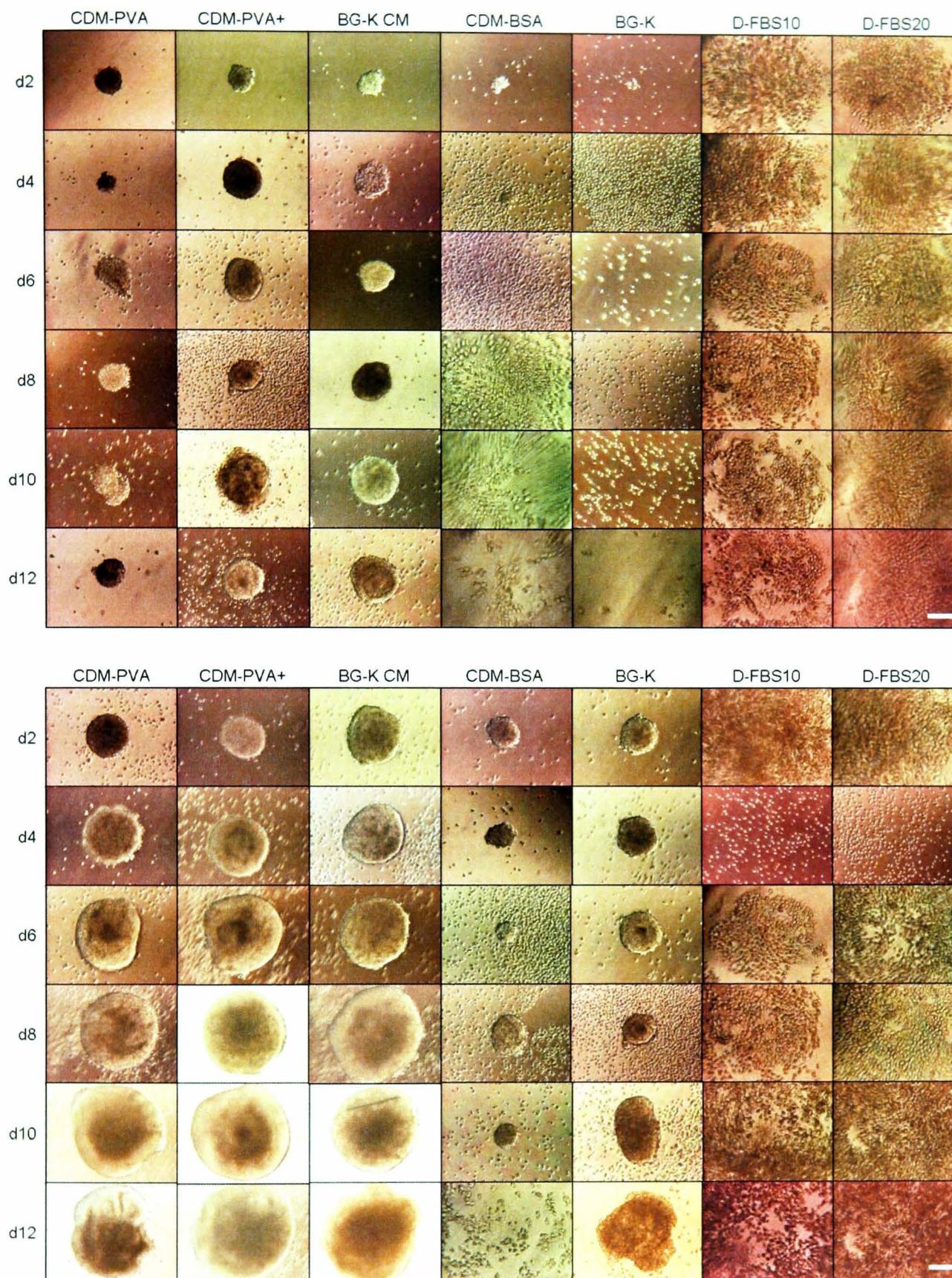
Figure 3-7: Effect of different media on HUES-7 hEB formation and development using hEBs formed from 3000 and 10000 cells

HUES-7 hEBs were formed from 3000 (top) and 10000 (bottom) cells per well in uncoated V-bottom plates in CDM-PVA, CDM-PVA+, BGK CM, CDM-BSA, BGK, D-FBS10, D-FBS20. hEBs were maintained in the wells and media were changed every 3 days. hEBs were removed from plates and photographed every 2 days. Data collected from two experimental replicates. White scale bar = 100 μm.
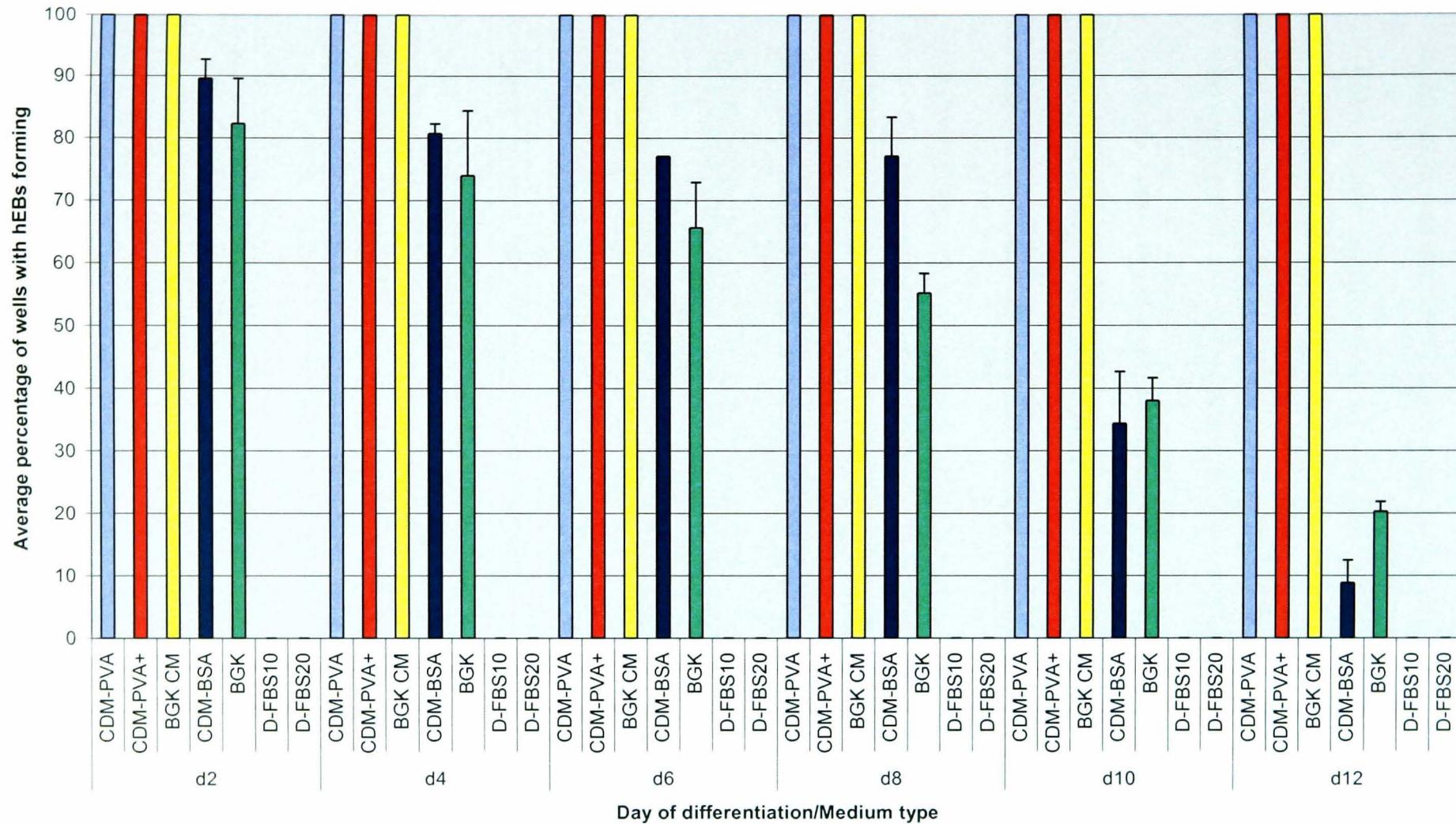
Figure 3-8: Analysis of HUES-7 hEB formation in different media

HUES-7 cells were plated out at 10000 cells per well in uncoated V-bottom (V-96) plates in CDM-PVA, CDM-PVA+, BGK CM, CDM-BSA, BGK, D-FBS10 or D-FBS20. hEBs were maintained in the wells and media were changed every 3 days. Numbers of wells with 1 or more hEBs present were recorded every 2 days over 12 days of differentiation. Each data point represents the average percentage of wells (±SEM) of 2 independent experiments (192 wells in total). In total 6912 wells were counted in these experiments.

152

3.3.4 Histology of hEBs

To assess the effects of hEBs formation method on the development and internal structure formation, hEBs were sectioned and stained with haematoxylin and eosin (H&E) which highlight nuclei and cytoplasm respectively. HUES-7 hEBs were formed either by mass suspension culture of cells cultured on MEFs and harvested with collagenase IV and scraping (Figure 3-9) or by forced aggregation of trypsin-passages cells cultured on Matrigel. For the forced aggregation, V-96 well plates were seeded with 1000, 3000 and 10000 HUES-7 hESCs in BGK CM (Figure 3-9) or CDM-PVA (Figure 3-10). Medium was changed on d3 and hEBs were collected on d2, d4 and d6.

Forced aggregation hEBs cultured in BGK CM appeared more dense and uniform that mass culture hEBs between d2-d4 and the cells forming mass culture hEBs appeared to have larger cytoplasms. Similar results were seen for hEBs formed from either 1000, 3000 or 10000 cells. Distinct change in both forced aggregation and mass culture hEBs was detected at d6 with large internal cavities forming. In mass culture hEBs a single large central cavity formed whereas in forced aggregation hEBs numerous cavities formed throughout the hEBs. Forced aggregation hEBs formed in CDM-PVA appeared similar to those formed in BGK CM between d2-d4 but at d6 the CDM-PVA hEBs were substantially less cavitated and no hEBs formed from 1000 cells remained.
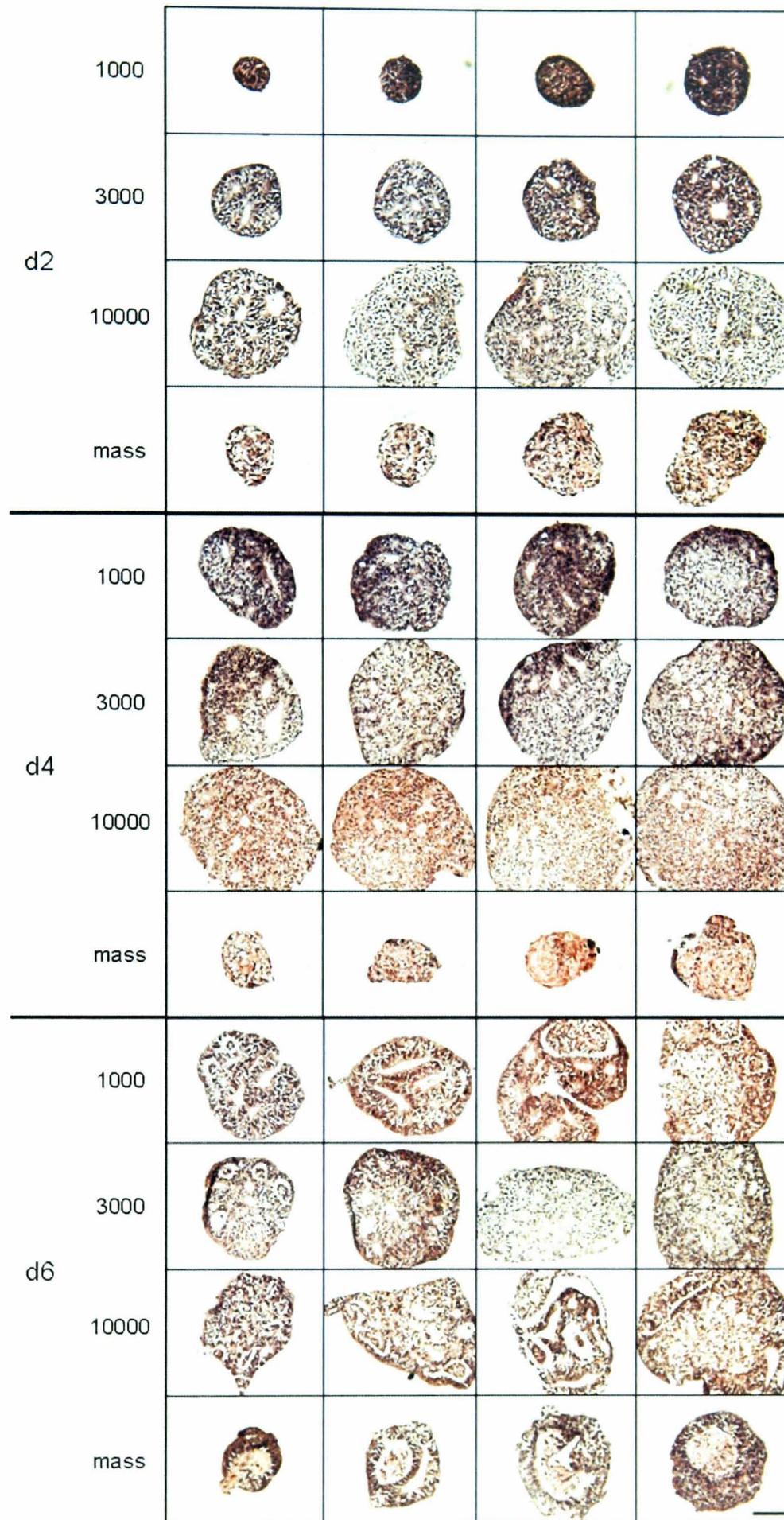
Figure 3-9: Haematoxylin and eosin staining of HUES-7 hEBs formed by forced aggregation and mass culture in BGK CM

Images of representative hEBs formed in BGK CM from 1000, 3000 and 10000 cells and mass culture and stained with H&E at d2, d4 and d6. Black scale bar = 100 μm.
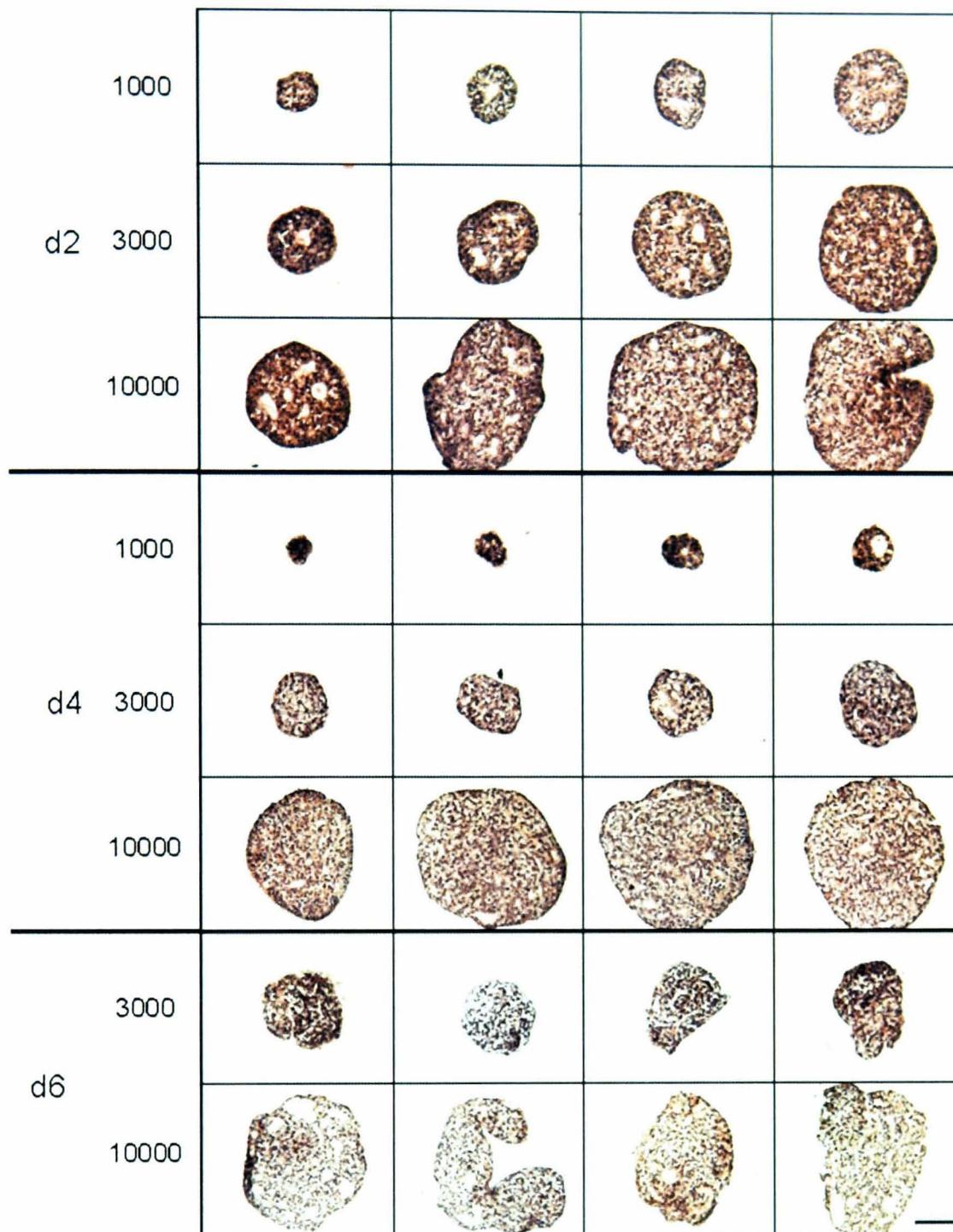
Figure 3-10: Haematoxylin and eosin staining of HUES-7 hEBs formed by forced aggregation in CDM-PVA

Images of representative hEBs formed in CDM-PVA from 1000, 3000 and 10000 cells stained with H&E at d2, d4 and d6. Black scale bar = 100 μm.

3.3.5   Inter-line comparison of hEB development using BGK CM and the forced aggregation system

To further study the forced aggregation system using V-96 plates, the kinetics of hEB growth in relation to input cell number, days of differentiation and media were investigated. hEBs were formed from 1000, 3000 and 10000 HUES-7, BG01,

155

NOTT1 and NOTT2 hESCs by forced aggregation in BGK CM. Cells were seeded in triplicate and one plate at each density was cultured until d2, d4 or d6, at which time 40 hEBs were removed and average hEB size was calculated (see Figure 3-11). Analysis of hEB size indicated a high degree of reproducibility between experiments and both increasing input cell number and day of differentiation contributed to increasing size (Figure 3-11). Similar overall growth profiles were observed between lines. However, significant differences in growth profiles were observed during the first 6 days of differentiation (p = 0.437 to 0.001; one-way analysis of variance (ANOVA)).
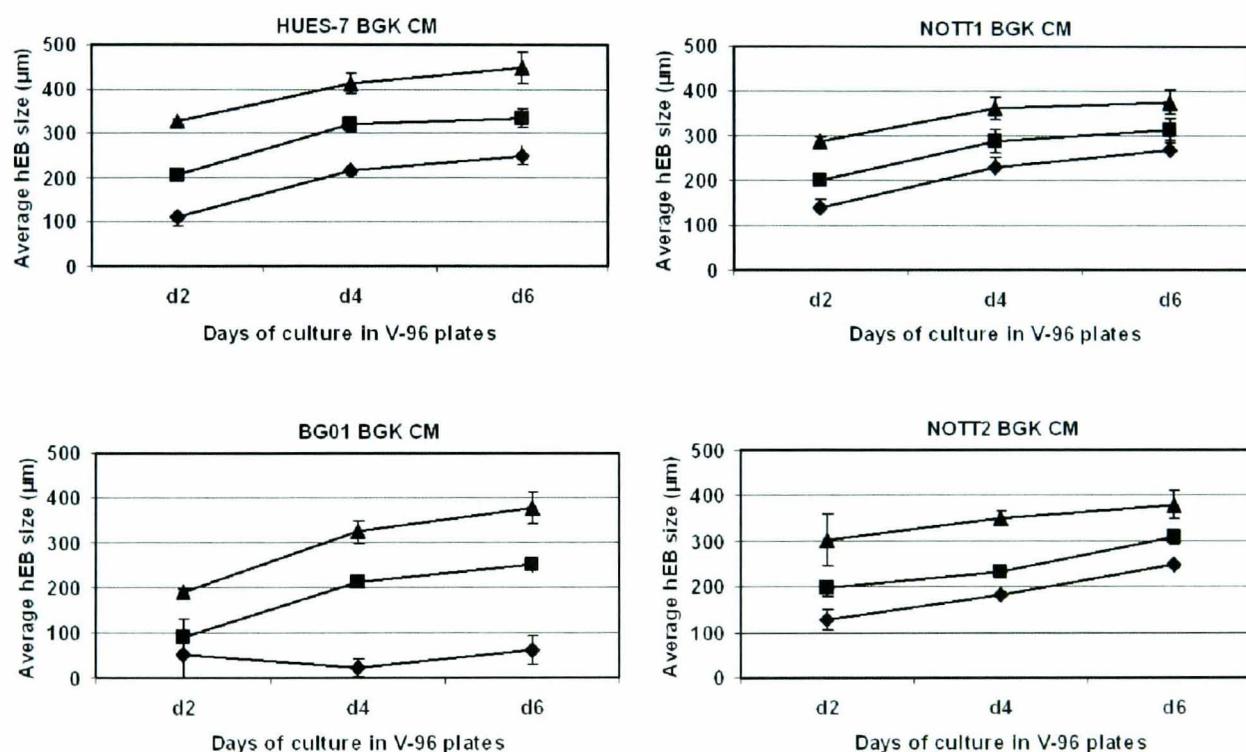
	Day of transfer to D-FBS		
Cell number	Day 2	Day 4	Day 6
1000	0.364	**0.002**	0.062
3000	0.325	**0.001**	0.437
10000	0.429	**0.001**	**0.042**

Figure 3-11: Size of hEBs produced from 4 hESCs in BGK CM

hEBs were formed in BGK CM from the hESC lines HUES-7, BG01, NOTT1 and NOTT2 from 1000 (♦), 3000 (■) or 10000 (▲) cells in V-bottom plates and assessed for size every 2 days. Each data point represents average (±SEM) of between 2 and 4 independent experiments. Table represents inter-line comparisons by one-way ANOVA, numbers in bold indicate significant differences between lines. Data produced in collaboration with C. Denning and D. Anderson.

3.3.6 Inter-line comparison of hEB development using CDM-PVA and CDM-PVA+ and the forced aggregation system

To study the effect of CDM-PVA and CDM-PVA+ on the kinetics of hEB growth in relation to input number hEBs were formed from 1000, 3000 and 10000 HUES-7, BG01 or NOTT1 hESCs in either CDM-PVA or CDM-PVA+ (Figure 3-12). For hEBs formed in both CDM-PVA and CDM-PVA+, hEBs initiated from 10000 cells increased in size from d2 to d6 of differentiation. However, the size of hEBs formed from 3000 cells remained static or declined and those formed from 1000 cells declined suggesting this medium is less efficient that CM for hEB growth. Similar overall growth profiles were observed between lines. However, significant differences in growth profiles were observed during the first 6 days of differentiation ($p = 0.880$ to 0.007; one-way ANOVA).

Figure 3-12: Size of hEBs produced from 3 hESC lines in CDM-PVA and CDM-PVA+

hEBs were formed in CDM-PVA and CDM-PVA supplemented with activin A and FGF2 (CDM-PVA+) from the hESC lines HUES-7, BG01, NOTT1 and from 1000 (♦), 3000 (■) or 10000 (▲) cells in V-bottom plates and assessed for size every 2 days. Each data point represents average (±SEM) of between 2 and 4 independent experiments. Table represents inter-line comparisons by one-way ANOVA, numbers in bold indicate significant differences between lines Data produced in collaboration with C. Denning and D. Anderson.

3.3.7 Cardiomyocyte differentiation

The reproducibility of the V-96 forced aggregation system and the ability to dictate hEB size by altering input cell number provided an opportunity to carry out a systematic comparison of mesodermal differentiation efficiency between the four

hESCs. Cardiomyocytes were used as an indication of successful mesoderm induction due to the speed, simplicity and low cost of their differentiation in comparison to haematopoietic lineages and the ability to accurately score successful differentiation by simply counting the number of beating wells which has been demonstrated as proportional to αMHC gene expression (Burridge *et al.*, 2007). hEBs were formed form 1000, 3000 or 10000 HUES-7, BG01, NOTT1 or NOTT2 hESCs in BGK CM (Figure 3-13) or CDM-PVA and CDM-PVA+ (Figure 3-14) and cultured until d2, d4 or d6 of differentiation. hEBs were then switched to D-FBS20 in uncoated 90 mm dishes for 6 days before transfer to uncoated U-96 plates and maintained until d24 of differentiation (Figure 3-1) when the number of wells with beating areas were counted.

For all four hESC lines, formation in BGK CM and transfer to D-FBS20 on d2 yielded limited number of beating hEBs. Similarly, cardiomyocyte differentiation was consistently poor using 1000 cells with transfer on d2, d4 or d6. There were significant inter-line differences in absolute efficiency of the most successful conditions for cardiomyocyte production: HUES-7 (3000 cell, d4), 9.5±0.9%; BG01 (10000 cells, d6) 1.6±1.0%; NOTT1 (10000 cells d6), 5.3±3.1%; NOTT2 (1000 cells d6), 6.6±2.4%; $p = 0.008$, one-way ANOVA.

HUES-7 hEBs formed in CDM-PVA from 10000 cells and switched to D-FBS20 at d2 of differentiation produced 4.2±2.9% beating areas at d24. This was increased significantly to 23.6±3.6% by formation in CDM-PVA+ ($p = 0.01$, T-test).
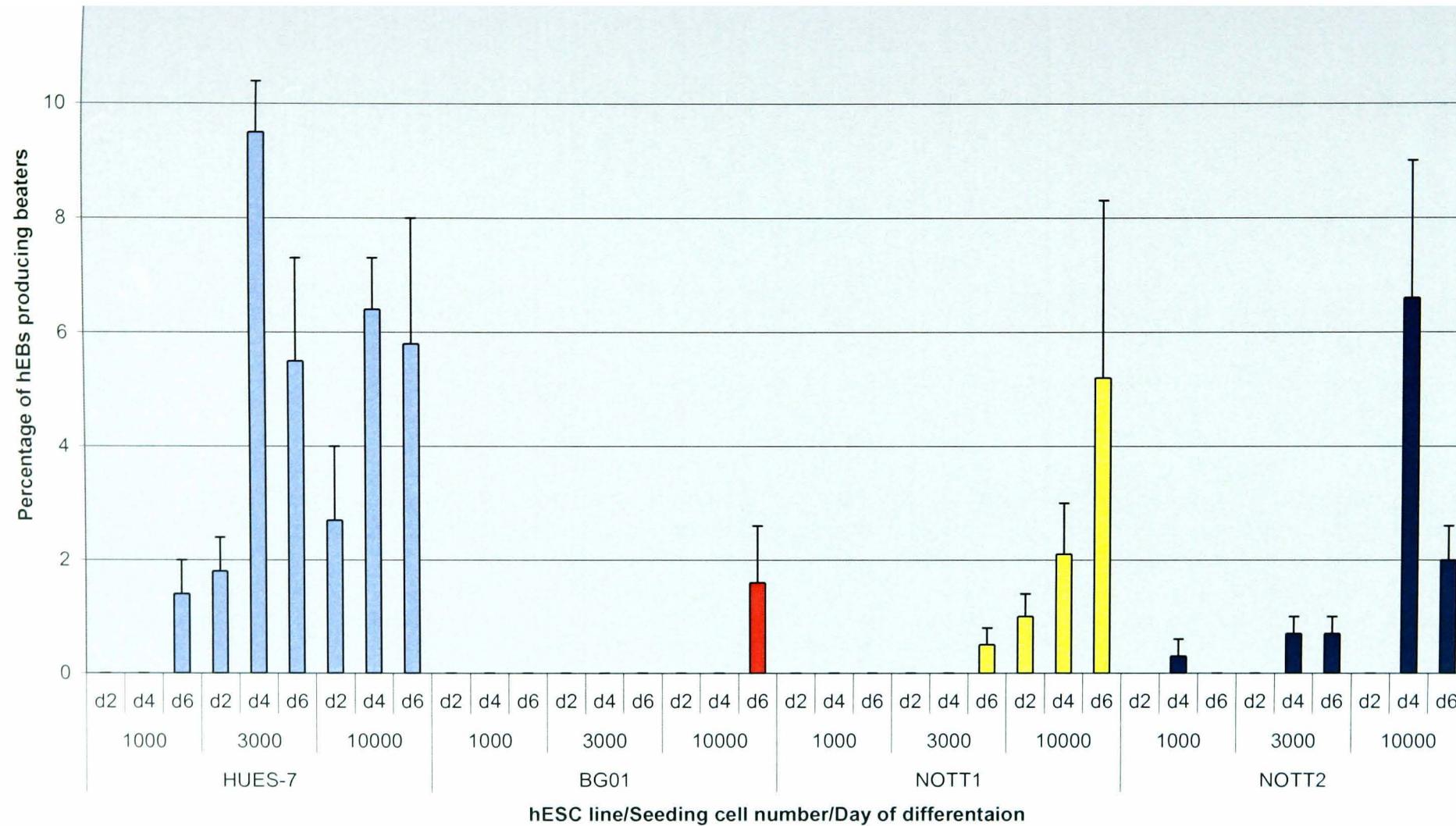
Figure 3-13: Inter-line comparison of percentage of beaters produced

hEBs were formed in BGK CM from the hESC lines HUES-7, BG01, NOTT1 and NOTT2 and from 1000 (left), 3000 (centre) or 10000 (right) cells per well in uncoated V-bottom plates. hEBs were transferred from the V-bottom plates on either day 2, day 4 or day 6 of differentiation before switching to 90 mm Petri dishes for 6 days then transferring to uncoated U-bottom plates. At day 24 wells were assessed for the beating areas. Each data point represents the average percentage of wells with beating areas (±SEM) of between 2 and 4 independent experiments (192-384 wells in total). Data produced in collaboration with C. Denning and D. Anderson.

160
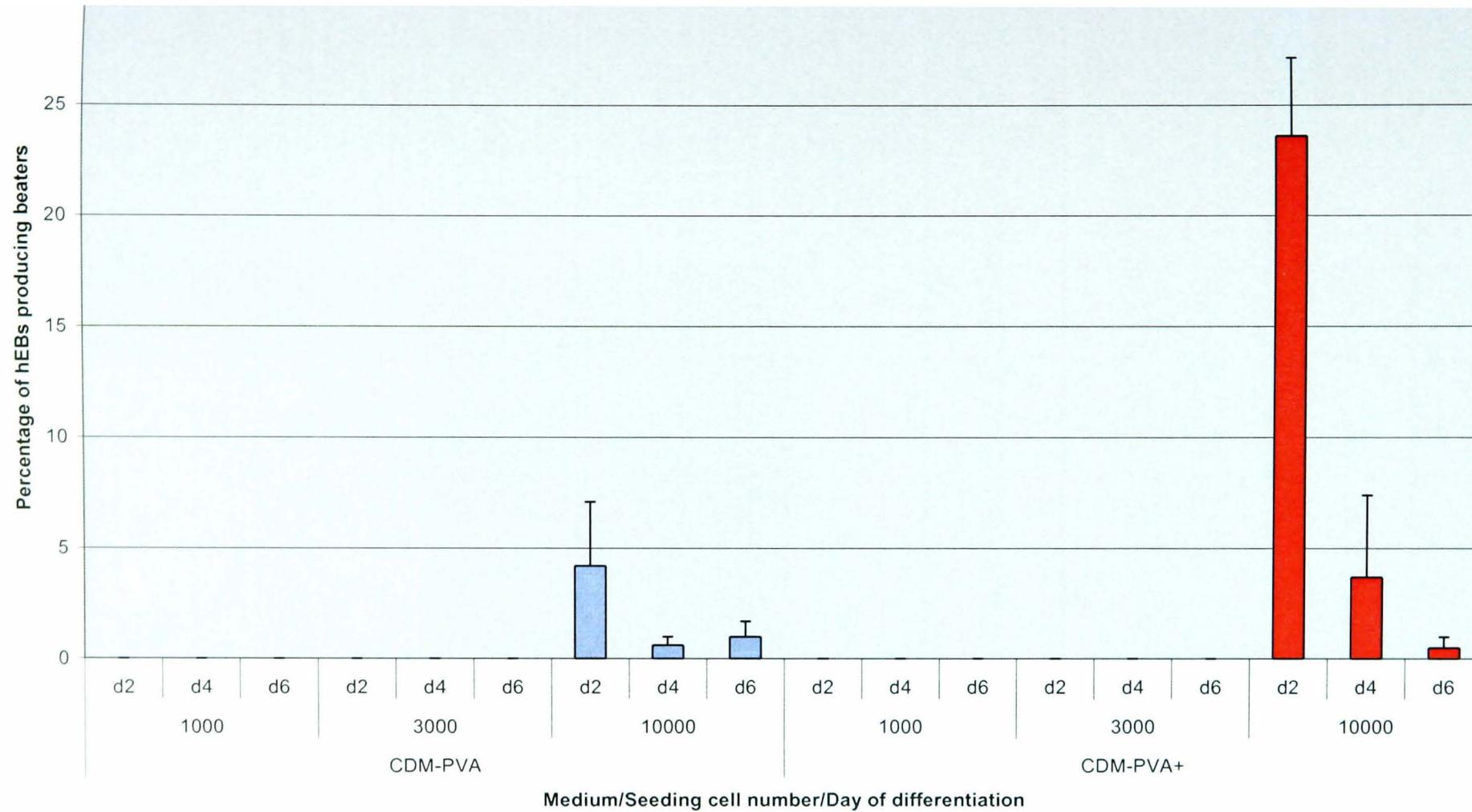
Figure 3-14: Comparison of percentage of beaters produced in CDM-PVA and CDM-PVA+

hEBs were formed in from the hESC lines HUES-7, BG01, NOTT1 and NOTT2 and from 1000 (left), 3000 (centre) or 10000 (right) cells per well in uncoated V-bottom plates in either CDM-PVA or CDM-PVA supplemented with activin A and FGF2 (CDM-PVA+). hEBs were transferred from the V-bottom plates on either day 2, day 4 or day 6 of differentiation before switching to 90 mm Petri dishes for 6 days then transferring to uncoated U-bottom plates. At day 24 wells were assessed for the beating areas. Each data point represents the average percentage of wells with beating areas (±SEM) of between 2 and 4 independent experiments (192-384 wells in total). Data produced in collaboration with C. Denning and D. Anderson.

3.3.8 Haematopoietic differentiation

Although large scale analysis of the effect of hESC input number, days in culture, day of transfer and media used were prohibitively expensive, a small scale analysis of forced aggregation hEB propensity to form blood was performed. V-96 forced aggregation hEBs were formed form 10000 cells in CDM-PVA+ (Figure 3-13) and cultured until d4 of differentiation. hEBs were then switched to D-FBS20 in uncoated 90 mm dishes for 12 days before transfer to MethoCult growth factor enriched methylcellulose and cultured for 30 days before staining with Wright-Giemsa. A small number of cobblestone areas, endothelial-like outgrowths and colonies with red colouration were noted during growth in methylcellulose. Using Wright-Giemsa staining cells from these colonies were identified as erythrocytes and macrophages.
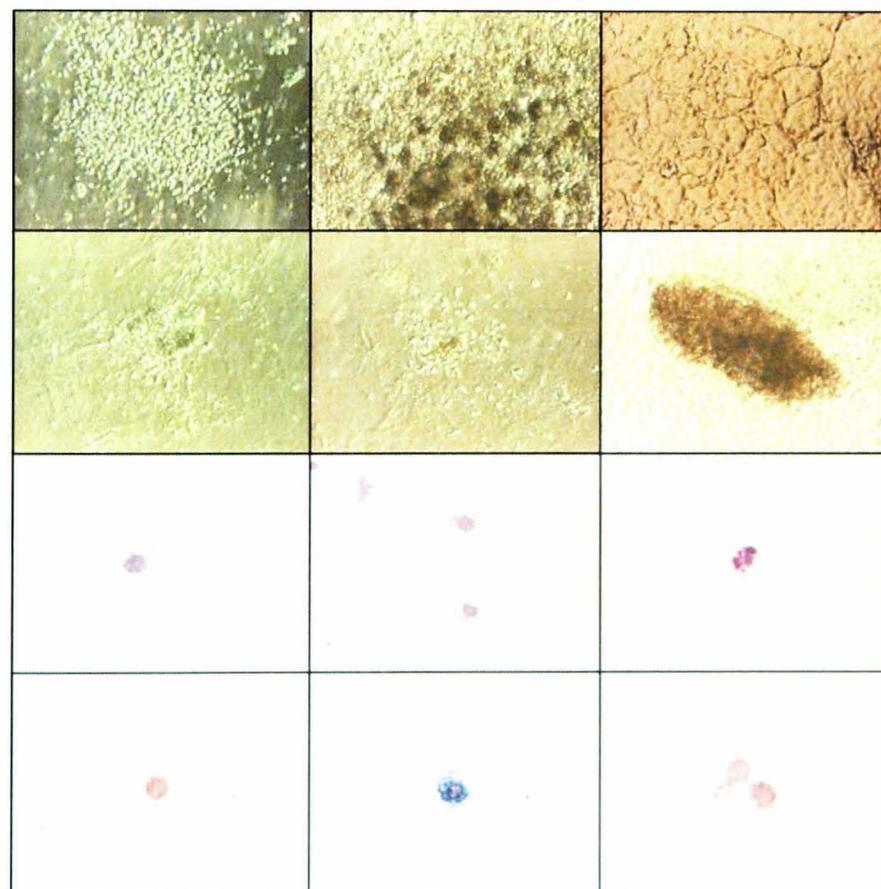
Figure 3-15: Haematopoietic colonies and Wright-Giemsa stained cells

Images of colonies after 30 days suspension in MethoCult (top) and Wright-Giemsa stained cells (bottom).

3.4 DISCUSSION

The object of this study was to develop a system for the controlled formation of hEBs to improve the size of the mesodermal population and provide a standardised platform for the analysis of inter-line variability.

3.4.1 Analysis of traditional mass culture hEB formation

Traditional protocols for hEB formation initiate suspension by harvesting colonies directly from MEFs using manual dissection, scraping, enzymatic digestion or a combination of techniques. Consistent with previous reports (Ng *et al.*, 2005b, Yoon *et al.*, 2006) this strategy resulted in a high degree in heterogeneity in hEB size in hEBs formed from either HUES-7 or BG01 hESCs grown on MEFs with Collagenase IV passage or grown on Matrigel with Collagenase IV or trypsin passage (Table 3-4 and Figure 3-2). Previous experiments in our lab have demonstrated high variability in haematopoietic differentiation, likely a consequence of the variability in cell numbers that form each hEB. This experiment also demonstrated that hEBs were able to form from the aggregation single cell trypsin dissociated HUES-7 grown on Matrigel without MEF contamination.

3.4.2 Establishing a forced aggregation system

Ng *et al.* (2005b) published data demonstrating successful hEB formation from a known number of HES-2, HES-3 or HES-4 hESCs using forced aggregation. This system involves centrifugation at 500 g for 4 minutes at 4°C using 96-well plates with an ultra low attachment (ULA U-96) coating along with a semi-chemically defined medium supplemented with growth factors. After 8-12 days hEBs were then transferred to flat bottom plates and with the introduction of blood inducing growth factors, high levels of blood differentiation could be achieved. Although hEB size

data was not reported, efficient haematopoietic development required a minimum of 500 cells per well and input number was critical for directing cells to the haematopoietic lineage with 3000 cells most successful.

While this strategy proved useful as a proof of concept, there were several potential limitations. Firstly, ULA U-96 plates were prohibitively expensive for large scale experiments. Secondly, differentiation studies were performed using hESCs derived from a single institute therefore the performance of this study in independently-derived hESCs was not established. Thirdly, this system involved the addition of a large number haematopoietic inducing growth factors without insight into the individual effect of the growth factors. Finally, this system involved the use of hESCs cultured on MEFs, albeit at a lower density, and a mixed population of the two cell types were used in the aggregation experiments. It has been suggested that contaminating MEFs may have the potential to interfere with differentiation by competing with cell-cell interaction and insulating communication between mESCs (Weitzer, 2006).

Comparisons were made using standard uncoated U-bottom and V-bottom plates alongside ULA plates. HUES-7 cells grown on Matrigel and force aggregated in ULA plates produced >90% hEB formation, consistent with observations using HES-3 cells grown MEFs (Ng *et al.*, 2005a). Centrifugation of HUES-7 cells in untreated U-bottom plates resulted in erratic and/or poor hEB formation (Figure 3-4 and Figure 3-6). In contrast V-bottom plates produced hEBs at a similar efficiency to ULA U-96 plates of hEB formation per well. The differences detected in hEB formation efficiency between V-96 and U-96 plates, along with the success of ULA U-96 plates, suggests that the force exerted upon the cells has a prominent effect on hEB formation. The success of hEB formation in V-bottom plates maybe attributed an

increase in the compression of the hESCs during the forced aggregation caused by the angle and more defined point of the V-bottom well. The differences in hEB formation efficiency seen between the U-96 and ULA-96 plates, which have identical dimensions, suggests that the reduction in friction on the plate surface due to the ultra-low attachment coating also aids hEB formation (see Figure 3-16).
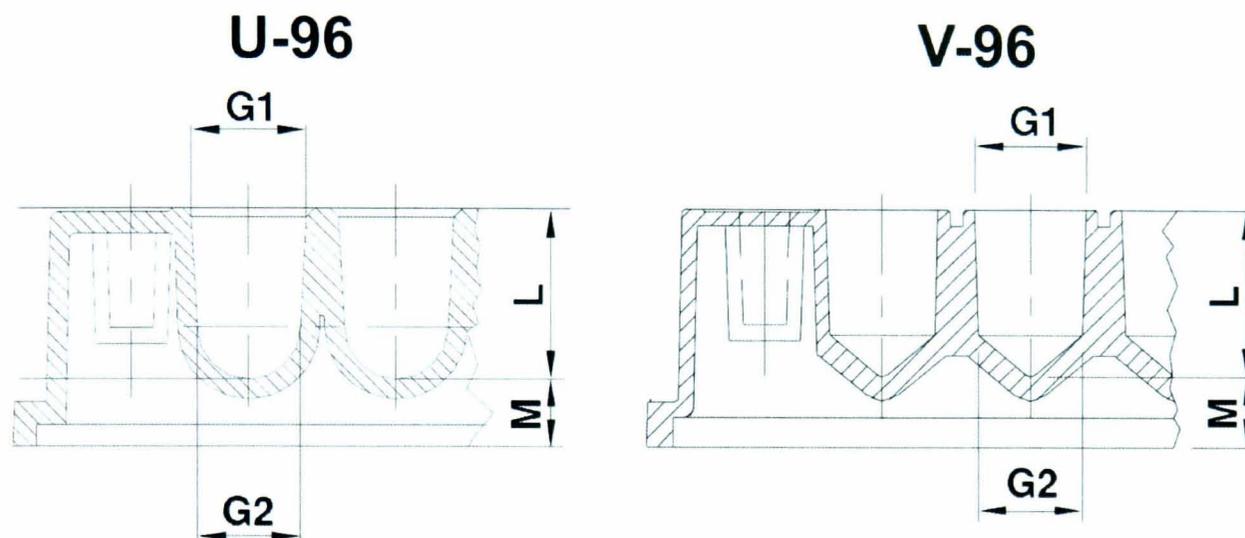
Dimension	Size (mm)	
	U-96	V-96
G1	7.0	6.8
G2	6.3	6.4
L	10.3	9.8
M	4.1	4.6

Figure 3-16: Comparison of U-96 and V-96 well dimensions

Diagram demonstrating the differences in well dimensions between U-96 and V-96 plates. Diagrams adapted from http://www.nuncbrand.com

The presence of a single hEB or a number of hEBs in each well was also observed (Figure 3-5) and demonstrated that wells seeded with 3000 cells produced a higher proportion on multiple hEBs per well. hEBs formed in ULA U-96 plates showed higher levels of agglomeration than those formed in V-96 plates which has been demonstrated as the major process limiting cell proliferation and differentiation (Dang *et al.*, 2002).

Visual analysis of hEB formation and development was also observed with HUES-7 hESCs (Figure 3-6). In U-bottom plates hESCs formed no hEBs with 1000 or 3000

cells and numerous small hEBs in each well from 10000 cells. ULA U-96 plates formed no hEBs with 1000 cells, small hEBs with 3000 cells and hEBs comparable to those made in V-bottom plates with 10000 cells, this is in contrast to Ng *et al.*, (2005a) who suggested that the most successful hEB formation came from 1000 cells/well. After 12 days maintenance in the plates with conditioned medium these hEBs started to form more complex structures suggesting that even in the presence of a medium that is used as standard for maintaining pluripotency differentiation can be induced by forcing the cells into a 3D formation.

3.4.3   Effect of media on hEB formation in the forced aggregation system

A variety of media were tested to determine capacity for supporting hEB formation (Figure 3-7 and Figure 3-8). Of the 7 media tested BGK CM, CDM-PVA and CDM-PVA+ produced the highest efficiency of hEBs formation with efficiency decreasing in BGK, CDM-BSA, D-FBS10 and D-FBS20. BGK CM, CDM-PVA and CDM-PVA+ all yielded hEBs that were maintained through to d12. The underlying mechanisms responsible for the differences observed between hEB formation in different media are unknown but expression levels of key adhesion factors, such as CDH1 (discussed in Chapter 4), are likely targets for further studies. It has been demonstrated that over 60 cell-adhesion related genes are up-regulated in undifferentiated HS237 hESCs upon transfer from an FBS containing medium to a medium containing Knockout™ Serum Replacement (Skottman *et al.*, 2005).

3.4.4   Size of hEBs in conditioned medium and chemically defined medium

The kinetics of hEB growth in relation to input cells number and days of differentiation was assessed in four hESC lines HUES-7, BG01, NOTT1 and NOTT2. For hEBs formed at all seeding densities, both increasing cell input number

and day of differentiation contributed to increasing size. This study was extended to include the hESC lines BG01, NOTT1 and NOTT2 and similar growth profiles were observed (Figure 3-11).

Similar experiments to those above were performed using HUES-7, BG01 and NOTT1 hEBs formed in CDM-PVA and CDM-PVA+ (Figure 3-12). Overall hEBs formed in CDM-PVA and CDM-PVA+ were similar but only increased in size when seeded from 10000 cells suggesting that only this density is able to overcome the absence of factors present in BGK CM.

3.4.5 Histology of hEBs

HUES-7 hEBs were formed in BGK CM and CDM-PVA using forced aggregation and compared to hEBs formed using suspension mass culture. Samples were embedded, sectioned and haematoxylin and eosin stained to show nuclei and cytoplasm as well as levels of development and the formation of internal structures. Results correlated well with hEB size results (Figure 3-11 and Figure 3-12). At d6 BGK CM mass suspension culture hEBs appeared to consist of an outer epithelial layer with a central cavity (Figure 3-9), similar to that seen in mEBs (Weitzer, 2006). Cavitation of hEBs has been demonstrated (Itskovitz-Eldor *et al.*, 2000, Conley *et al.*, 2004a, Khoo *et al.*, 2005) but it is not currently known how well this correlates with mEB cavitation. Forced aggregation BGK CM and CDM-PVA hEBs appeared more dense than mass culture hEBs at d2-d4, likely a result of the forced aggregation procedure (Figure 3-12). At d6, in both BGK CM hEBs numerous random cavities were seen, which were smaller in CDM-PVA hEBs (Figure 3-9). The random nature of this cavities, rather than one large central cavity, and the lack of any identifiable epithelial layer suggests that forced aggregation hEBs do not differentiate in the

same manner to mass culture hEBs although the cell lineages present could only be identified using immunohistochemistry.

3.4.6 Production of terminal lineages

The ability of hEBs formed by forced aggregation to form cardiomyocytes was assessed. FBS was included in the extended differentiation period because the absence of serum is reported to be detrimental to the maintenance of primary cardiomyocytes (Heng *et al.*, 2004). Each of the hESC lines yielded only a limited number beating hEBs, particularly poor were hEBs formed from 1000 cells (Figure 3-13). Most successful was HUES-7 hEBs formed from 3000 cells at d4 with 9.5±0.9% of hEB beating. Interestingly, HUES-7 formed the largest number of cardiomyocytes from 3000 cells at d4 whereas the other three lines produced the most cardiomyocytes from 10000 cells at d4 or d6. Similar experiments were also performed using HUES-7 with hEB formation in CDM-PVA and CDM-PVA+ (Figure 3-14) and demonstrated that CDM-PVA hEBs formed from 10000 cells resulted in 4.2±2.9% of beating hEBs at d24 whereas supplementation with activin A and FGF2 induced 23.6±3.6% beating hEBs (Figure 3-14). This suggests that the combination of CDM-PVA supplemented with activin A and FGF2 is a successful combination to induce cells of the mesodermal lineage. This percentage compares favourably to other groups who have formed cardiomyocytes by mass culture who achieved between 0-25% beating hEB efficiency when using mass culture mechanical/dispase dissociation and 18-22% when using hanging drop hEB formation (see Table 3-5).

Table 3-5: Reported efficiencies of beating hEB production from different laboratory groups, hESC lines and differentiation method

The tope section of the table contains methods that involve mass culture, whilst the bottom section contains alternative methods such as hanging drop and co-culture.

hESC line	hESC growth	passage method	Differentiation on culture media	Beating hEB efficiency	Reference
HES-1,2	MEFs/FBS	mechanical/ dispase	20% FBS	none	(Reubinoff et al., 2000)
H9.2	MEFs/FBS	mechanical/ dispase	20% FBS	8.10%	(Kehat et al., 2001)
H1, H7, H9, H9.1, H9.2	Matrigel/ KSR-CM	Coll IV	20% FBS	upto ~70%	(Xu et al., 2002a)
H1,7,9,14	MEFs/KSR	mechanical/ dispase	15% FBS	10-25%	(He et al., 2003)
Royan H1	MEFs/FBS	mechanical/ dispase	20% FBS	10%	(Baharvand et al., 2004)
H1	MEFs/FBS	mechanical/ dispase	20% FBS	~13%	(Xue et al., 2005)
H9.2	MEFs/KSR	mechanical/ dispase	20% FBS	21.50%	(Segev et al., 2005)
SA002	MEFs/ VitroHES	mechanical	20% FBS	~30%	(Norstrom et al., 2006)
Miz-hES2, HSF-6	MEFs/KSR	mechanical	20% FBS	5-8%	(Yoon et al., 2006)
H1	MEFs/KSR	mechanical	20% FBS	3-15%	(Bettiol et al., 2007)
BG01V, ReliCell-hES1	MEFs	mechanical	5% FBS + BMP2	7-9%	(Pal and Khanna, 2007)
BG01, HUES-7	Matrigel/ KSR-CM	trypsin	20% FBS	~2%	(Denning et al., 2006)
Miz-hES2, HSF-6	MEFs/KSR	mechanical/ hanging drop	20% FBS	18-22%	(Yoon et al., 2006)
HES2	MEFs/FBS	mechanical/ dispase onto END2 co-culture	20% FBS	15-20%	(Mummery et al., 2002)
HES2, HES3, HES4	MEFs/FBS	mechanical/ dispase onto END2 co-culture	20% FBS	35±10%	(Mummery et al., 2003)
H7	Matrigel/ KSR-CM	Coll IV/ monolayer based	activin A and BMP4	>30% of cells cardiomyocytes	(Laflamme et al., 2007)

Differences in developmental potential between hESC lines has been previous described (Mikkola *et al.*, 2006), including differences in preferential terminal differentiation, despite no difference in hEB formation, between two lines (Miz-hES4 and Miz-hES6) derived under the same conditions (Kim *et al.*, 2007b). The differences in developmental competence between hESC lines may be the result of the conditions and developmental stage under which the hESC lines were derived, male-female differences or genetic variation. Single nucleotide polymorphisms are suggested to contribute to the unique genetic profile of individual hESC lines

(Abeyta *et al.*, 2004). Epigenetic differences and X-inactivation status may also affect gene expression patterns (Allegrucci and Young, 2007, Hoffman *et al.*, 2005).

Once a suitable system was established for mesodermal lineage differentiation was established, the system was tested for haematopoietic lineage production. Successful differentiation, albeit very low numbers, of haematopoietic cells of the erythrocyte and macrophage lineage was obtained from HUES-7 hEBs. The number of haematopoietic cells formed was too low and variable to identify a pattern or most successful conditions that favour haematopoietic differentiation suggesting that additional factors that further induce haematopoiesis may be required such as those used by Ng *et al.* (2005b).

This study combines the use of a standardised method for culturing multiple hESC lines without feeders with a forced aggregation procedure to provide a system that produces highly homogenous hEBs which is optimised for mesodermal lineage differentiation. This system allows for accurate comparison between the differentiation capacities of different hESC lines and provides a platform for the further study of the effects of media, growth factors and plating on the process of differentiation.

4 SPATIAL AND TEMPORAL ASSOCIATION BETWEEN LOSS OF PLURIPOTENCY AND GERM LAYER FORMATION DURING HUMAN EMBRYOID BODY DIFFERENTIATION

4.1 INTRODUCTION

The reproducibility of the forced aggregation system detailed in Chapter 3 allows for production of large numbers of standardised hEBs. In turn this provides a platform for the analysis of the spatial and temporal association between the loss of pluripotency and germ layer induction during hEB differentiation. This chapter details the spatial relationships of cells expressing markers for POU5F1, NANOG (pluripotency), T (mesoderm), SOX17 (endoderm) and SOX1 (ectoderm) during the initial stages of differentiation (16 days). The inter-line variability in early differentiation in hEBs formed from 4 hESC lines is also examined. In addition the effect of CDM supplemented with activin A and FGF2 on the molecular induction of differentiation is also analysed to determine whether the mesoderm component can be enhanced by these additives.

The early stages of hESC commitment and differentiation in early hEBs and the relationships between cell types are largely uncharted (Laslett *et al.*, 2007). Currently in addition to data extrapolated from work on EBs derived from rhesus monkey ESCs, common marmoset ESCs and human embryonal carcinoma (F9) cells, most clues are derived from mEBs. This data is usually interpreted using information from mouse embryonic development which provides a clue to the expected timing and cell type relationships during hEB differentiation (reviewed by Tam and Loebel, 2007).

4.1.1 Markers of pluripotency and germ layer induction in mouse embryos

Although attempts have been made to standardise marker genes for the detection of differentiation in ESCs (Willems *et al.*, 2006), often the selected genes appear too late in development to be of use for the identification of germ layer induction. To examine the ontogeny of germ layer formation, the effect of culture conditions and how this differentiation correlates to previously published studies of early post-implantation development from both mouse and human, within this chapter the following panel of molecular marker genes were selected: POU5F1 and NANOG for pluripotency; T, MIXL1, GSC, SOX17 and FOXA2 for mesendoderm; and SOX1 and SOX3 for ectoderm.

For simplicity, the mouse embryo stage terms used refer to the following stages of development: E6.25, pre-streak; E6.5-6.75, early streak; E7.0-7.5, mid-streak; E7.25-7.75, late streak; E7.5-8.0 neural plate; E7.75-8.0, headfold; E8.0+, somites. Derived from Downs and Davies (1993) and the Edinburgh Mouse Atlas staging criteria (http://genex.hgu.mrc.ac.uk/Databases/Anatomy/MAstaging.shtml).

4.1.1.1 Pluripotency markers

4.1.1.1.1 POU5F1

POU5F1 (POU domain, class 5, transcription factor 1, also known as OCT4) is a nuclear transcription factor (reviewed by Pan *et al.*, 2002). POU5F1 was discovered in mice (Scholer *et al.*, 1990b) as a POU (Pit-Oct-Unc) domain-containing transcription factor that binds the octamer sequence, ATGCAAAT (Herr and Cleary, 1995). Pre-implantation expression of *Pou5f1*, is first detected at the four- to eight-cell stage (Yeom *et al.*, 1996, Palmieri *et al.*, 1994). *Pou5f1* expression is uniform at the morula stage, however as the outer cells differentiate to trophectoderm, *Pou5f1* is

down-regulated and becomes restricted to the ICM of the blastocyst (Rosner *et al.,* 1990, Scholer *et al.,* 1990a). As development continues *Pou5f1* expression becomes restricted to the epiblast and subsequent primitive ectoderm (Rosner *et al.,* 1990, Scholer *et al.,* 1990a) and by E8.5 is only maintained in PGCs (Yeom *et al.,* 1996, Yoshimizu *et al.,* 1999). POU5F1 has been demonstrated to be required for PGC cell survival in mice (Kehler *et al.,* 2004). In the mouse embryo POU5F1 is essential to establish pluripotency and in *Pou5f1*$^{-/-}$ embryos, cells from the ICM in the blastocyst do not fully mature and are restricted to the extra-embryonic trophoblast lineage (Nichols *et al.,* 1998). Human POU5F1 has two isoforms, both containing identical POU DNA binding domains and C-terminal domains, but differ in their amino-terminal domains (Lee *et al.,* 2006). POU5F1 also has six proposed pseudogenes (Pain *et al.,* 2005).

4.1.1.1.2 NANOG

NANOG is a homeobox family transcription factor originally identified in mESCs (Chambers *et al.,* 2003, Mitsui *et al.,* 2003). In the mouse embryo *Nanog* is first detected in the compacted morula then restricted to the ICM of the blastocyst. At E5.5, *Nanog* is expressed asymmetrically in the proximal epiblast at the embryonic/extra-embryonic junction. At E6.0, *Nanog* expression extends distally in the epiblast at the site of the presumptive primitive streak. At E6.5, *Nanog* is localised to the epiblast of the emerging primitive streak but is not detected in the embryonic visceral endoderm. At E7.0, *Nanog* is detected anteriorly within the epiblast as the streak forms and elongates along the embryonic anterior-posterior axis between E7-7.5, with maximal expression in epiblast cells flanking the primitive streak. Expression is lost in cells as the enter they primitive streak and *Nanog* is undetectable by E9.5, except for the genital ridges at E11.5, containing PGCs

(Chambers *et al.*, 2003, Hart *et al.*, 2004). In humans *NANOG* has ten proposed processed pseudogenes and one tandem duplicate (Booth and Holland, 2004).

4.1.1.2 Primitive streak markers

4.1.1.2.1 T

T (brachyury) is a transcription factor that is commonly used as a panmesodermal marker (Herrmann *et al.*, 1990). However T has been detected in definitive endoderm (Kispert and Herrmann, 1994) and it is possible that expression of some primitive streak genes is maintained for a short period after differentiation to definitive endoderm (Yasunaga *et al.*, 2005). Like all T-box family members, T binds to the DNA consensus sequence, TCACACCT, at the T-box region in its N-terminus (reviewed by Wilson and Conlon, 2002). In the mouse embryo, T expression is first detected at E5.5 at the extra-embryonic ectoderm/proximal epiblast boundary (Thomas and Beddington, 1996, Perea-Gomez *et al.*, 2004, Rivera-Perez and Magnuson, 2005). T then localises to the nascent primitive streak by E6.5 (Thomas *et al.*, 1998, Inman and Downs, 2006). Between E6.75 and 7.0, T is detected along the length of the primitive streak and in the nascent mesoderm (Inman and Downs, 2006). At E7.5 T expression is detected in the notochordal plate and extra-embryonic mesoderm (Kispert and Herrmann, 1994). At later stages T expression is seen in the node, notochord and tail bud of neural plate and somite stage embryos (Wilkinson *et al.*, 1990, Wilson *et al.*, 1993). T has also been noted to be maintained in migrating PGCs (Saitou *et al.*, 2002). *T* ⁻ embryos die at around E10 due to defective anterior mesoderm formation, malformed anterior somites and absent posterior somites (Kispert and Herrmann, 1994). Recently *T* has been demonstrated to be expressed in the mouse blastocyst in a ICM specific manner along with *Pou5f1* and *Nanog*

(Yoshikawa *et al.*, 2006). The human homologue of *T* (Edwards *et al.*, 1996) has been associated with spina bifida (Morrison *et al.*, 1996).

4.1.1.2.2 MIXL1

MIXL1 (mesoderm induced homeobox-like 1) is the only identified human member of the *Xenopus* Mix/Bix family of homeobox proteins (Robb *et al.*, 2000, Sahr *et al.*, 2002, Guo *et al.*, 2002). In the mouse, *Mixl1* is essential in for axial mesendoderm morphogenesis, as well as endoderm differentiation (Robb *et al.*, 2000). *Mixl* is first expressed in posterior visceral endoderm and posterior epiblast at E5.5-6 before localising to the primitive streak and nascent mesoderm at E6.5-7.5 (Pearce and Evans, 1999). *Mixl1* then localises to the mesoderm of the developing midgut and hindgut (but not the definitive endoderm), and finally in the tailbud before switching off after E9.5 (Pearce and Evans, 1999, Robb *et al.*, 2000, Mohn *et al.*, 2003, Mossman *et al.*, 2005).

4.1.1.2.3 GSC

GSC (goosecoid) is a homeodomain protein (Blum *et al.*, 1992) commonly used as a marker for mesendoderm (Tada *et al.*, 2005). However, *Gsc* is not entirely specific to the mesendoderm as it is also expressed in the anterior visceral endoderm during early development (Perea-Gomez *et al.*, 2002). *Gsc* is expressed in the anterior end of the primitive streak at E7.0-E7.5 followed by expression in the anterior end of the embryo at E8.0 (Filosa *et al.*, 1997). At E8.5, *Gsc* is expressed in all three germ layers (ventral neuroepithelium of the forebrain, prechordal mesoderm and foregut endoderm), followed expression in the ventral diencephalon of the brain and oral epithelium at E9.5 (Blum *et al.*, 1992, Filosa *et al.*, 1997). At E10.5, GSC expression

becomes restricted to portions of the facial process, branchial arches, limbs and body wall (Gaunt *et al.*, 1993).

4.1.1.2.4 EOMES

EOMES (eomesodermin, also known as TBR2) is a T-box nuclear transcription factor related to T (Hancock *et al.*, 1999). EOMES is expressed in mouse oocytes and in both the ICM and trophectoderm of the E3.5 blastocyst stage embryo (McConnell *et al.*, 2005). *Eomes* has then been shown to localise to the trophectoderm then the extra-embryonic ectoderm between E5.0 and 6.5 and the posterior epiblast and primitive streak and nascent mesoderm between E5.75 and 7.5 (Russ *et al.*, 2000). *Eomes* is then detected in the developing forebrain and olfactory lobes at E12.5-14.5 (Russ *et al.*, 2000) and the hippocampus from E18.5 (Kimura *et al.*, 1999).

4.1.1.2.5 SOX17

SOX17 (SRY (sex determining region Y)-box 17) is a transcription factor originally identified as a stage-specific transcription factor during spermatogenesis (Kanai *et al.*, 1996). *Sox17* is commonly used as a marker of definitive and visceral endoderm although it is not expressed in the anterior visceral endoderm (Kanai-Azuma *et al.*, 2002). *Sox17* can form two splice variants that are both translated into proteins, with the shorter form displaying no apparent DNA-binding activity (Kanai *et al.*, 1996). SOX-type transcription factors share a conserved high mobility group (HMG)-box, minor grove DNA-binding domain (Pevny and Lovell-Badge, 1997). SOX proteins bind to specific DNA sequences by a core consensus sequence ATTGTT, although flanking sequences and accessory factors are often involved (reviewed by Wilson and Koopman, 2002, Kamachi *et al.*, 2000, Pevny and Lovell-Badge, 1997). *Sox17* is

first detected in the visceral endoderm nearest the epiplacental cone at E6.0 (Kanai-Azuma *et al.*, 2002). It is then expressed across the entire extra-embryonic visceral endoderm at E6.5, but is undetectable in the embryonic visceral endoderm (Kanai-Azuma *et al.*, 2002). At E7.0, *Sox17* is expressed in the endoderm subjacent to the anterior end of the primitive streak, and in the endoderm underlying the neural plate by E7.5 (Kanai-Azuma *et al.*, 2002). At E8.5, *Sox17* is expressed in the middle and posterior gut endoderm (Tam *et al.*, 2004). *Sox17*$^{-/-}$ embryos are deficient in gut endoderm (Kanai-Azuma *et al.*, 2002).

4.1.1.2.6 FOXA2

FOXA2 (fork head box A2, previously known as HNF3β) is a transcription factor that also interacts with chromatin. At the pre-streak stage, *FoxA2* is expressed in the visceral endoderm (Ang *et al.*, 1993). In the early streak stage, *FoxA2* expression is localised to the anterior portion of the primitive streak, and by mid-streak a large group of cells within the anterior third of the streak express *FoxA2* before becoming restricted to the node, to anteriorly migrating mesoderm and to endoderm cells of the head process (Filosa *et al.*, 1997). At the headfold stage *FoxA2* is expressed in all three germ layers; in the notochord, neural plate, and underlying midline endoderm and the medial and lateral regions of the foregut and prechordal mesoderm (Ang *et al.*, 1993, Monaghan *et al.*, 1993, Ruiz i Altaba *et al.*, 1993, Sasaki and Hogan, 1993, Hart *et al.*, 2002, Filosa *et al.*, 1997). At E16.5, *FoxA2* is expressed in predominantly in the liver but is also detected in the lung, pancreas, intestine and stomach (Ang *et al.*, 1993). Gene targeting of *FoxA2* in visceral endoderm has distinguished an essential role in primitive streak morphogenesis (Dufort *et al.*, 1998).

4.1.1.3 Ectodermal markers

4.1.1.3.1 SOX1

SOX1 (SRY (sex determining region Y)-box 1) is a transcription factor, first cloned in humans (Malas *et al.*, 1997). It is one of the earliest transcription factors to be expressed in definitive ectoderm (Pevny *et al.*, 1998). In mouse embryos, *Sox1* is first detected in the columnar ectoderm cells in the anterior half of late-streak embryos and is maintained in all neuroepithelial cells along the entire antereoposterior axis as the neural plate bends at E8.0-8.5 and fuses to form the neural tube at E9.0-9.5 (Pesce *et al.*, 1998). As development proceeds, *Sox1* is down-regulated in along the dorsoventral axis of the neural tube. By E13.5, *Sox1* is restricted to a thin ventral zone in the central nervous system (Pevny *et al.*, 1998, Wood and Episkopou, 1999). *Sox1*$^{-/-}$ mice do not exhibit any obvious abnormalities except for reduction in the size of the lens of the eye and cataract (Nishiguchi *et al.*, 1998).

4.1.1.3.2 SOX3

SOX3 (SRY (sex determining region Y)-box 3) is a transcription factor first identified in humans (Stevanovic *et al.*, 1993). In mouse embryos, *Sox3* is expressed at E6.5 in a band of extra-embryonic ectoderm at the embryonic/extra-embryonic boundary (Wood and Episkopou, 1999). At E7.0 *Sox3* expression becomes restricted to the anterior ectoderm whilst extra-embryonic expression becomes restricted to the chorion. At E7.5 *Sox3* expression spreads from the anterior to the posterior epiblast in cells that contribute to the paraxial mesoderm. At E8.0 *Sox3* is expressed in an anterior-posterior gradient up-regulated in the posterior ectoderm during late streak and neural plate stages and is concomitantly down-regulated in the chorion. From

E8.0 onwards *Sox3* is expressed in the neuroectoderm (Wood and Episkopou, 1999).

At E9.5-10.5 *Sox3* maintained in the full length of the developing central nervous

system including brain and spinal cord. At E11.5 *Sox3* expression is maintained

throughout the foetal brain and by E13.5 expression has become limited to the

ependymal layer where undifferentiated neural progenitor cells are still actively

dividing (Collignon *et al.*, 1996).

Table 4.1 summarises the sites of expression of markers selected for use in this

study.

Table 4-1: Summary of expression of pluripotency and germ layer markers during gastrulation

Summery of the expression patterns of markers used to detect pluripotency and germ layer induction. ICM: inner cell mass, ESC: embryonic stem cell, PS: primitive streak, D. Endo: definitive endoderm, Pr. Endo: primitive endoderm, VE: visceral endoderm, PE: parietal endoderm, TE; trophectoderm.

Gene name	Symbol	ICM/ESC	PS	Ectoderm	Mesoderm	D. Endo	Pr.End/VE/PE	TE	Refs
POU domain, class 5, transcription factor 1	POU5F1	*						*	Scholer *et al.*, 1990
Nanog homeobox	NANOG	*							Chambers *et al.*, 2003
T, brachyury homolog (mouse)	T		*		*				Hermann *et al.*, 1990, Inman and Downs, 2006
Mix1 homolog-like 1	MIXL1		*		*		*		Pearce and Evans, 1999, Ng *et al.*, 2005a
goosecoid	GSC		*		*	*	*		Blum *et al.*, 1992, Tada *et al.*, 2005
eomesodermin homolog (Xenopus laevis)	EOMES		*		*			*	Ciruna and Rossant, 1999
SRY (sex determining region Y)-box 17	SOX17					*	*		Katoh *et al.*, 2002, Matsuura *et al.*, 2006
forkhead box A2	FOXA2		*		*	*	*		Levinson-Dushnik and Benvenisty, 1997
SRY (sex determining region Y)-box 1	SOX1			*					Malas *et al.*, 1997, Wood and Episkopou, 1999
SRY (sex determining region Y)-box 3	SOX3			*					Stevanovic *et al.*, 1993

4.1.2 Ontogeny of pluripotency and germ layer marker gene expression during mEB differentiation

There is surprisingly little data available on the spatial expression of germ layer markers in mEBs. In part, this is due to the requirement for mEB to adhere to facilitate the later stages of mesendoderm differentiation (Bader *et al.*, 2001) that makes visualisation by sectioning difficult.

Leahy *et al.*, (1999) used RNA *in situ* hybridisation to in mEBs to examine *Pou5f1*, *T*, and *Gata4* (expressed in primitive and definitive endoderm). This group found *Pou5f1* strongly expressed a d1-4 throughout the mEBs before becoming patchy at d5 and down-regulated between d7 and 10. *T* expression was first seen at d3, markedly increased at d4 in a patchy formation localising one side or point of elongation before becoming more restricted to areas at the edge of the mEBs at d5-6 and declined after d7, with traces of expression found through to d10. By whole mount *in-situ* hybridisation *T* has been shown to be expressed in a "clustered (patch like) formation" in mEBs at d5, d6 and d7, making up an estimated 3-8% of the total mEB cell number (Yamada *et al.*, 1994). In addition this study demonstrated that the proportion of *T* expressing cells could be increased by the addition of activin A (150 ng ml^{-1}) or FGF2 (300 ng ml^{-1}), although no statistical analysis was performed (Yamada *et al.*, 1994). MIXL1 was expressed throughout mEBs at d4 (Ng *et al.*, 2005a).

SOX17 and FOXA2 were detected by immunohistochemistry, in points of elongation at the periphery of the mEBs, in gut-like epithelial structures after 6 days culture as hanging drops without LIF. Expression intensity decreased after an additional 7 days on gelatine coated dishes and disappeared after 20 days total culture (Matsuura *et al.*, 2006).

These results suggest there is a definable order to differentiation within mEBs but no conclusion can be drawn to the germ layer spatial relationships from the available data.

In mouse, the transcriptional profiling of pluripotency and germ layer marker expression has involved harvesting mEB samples every day over the first 6 days, with analysis of early markers via RT-PCR, real-time RT-PCR or microarrays (Ng *et al.*, 2005a, Mossman *et al.*, 2005, Willey *et al.*, 2006, Hirst *et al.*, 2006). These studies demonstrate that the expression level of pluripotency genes such as *Pou5f1*, *Nanog*, *Sox2* and *Zpf42 (Rex1)* are reduced over the first 5-6 days of differentiation, that epiblast markers such as *Cdh1* and *Fgf5* are expressed until d4-6 (with highest levels at d3) and markers of the primitive streak such as *T*, *Mixl1*, *Gsc* and *Wnt3a* are expressed from d2 to d5 (with highest levels at d3-d4). Markers of endoderm such as *Gata6*, *Plat*, *Lamb1*, *Ker19* and *Nr2f1* are expressed in undifferentiated mESCs and up-regulated at d6. Overall, whilst these studies have demonstrated that genes for epiblast, primitive streak, mesoderm, and endoderm markers are sequentially expressed, there is a caveat that mRNA expression may not faithfully recapitulate mature protein expression.

4.1.3 Ontogeny of pluripotency and germ layer marker gene expression during hEB differentiation

The spatial and temporal expression of pluripotency and germ layer markers is even less well studied in hEBs. In hEBs formed by mass culture, POU5F1 is expressed across H9 and H13 hEBs at d2 (Dvash *et al.*, 2006), in small areas towards the periphery of some FES20 hEBs at d7 and ubiquitously in FES30 hEBs at d7 (Mikkola *et al.*, 2006). POU5F1 has also been detected predominantly at the periphery of HES2 hEBs at d3 whereas it is more restricted to discrete regions of the

periphery at d5 and broadly undetectable at d7 (Conley *et al.*, 2007). Interestingly POU5F1 expression was detected in the core of mass culture d3-d5 rhesus monkey EBs (Mitalipov *et al.*, 2002).

T is expressed towards the centre of in a small proportion of larger d7 hEBs formed from FES22 hESCs, although no expression was seen in FES30 hEBs under the same conditions (Mikkola *et al.*, 2006), highlighting the potential for inter-line variability. Expression of later markers for mesoderm (PECAM1), endoderm (AFP) and ectoderm (NEFH) was detected by confocal immunofluorescence on sections of d7 HES-2 hEBs (Conley *et al.*, 2004a). Although this study described the expression of markers of each of the germ layers in clusters of cells within the hEBs, and reported that PECAM1 expression was also localised to a point of elongation at the periphery of the hEBs, no details their co-expression of was provided (Conley *et al.*, 2004a).

In contrast to immunohistochemistry and immunofluorescence data, differences in pluripotency and germ layer marker expression between undifferentiated hESCs and differentiating hEBs have been well studied using RT-PCR and microarrays. Using RT-PCR the expression of pluripotency markers such as *POU5F1*, *NANOG* and *ZPF42* was detected from d0 to d21 of H1 and H9 hEB differentiation with mesoderm markers *T* and *TBX5* and endoderm marker *SOX17* detected between d7 and d21 (Barberi *et al.*, 2007). In force aggregated hES2, hES3 and hES4 hEBs (cultured in CDM supplemented with haematopoietic inducing growth factors), *POU5F1* was expressed from d0 to d26 whilst *T* and *MIXL1* were detected from d4 to d8 (Ng *et al.*, 2005b). In H1 and HES2 hEBs (cultured in an aggregation medium supplemented with FGF2, BMP4 and VEGF), *POU5F1* was expressed from d0 and reduced towards d8, *T* was expressed at low levels from d1-d6, peaking at d2-d3 and *FOXA2* was expressed from d1-d8 (Kennedy *et al.*, 2007). Serum-free neural

induction medium suspension of HS346 hESCs resulted in expression of *POU5F1* from d0-d24, *NANOG* from d0-d14, *SOX1* from d14-d42 and no detection of *T* or *AFP* (Nat *et al.*, 2007). When using a 'neuralising medium' on H9 and HUES-7 hEBs, expression of *POU5F1* and *NANOG* was detected up to d8. Expression of *T* was detected in undifferentiated cells and hEBs up to d12 and expression of *FOXA2* was also detected in undifferentiated cells and hEBs up to d8 and *SOX1* was detected at d8-d16 (Joannides *et al.*, 2006). In H9 hEBs cultured in CDM *POU5F1* was detected at d0-d8, *SOX17* was detected at d12 and d16 and *NEUROD1*, a marker for neuroectoderm, was detected at d8-d16 (Vallier *et al.*, 2005).

Using microarrays, hEBs created using the suspension culture method and harvested at d12-d14 of differentiation (Miura *et al.*, 2004, Brandenberger *et al.*, 2004b, Bhattacharya *et al.*, 2005, Li *et al.*, 2006a, Cai *et al.*, 2005, Liu *et al.*, 2006a) or on d2, d10 and d30 (Dvash *et al.*, 2004) have been analysed and identify numerous new genes that are >3 fold up-regulated after differentiation. Unfortunately these studies do not cover intermediate time-points and therefore do not allow us insight into the process of pluripotency down-regulation and germ layer induction. Others that have included time-points every 2 days have concentrated on a small number of genes, such as those associated with pluripotency (Calhoun *et al.*, 2004, Noaksson *et al.*, 2005).

4.1.4 Aims

The initial stages of mEB differentiation have been well studied and appear to successfully recapitulate *in vivo* mouse embryo development, but equivalent stages in hEBs have been poorly characterised. Using a carefully selected panel of pluripotency and early gastrulation markers, this chapter aims to elucidate the spatial and temporal relationship between pluripotency/germ layer markers within hEBs. In order to determine whether mesoderm component can be enhanced, the effect of FGF2 and activin A on germ layer induction will also be evaluated.

The specific aims of this chapter were:

- To optimise immunohistochemistry methods for pluripotency and early germ layer marker detection in differentiating hEBs.

- To compare the effects of different methods of hEB formation on marker expression.

- To investigate the spatial and temporal association between loss of pluripotency and germ layer formation.

- To investigate inter-line variability in hEBs from 4 hESC lines.

4.2 METHODS

hESC lines HUES-7, NOTT1, NOTT2 and BG01 were cultured in identical conditions using Matrigel and MEF CM, derived from the same MEF batch, and passaged with trypsin. hEBs were aggregated by forced aggregation as described in Chapter 3 (3.2.2) using 10000 cells. hEBs were maintained the in V-bottom plates in MEF CM for 4 days before transfer to Petri dishes containing differentiation medium consisting of 20% FBS. FBS with the same batch number was used for producing MEF CM and differentiation medium. All lines formed consistent high proportions of hEBs (>95%) as detailed in 3.3.2. HUES-7 hEBs were also formed in CDM supplemented with activin A and FGF2 as previous described (3.2.2) and are referred to as HUES-7 CDM hEBs. Mass culture hEBs were also formed as previously described (3.2.2). The hESC line H1 (Thomson *et al.*, 1998) was also used after transfer to the same feeder-free culture conditions as used for the other 4 hESC lines.

4.2.1 RT-PCR

4.2.1.1 Sample collection and RNA isolation

hEB and undifferentiated hESC samples were washed twice in D-PBS (Invitrogen), centrifuged at 500 *g* for 4 min and flash frozen in liquid nitrogen then stored at -80 °C. RNA was isolated using RNeasy Mini columns (QIAGEN), including steps for DNase DNA digestion (QIAGEN) following manufacturers instructions. Optical densities were established using a ND-1000 spectrophotometer (NanoDrop Technologies). Samples used in 4.3.9 were as follows: BG01 p49 cultured on Matrigel in CM and passaged with trypsin; HUES-1 p31, HUES-7 p26, HUES-8 p37 and HUES-9 p30 all culture on MEFs and passaged with trypsin kindly gifted by Chad Cowan and Doug Melton, University of Wisconsin, USA; hES-NL-1 p22 and

HES-2 p56 cultured on MEFs and passaged with collagenase kindly gifted by Christine Mummery, University of Utrecht, The Netherlands. Control samples were also assessed: week 6 foetal brain (Virogen) and week 20 foetal testis (BioChain); week 10 foetal heart and foetal liver RNA were kindly gifted by Dr. Rhodri Jones, with The University of Nottingham and NHS Trust ethical approval.

4.2.1.2 Reverse transcription

cDNA was synthesised from RNA samples isolated above or from commercial RNA using the First-Strand cDNA Synthesis Kit (GE Healthcare) with pd(N)$_6$ random hexamers following manufacturer's instructions using 200 ng of RNA from each sample.

4.2.1.3 PCR

Primers were designed using sequence data from the NCBI Entrez Gene database (http://www.ncbi.nlm.nih.gov/entrez/query.fcgi?db=gene) using online Primer3 software (http://frodo.wi.mit.edu/primer3/input.htm). Primer sequences are shown in Table 4-2. PCR was performed using HotStarTaq PCR kit (QIAGEN) in a 25 µl volume using ¼ of the manufacturers recommended constituents; 200 µM each dNTP (Invitrogen), 0.4 µM each primer (Sigma-Genosys), 0.5 µl of cDNA and 1.5-3.5 mM MgCl$_2$ and/or Q solution as required. PCR tubes were placed in Flexigene or TC-512 thermal cycler (Techne) with the following program: initial activation, 95 °C 15 min; 35 3-step cycles of 95 °C 1 min, 50-68 °C 1 min (5 °C below T$_m$, typically 57 °C), 72 °C 1 min; final extension, 72 °C 10 min. Primers were optimised first for Mg^{2+} concentration using T$_m$ −5 °C then temperature and finally cycle number. Optimised conditions for each primer set are shown in Table 4-2.

Table 4-2: PCR primers used for detection of pluripotency and germ layer marker gene expression

Abbreviations: Tm, melting temperature; Ta, annealing temperature; Mg2+, magnesium concentration; C#, cycle number.

Name	Detects	Positive control	Primers	Tm (°C)	mRNA (bp)	gDNA (bp)	Ta (°C) used	Mg2+ (mM)	C#	Reference and accession number
POU5F1 5'	Pluripotent cells	hESC	gaaggtattcagccaaac	64.2	644	1192	57	3.5	26	Courtesy of Helen Priddle
POU5F1 3'			cttaatccaaaaaccctgg	63.9						NM_002701
NANOG 5'	Pluripotent cells	hESC	aggcaaacaacccacttctg	59.1	263	1507	59	3.5	28	Courtesy of Helen Priddle
NANOG 3'			tcttcggccagttgtttttc	59.6						NM_024865
T 5'	Mesoderm	hESC	agagcctgcagtaccgagtg	64.5	546	1826	59	1.5	36	
T 3'			tgaactgggtctcagggaag	64.2						NM_003181
MIXL1 5'	Mesoderm	hESC	ggtaccccgacatccacttg	66.2	341	1772	59	1.5	32	(Guo et al., 2002)
MIXL1 3'			ctcccatgagtccagctttg	64.1						NM_031944
GSC 5'	Mesoderm	hESC	gctctcgagaacctcttcca	63.6	257	563	59	2.5	34	Courtesy of Helen Priddle
GSC 3'			tcagctgtccgagtccaaat	64.8						NM_173849
EOMES 5'	Mesoderm/ Trophectoderm	hESC	gtcctcaggggtcggagc	57.9	870	3200	59	Q+2.5	40	(Kimura et al., 1999)
EOMES 3'			aataacggtgttttggtagg	67.4						NM_005442
SOX17 5'	Endoderm	Fetal liver	ctttcatggtgtgggctaagg	65.4	193	805	59	2.5	34	
SOX17 3'			cggtacttgtagttggggtggt	65.7						NM_022454
FOXA2 5'	Endoderm	Fetal liver	gacaagtgagagagcaagtg	57.6	234	234	53	1.5	34	(Ginis et al., 2004)
FOXA2 3'			acagtagtggaaaccggag	59.1						NM_021784
SOX1 5'	Ectoderm/Neural	Fetal brain	caatgcggggaggagaagtc	64	464	464	59	1.5	30	(Li et al., 2005)
SOX1 3'			ctctggaccaaactgtggcg	64.1						NM_005986
SOX3 5'	Ectoderm/Neural	Fetal brain	catgggctcggtagtgaagt	64	213	213	59	1.5	36	Courtesy of Virginie Sottile
SOX3 3'			cgttccgttgactgcagtc	64.6						NM_005634
18S 3'	All cells	rRNA	Proprietary	na	324	324	61	3.5	14	X03205

4.2.1.4 Agarose gel electrophoresis

1.5% agarose (Invitrogen) gels were prepared in 0.5 x TBE (VWR). Whilst molten, ethidium bromide (Sigma) was added to a final concentration of 20 ng ml^{-1}. Samples were supplemented with Gel Loading Buffer (Sigma) run in comparison to 100 Base-Pair Ladder (GE Healthcare). Gels were run in 0.5 x TBE supplemented with 20 ng ml^{-1} ethidium bromide at 100 V for 1.5 hr then visualised using a UV transilluminator and photographed using a Raytek cooled CCD camera system incorporating a FujiFilm LAS-1000 CCD camera and AIDA software.

4.2.2 Fluorescence activated cell sorting

For each of the three cell lines HUES-7, NOTT1 and NOTT2, a single cell suspension was made using 0.05% trypsin (Invitrogen) from ~15 million cells cultured on Matrigel in MEF conditioned medium. Cells were washed in D-PBS (Invitrogen), blocked in 20% FBS and incubated in SSEA3 or SSEA4 primary antibody (1 in 200, Chemicon) for 30 min and FITC conjugated Rabbit anti-Mouse (Jackson ImmunoResearch) secondary antibody for 30 min. Cells were passed through a Beckman Coulter FACS and the top 20% most fluorescent were collected. ~5x10^6 cells were recovered from each sample and RT-PCR was performed to analyse the expression of pluripotency and germ layer markers. A proportion of each sample was attached to a Superfrost Plus slide (Menzel-Gläser) using a Shandon Cytospin (Thermo) at 1000 rpm for 4 min and allowed to dry overnight before the addition of 1 drop of VectorShield with DAPI (Vector Laboratories) and a coverslip. Images were captured using a Leica DMRB upright fluorescent microscope, Hammatsu camera and Improvision OpenLab 4.0.2 and Volocity 4.0.1 software.

FACS figures were assembled using Weasel v2.3 (http://www.biotechcentre.net.au/cytometry/index.html).

4.2.3 Embedding and sectioning of mouse embryos and hEBs

For mouse E6.5 and E7.5 embryos, pregnant MF1 mice were killed by cervical dislocation according to home office schedule 1 at midday either 6 or 7 days after plugs were discovered. For E6.5 embryos whole decidua were removed from the uterus and fixed in 4% PFA (Sigma) in D-PBS for 1 hour. For E7.5 embryos, deciduas were dissected and embryos isolated and fixed in 4% PFA in D-PBS for 15 min. All embryos were embedded and sectioned in the same manner as hEBs as detailed in 3.2.3.

4.2.4 Immunofluorescence on whole mouse embryos and intact hEBs

Whole E6.5 and E7.5 mouse CD1 embryos were obtained as in 0, dissected from the decidua and Reichert's membranes were removed. hEBs were produced as described in 3.2.2. Both embryos and hEBs were fixed in 4% PFA for 15 min. Embryos/hEBs were washed three times in 0.1% Tween 20 (Sigma)/D-PBS then permeablised in 0.5% Triton X-100 (Sigma)/PBS for 30 min (10 min for hEBs). Embryos/hEBs were blocked overnight at 4 °C in 0.1% Tween 20, 1% Rabbit Serum/PBS. Embryos/hEBs were incubated for 1 h at room temperature with primary antibodies in 0.1% Tween 20, 1% Rabbit Serum/PBS. Embryos/hEBs were washed three times for 20 min with 0.1% Tween 20/PBS. Embryos/hEBs were incubated for 1 h at room temperature with a rabbit anti-goat or rabbit anti-rat FITC conjugated antibody (Jackson ImmunoResearch) in 0.1% Tween 20/PBS. Images were captured using a Leica DMIRE SP2 laser confocal microscope and Leica software.

4.2.5 Immunohistochemistry of sections

Slides were processed using a Vision Biosystems Bond-max immunohistochemistry (IHC) robot. Bond-max is fully automated and allows for simultaneous staining of 30 slides including dewaxing and epitope retrieval. The system was used in conjunction with Vision Bioystems proprietary Bond Refine Detection System, a biotin-free kit which provides peroxide block, secondary antibody, compact polymer reagent, DAB chromatin system and haematoxylin counterstain. The compact shape of the polymer reagent allows multiple conjugates to bind in close proximity and access to antigen sites inaccessible with convention long chain polymers. This results in high signal amplification for the detection of antigens at low concentrations and allows increased primary antibody dilutions for increased sensitivity. The Bond Refine Detection System is designed to work with Vision Biosystems proprietary primary antibodies raised in mouse or rabbit, to circumnavigate this issue a custom program was developed replacing preparatory primary antibody with those listed in Table 4-3. For primary antibodies raised in goat or rat the secondary antibody from Bond Refine Detection System was also replaced with either an unconjugated rabbit anti-goat antibody (Jackson ImmunoResearch) or an unconjugated mouse-absorbed rabbit anti-rat antibody (Vector Labs) respectively. The following parameters were used: Peroxidase Block 5 min; Primary antibody 30 min, Secondary antibody 15 min, Polymer 15 min, Mixed DAB 0 min, Mixed DAB 10 min, Haematoxylin 5 min. Slides were then processed through 100% ethanol and xylene before affixing a cover slide with DePeX mounting medium (VWR). Images were captured using a Leica DMRB (embryos) or DM4000B (hEBs) upright microscope. Qimaging Micropublisher camera and Improvision OpenLab 4.0.2 or 5.0.2 and Volocity 4 software.

4.2.6 Immunohistochemistry on slides of undifferentiated hESCs

All lines were cultured on Matrigel with MEF conditioned medium before transfer to Matrigel coated 4 well slides and growth for 48 hr. HUES-7 p21, NOTT1 p27, NOTT2 p33, BG01 p52 and H1 p19+11 Hoffman Objective images were taken after PFA fixation to minimise fixation related artefacts. Slides were processed through the Bond-max in the same manner as sections except excluding the dewax step.

Table 4-3: Antibodies used with Vision Biosystems Bond-max

Protein	Raised in	Antibody	Manufacturer	Reference
POU5F1	Mouse	monoclonal Oct-3/4, detects both POU5F1 isoforms	Santa Cruz	(Schultz *et al.*, 2004)
NANOG	Goat	polyclonal Anti-human NANOG	R&D Systems	(Cai *et al.*, 2005b)
T	Goat	polyclonal Anti-human Brachyury	R&D Systems	(Cai *et al.*, 2005b)
MIXL1	Rat	monoclonal MIXL1, clone 6G2	Courtesy of Andrew Elefanty and Anna Mossman, Monash University, Melbourne, Australia	(Mossman *et al.*, 2005)
SOX17	Goat	polyclonal Anti-human SOX17	R&D Systems	(Cai *et al.*, 2005b)
SOX1	Goat	polyclonal Anti-human SOX1	R&D Systems	(Cai *et al.*, 2005b)

4.3 RESULTS

4.3.1 Validation of primitive streak markers in whole gastrulating mouse embryos using immunofluorescence

Before immunofluorescence was used to determine the spatial expression of markers of the primitive streak (mesendoderm) and early mesoderm in whole hEBs, the specificity of these markers was first examined on whole CD1 mouse embryos at E7.5. Expression of T was clearly detected along the strip of primitive streak cells on the posterior side of the embryo and lower expression was detected in the allantoic bud (extra-embryonic mesoderm), MIXL1 was detected in individual cells on the posterior side of the embryo but was less clearly localised to the primitive streak. Images of embryos stained with anti-T and anti-MIXL1 antibodies and respective negative controls with primary antibodies omitted are shown in Figure 4-1.
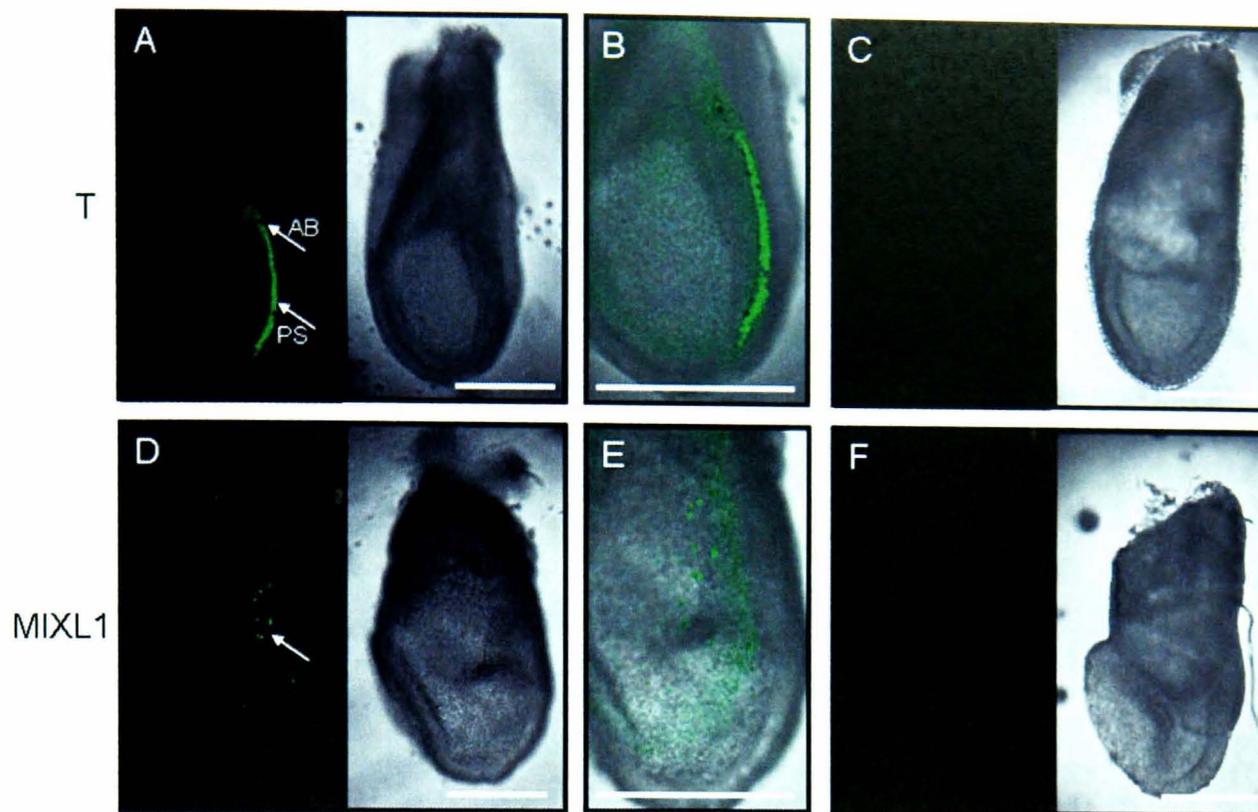
Figure 4-1: Expression of T and MIXL1 in the primitive streak of gastrulating mouse embryos

Whole E7.5 mouse embryos were stained with anti-T (A and B) or anti-MIXL1 (D and E) antibodies followed by secondary antibodies conjugated to FITC to reveal T or MIXL1 expressing cells in the primitive streak. Representative FITC filter images observed using a confocal microscope are shown on the left and phase images on the right. Enlarged and merged images are shown in B and E. Arrows indicate T or MIXL1 expressing cells in the posterior region of the embryo. PS, primitive streak; AB, allantoic bud. Representative images of embryos stained in the same manner as embryos in A and C with the primary antibody omitted (control) are shown in B and D respectively. Mouse embryo experiments were repeated independently twice. Data above is recorded from the second replicate. Approximately 6 embryos for each of the 4 conditions were observed under a confocal microscope.

Scale bar = 250 μm.

4.3.2 Detection of primitive streak markers in hEBs using immunofluorescence

In order to determine whether T and MIXL1 expression could be detected in hEBs, d8-12 HUES-7 hEBs were formed by the forced aggregation method detailed in Chapter 3 (3.2.2). Immunofluorescence was performed, using 30 hEBs for each sample, to detect the expression of T and MIXL1 using an identical protocol to that used for mouse embryos in 4.3.1. d8-d12 hEBs were selected for examination on the basis of previous RT-PCR detection of *T* and *MIXL1* at these stages by Ng *et al.* (2005a). hEBs were formed every two days over six days allowing d8-d12 samples to be collected on the same day to standardise exposure to PFA fixation. Representative results are shown in Figure 4-2. Both markers were detected in d8–d12 hEBs. T was expressed at a higher level than MIXL1 and was localised mostly to the outside. MIXL1 expression demonstrated a more punctate and rather more dispersed pattern of expression throughout the hEBs.
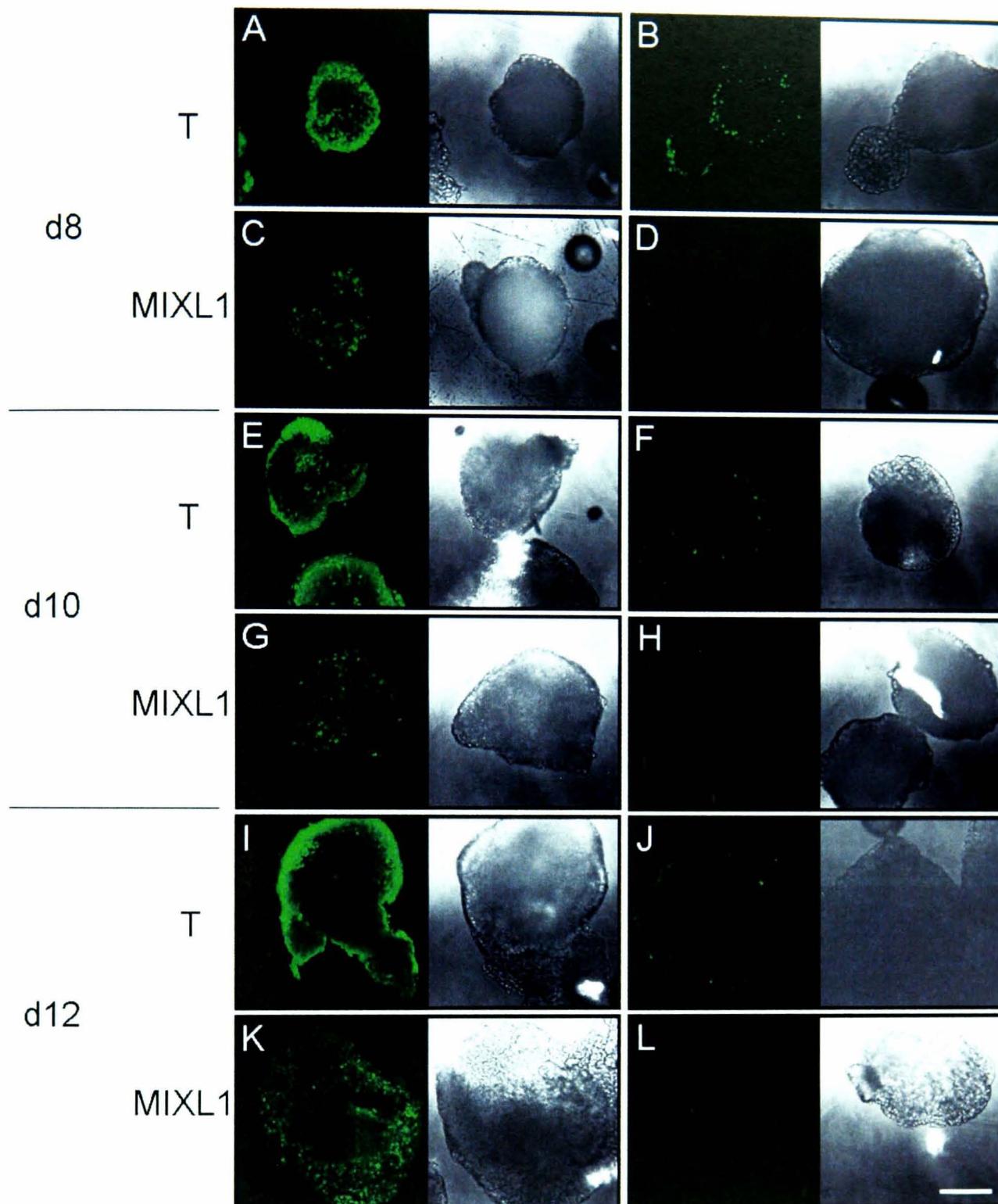
Figure 4-2: Expression of T and MIXL1 in d8-d12 HUES-7 hEBs

Whole HUES-7 hEBs formed by forced aggregation of 10 000 cells at d8, d10 and d12 were stained with anti-T (A, E, I) or anti-MIXL1 (C, G, K) antibodies followed by secondary antibodies conjugated to FITC to reveal T or MIXL1 expressing cells. Representative FITC filter images observed using a confocal microscope are shown on the left and phase images on the right. Images of hEBs stained in the same manner as hEBs in A, E, I and C, G, K with the primary antibody omitted are shown in B, F, J and D, H, L respectively.

Scale bar = 250 μm.

4.3.3 Validation of pluripotency and germ layer markers in mouse embryos using immunohistochemistry

Since, in whole mount hEBs, immunofluorescence revealed only peripheral staining of T and MIXL1, sections were then examined to investigate whether improved detail could be resolved. The use of sections also allowed the prevention of issues associated with lack of antibody penetration. The availability of a Vision Biosystems Bond-max™ automated immunohistochemistry system, which allows for high throughput analysis and provides high levels of inter-run comparability, lead to this system being chosen over manual immunofluorescence staining. In addition to investigating the expression of primitive streak/mesendoderm markers the high-throughput system allowed for simultaneous analysis of pluripotency and germ layer markers to better define the relationship between remaining pluripotent cells and cells that have begun germ layer specification. Serial sections of the hEBs (5 μm) allowed comparative staining of multiple markers in the same region of an individual hEB. Five markers were chosen; POU5F1 and NANOG to detect pluripotent cells, SOX1 to detect ectoderm/early neuroectoderm, SOX17 for endoderm and T for mesendoderm (and, in later development, mesoderm). The anti-T antibody was used rather than anti-MIXL1 due to the more restricted expression pattern of T observed within the primitive streak during gastrulation in section 4.3.1 and also conflicting evidence of *Mixl1* expression in the visceral endoderm (Pearce and Evans, 1999, Robb *et al.*, 2000, Mohn *et al.*, 2003).

To validate the specificity of these markers within the hEB system, immunohistochemistry was performed on sections of early primitive streak (E6.5) and gastrulating (E7.5) MF1 mouse embryos. Each of the five markers were

previously shown to be expressed in a restricted location (See 4.1.1.1-4.1.1.3 and Table 4-1)

In the E6.5 embryo POU5F1 expression was restricted to the forming early primitive ectoderm, with nuclear staining in both epiblast and epithelial primitive ectoderm cells (Figure 4-3A). More loosely packed cells with larger cytoplasm formed a strip of POU5F1 expressing cells along the posterior/distal portion of the embryo. Low level expression of POU5F1 was also noted in a small number of cells of the forming embryonic visceral endoderm at the distal tip of the embryo and cells of the extra-embryonic visceral endoderm. Some staining, potentially due to antibody trapping, was also seen in the location of Reichert's membrane on the anterior and posterior sides of the extra-embryonic portion of the embryo.

In the E7.5 embryo POU5F1 was strongly detected throughout the primitive ectoderm, which by this stage had formed a distinctive epithelial morphology, with some nuclear and cytoplasmic locations staining (Figure 4-3B). POU5F1 was also detected throughout the extra-embryonic visceral endoderm and in the recently formed primitive streak and scattered cells of the embryonic visceral endoderm.

NANOG expression was substantially different to POU5F1 expression (Figure 4-4A) and with only low levels detected in scattered cells within the epiblast/primitive ectoderm of the E6.5 embryo. In the E7.5 embryo (Figure 4-4B), very low NANOG expression was seen in both the nucleus and cytoplasm of a few scattered cells of the columnar primitive ectoderm and the primitive endoderm towards the distal end of the embryo.

T expression was seen in two distinct areas in the E6.5 embryo (Figure 4-5A). T was strongly expressed in the nucleus of cells in a tightly packed single cell-thickness

area assumed to be the anterior mesendoderm. This layer of cells exists outside of the epiblast/primitive ectoderm, immediately anterior to the distal tip of the embryo at the location of the presumptive headfold/node. T was also expressed in the region of the forming primitive streak. This area extended up to the nascent allantoic bud.

At E7.5, T was strongly expressed in an embryonic region between the visceral endoderm and the epithelial primitive ectoderm (Figure 4-5B). The epithelial primitive ectoderm of this area also expressed T, albeit at a lower level. Distally to this region, T was expressed throughout the posterior side of the embryo including the visceral endoderm in an area of cells showing little epithelial organisation. Below this area was a cluster of cells not expressing T surrounding the area of the T-expressing node. As in E6.5 towards the anterior portion of the distal tip of the embryo at the location of the presumptive headfold/node, a single cell layer of cells was seen to strongly express T. On the anterior side of the embryo, T was detected between the primitive ectoderm and the anterior visceral endoderm. T was also observed in the extra-embryonic regions of inside of the both the anterior and posterior extra-embryonic visceral endoderm and within cells of the amniotic and chorionic mesoderm.

SOX17 was expressed in similar regions of in both the E6.5 and E7.5 embryo. Expression was detected in the nucleus of cells in the single cell-thickness visceral endodermal layer around the outside of the whole embryo. At E6.5 SOX17 expression was also seen at very low levels in the epiblast/primitive ectoderm, with more dominant expression in the nucleus (Figure 4-6A). In the E7.5 embryo expression was most obvious in the visceral endoderm but was also present in the cytoplasm of the epithelial primitive ectoderm (Figure 4-6B). Of note, no expression

of SOX17 was observed in the nascent primitive streak areas of either the E6.5 or E7.5 embryos.

Nuclear SOX1 expression was observed throughout the E6.5 embryonic and extra-embryonic epiblast/primitive ectoderm, in particular in the non-epithelial cells towards the anterior side of the E6.5 embryo (Figure 4-7A). In the E7.5 embryo SOX1 expression in the embryonic and extra-embryonic primitive ectoderm appeared confined to the cytoplasm (Figure 4-7B).

Negative controls with the primary antibody omitted are included in Figure 7-1.
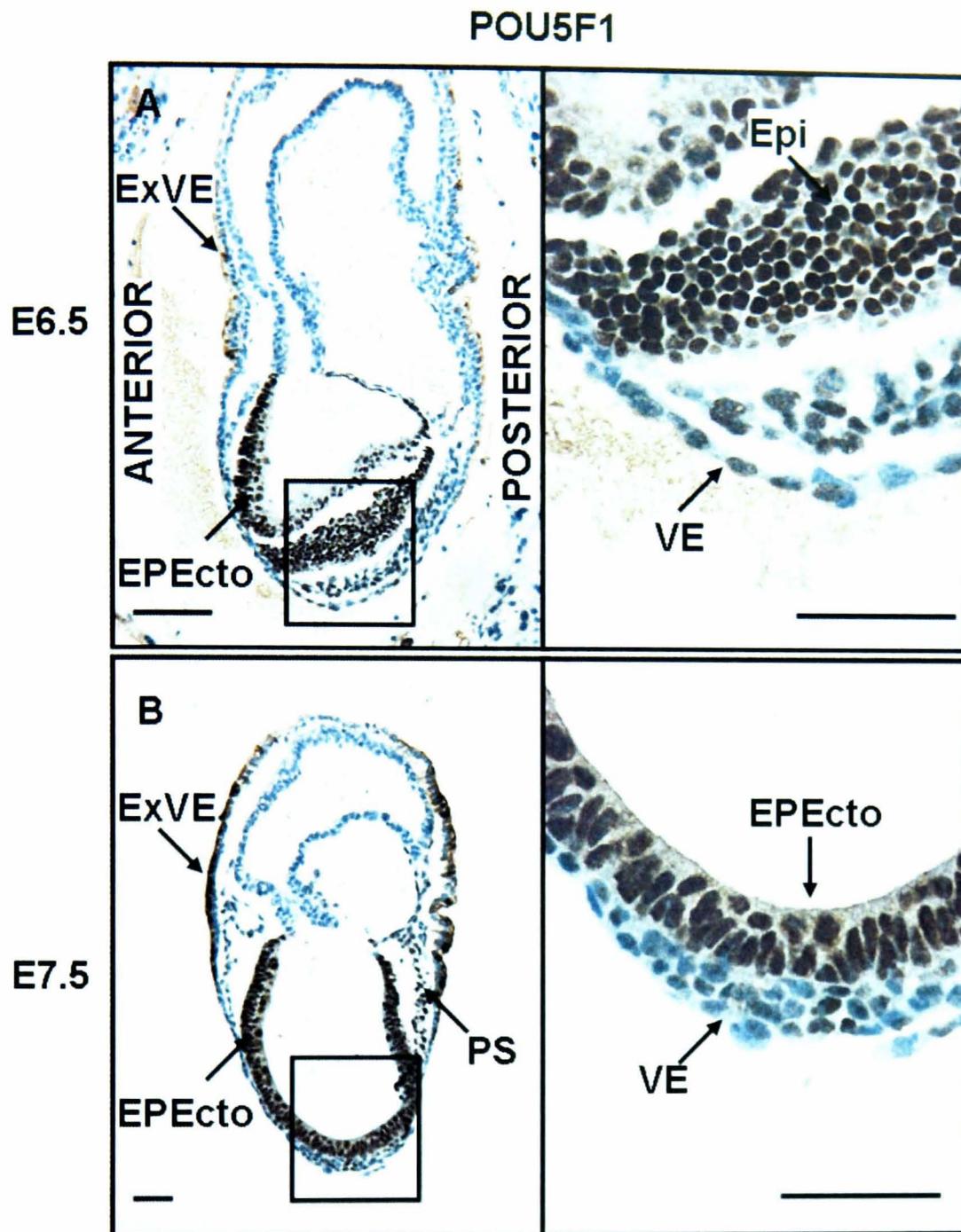
POU5F1

Figure 4-3: Expression of POU5F1 in early streak and gastrulating mouse embryos

Sections of E6.5 (A) and E.75 (B) mouse embryos after immunohistochemistry for detection of the expression of POU5F1. Images of full embryo on the left (A using 10 x objective and B using 5 x objective) and magnified area of interest of the right (20 x objective). A) Showing expression throughout the epiblast/primitive ectoderm. B) Showing expression in the now fully epithelial primitive ectoderm and lower level expression in the visceral endoderm. E7.5 experiments were repeated twice independently and E6.5 once. ExVE: extra-embryonic visceral endoderm; EPEcto: epithelial primitive ectoderm; Epi: Epiblast; VE: visceral endoderm; PS: primitive streak.

Scale bar = 50 μm.
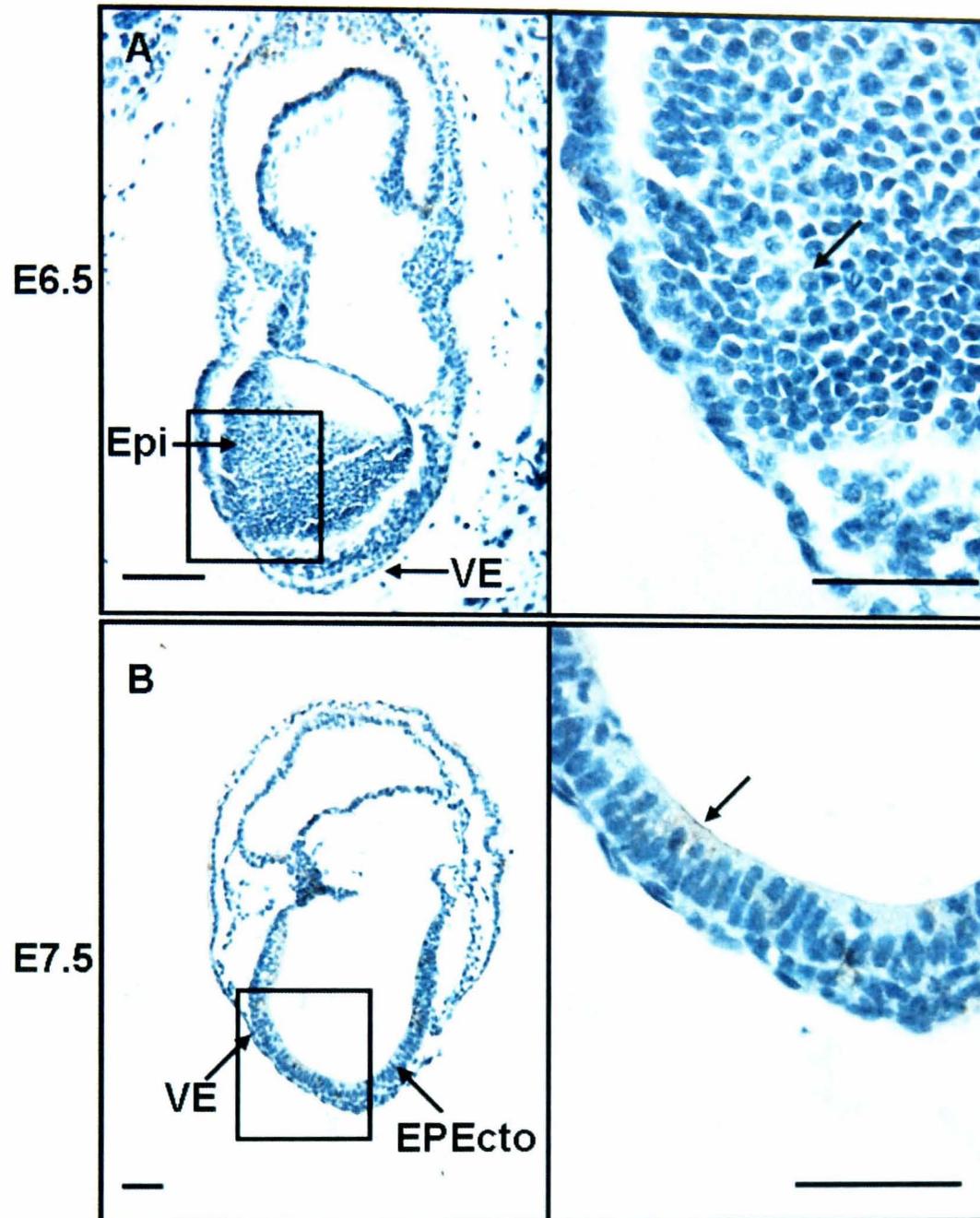
NANOG

Figure 4-4: Expression of NANOG in early streak and gastrulating mouse embryos

Sections of E6.5 (A) and E.75 (B) mouse embryos after immunohistochemistry for detection of the expression of NANOG. Images of full embryo on the left (A using 10 x objective and B using 5 x objective) and magnified area of interest of the right (20 x objective). A) Showing expression in few scattered cells of the epiblast/primitive ectoderm (arrow). B) Showing expression in the cytoplasm of cells within the primitive ectoderm (arrow). EPEcto: epithelial primitive ectoderm; Epi: epiblast; VE: visceral endoderm.

Scale bar = 50 μm.
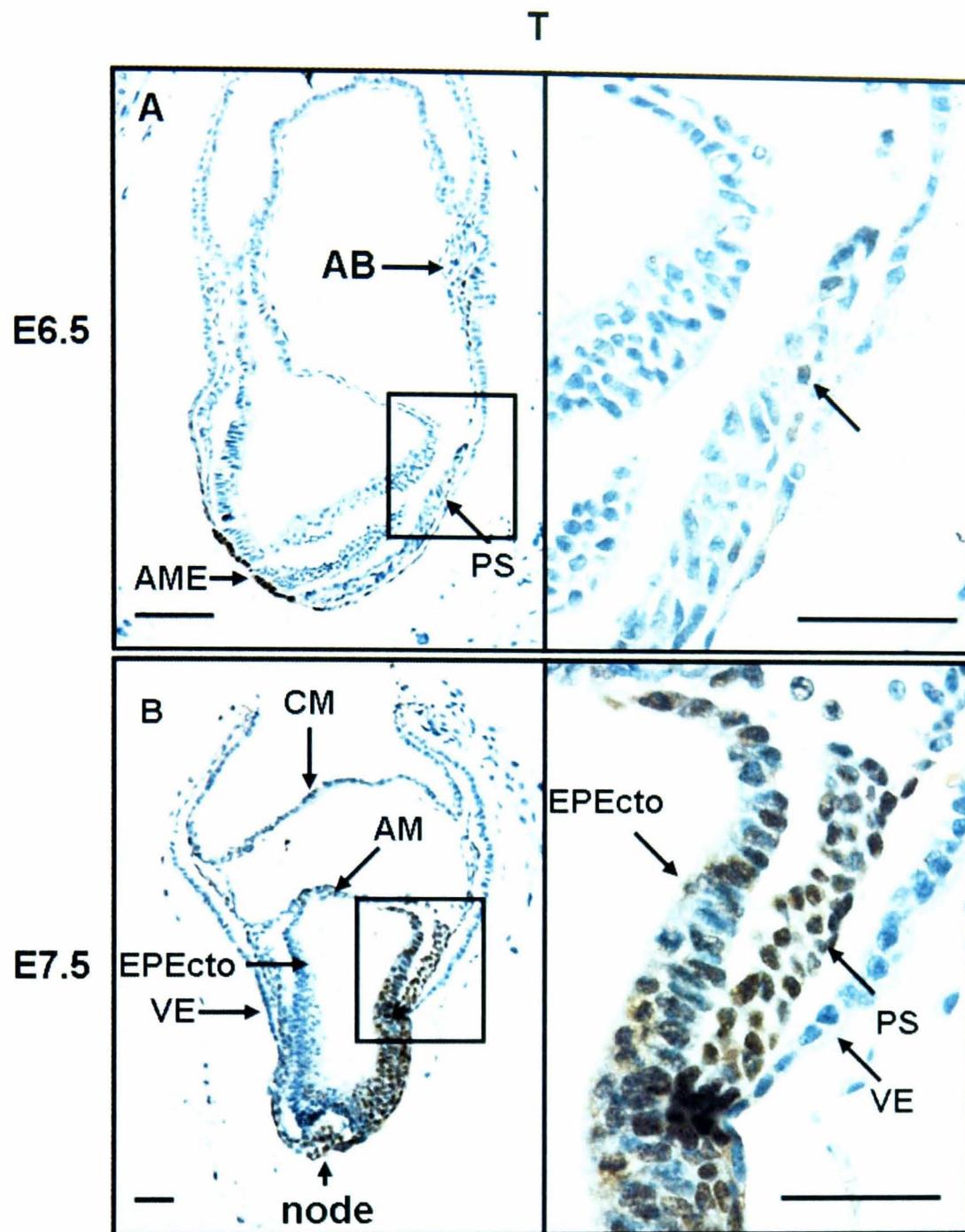
Figure 4-5: Expression of T in early streak and gastrulating mouse embryos

Sections of E6.5 (A) and E.75 (B) mouse embryos after immunohistochemistry for detection of the expression of T. Images of full embryo on the left (A using 10 x objective and B using 5 x objective) and magnified area of interest of the right (20 x objective). A) Showing expression towards the allantoic bud, forming primitive streak area (arrow) and anterior mesendoderm. B) Showing expression in the primitive streak, the posterior primitive ectoderm and the node. AB, allantoic bud; AME, anterior mesendoderm; PS, primitive streak; VE: visceral endoderm; CM, chorionic mesoderm; AM, amniotic mesoderm, EPEcto: epithelial primitive ectoderm.

Scale bar = 50 µm.
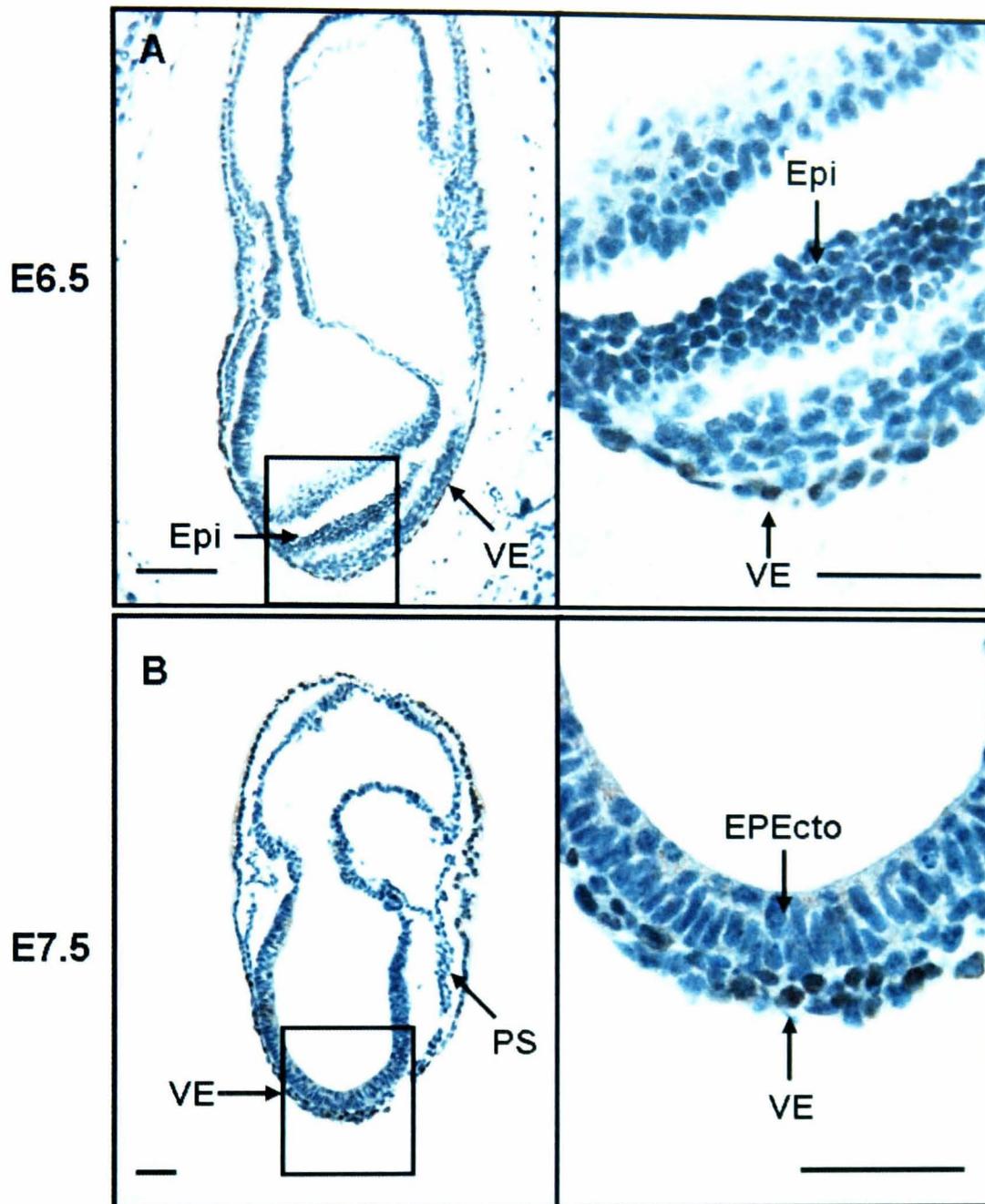
SOX17

Figure 4-6: Expression of SOX17 in early streak and gastrulating mouse embryos

Sections of E6.5 (A) and E.75 (B) mouse embryos after immunohistochemistry for detection of the expression of SOX17. Images of full embryo on the left (A using 10 x objective and B using 5 x objective) and magnified area of interest of the right (20 x objective). A) Showing expression in the single cell-thickness visceral endoderm around the periphery of the embryo strongest at the most distal point of the embryo and in the epiblast/primitive ectoderm. B) Showing expression in the visceral endoderm which has no thickened to ~2 cells thick and cytoplasmically within the epithelial primitive ectoderm. Epi, epiblast; VE: visceral endoderm; PS, primitive streak; CM; EPEcto: epithelial primitive ectoderm.

Scale bar = 50 μm.
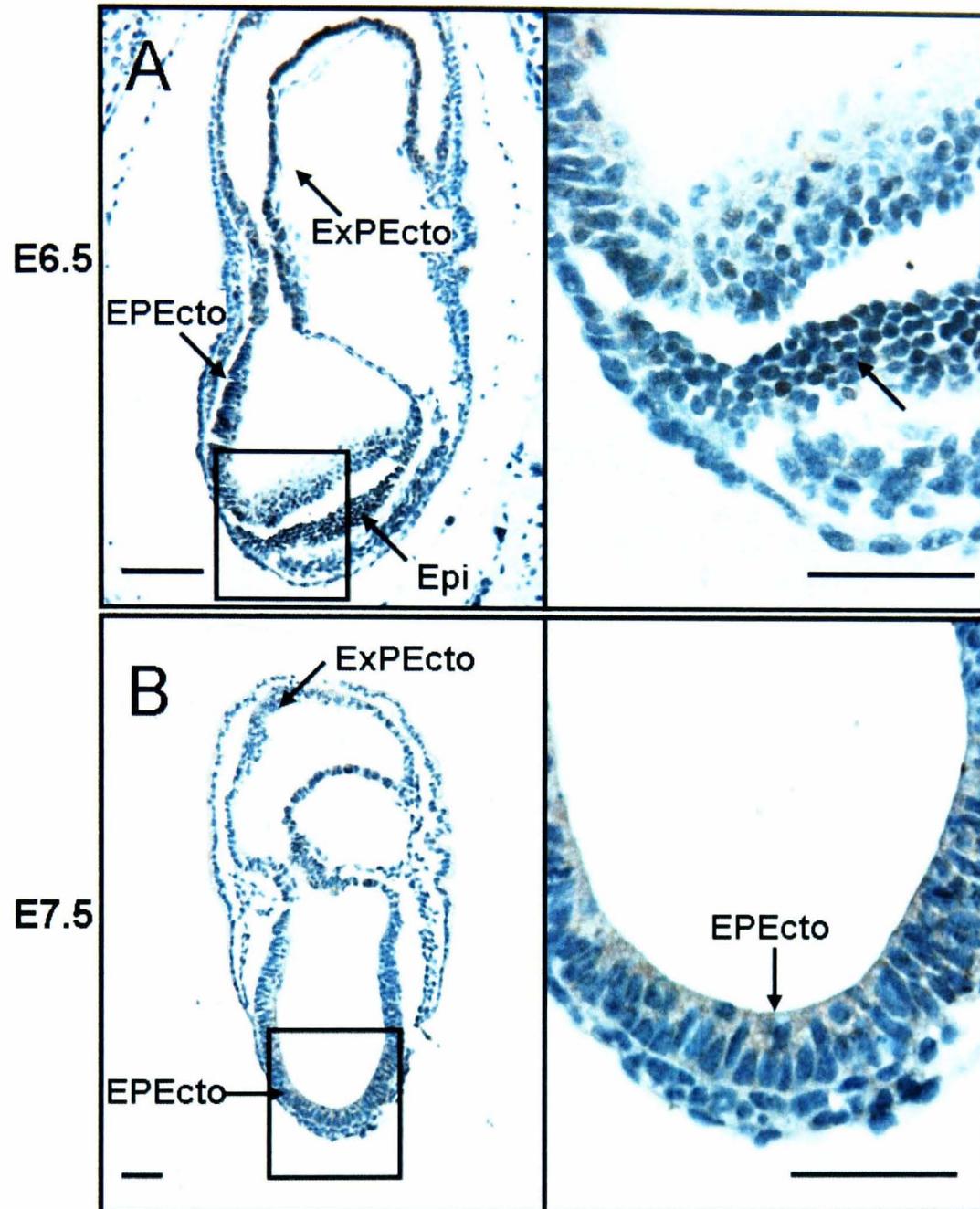
SOX1

Figure 4-7: Expression of SOX1 in early streak and gastrulating mouse embryos

Sections of E6.5 (A) and E.75 (B) mouse embryos after immunohistochemistry for detection of the expression of SOX1. Images of full embryo on the left (A using 10 x objective and B using 5 x objective) and magnified area of interest of the right (20 x objective). A) Showing expression in the extra-embryonic and embryonic epiblast/primitive ectoderm, particularly in the non-epithelial cells (arrow). B) Showing expression in the cytoplasm of cells of the extra-embryonic and embryonic primitive ectoderm. ExPEcto, extra-embryonic primitive ectoderm, EPEcto: epithelial primitive ectoderm; Epi: epiblast; VE: visceral endoderm.

Scale bar = 50 μm.

4.3.4 Comparison of pluripotency and germ layer marker expression in d2 HUES-7 hEBs formed using mass culture or forced aggregation

hEBs were analysed using the immunohistochemistry protocols validated on mouse embryos (4.3.3). First compared was the effect of the method of hEB formation on marker expression. Previous experiments using haematoxylin and eosin staining (3.3.4) had identified substantial differences in the structure of the hEBs produced by the two methods, even immediately after formation. Figure 4-8 shows the expression of POU5F1, NANOG, T, SOX17 and SOX1 in serial sections of d2 mass culture and forced aggregation HUES-7 hEBs.

Mass culture hEBs (Figure 4-8A) displayed substantial variation in pluripotency marker expression with nuclear POU5F1 expression only detected in some hEBs of a small size (<200 μm, denoted by circle) and isolated small clusters within the larger hEBs (>1000 μm, denoted by square). Low level nuclear POU5F1 expression was also detected in scattered cells throughout the mass culture hEBs (arrows). NANOG was more ubiquitously expressed than POU5F1. In larger mass culture hEBs, regions of both nuclear and cytoplasmic expression were detected (arrows). Highest nuclear expression was detected in regions of high POU5F1 expression (square) and at the periphery of some hEBs. NANOG was also highly expressed in the smaller hEBs that expressed POU5F1 (circle). Uniform nuclear POU5F1 expression was detected throughout all forced aggregation hEBs (Figure 4-8B). Nuclear NANOG expression was also detected in the majority of cells of the forced aggregation hEBs, albeit at lower levels than POU5F1 and at higher levels at the periphery.

In the mass culture hEBs nuclear T, SOX17 and SOX1 expression was detected in many cells. In the larger mass culture hEBs T was expressed in scattered, isolated cells at the centre of the hEBs (arrows) whereas cells expressing SOX17 appeared

localised together (arrows) and SOX1 appeared more ubiquitously and cytoplasmically expressed (arrows). In the some of the smaller hEBs that expressed high levels of POU5F1 and NANOG, high levels of nuclear T, SOX17 and SOX1 expression were also detected (circle). In the forced aggregation hEBs, only very low levels of (nuclear) T, SOX17 and SOX1 expression were evident throughout the hEBs, with slightly more intense staining towards the periphery.

These results reinforce the more, reproducible differentiation observed using the forced aggregation system in comparison the traditional mass culture system, as observed in Chapter 3 (3.3.1-3.3.2). Pluripotency/germ layer maker expression patterns in mass culture hEBs are highly variable, with an apparent relationship to hEB size detected. In contrast, expression patterns in forced aggregation hEBs exhibit almost no variation between hEBs.

A, Mass cultured

| POU5F1 | NANOG | T | SOX17 | SOX1 |

B, Forced aggregation
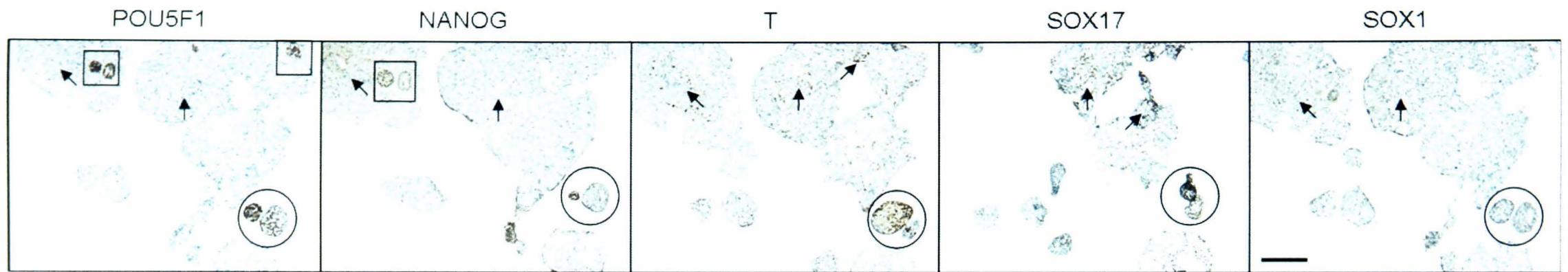
| POU5F1 | NANOG | T | SOX17 | SOX1 |
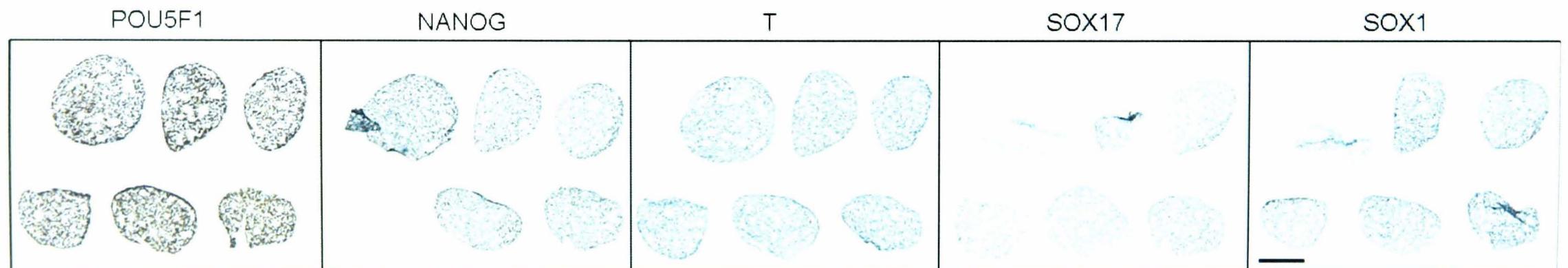
Figure 4-8: Expression of POU5F1, NANOG, T, SOX17 and SOX1 and in mass culture and forced aggregation hEBs

Sections of mass culture and forced aggregation HUES-7 hEBs at d2 after immunohistochemistry for detection of the expression of POU5F1, NANOG, T, SOX17 and SOX1. Images were taken at the same time using a 10 x objective. A) Showing nuclear co-expression of all five markers in smaller mass culture hEBs (circles), nuclear co-expression of pluripotency markers within larger mass culture hEBs (squares) and areas of marker expression within larger hEBs (arrows). B) Showing high level expression of POU5F1 and slightly lower level expression of NANOG and low level expression of T, SOX17 and SOX1 in forced aggregation hEBs. Scale bar = 200 µm

4.3.5 Ontogeny of pluripotency and germ layer marker expression in mass culture and forced aggregation HUES-7 hEBs throughout differentiation

To map pluripotency and germ layer marker expression in mass culture HUES-7 hEBs, samples were collected for analysis every two days over 16 days of differentiation. 30-40 hEBs from each time-point were embedded and serial sections were assessed using immunohistochemistry for the pluripotency and germ layer markers POU5F1, NANOG, T, SOX17 and SOX1. cDNA was prepared from 10-15 hEBs of the same samples and used for RT-PCR with an extended panel of pluripotency and germ layer markers: pluripotency, *POU5F1* and *NANOG*; mesendoderm, *T*, *MIXL1* and *GSC*; endoderm, *SOX17* and *FOXA2*; ectoderm, *SOX1* and *SOX3*.

4.3.5.1 Timing of expression of pluripotency and germ layer markers in mass culture HUES-7 hEBs detected by RT-PCR

RT-PCR (Figure 4-9) demonstrated that the pluripotency markers *POU5F1* and *NANOG* were both highly expressed in undifferentiated cells (d0). Both were substantially down-regulated at d2, before further reducing in expression gradually to d14, with no or very low expression detectable at d16. Immunohistochemistry results were consistent with this data, showing that POU5F1 and NANOG gradually reduced in expression during hEB differentiation, but that both were still detectable in a very small number of cells at d16 (Figure 4-10).

Of the three mesendodermal markers, *T* was expressed at relatively low levels in undifferentiated cells compared to *MIXL1* and *GSC*. mRNA expression of all three mesendodermal markers peaked at d2-d6 before gradually reducing towards d16 (Figure 4-9). T protein was also detected in undifferentiated cells (Figure 4-18) and,

during differentiation, it was expressed at highest levels from d2-d10 (although it was still evident at d16), see Figure 4-10.

Expression of the endodermal markers, *SOX17* and *FOXA2*, was seen at low levels in the undifferentiated cells and both makers were consistently expressed through d2-d16 (Figure 4-9). SOX17 protein was expressed in undifferentiated cells (Figure 4-18) and throughout differentiation with highest expression at d14-d16 (Figure 4-10).

Of the two ectodermal markers, *SOX1* was expressed at very low levels in undifferentiated cells, and *SOX*3 was not detected. *SOX1* and *SOX3* expression gradually increased, peaking at d8-d10 before gradually reducing to d16 (Figure 4-9). SOX1 protein was detected in undifferentiated cells (Figure 4-18) and cytoplasmic expression was seen throughout differentiation and weak nuclear expression could be detected from d8-d16 (Figure 4-10).
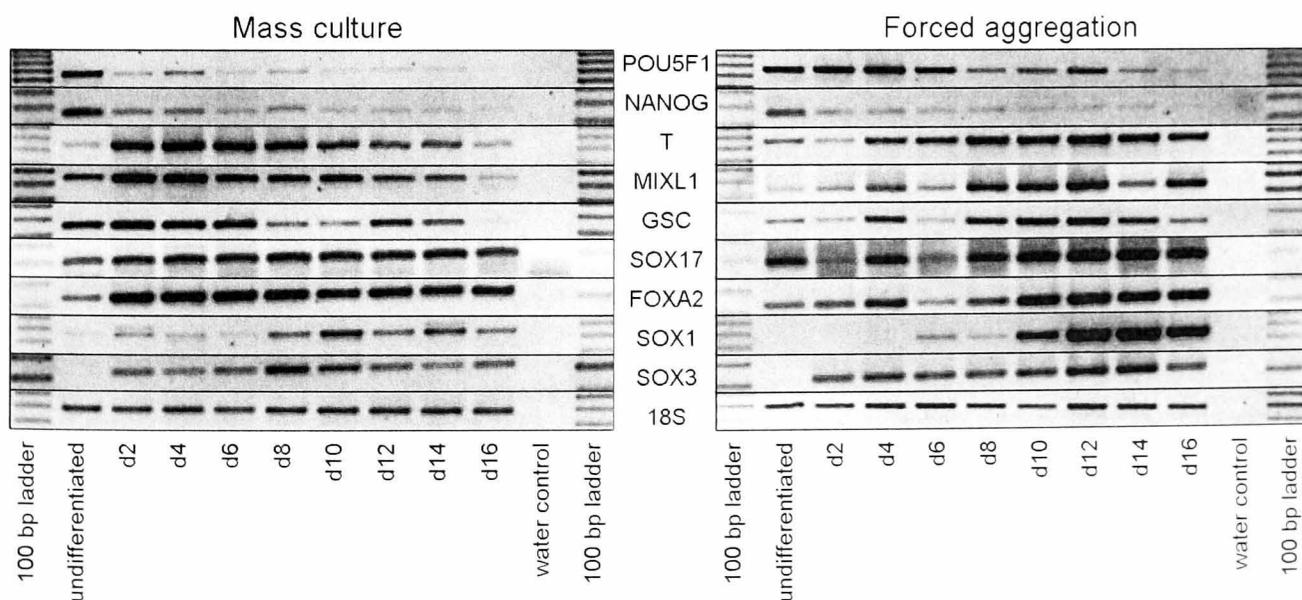
Figure 4-9: Expression of pluripotency and germ layer markers in HUES-7 hEBs formed by mass culture and forced aggregation detected by RT-PCR

4.3.5.2 Spatial expression of POU5F1, NANOG, T, SOX17 and SOX1 in mass culture HUES-7 hEBs detected by immunohistochemistry

Overall, sections of mass culture hEBs demonstrated highly variable morphology in hEBs at d2 (Figure 4-10). Numerous hEBs of >1000 μm in diameter (4 visible in images) were produced along with smaller hEBs of ≤200 μm (11 visible in images). Internal cavities were present at this time-point but appeared to be formed by the aggregation process rather than by cavitation, since no characteristic epithelial cell layer or basement membrane was visible. Over d4-d8, hEBs became more uniform in size with diameters ranging from 300-600 μm and one or more internal cavities present in the majority of hEBs from d6. hEB size was constant from d8 onwards despite an increase in the number and size of cavities and the formation of internal structures.

4.3.5.2.1 Mass culture day 2

At d2, the first time-point examined after hEBs were induced to form, approximately 50% of the smaller (<200 μm) mass culture hEBs demonstrated nuclear co-expression all of the five markers (Figure 4-10, denoted by circles). POU5F1, NANOG, T and SOX1 were co-expressed in some small regions of the larger hEBs (>1000 μm, denoted by circles). NANOG was additionally expressed cytoplasmically in the some of the larger hEBs (denoted by arrows, example in inset). T and SOX1 were expressed both cytoplasmic and scattered nuclear locations towards the centre of the larger hEBs (arrows). Nuclear SOX17 expression, whereas not clearly co-expressed with the other markers in larger hEBs, was detected in substantial areas across the larger hEBs (arrows).

4.3.5.2.2 Mass culture day 4

The pattern of co-expression seen at d2 was maintained at d4 with all five markers co-expressed in some of the smaller hEBs (<300 μm, circles) along with some areas of the intermediate sized hEBs (300-600 μm, circles). In one hEB POU5F1, T and SOX17 were independently expressed in spatially separate areas (denoted by red square). Larger hEBs (600-1000 μm) and a small number of intermediate sized hEBs demonstrated no expression of POU5F1 or NANOG but both clusters of low level nuclear and cytoplasmic expression of T, SOX17 and SOX1 (arrows).

4.3.5.2.3 Mass culture day 6

At d6, hEBs had become more uniform in size and internal cavities surrounded by an epithelial layer were visible. Nuclear co-expression of POU5F1, NANOG, T and SOX17 was detected in distinct clusters of cells in approximately 60% (9/14) larger sized hEBs (example inset and circles). Cytoplasmic expression of NANOG, T, SOX17 and SOX1 was detected in patches particularly in hEBs in which clusters of nuclear expression were not detected (arrows).

4.3.5.2.4 Mass culture day 8

At d8, pluripotency marker expression was reduced in comparison to d6 and was, in some hEBs, spatially separate from mesoderm/endoderm marker expression. POU5F1 expression was only detected in approximately 25% of hEBs (7/27). Spatially, POU5F1 was observed throughout some smaller hEBs, at the periphery of immediate sized hEBs and surrounding some cavities or in loose cells in the centre of larger hEBs (circles). NANOG was expressed cytoplasmically in all larger hEBs (arrows) in addition to nuclear locations expressing POU5F1 (circles) and a few additional locations (squares). Nuclear T and SOX17 expression was detected in some locations similar to POU5F1 and NANOG (circles). Nuclear cytoplasmic T

expression also partially co-localised with high levels of SOX17 expression in larger hEBs (squares). For the first time, SOX17 was also expressed in areas lacking T expression, in some intermediate size hEBs (squares). SOX1 was expressed cytoplasmically in areas exhibiting nuclear expression of both T and SOX17 (arrows).

4.3.5.2.5 Mass culture day 10

At d10, mesoderm and endoderm markers were expressed in additional locations in comparison to the pluripotency markers. Nuclear expression of POU5F1 was detected in small areas of ~25% (4/16, circles) of the larger hEBs. NANOG was expressed cytoplasmically in all d10 hEBs, with nuclear expression in similar areas to POU5F1 (albeit in a larger area of cells). Nuclear expression of T was seen in large clusters centred on areas of POU5F1 expression as well as in areas not expressing POU5F1 (squares). T was also expressed cytoplasmically in all hEBs. Strong nuclear and cytoplasmic expression of SOX17 was seen in all hEBs with strongest nuclear expression in areas of expressing T (squares). Weak nuclear and cytoplasmic expression of SOX1 was seen in similar areas to those expressing T and SOX17 (squares).

4.3.5.2.6 Mass culture day 12

Although only a few hEBs were analysed at d12 (n=4), no expression of POU5F1, and only weak cytoplasmic staining of NANOG and T was detected (arrows). Nuclear expression of SOX17 in a tight cluster of cells was detected along with some cytoplasmic staining (squares). Nuclear SOX1 expression was seen in some isolated cells at the periphery of one of one hEB.

4.3.5.2.7 Mass culture day 14

At d14, little pluripotency marker expression remained, although substantial germ layer marker expression was obviously detected. Clusters of approximately 5 cells expressing POU5F1 were seen at the periphery of approximately 33% (6/18) of hEBs (circles). Cytoplasmic NANOG expression was seen in all hEBs along with strong nuclear expression in areas also expressing POU5F1 (circles). T was expressed cytoplasmically throughout some intermediate sized hEBs and at the centre of others whilst at the periphery of larger hEBs (squares). SOX17 was expressed cytoplasmically in similar locations to T but also with strong nuclear staining at the centre of intermediate sized hEBs and at the periphery of larger hEBs. SOX1 expression was similar to SOX17 although nuclear expression was weaker.

4.3.5.2.8 Mass culture day 16

At d16 substantial nuclear expression was only visible for SOX17. Almost no POU5F1 expression was visible except a few cells in two hEBs (circles). Nuclear expression of NANOG and T were similar to POU5F1 (circles) with additional cytoplasmic expression present in all hEBs. SOX17 was cytoplasmically expressed in all hEBs and with strong nuclear expression at the centre of the majority (15/23) of hEBs (squares). Low level nuclear expression of SOX1 was detected surrounding surround cavities of some of the larger hEBs (squares).

4.3.5.2.9 Comparison of marker expression between mass culture and forced aggregation HUES-7 hEBs

Along with the substantial difference in size and cardiomyocyte potential (Chapter 3) a number of differences in developmental programming/ontogeny were noted between mass culture and forced aggregation hEBs. Most obvious was the spatial disparity between POU5F1 and NANOG expression at d2 between the two

techniques, as described in 4.3.4. Expression of POU5F1 was maintained at high levels in forced aggregation hEBs throughout d2-d6 as shown by both immunohistochemistry (Figure 4-12) and RT-PCR (Figure 4-9). In contrast, in mass culture hEBs, only some smaller hEBs and small areas larger hEBs expressed POU5F1 at d2. These low levels POU5F1 expression were maintained until d16.

In mass culture hEBs (Figure 4-10), *NANOG* expression was similar to *POU5F1* expression by RT-PCR despite higher levels of cytoplasmic expression throughout differentiation. In comparison, in forced aggregation hEBs, *NANOG* expression was more quickly down-regulated than *POU5F1* expression detected by both RT-PCR and immunohistochemistry assays.

By RT-PCR both mesendoderm and endoderm markers appeared most highly expressed at d2-d4 in mass culture hEBs compared to maximal expression at d10-d12 in forced aggregation hEBs (Figure 4-9). Notably, by immunohistochemistry, SOX17 expression was seen to spatially diverge from POU5F1/NANOG/T expression in mass culture hEBs at d8, despite the constant level of expression detected by from d2-d16 by RT-PCR (Figure 4-9), whereas, in forced aggregation hEBs, this separation occurred later at d12.

mRNA expression for the ectodermal markers, *SOX1* and *SOX3*, peaked at d12-d14 in forced aggregation hEBs, concordant with a similar a peak in SOX1 protein expression. In comparison, in mass culture hEBs, no peak in either *SOX1* or *SOX3* expression any of the time-points or substantial nuclear of SOX1 expression was detected.

Overall, gene and protein expression in mass culture hEBs was characterised by a slow down-regulation of the markers from d2 to d16. In comparison forced

aggregation hEBs appeared to have a more distinct pattern of pluripotency marker down-regulation and subsequent germ layer marker up-regulation.

Figure 4-10: (pages 217 to 220) Expression of POU5F1, NANOG, T, SOX17 and SOX1 in d2-d16 HUES-7 hEBs formed by mass culture

Sections of mass culture HUES-7 hEBs at d2-d16 after immunohistochemistry for the detection of POU5F1, NANOG, T, SOX17 and SOX1. Upper images were taken using a 5 x objective and lower images with a 20 x objective.

Images demonstrate the timing and co-localisation of marker expression with:

Circles highlighting areas of conserved expression between pluripotency and germ layer markers.

Squares highlighting areas of contrasting expression between pluripotency and germ layer markers

Arrows highlight areas of cytoplasmic and/or scattered nuclear expression.

Scale bar = 500 μm.

POU5F1   NANOG   T   SOX17   SOX1

d6

d8

POU5F1   NANOG

d10

d12

d14

d16
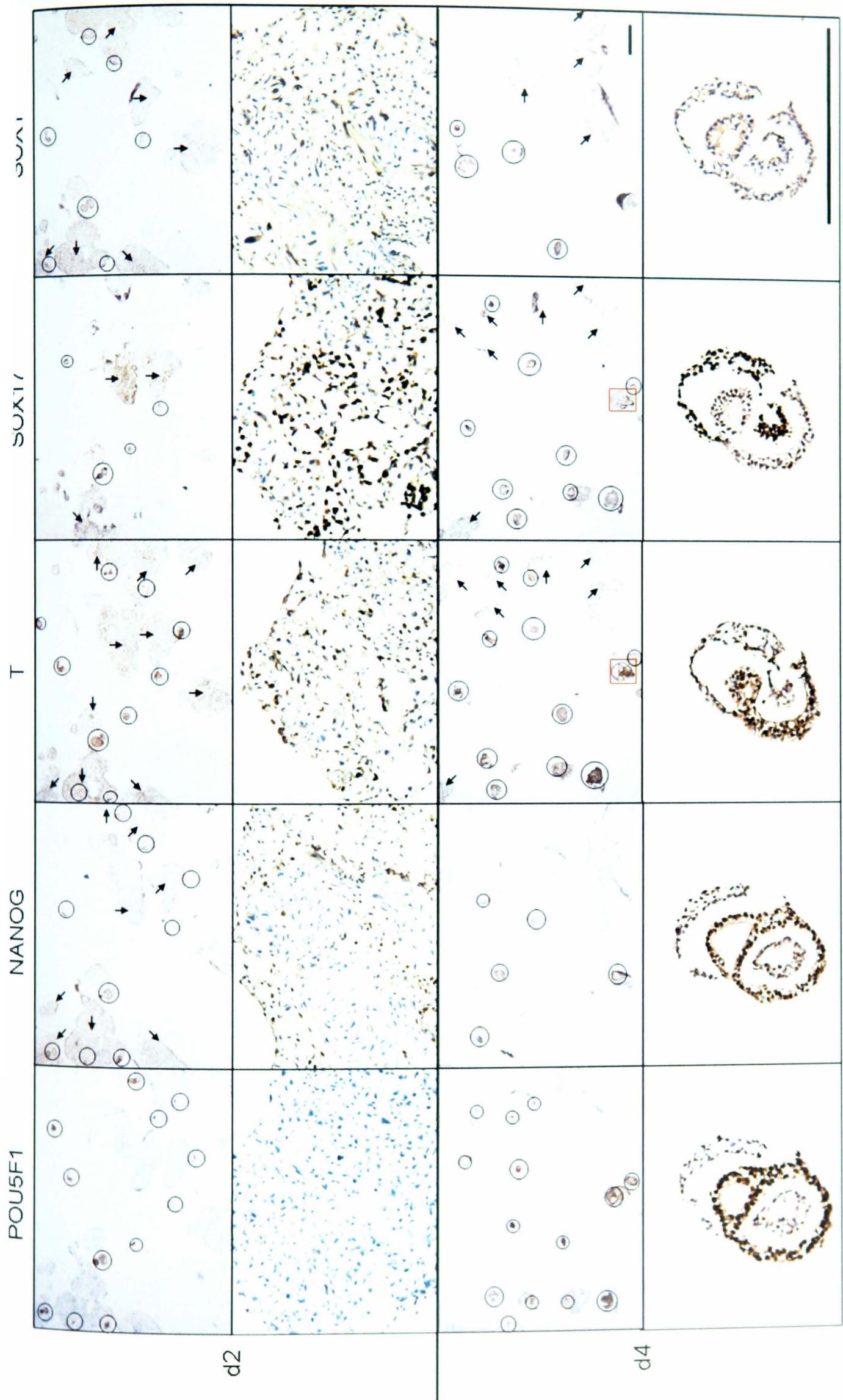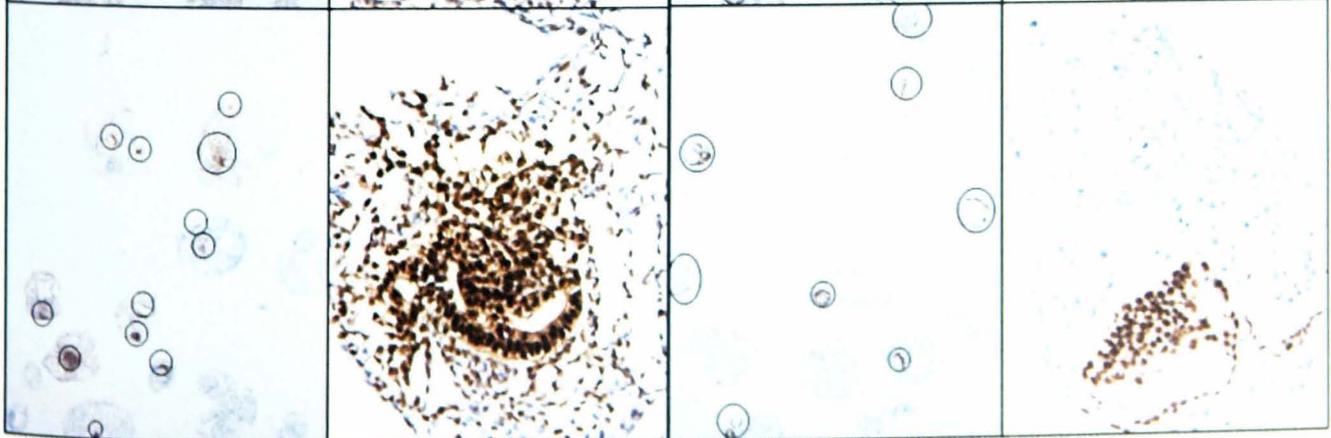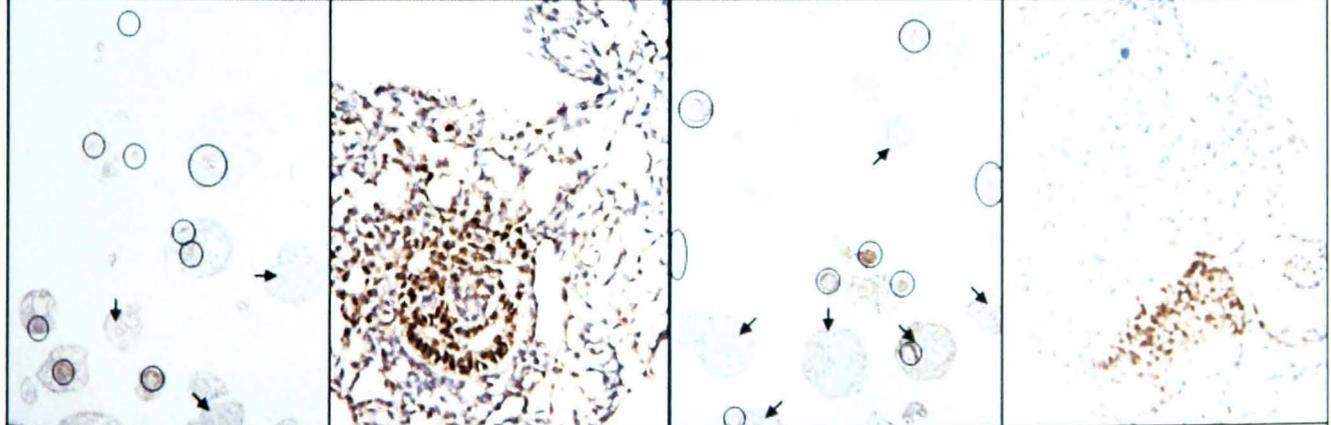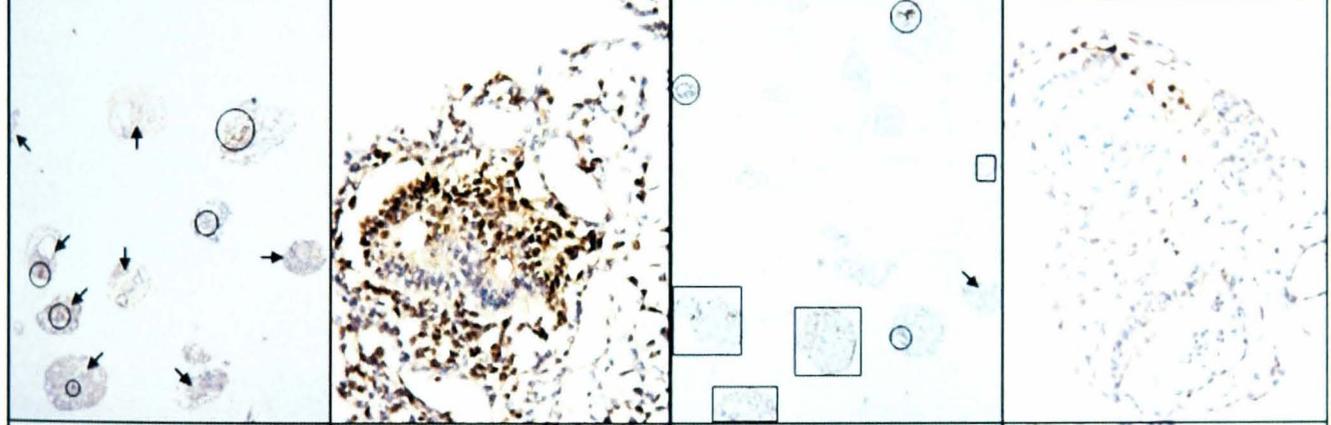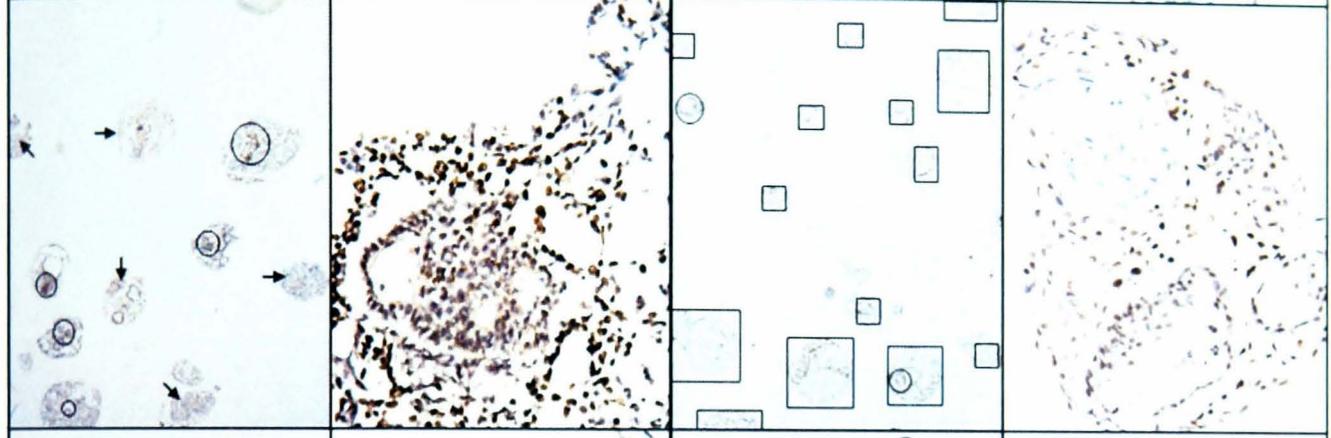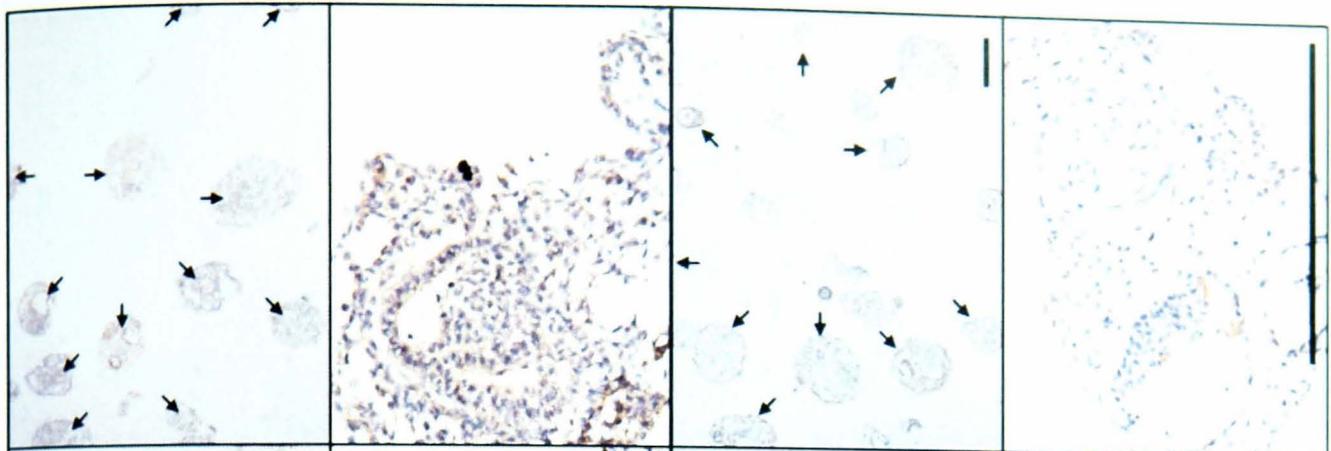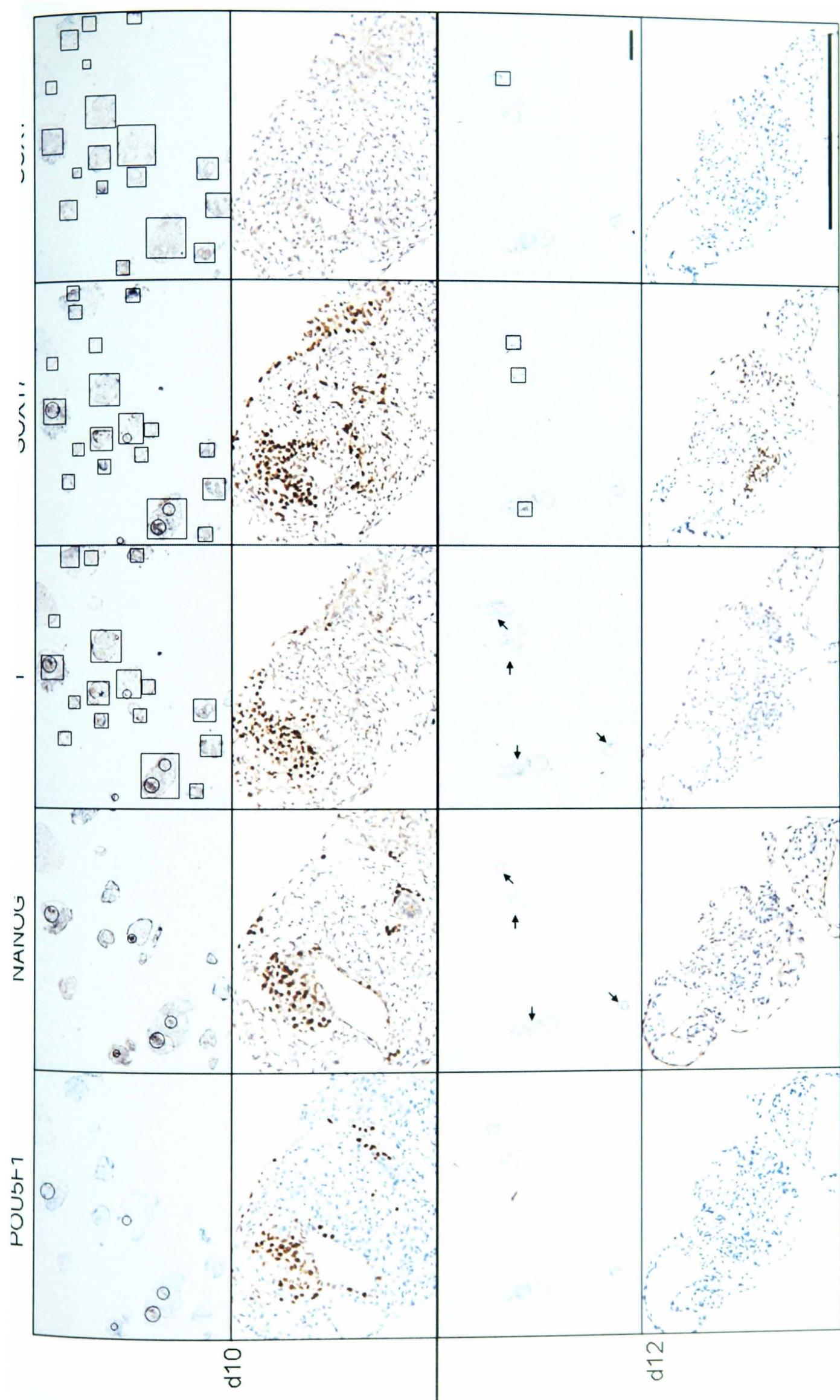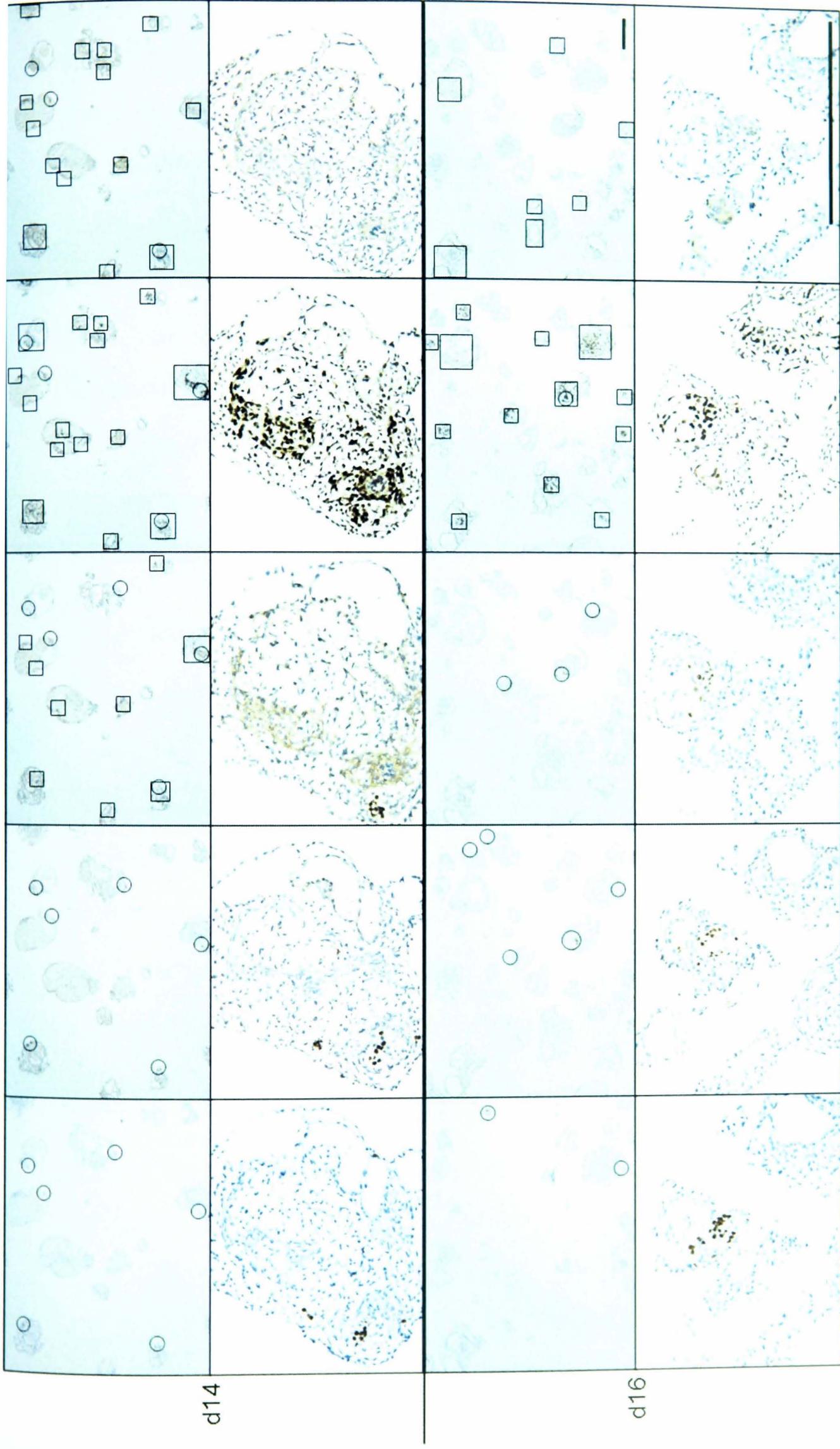
4.3.6 Ontogeny and spatial organisation of pluripotency and germ layer marker expression in forced aggregation hEBs formed from HUES-7, NOTT1, NOTT2 and BG01 hESCs

In order to examine any variation the patterns and timing forced aggregation hEB induced differentiation between hESC lines, HUES-7, BG01, NOTT1 and NOTT2 hEBs were formed as described in Chapter 3 (3.2.2) and assessed using immunohistochemistry and RT-PCR. hEBs were selected for photography (Figure 4-12 to Figure 4-15) based on being most representative of the expression pattern of hEBs on a given slide. Serial sections of each hEB were stained for POU5F1, NANOG, T, SOX17 and SOX1.

4.3.6.1 Forced aggregation day 2

In HUES-7 (Figure 4-12), NOTT1 (Figure 4-13), NOTT2 (Figure 4-14), and BG01 (Figure 4-15) hEBs at d2, numerous small cavities were visible. Strong nuclear POU5F1 expression was detected ubiquitously and NANOG was expressed in scattered cells across the hEBs from all 4 lines, albeit at a lower level that POU5F1 (concordant with RT-PCR data for *POU5F1* and *NANOG* expression; Figure 4-11). Low levels of nuclear SOX17 expression were also detected ubiquitously throughout the hEBs. Both T and SOX1 were detected cytoplasmically at very low levels.

4.3.6.2 Forced aggregation day 4

At d4, cavities had increased in size and high levels of nuclear POU5F1 expression were maintained throughout the hEBs from all lines. NANOG was expressed more highly than at d2, with slightly lower expression at the centre of the hEBs. This higher level of expression at d4 was also detected by RT-PCR. Relative to d2, higher levels of cytoplasmic T expression, particularly towards the periphery (in a similar

manner to NANOG) were detected, mirroring the increase in T mRNA detected by RT-PCR. In BG01, but not in the other 3 lines, hEBs exhibited additional nuclear expression of T in localised patches of cells at the edge of the hEBs (Figure 4-15, denoted by square), in areas still expressing POU5F1 and NANOG. Ubiquitous nuclear SOX17 expression was detected at similar or slightly higher levels relative to d2, corresponding to a small increase in $SOX17$ detected by RT-PCR in all lines.

4.3.6.3 Forced aggregation day 6

By d6, cavities had increased in size in all lines and POU5F1 was typically down-regulated towards the centre of the hEBs. NANOG was down-regulated more POU5F1 and expressed only towards the periphery of NOTT1, NOTT2 and BG01 hEBs. However HUES-7 hEBs expressed NANOG in a few cells scattered across the hEBs. RT-PCR results mirrored the faster down-regulation of NANOG than POU5F1. Low levels of cytoplasmic T expression were generally maintained, with some clusters of nuclear expression evident towards the periphery of BG01 hEBs. Both nuclear and cytoplasmic expression of SOX17 was detected throughout all hEBs with slight increases in expression in the areas of nuclear T expression in BG01 hEBs (square). Low levels of cytoplasmic SOX1 expression were generally and these were localised more towards the periphery of BG01 hEBs (arrow) than for the other lines.

4.3.6.4 Forced aggregation day 8

At d8, POU5F1 continued to down-regulate down-regulated and was restricted to a few clusters of cells at the periphery of the hEBs for all lines. NANOG expression was detected in a subset of these clusters (circles). For the first time, strong nuclear expression of T was detected and, notably, this was co-expressed with POU5F1

(circles). RT-PCR detected a general increase in expression of all three mesendoderm markers *T*, *MIXL1* and *GSC* in hEBs for the different lines. Nuclear SOX17 expression was detected across the hEB sections, with strongest areas of expression co-localising with POU5F1/T expression (circles). In NOTT2, these areas of SOX17 expression that corresponded to areas of T expression demonstrated a distinctly different, less compact morphology than the other lines (circle). In NOTT2 and BG01, low levels of nuclear and cytoplasmic SOX1 expression were detected in different areas to those expressing POU5F1/T/SOX17 (squares).

4.3.6.5   Forced aggregation day 10

At d10, there were no obvious interline differences from most hEBs. Cavities had lost their circular shape and single cell-layers were often left between some of the cavities. Nuclear POU5F1 and NANOG expression were generally maintained around the periphery of the hEBs and in vicinity of some cavities. As with previous time-points, NANOG expression existed only in a subset of POU5F1 expressing areas (circles). Nuclear T and SOX17 expression was detected in the vicinity of cavities, in the same locations expressing POU5F1/NANOG (circles). SOX17 was also expressed at low levels throughout the hEB (arrows). SOX1 expression was nuclear and was always spatially distinct from the other four markers (squares).

4.3.6.6   Forced aggregation day 12

At d12, more interline variation was discernable. In HUES-7 hEBs three separate areas of nuclear marker expression were discernable. POU5F1 and NANOG were co-expressed at the periphery of the hEBs and in areas surrounding portions of some cavities. T and SOX17 were, for the first time, expressed in distinctly spatially separate regions, with T expression more closely matching areas of POU5F1

expression (circles). Nuclear expression of SOX17 was particularly strong in the regions of single cell-thickness that separated the cavities (squares). Some cytoplasmic expression of SOX17 (arrows) correlated to areas cytoplasmic and nuclear SOX1 expression (squares).

In NOTT1 hEBs POU5F1 and NANOG were tightly co-expressed in regions adjacent to the cavities (circles). T and SOX17 were co-expressed in regions of scattered cells within larger cavities (circles) that also expressed low levels of POU5F1 and NANOG (arrow). SOX1 was expressed in large areas across the hEBs that did not express any of the other four markers (circle), and well formed SOX1-expressing neural rosettes were visible (arrows).

NOTT2 hEBs had lost the round morphology seen at earlier stages and become more adhesive. Marker expression was substantially reduced and only nuclear T and POU5F1 co-expression was detected.

BG01 hEBs also lost their round morphology and were more adhesive by d12. In these hEBs, nuclear co-expression of POU5F1 and NANOG was detected in small, scattered clusters of cells (circles), low levels of nuclear T expression were detected in small or scattered areas of cells (square) and nuclear expression of SOX17 was detected in small clusters of cells (arrow). In the hEB shown in Figure 4-15, SOX1 was expressed on the interior surface of a neural rosette-like cluster of cells that exhibited an epithelial-like morphology (arrow and square).

4.3.6.7 Forced aggregation day 14

At d14 very little POU5F1 or NANOG expression could be detected in hEBs from any of the hESC lines. Nuclear T expression was detected in a few small clusters, co-localising with POU5F1 in NOTT1 and NOTT2 hEBs (circles). SOX17 was

expressed with T in HUES-7 hEBs (squares) whereas it was expressed in an entirely separate location in hEBs formed from NOTT1, NOTT2 and BG01 (outlined and squares). SOX1 expression was detected in HUES-7, NOTT1 and NOTT2 hEBs in areas separate from any of the other markers.

4.3.6.8 Forced aggregation day 16

The hEBs from all 4 lines became substantially more adherent at d16 and no longer retained their rounded morphology. In HEUS-7, NOTT1 and NOTT2 hEBs (as with d14) very little POU5F1 and NANOG expression remained (arrows and circles). Low levels of both nuclear and cytoplasmic T expression were detected in small clusters of HUES-7 and NOTT2 hEBs (squares) which were in spatially distinct areas from SOX17. Nuclear and SOX1 expression was detected at low levels throughout the hEBs from both of these lines.

In NOTT1 hEBs, cytoplasmic SOX17 expression was detected in an area of elongated cells that also expressed SOX17 in the cytoplasm (square). One BG01 hEB exhibited a very distinctive morphology at d16 (complex morphology was also seen in two other examples, data not shown). In the hEB shown, nuclear POU5F1 expression was detected in a compact layer at the periphery of the hEB (arrow) and two clusters just inside this layer (circles). T was co-expressed with POU5F1 in the inner layer, but was also in a central region not expressing POU5F1 (square). SOX17 was expressed in a layer surrounding a cavity inside of the T expressing layer and also in numerous other, more central locations. SOX1 was expressed in two neural rosettes towards the centre of this hEB.
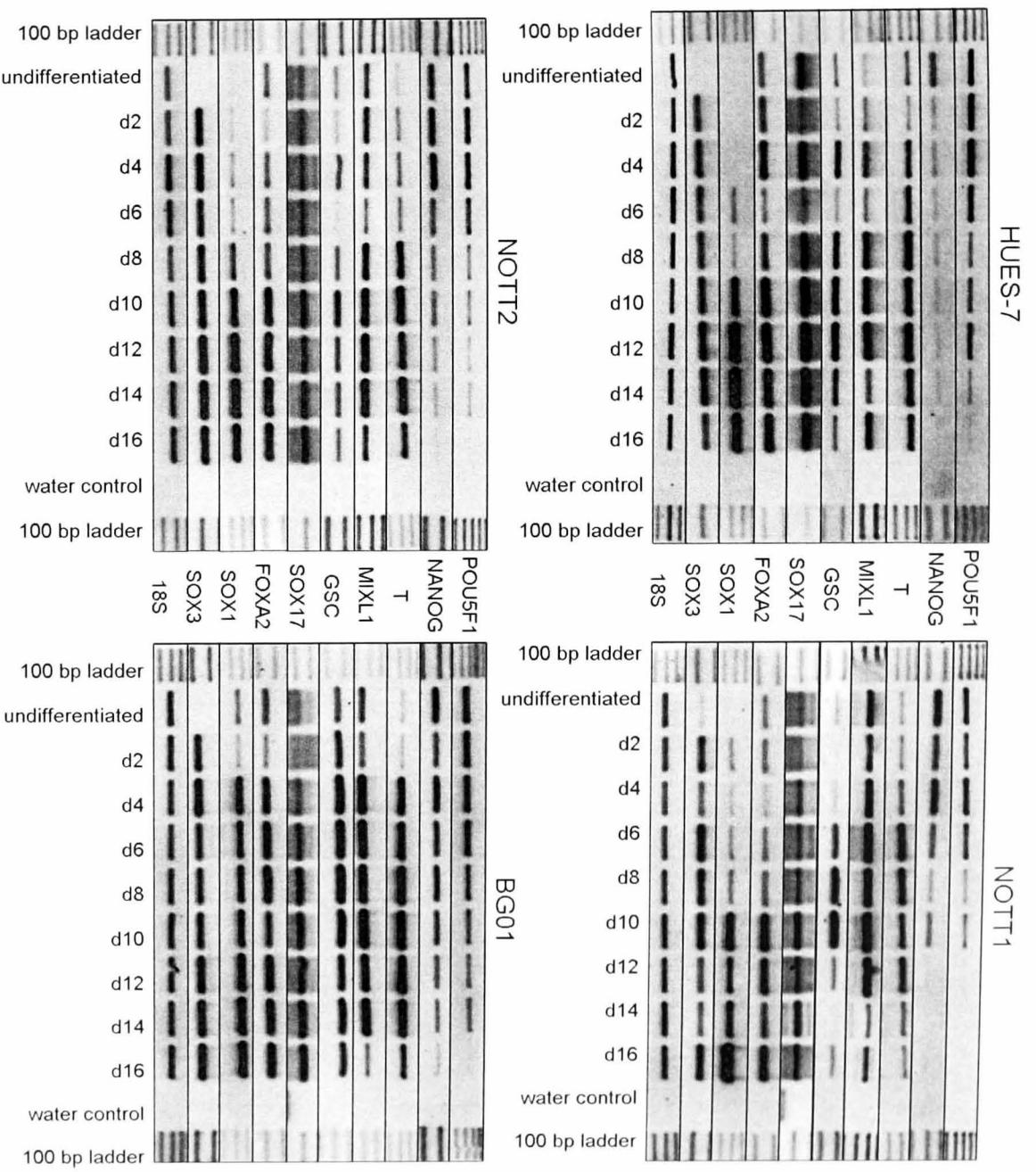
Figure 4-11: Expression of pluripotency and germ layer markers in HUES-7, NOTT1, NOTT2 and BG01 hEBs as detected by RT-PCR
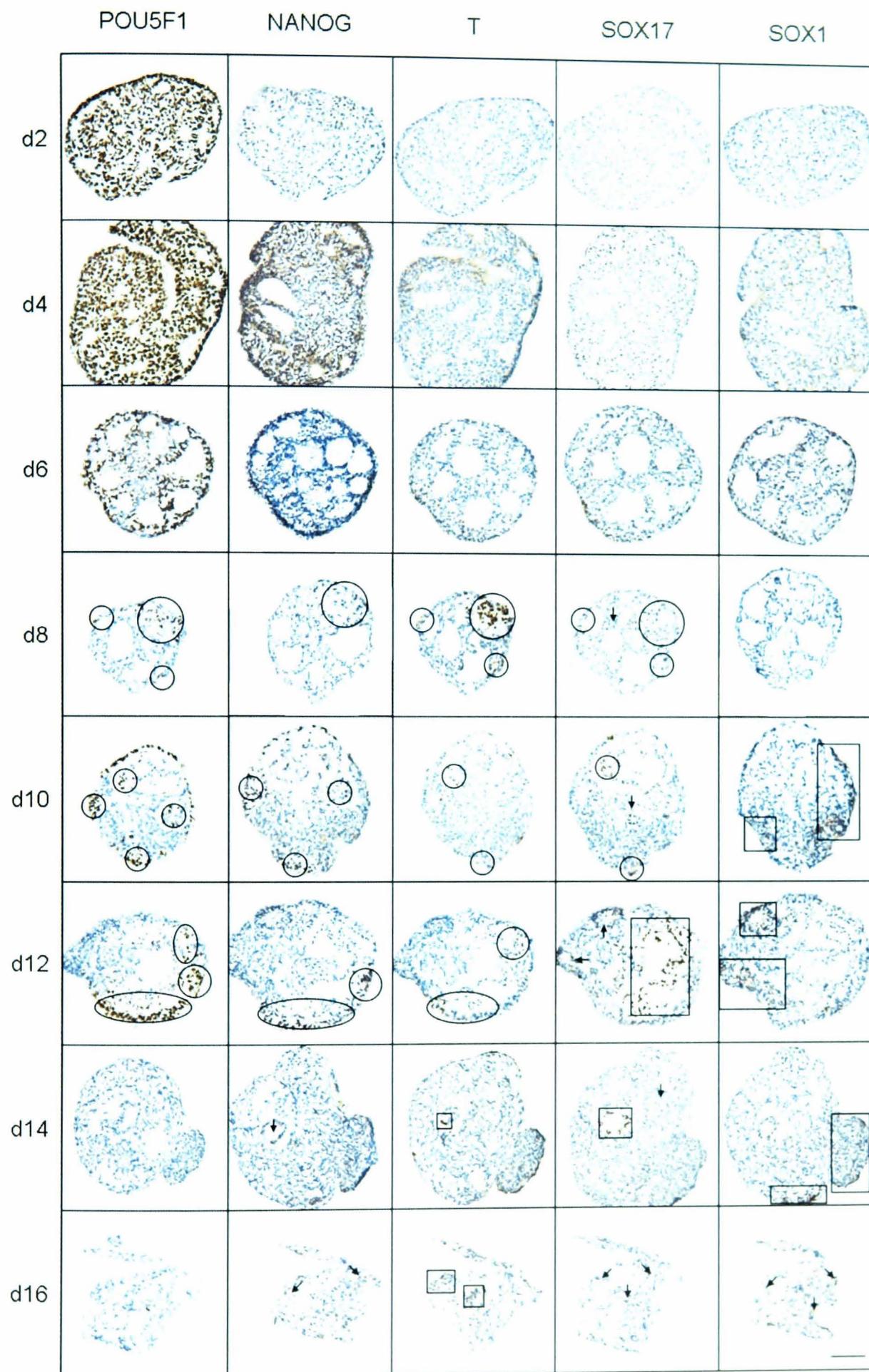
**Figure 4-12: Co-expression of pluripotency and germ layer markers in HUES-7 hEBs**

Circles highlight areas of conserved expression between pluripotency and germ layer markers. Squares highlight areas of contrasting expression between pluripotency and germ layer markers. Arrows highlight areas of cytoplasmic and/or scattered nuclear expression. Scale bar = 100 µm.
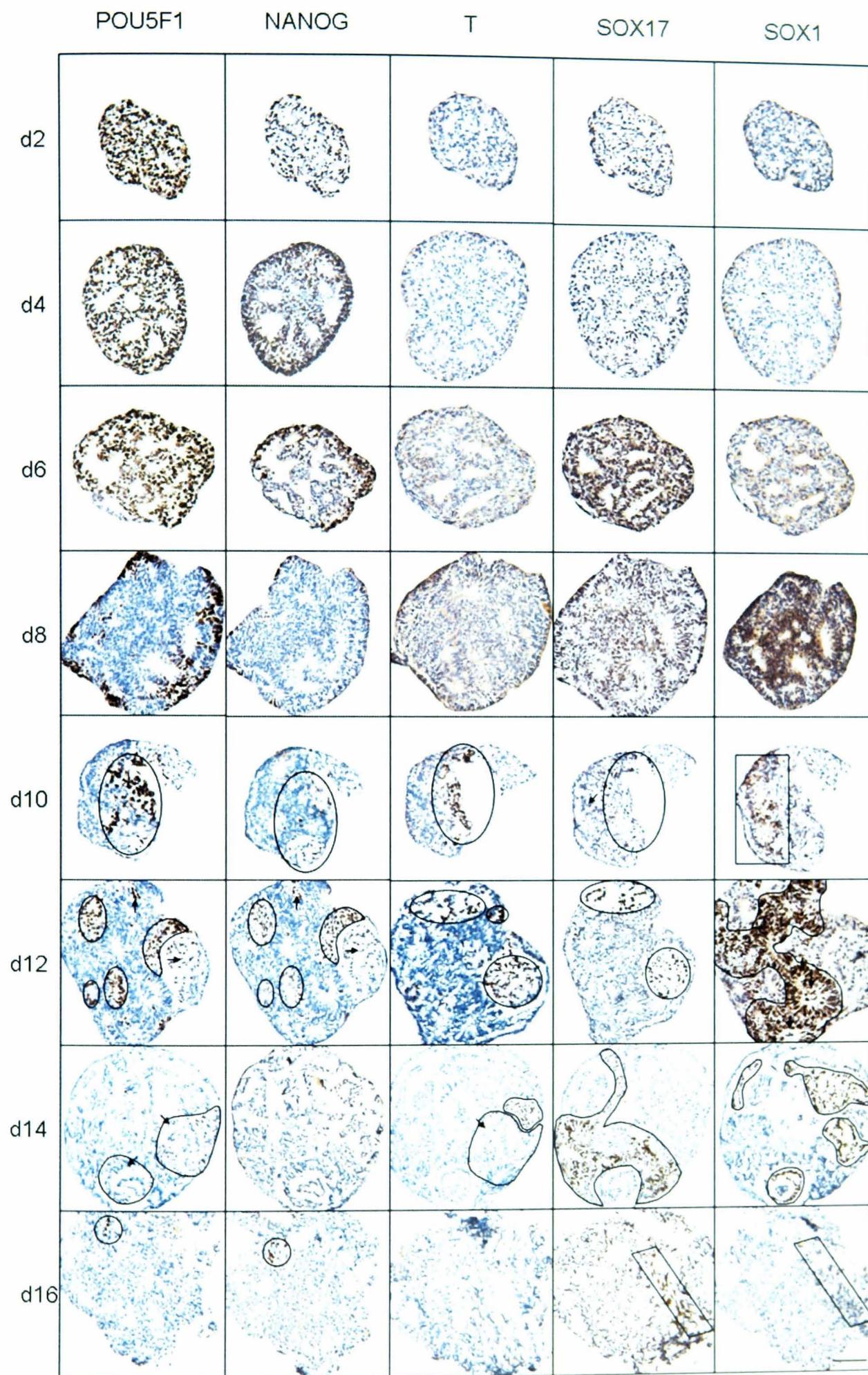
Figure 4-13: Co-expression of pluripotency and germ layer markers in NOTT1 hEBs

Circles highlight areas of conserved expression between pluripotency and germ layer markers. Squares highlight areas of contrasting expression between pluripotency and germ layer markers. Arrows highlight areas of cytoplasmic and/or scattered nuclear expression. Scale bar = 100 μm.
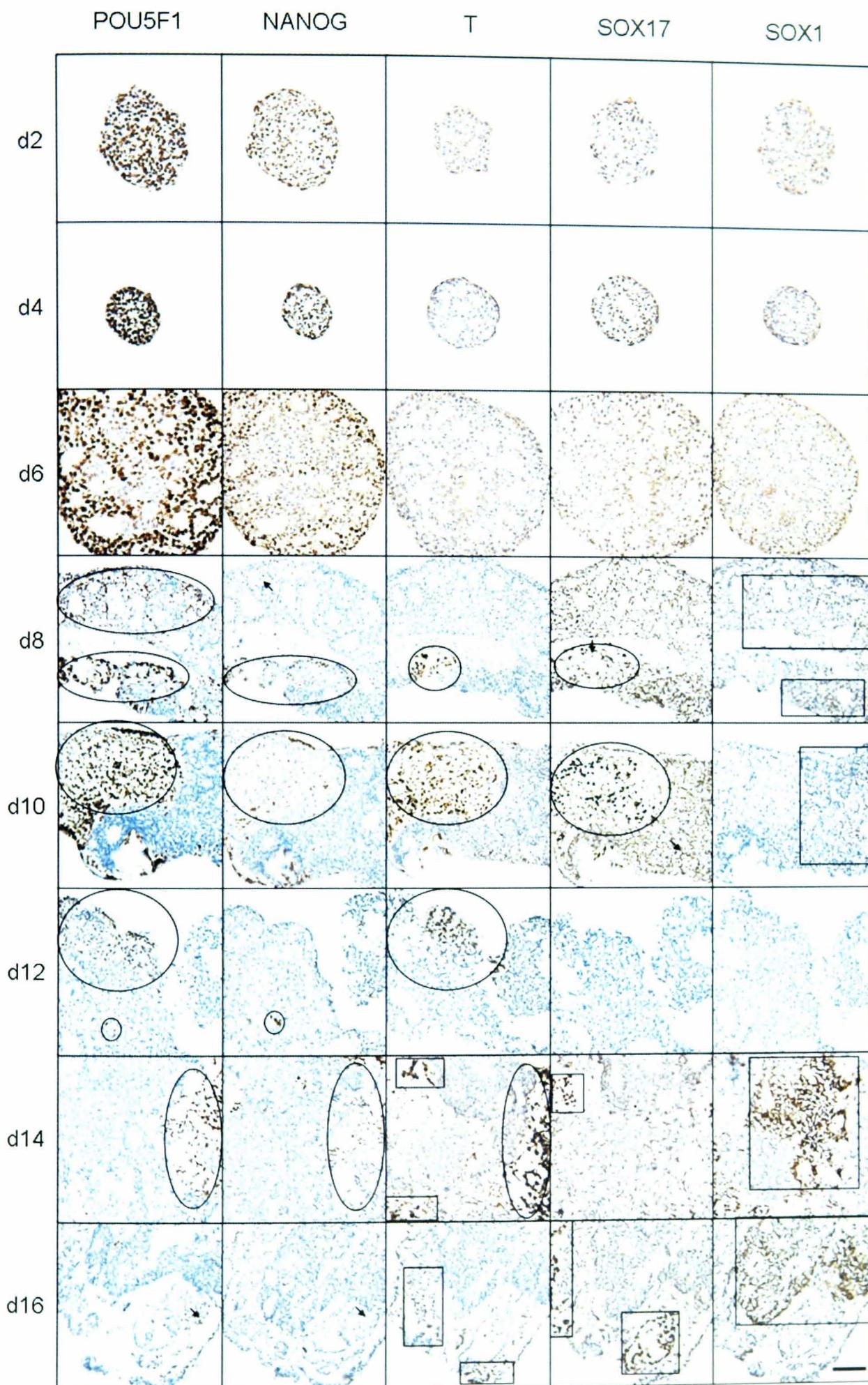
Figure 4-14: Co-expression of pluripotency and germ layer markers in NOTT2 hEBs

Circles highlight areas of conserved expression between pluripotency and germ layer markers. Squares highlight areas of contrasting expression between pluripotency and germ layer markers. Arrows highlight areas of cytoplasmic and/or scattered nuclear expression. Scale bar = 100 μm.
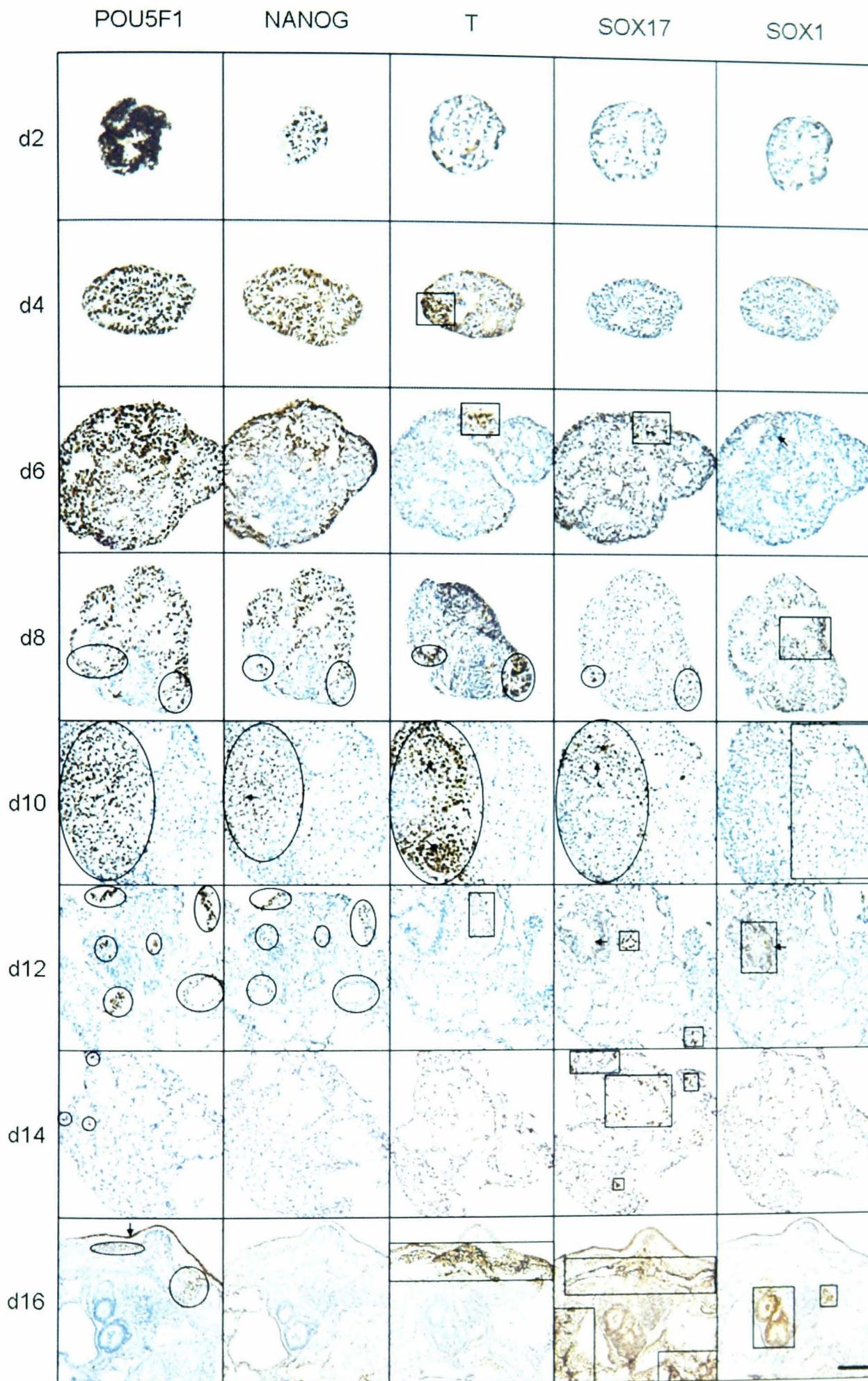
Figure 4-15: Co-expression of pluripotency and germ layer markers in BG01 hEBs

Circles highlight areas of conserved expression between pluripotency and germ layer markers. Squares highlight areas of contrasting expression between pluripotency and germ layer markers. Arrows highlight areas of cytoplasmic and/or scattered nuclear expression. Scale bar = 100 μm.

4.3.7   Effect of CDM, activin A and FGF2 on co-expression of pluripotency and germ layer markers in forced aggregation HUES-7 hEBs

The effect of HUES-7 hEB formation in chemically defined medium with PVA and supplemented with activin A and FGF2 (referred to simply as CDM) was also assessed, and referred to as HUES-7 CDM hEBs. HUES-7 hESCs were chosen for demonstrating the effect of CDM as experiments in Chapter 3 had demonstrated these conditions to provide the highest proportion of beating cardiomyocytes.

4.3.7.1   POU5F1

In HUES-7 CDM hEBs at d2, POU5F1 was expressed in scattered cells at a lower level than HUES-7 hEBs (Figure 4-17). A lower level of *POU5F1* expression in HUES-7 CDM hEBs than HUES-7 hEBs was also detected by RT-PCR (Figure 4-16). In d4 HUES-7 CDM hEBs, nuclear POU5F1 expression was detected relatively lower levels than HUES-7 hEBs. *POU5F1* mRNA was also reduced in HUES-7 CDM hEBs from d2 to d4 and was substantially lower than expression in HUES-7 hEBs. *POU5F1* expression was almost undetectable by RT-PCR at d6 in HUES-7 CDM hEBs and completely undetectable at d8 whereas expression was still detected at d16 in HUES-7 hEBs.

4.3.7.2   NANOG

In the HUES-7 CDM hEBs at d2, nuclear NANOG expression was comparable to HUES-7 hEBs, only detectable in few scattered cells throughout the hEBs with higher expression towards the periphery. *NANOG* mRNA was also expressed at similar levels in each of the hEB types. At d4, NANOG expression was higher relative to d2 in both HUES-7 CDM hEBs and HUES-7 hEBs, although an increase was not detected by RT-PCR. By d6, NANOG expression was restricted to the

periphery of both hEB types. *NANOG* expression at d6 was detected in HUES-7 CDM hEBs by RT-PCR at a very low level but not thereafter. From d8 onwards NANOG was expressed cytoplasmically in HUES-7 CDM hEBs at a low level whereas nuclear NANOG expression remained detectable in HUES-7 hEBs up to d14. By RT-PCR, NANOG levels in HUES-7 hEBs diminished from d8-d16.

4.3.7.3 *T, GSC and MIXL1*

A low level of cytoplasmic T expression was detected in both HUES-7 CDM hEBs and HUES-7 hEBs at d2. *T* and *MIXL1* mRNA were expressed at similar levels in each of the hEB types. At d4, a high level of nuclear expression of T expression was detected in HUES-7 CDM hEBs whereas only cytoplasmic expression was detected in HUES-7 hEBs. A concordant high level of *T, MIXL1* and *GSC* expression was detected by RT-PCR. These high levels of expression were quickly down-regulated and by d6 only low levels of nuclear T expression were detected in HUES-7 CDM hEBs. Correspondingly, low levels of each of the three mesendodermal marker mRNAs were detected at d6. At d8, only low levels of cytoplasmic T expression were detected in HUES-7 CDM hEBs in HUES-7 hEBs T was detectable at high levels. After d8, low levels of cytoplasmic T expression were detectable in HUES-7 CDM hEBs until d16, *GSC* was undetectable from d10 onwards and the already low levels *T* and *MIXL1* expression further reduced but were still detectable at d14/d16 by RT-PCR. In comparison nuclear T expression was detected in HUES-7 hEBs until d14. All three mesendodermal markers peaked in expression from d8-d12 and were still detectable at d16 by RT-PCR.

4.3.7.4 SOX17 and FOXA2

SOX17 was more highly expressed in HUES-7 CDM hEBs at d2 than in HUES-7 hEBs although, in both hEB types, expression was detected in scattered cells. *SOX17* and *FOXA2* mRNA was detected at similar levels. At d4 and d6 SOX17 was expressed at substantially higher levels in HUES-7 CDM hEBs than in HUES-7 hEBs, a result recapitulated by RT-PCR which detected a peak of *SOX17* and *FOXA2* expression at d6. In contrast, *SOX17* and *FOXA2* expression in HUES-7 hEBs peaked at d10-d14. From d8 onwards, low levels of both nuclear and cytoplasmic SOX17 expression could be detected in HUES-7 CDM hEBs, along with a steady down-regulation of both *SOX17* and *FOXA2* towards d16.

4.3.7.5 SOX1 and SOX3

Although cytoplasmic expression of SOX1 was detected at d4-d6 and nuclear expression was detected at d10-d16, only low level cytoplasmic expression through d4-d16 was detected in HUES-7 CDM hEBs. Very low expression of *SOX1* was detected at d12 in HUES-7 CDM hEBs coinciding with a peak in HUES-7 hEB *SOX1* expression. *SOX3* expression was detected decreasing from d2-d14 whereas expression in HUES-7 hEBs peaked at d12-d14.
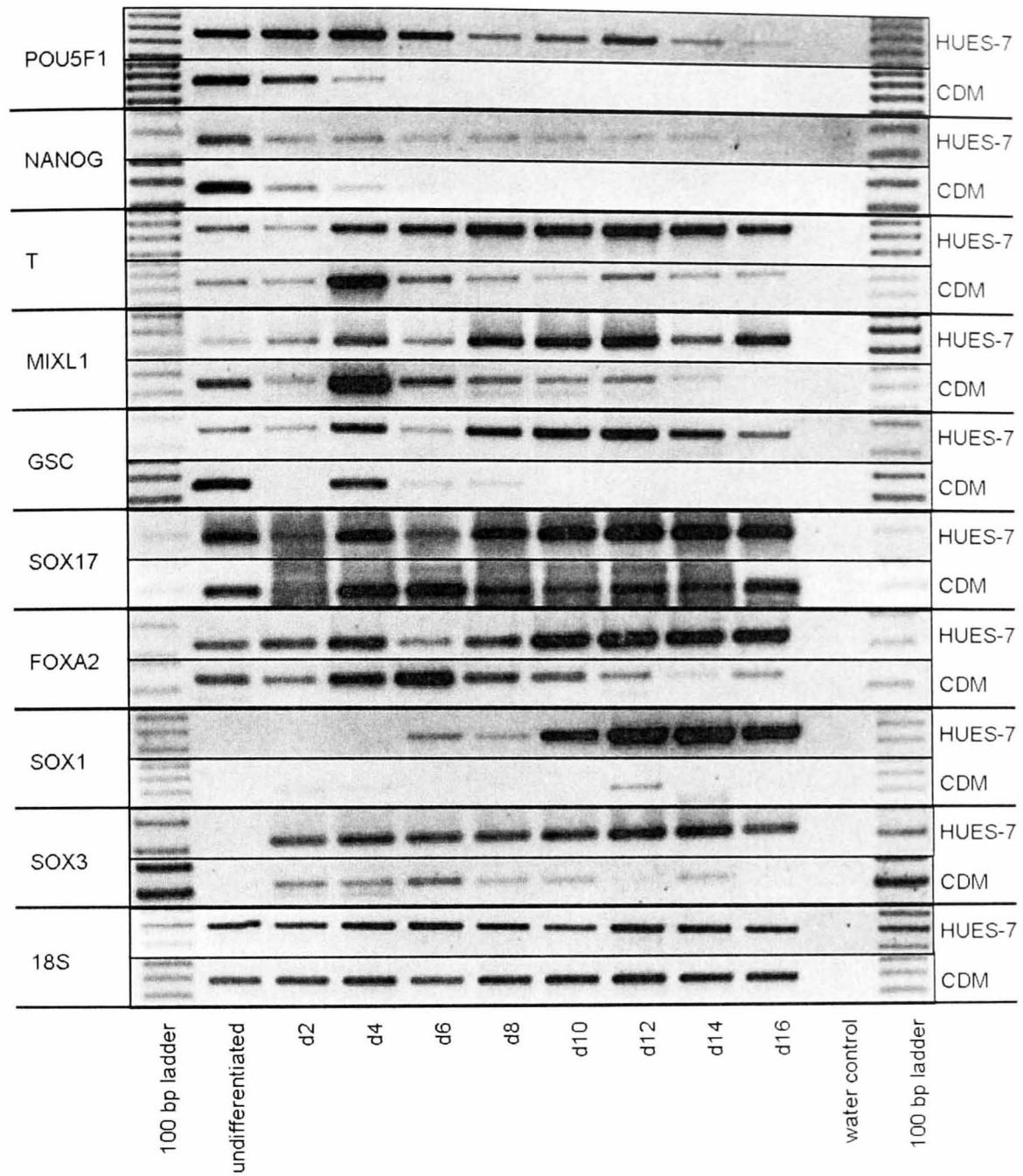
Figure 4-16: Expression of pluripotency and germ layer markers in HUES-7 and HUES-7 CDM hEBs detected by RT-PCR

POU5F1

HUES-7

HUES-7
CDM

NANOG

HUES-7

HUES-7
CDM

T

HUES-7

HUES-7
CDM

235
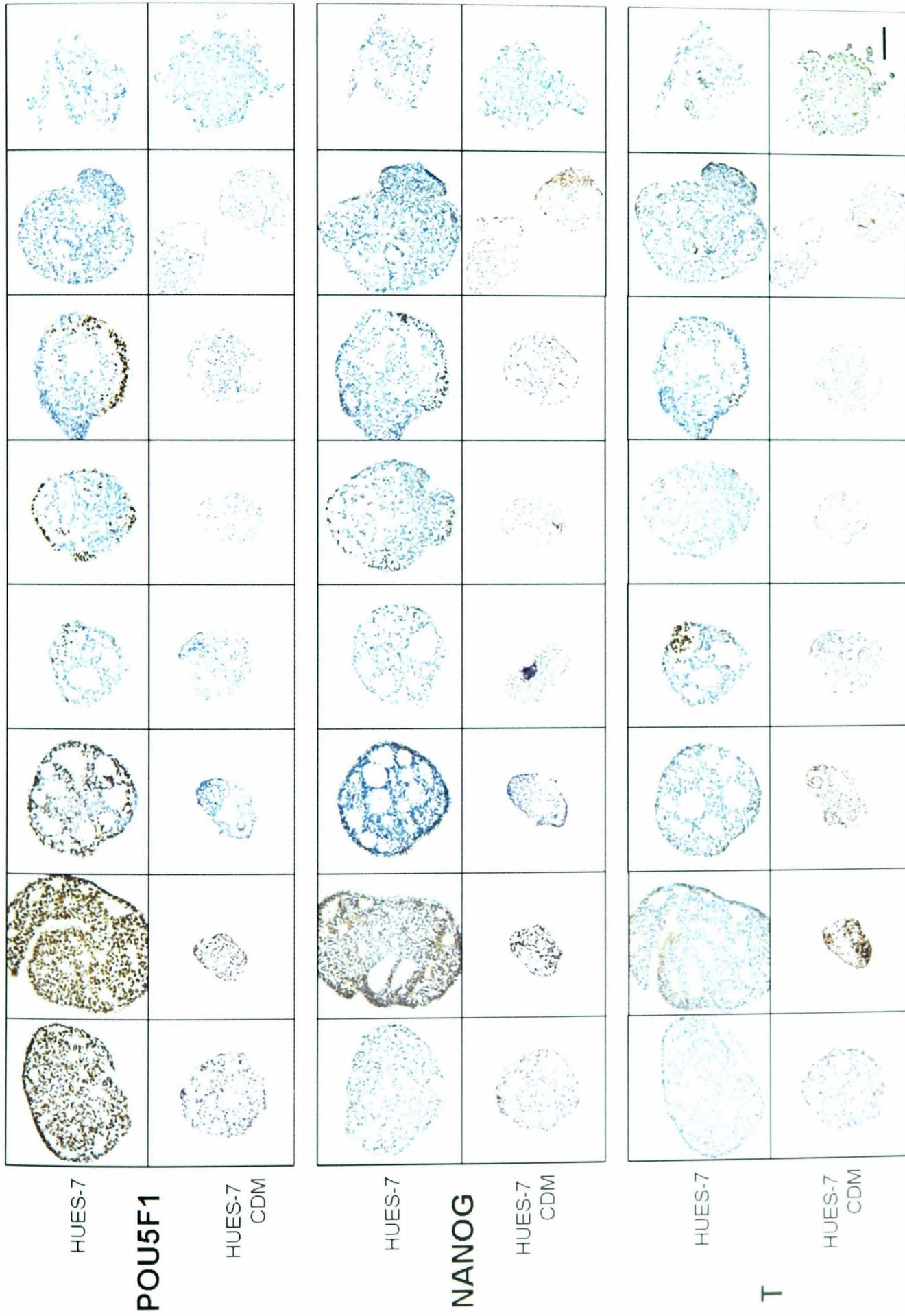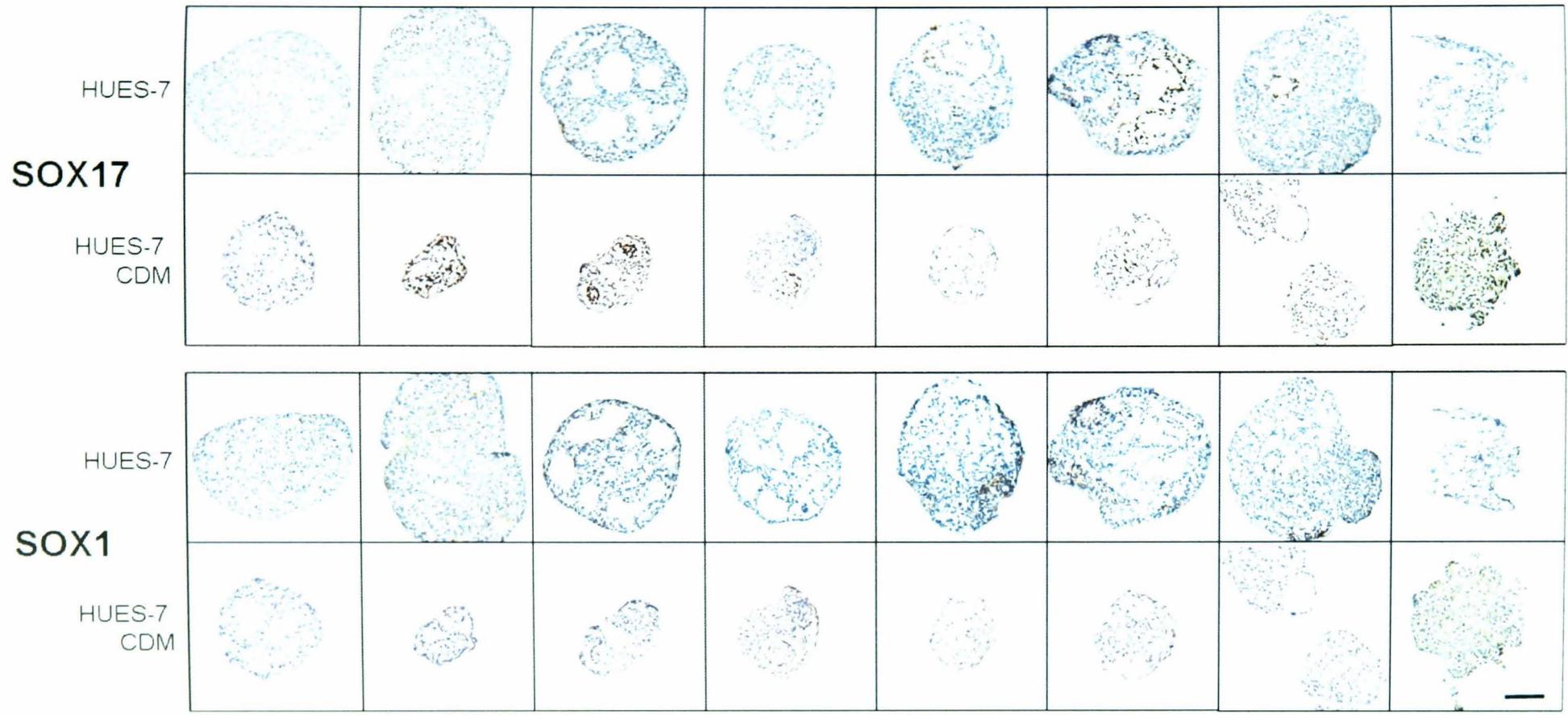
Figure 4-17: Co-expression of pluripotency and germ layer markers in HUES-7 hEBs formed in CDM

Circles highlighting areas of conserved expression between pluripotency and germ layer markers. Squares highlighting areas of contrasting expression between pluripotency and germ layer markers. Scale bar = 100 μm.

4.3.8 Comparison of the expression of pluripotency and germ layer markers in five undifferentiated hESC lines

The automated immunohistochemistry system established above was used to detect the expression of T, SOX17, SOX1, POU5F1 and NANOG in the undifferentiated cells of five hESCs lines grown on Matrigel for at least five passages in identical conditions (Figure 4-18).

For each of the markers both nuclear and cytoplasmic expression was detected. All five lines expressed high levels of POU5F1 and NANOG. T expression was detected at low levels in all cells with some individual cells expressing T at higher levels particularly in the H1 hESCs. SOX17 and SOX1 appeared to be expressed ubiquitously at very low levels in HUES-7, NOTT1, NOTT2 and BG01. In the H1 hESCs, SOX17 and SOX1 were additionally expressed at higher levels in some individual cells.

	In culture	POU5F1	NANOG	T	SOX17	SOX1	Control

HUES-7

NOTT1

NOTT2

BG01

H1
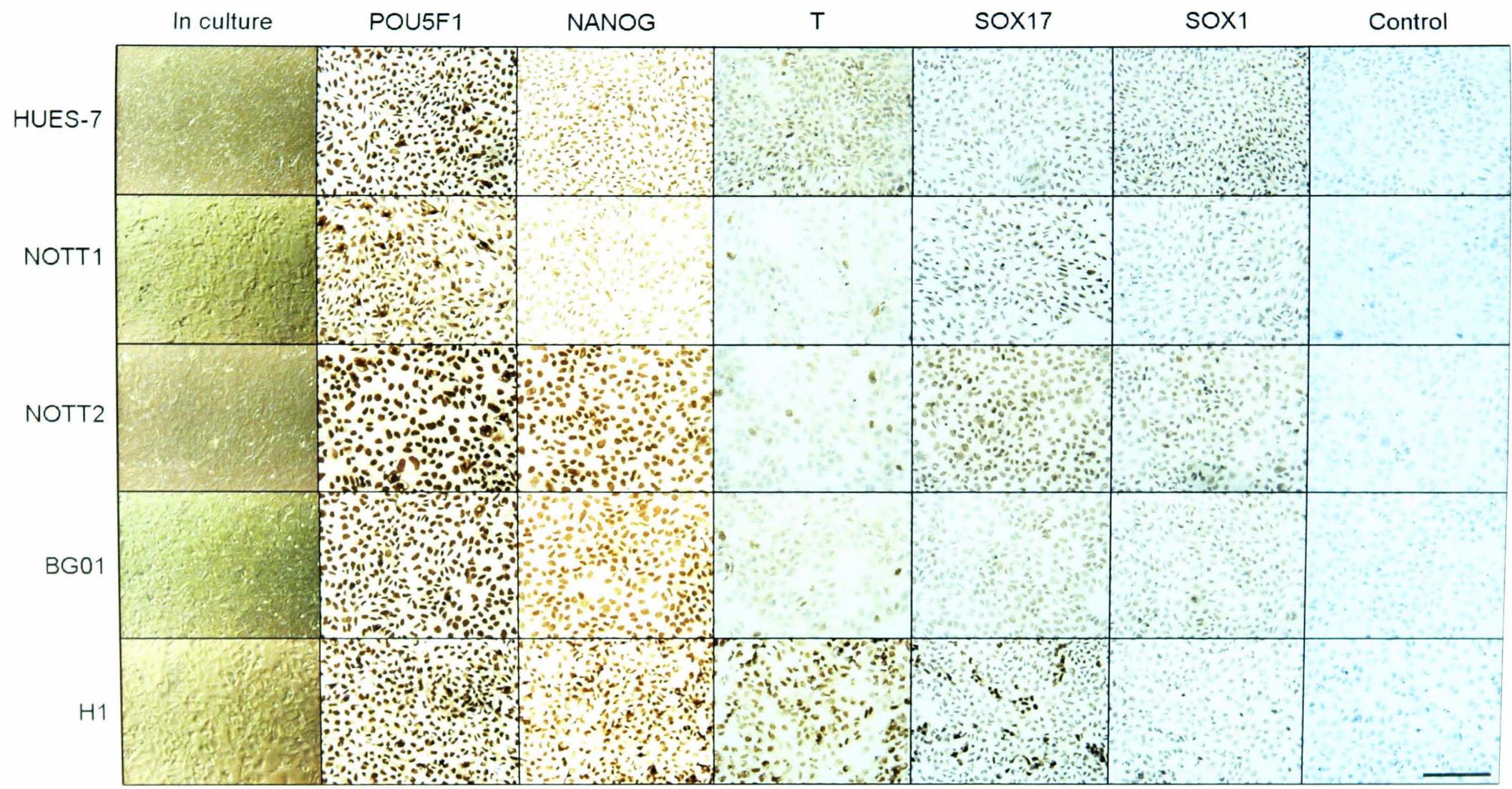
Figure 4-18: Comparison of the expression of pluripotency and germ layer markers in five undifferentiated hESC lines

The expression of POU5F1, NANOG, T, SOX17 and SOX1 in HUES-7, NOTT1, NOTT2, BG01 and H1 undifferentiated hESCs detected by immunohistochemistry. Hoffman objective images are included of each of the lines in culture. All lines demonstrated typical undifferentiated morphology. The experiment was repeated twice with different passages. Scale bar – 50 µm.

4.3.9 Expression of mesendodermal markers in seven undifferentiated hESC lines maintained under different conditions

Once it was established that mesendodermal genes were expressed in each of the undifferentiated hESC lines analysed above (Figure 4-11 and Figure 4-18), and with the overall aim to improve mesodermal lineage specification, seven different hESC lines were analysed for mesendodermal marker expression. Six of the lines were maintained in other laboratories using different culture conditions. All seven lines were analysed for the expression of an increased panel of mesendodermal genes (*EOMES, T, GSC* and *MIXL1*) to establish if the detected gene expression above was due to the culture conditions used.

RT-PCR was performed on cDNA produced from cell pellets obtained from different undifferentiated hESC lines cultured in three separate laboratories (Figure 4-19): BG01 from our own laboratory, HUES-1, HUES-7, HUES-8 and HUES-9 from the University of Wisconsin and hES-NL-1 & HES-2 from the Interuniversity Cardiology Institute of the Netherlands. All but BG01 were cultured on MEFs in FBS-containing medium. Week 6 human foetal brain, week 10 foetal heart, week 10 foetal liver and week 20 foetal testis samples are also obtained and analysed to establish the timing of maintenance of mesendodermal gene expression in humans.

Expression of *EOMES, T, GSC* and *MIXL1* was detected at similar levels in HUES-1, HUES-7, HUES-8, HUES-9, hES-NL-1 and HES-2. BG01 hEBs expressed *GSC* and *MIXL1* at similar levels to the other lines, but *T* expression was substantially lower and *EOMES* was almost undetectable. *MIXL1* and *GSC* were found to be expressed in each of the 4 human foetal samples, *EOMES* was expressed in foetal brain and heart and *T* was expressed only in foetal testis.
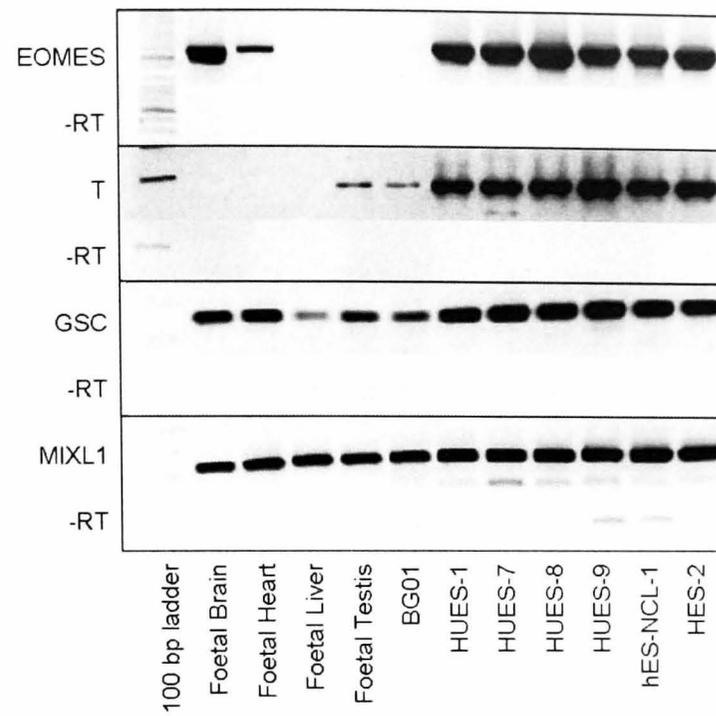
Figure 4-19: Expression of mesendodermal genes in seven hESC lines and human foetal organs determined by RT-PCR

RT-PCR assessment of the expression of *EOMES*, *T*, *GSC* and *MIXL1* in seven hESC lines cultured in different laboratories and comparison to human foetal organ control samples.

4.3.10 Expression of pluripotency and germ layer markers in SSEA3$^+$ and SSEA4$^+$ FACS-sorted undifferentiated hESCs

To establish if germ layer marker expression detected in undifferentiated cells was due to a ubiquitous low level of expression or to the presence of a 'differentiated' subpopulation, undifferentiated cells from the hESC lines NOTT1, NOTT2 and HUES-7 were labelled with SSEA3 and SSEA4 antibodies and sorted using FACS. Samples incubated without primary antibody (i.e. secondary only) were used to establish the baseline fluorescence background for flow cytometry analysis.

Figure 4-20 shows that both HUES-7 and NOTT1 cells maintained a substantial (98.1% and 88.2% respectively) SSEA4 positive population, with lower (but still substantial) SSEA3 positive populations (79.4% and 81.1%). A much smaller SSEA3 positive fraction (65.1%) was detected in NOTT2 cells. In the NOTT2 SSEA4 positive population two distinct levels of intensity were seen, with 20% of cells in the higher intensity peak and 40% in the lower intensity peak. From each sample SSEA3 and SSEA4 high and low fractions were isolated by sorting the 20% highest or lowest fluorescent intensity cells for SSEA3 and SSEA4 respectively.

For visual confirmation of antibody specificity, approximately 10% of the volume each sample was removed placed onto slides and treated with Vectashield with DAPI. Slides were visualised with a fluorescent microscope with DAPI and FITC filters. Merged DAPI/FITC images show that the expression of either SSEA4 or SSEA3 is visually higher in the FACS high populations than the FACS low populations (Figure 4-21). The remainder of the sample was analysed using RT-PCR for a panel of pluripotency and germ layer markers. Although differences in mesendoderm and endoderm marker expression were detected in each of the lines after FACS separation, no apparent correlation between the level of mesendoderm

and endoderm marker expression and the level of SSEA3 or SSEA4 expression was determined (Figure 4-22).
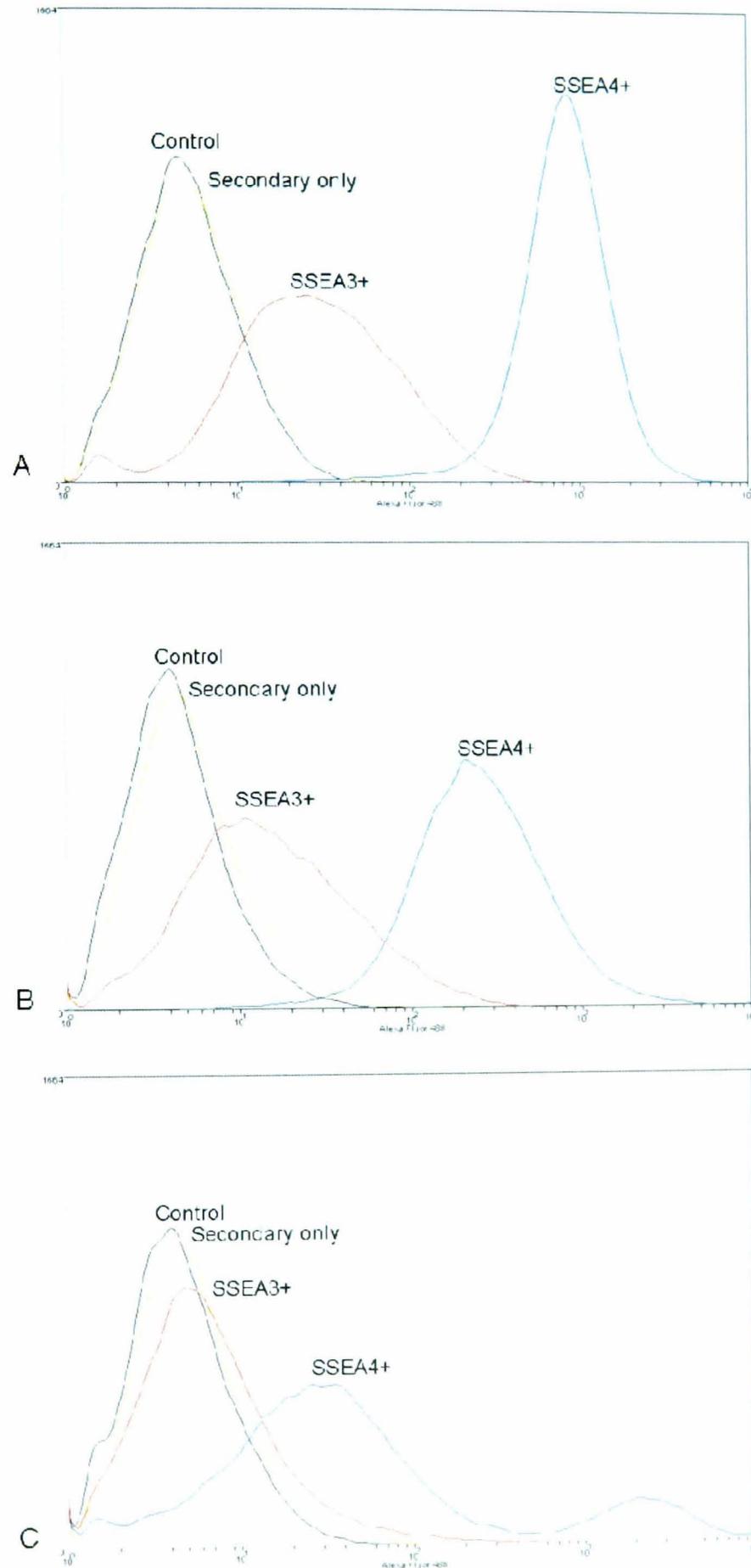
Figure 4-20: FACS of undifferentiated hESC lines for pluripotency markers

FACS readouts for hESC lines analysed for the expression of the pluripotency markers SSEA3 and SSEA4. (A) HUES-7 (B) NOTT1 and (C) NOTT2.
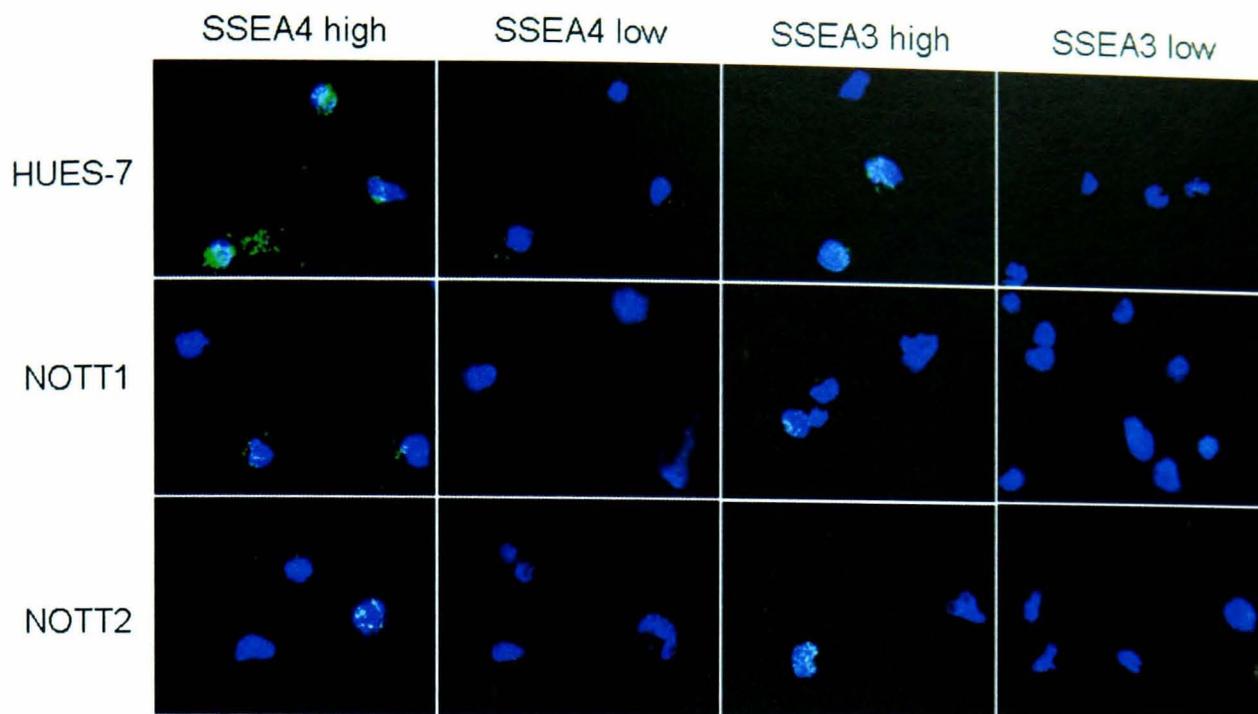
Figure 4-21: Expression of SSEA3 and SSEA4 in undifferentiated HUES-7, NOTT1 and NOTT2 cells after FACS separation

Merged DAPI/FITC images of SSEA4 and SSEA3 high or low sorted undifferentiated HUES-7, NOTT1 and NOTT2 cells.
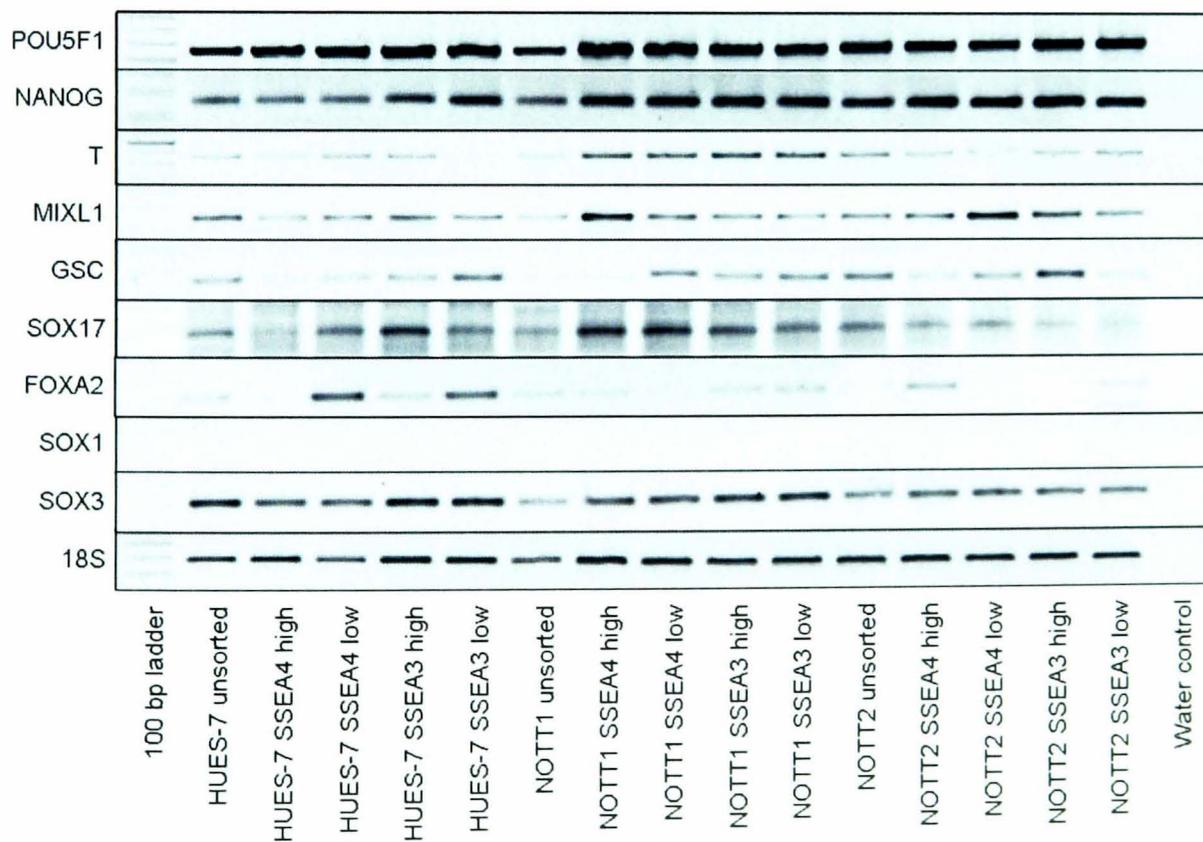
Figure 4-22: Expression of pluripotency and germ layer markers in SSEA3 and SSEA4 sorted hESCs

Undifferentiated HUES-7, NOTT1 and NOTT2 were FACS separated for high or low expression of SSEA3 and SSEA4 and samples were analysed for expression of pluripotency and germ layer markers by RT-PCR.

4.4 DISCUSSION

The objective of this study was to identify the spatial and temporal interaction of cells expressing makers of pluripotency and the three germ layers during hEB differentiation. Traditional methods of hEB formation lead to heterogeneity in hEB size and contamination with feeder cells, whereas forced aggregation of a defined number of hESCs grown in feeder-free conditions allows the reliable production of homogeneous hEBs and improves inter-hEB comparability as described in Chapter 3.

4.4.1 Immunofluorescence of T and MIXL1 in mouse embryos and hEBs and antibody validation in the immunohistochemistry system

At E7.5 in the mouse embryo, the primitive streak, from which mesoderm and definitive endoderm will form, has arisen along the anterior side of the embryo (Keller, 2005). Using immunofluorescence, a high level of T expression was detected in the area of the primitive streak and a lower level expression was detected in the allantoic bud (Figure 4-1), similar the expression pattern seen by others using *in situ* hybridisation (Perea-Gomez *et al.*, 1999). Although MIXL partially localised to the primitive streak area, as previously reported using immunofluorescence (Mossman *et al.*, 2005), it was also evident at low levels in non-primitive streak areas suggesting that MIXL1 is not as restricted as T. In hEBs both T and MIXL localised to the periphery at d8, d10 and d12 of differentiation (Figure 4-2) suggesting that mesendodermal differentiation had occurred on the outside of these hEBs. Although informative, these experiments demonstrated that more precise and detailed methods were required to visualise differentiation in hEBs. Therefore subsequent experiments were performed using sections of hEBs to allow visualisation of the interior of the hEBs. Additionally, an automated immunohistochemistry system was used to allow high throughput analysis. To validate the automated immunohistochemistry system,

E6.5 and E7.5 mouse embryos were analysed for expression of POU5F1 (Figure 4-3), NANOG (Figure 4-4), T (Figure 4-5), SOX17 (Figure 4-6), and SOX1 (Figure 4-7). Each marker exhibited the pattern of expression previously reported in the EMAGE database (http://genex.hgu.mrc.ac.uk/Emage/database/emageIntro.html) validating this system for use on sections of hEBs. The expression of SOX1 was particularly low in the E7.5 embryos and the interpretation of this result would have been further enhanced by the inclusion of a positive control such as a mouse embryonic brain section. Negative controls produced by omitting the primary antibody (Figure 7-1) demonstrated very low levels of background staining although these experiments would have been further enhanced by using isotype or pre-immune serum controls to estimate the non-specific binding of target primary antibodies to cell surface antigens.

4.4.2   Comparison of pluripotency and germ layer marker expression in mass culture HUES-7 hEBs

To establish a baseline with which to compare the differentiation of hEBs produced by forced aggregation, cultures of HUES-7 hESCs grown on MEF were collagenase treated, scraped and suspended in mass culture. Comparing mass culture and forced aggregation hEBs at d2 demonstrated substantial differences in expression pattern (Figure 4-8). Whilst forced aggregation hEBs demonstrated a high level of homogeneity of marker expression between different hEBs, mass culture hEBs were highly variable in size and shape and expression of the five markers varied substantially between hEBs. This suggests that mass culture hEBs, even at d2, have already begun to differentiate in a non-synchronous manner.

During subsequent differentiation of mass culture hEBs, co-localisation was noted between T, POU5F1, NANOG and SOX17 (Figure 4-10). This co-localisation of

POU5F1, NANOG, T and SOX17 may represent cells progressing from primitive ectoderm to mesendoderm and endoderm, indeed the co-expression of POU5F1 and the primitive streak marker MIXL1 in hESCs has been previously reported (Mossman *et al.*, 2005). Although these four markers co-localised within the hEBs, and in some cases they were expressed at the centre of the hEBs (Figure 4-10, d6), overall there appeared to be no correlation between where the markers were expressed between different hEBs, reiterating the chaotic differentiation that occurs in mass culture hEBs. SOX1 was expressed cytoplasmically at low levels throughout differentiation suggesting that the mass culture method for hEB formation does not promote high levels of differentiation towards definitive ectoderm. In addition, a large proportion of cells within mass culture hEBs expressed none of the markers for pluripotency or the three germ layers, even at d2, suggesting that these cells are either at an intermediate stage between pluripotency and germ layer (possibly a non-SOX1 expressing definitive ectoderm), are of extra-embryonic lineages such as trophectoderm (Xu *et al.*, 2002b) and may express markers such as CDX2 (Strumpf *et al.*, 2005), or have already progressed past the early germ layer stages.

In mass culture hEBs, an immediate down-regulation of pluripotency markers was detected at d2 by RT-PCR (Figure 4-9), and this low level of expression was maintained until d14. Mesendodermal markers were highest at d2-d4 and slowly declined towards d16 whereas the expression of endoderm markers was sustained throughout differentiation. An increase of ectodermal marker expression was detected from d8 onwards. In comparison, in forced aggregation hEBs a clear pattern of pluripotency down-regulation was followed by up-regulation of mesendodermal endodermal and ectodermal markers similar to a previously report in the HES2 line (Ng *et al.*, 2005b). This extended maintenance of pluripotency and germ layer

marker expression is in mass culture hEBs most likely due to the highly heterogeneous population of hEBs and demonstrates that there are substantial differences in the timing of differentiation between mass culture and forced aggregation hEBs, at least in the HUES-7 and HES2 (Adjaye *et al.*, 2005) lines studied

Overall, therefore in mass culture HUES-7 hEBs, no standard pattern of differentiation could be detected. Interestingly, very few mass culture hEBs appeared to follow the standard cystic EB pattern of differentiation typical of mEBs as described by Weitzer (2006). Additionally, very little spatial separation of marker expression was seen in mass culture hEBs. In mEBs the production of visceral endoderm as a layer around the periphery of mEBs is responsible for the production of the basement membrane, which induces epithelial primitive ectoderm formation and, in turn, allows cystic mEB formation (Li *et al.*, 2001a). No visceral endoderm layer (which would be marked by SOX17, as demonstrated by mouse embryo immunohistochemistry) was detected in mass culture hEBs and a lack of this cell type may be responsible for the lack of cystic structure in these hEBs. As noted in the Introduction (1.2.6.5), the basement membrane is also required for mEB attachment and the subsequent formation of parietal endoderm. Since the latter lineage facilitates the induction of mesoderm, the lack of this inducer which may, along with the heterogeneous and non-synchronous differentiation, be the cause of poor formation of terminal mesodermal lineages such as blood and cardiomyocytes previously observed from mass culture hEBs (Denning *et al.*, 2006).

4.4.3 Expression of germ layer and pluripotency markers in forced aggregation hEBs

Improvements in terminal mesodermal lineage differentiation noted in Chapter 3 from hEBs produced by forced aggregation raised the question of what physical factors are responsible for this improvement and how future improvements could be made. To establish a spatial and temporal map of differentiation in this system and determine whether this methodology standardises differentiation across lines, hEBs formed from four hESC lines were examined for the expression of POU5F1, NANOG, T, SOX17 and SOX1 by immunohistochemistry.

Differences between the spatial pattern of differentiation in hEBs from separate hESC lines has been reported (Mikkola *et al.*, 2006). This work demonstrated that, in hEBs formed from two hESC lines (FES22 and FES30) by mass culture, there were substantial differences between the expression of POU5F1 and T at d7 of differentiation. FES22 hEBs expressed small amounts of POU5F1 towards the periphery of the hEBs and T towards the centre. In contrast, FES30 hEBs expressed high levels of POU5F1 throughout the majority of hEBs and at the periphery of a small number of hEBs, whereas no T expression was detected.

4.4.3.1 Limited cavitation in forced aggregation hEBs

The phenotype of hEBs formed by forced aggregation was broadly similar between 4 hESC lines but substantially different from that seen in conventional mEB development (Weitzer, 2006) and no obvious central cavities were noted (Figure 4-12 to Figure 4-15). As with mass culture hEBs, no SOX17 expression at the periphery was detected during early differentiation, as would be expected with the formation of a layer of visceral endoderm. In hEBs from each of the hESC lines there

did appear to be a single cell thickness layer of cells around the outside of the hEB although this layer expressed POU5F1 which is not expressed in primitive endoderm (Palmieri *et al.*, 1994, Rossant *et al.*, 2003). Therefore this further suggests that primitive endoderm is not formed and therefore the traditional cystic model of differentiation is not occurring. Forced aggregation hEBs did possess numerous, randomly located, small cavities at d2 which were increased in size at d4 and further increased at d6 in hEBs from each of the hESC lines analysed (Figure 4-12 to Figure 4-15). In later differentiation, the expression of T and SOX17 was either associated with these cavities, frequently in chains of single cells within the cavities, or at the points of extension/elongation of the hEBs. This suggests that cell movement may have a role in mesendoderm formation in hEBs.

4.4.3.2 Co-expression of pluripotency and mesendodermal (but not ectodermal) markers in forced aggregation hEBs

Markers of pluripotency were down-regulated from the centre of hEBs from d6 onwards, opposite to what has been found in mEBs (Weitzer, 2006). POU5F1 has been previously demonstrated to be restricted to the outside of the hEBs (Joannides *et al.*, 2006, Dvash *et al.*, 2006, Mikkola *et al.*, 2006) suggesting there are some substantial differences between mEB and hEB differentiation. Figure 4-23 presents a diagrammatic summary of the immunohistochemistry and RT-PCR results obtained in this chapter to demonstrate the spatial and temporal relationship between the various markers in hEBs from all four of the hESC lines analysed. Pluripotency markers are mostly down-regulated from d6-d10. At d8, mesendoderm markers are expressed in the same cells that are still expressing markers of pluripotency, indicating cells that are progressing from a pluripotent state to mesendoderm. At d10-d12 SOX1 is expressed in non pluripotency/mesendoderm expressing areas,

indicating that ectoderm is derived from a separate population. At d10-14 pluripotency and mesendoderm markers become expressed in separate populations. Mesendoderm subsequently diverges to form mesoderm and endoderm between d12-14, when markers of pluripotency are down-regulated and the expression of the three germ layer markers becomes spatially separate. Almost no overlap between POU5F1 and SOX1 expression was detected in hEBs from any line. This might suggest that despite that in the mouse embryo, primitive columnar ectoderm differentiates to neuroectoderm with little cell movement, and that columnar ectoderm cells in the anterior half of late-streak mouse embryos express SOX1 (Pevny *et al.*, 1998), this marker may be to late to detect a POU5F1/SOX1 co-expressing population in hESCs.
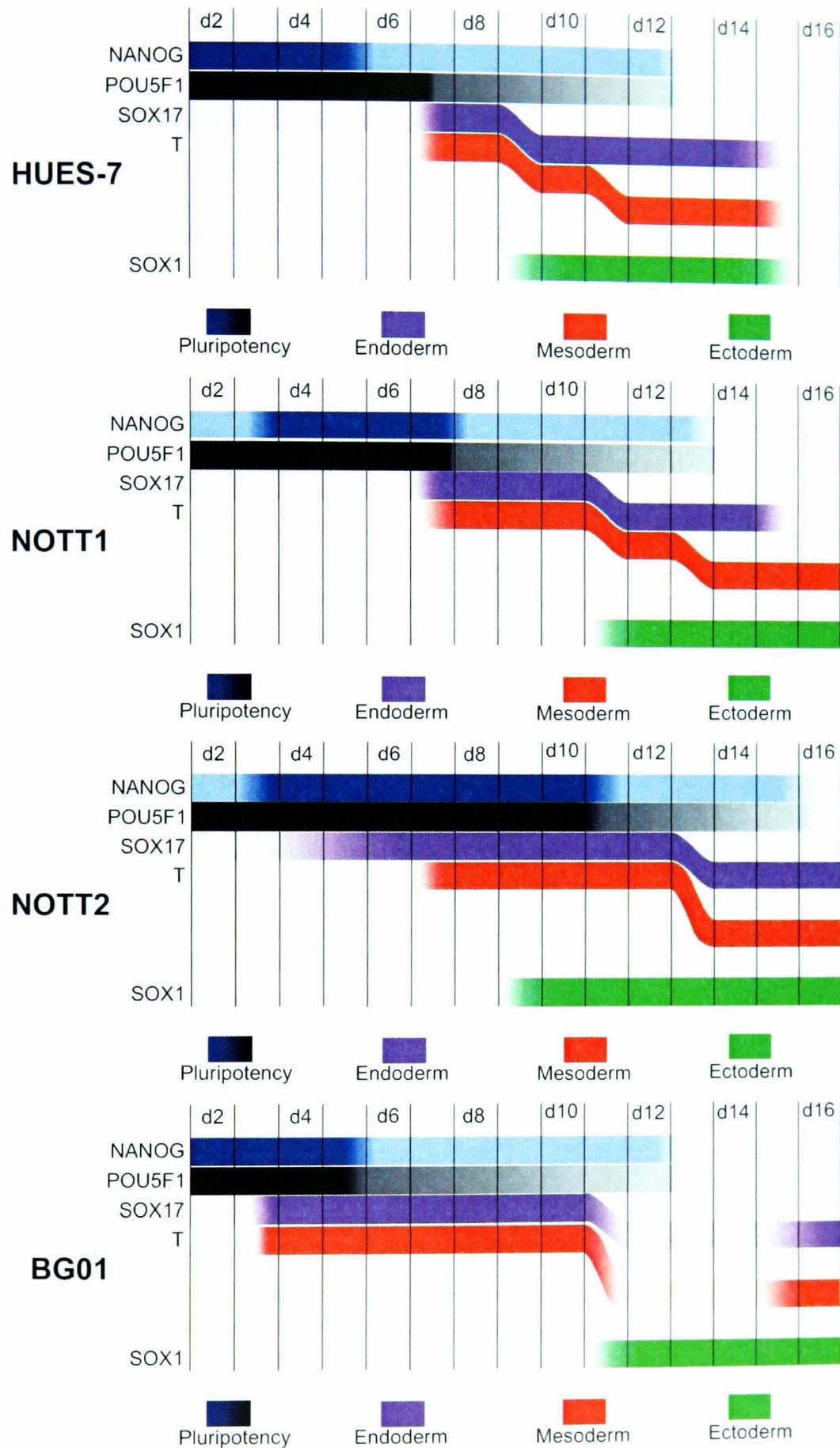
Figure 4-23: Diagrammatic representation of the timing and relationship between marker expression during HUES-7, NOTT1, NOTT2 and BG01 hEB differentiation

Sections of the coloured bars which are lighter represent a lower level of expression. Coloured bars which are adjacent to one-another represent co-localisation of markers at that time-point. Coloured bars that are not adjacent to one-another represent no co-localisation between markers.

4.4.4 Enhancement of mesendoderm with activin A and FGF2

When forming HUES-7 hEBs in a chemically defined medium supplemented with activin A and FGF2 (CDM), improvements were seen in the percentage cardiomyocytes produced at the end of differentiation (see Chapter 3). To assess the effect of this medium on hEB formation and differentiation, immunohistochemistry and RT-PCR was performed on a time course of samples as before (Figure 4-16 and Figure 4-17). HUES-7 CDM hEBs appeared as homogeneous in marker expression as the HUES-7 hEBs. Treatment with CDM leads to precocious and increased expression of mesodermal and endodermal markers at d4-6 in comparison to HUES-7 hEBs (diagrammatic representation, Figure 4-24). Pluripotency marker expression was down-regulated after d4. Ectoderm marker expression was also detected earlier from d8-10. This expression pattern in hEBs formed in CDM appeared to offer further improvement in the synchronicity of mesoderm induction, creating a larger population of cells at the same point in differentiation.
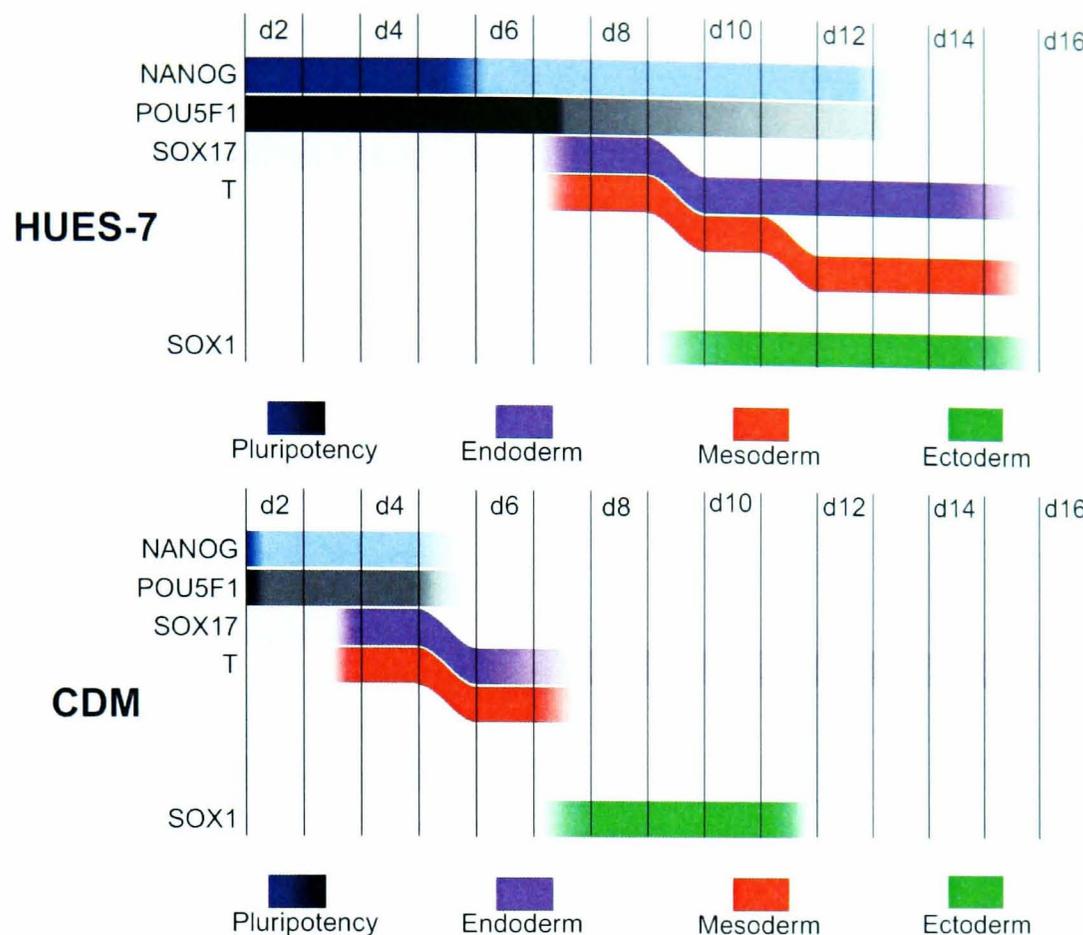
Figure 4-24: Comparisons of diagrammatic representations of forced aggregation HUES-7 hEBs and HUES-7 CDM hEBs

Lighter areas of the bars represent lower levels of expression. Adjoining bars represent areas of co-expression. Coloured bars which are adjacent to one-another represent co-localisation of markers at that time-point. Coloured bars that are not adjacent to one-another represent no co-localisation between markers.

4.4.5 Maintenance of POU5F1 expression in hEBs and potential for tumourigenesis

The maintenance of POU5F1 expression up to d16 of hEB differentiation as seen in these experiments has been demonstrated by other groups (Ng *et al.*, 2005a, Joannides *et al.*, 2006, Barberi *et al.*, 2007, Nat *et al.*, 2007) despite the conventional view that pluripotency is quickly down-regulated in differentiating ESCs (Johnson *et al.*, 2006). Undifferentiated hESCs are tumourigenic (Itskovitz-Eldor *et al.*, 2000) therefore any maintenance of pluripotency is important consideration for clinical applications. It is unclear if the expression of POU5F1 and NANOG so late in differentiation in these hEBs is due to the maintenance of a population of

undifferentiated cells or alternatively to the spontaneous generation of PGCs. In mice POU5F1 is expressed in PGCs during migration and maintained in male PGCs throughout foetal development and in the adult proliferating gonocytes, pro-spermatogonia and later in undifferentiated spermatogonia (Pesce *et al.*, 1998). NANOG is also expressed during PGC migration and becomes undetectable in females at E13.5-E14.5 and in males at E14.5-E16.5 (Yamaguchi *et al.*, 2005). Therefore both markers may potentially be expressed in PGCs derived from hESCs.

4.4.5.1 Transient up-regulation of NANOG expression in d4 hEBs

It was noted that hEBs formed from each of the 4 hESC lines examined to express higher levels of NANOG at d4 than d2, whereas POU5F1 was constant (Figure 4-12 to Figure 4-15). This result was recapitulated RT-PCR data from NOTT1 and BG01 but not HUES-7 or NOTT2 (Figure 4-11). Biphasic peaks of *NANOG* expression at d0 and d3 has been observed using microarray transcriptional profiling (Hirst *et al.*, 2006). This was suggested to be an *in vitro* recapitulation of the *NANOG* expression first seen in the ICM of the preimplantation mouse blastocyst and then later in the epiblast adjacent to the elongating primitive streak (Hart *et al.*, 2004). This may demonstrate the ability of the hEB system to mimic human development.

4.4.6 Mesendodermal marker expression in undifferentiated hESCs

This study detected markers of mesendoderm in undifferentiated (d0) hESCs by RT-PCR. To assess this was restricted to the culture conditions employed in our laboratory, cell pellets were obtained from 3 independent labs (including our own) using a variety of culture and passage methods. The RT-PCR results demonstrated at least some mesendodermal gene expression is in all lines assessed. The use of independently cultured lines shows that this result is not restricted to a particular

passage method or culture technique. Expression of T as well as FOXA2 has previously been detected in undifferentiated H9 hESCs (Joannides *et al.*, 2006).

Since the RT-PCR was performed at 35 cycles it is possible that only 'leaky' gene expression was detected, to assess if germ layer marker expression in undifferentiated hESCs was detectable at the protein level immunohistochemistry of T, SOX17, SOX1, POU5F1 and NANOG was performed in undifferentiated cells from five hESC lines cultured under the same feeder-free conditions. It was demonstrated that all three germ layer markers were expressed at low levels in most undifferentiated cells. These results also demonstrated that simultaneous expression of germ layer and pluripotency markers occurs in a subset of cells expressing the markers at a higher level. The mouse ICM has been identified as a heterogeneous population of unpredictable potential (Lake *et al.*, 2000) and *T* expression has been detected in all cells by ISH (Yoshikawa *et al.*, 2006). The co-expression of pluripotency and germ layer markers noted may represent either the readiness to differentiate or the cycling of cells from a state expressing high levels pluripotency markers and very low level of mesendoderm markers to a state still expressing high levels of pluripotency markers but also slightly elevated germ layer markers and back again by dedifferentiation, an ability suggested in mESCs by Niwa *et al.*, (2000) and Suzuki *et al.*, (2006). In addition it is possible that differentiated cells may have a role in the maintenance of the undifferentiated state (Bendall *et al.*, 2007).

4.4.7 Gene expression in pluripotency-sorted cells

The above result raised the question of whether undifferentiated hESCs maintain a population of differentiated cells within the undifferentiated population or if the cells are able to possess higher germ layer marker expression whilst maintaining their high

pluripotency marker expression. To answer this question, two cell surface markers demonstrated as the most descriptive for pluripotency (Henderson *et al.*, 2002), SSEA3 and SSE4 were used. Both of these markers are expressed on the cell surface of hESCs and are down-regulated as these cells differentiate (Thomson *et al.*, 1998, Reubinoff *et al.*, 2000). It has recently been demonstrated that hESCs can remain pluripotent after the depletion of SSEA3 and SSE4 (Brimble *et al.*, 2007) suggesting that these two markers are merely indicators rather than having a direct role in pluripotency. Cells were FACS sorted and the highest and lowest SSEA3 and SSEA4 expressing cells were isolated. RT-PCR was performed for the expression of markers of pluripotency and the three germ layers. Results showed that FACS sorting had no effect on germ layer marker expression suggesting that 'undifferentiated' hESCs are capable of expressing markers of the three germ layers without loosing expression of pluripotency markers.

The combination of immunohistochemistry and RT-PCR data in the present study provides a spatial and temporal map of hEB loss of pluripotency and germ layer formation. The forced aggregation system that has been shown to substantially improve cardiomyocyte formation is demonstrated to form hEBs which differentiate more synchronously that mass culture hEBs. A consistent pattern of differentiation is seen in hEBs from independently-derived hESC. Treatment with CDM supplemented with activin A and FGF2 is shown to induce precocious expression of mesendodermal markers at d2. The combination of forced aggregation and automated immunohistochemistry provides a platform to identify and quantify potential improvements in the differentiation of hESC-derived hEBs and a novel tool for studying early human development.

5 GENERAL DISCUSSION

To realise the full scientific and clinical potential of hESCs, strategies to overcome the high degree of heterogeneity of differentiated populations are required. The results presented here demonstrate the development of a forced aggregation system for the formation of hEBs from a defined number of hESCs. This system removes numerous variables in hEB formation and allowed the study of the temporal and spatial expression of markers of pluripotency and the three germ layers in hEBs. Also demonstrated is the formation of hEBs in CDM supplemented with activin A and FGF2, which resulted in an increase in mesendodermal marker expression at d2 of differentiation and the production of beating cardiomyocyte areas at d24 of differentiation in 23.6% of hEBs. Additionally, a successful method for the improved differentiation of pluripotent *Xenopus* animal cap cells to mesoderm, haemangioblasts and erythrocytes has been established.

5.1.1 A standardised system for hEB differentiation

The forced aggregation system developed in Chapter 3 provides a number of enhancements to the system demonstrated by Ng *et al.*, (2005b). Particularly significant is the formation of hEBs from a defined number of cells cultured on Matrigel. This allows the formation of hEBs of a reproducible size and removes any possible contamination on hEBs with MEFs. The use of a fully chemically defined medium, that replaces BSA used in previous experiments (Vallier *et al.*, 2004a, Ng *et al.*, 2005a), with PVA, is an important step for use in future clinical applications as well as for reducing the number of non-defined variables for differentiation studies. Together, these optimisations represent a significant enhancement to the hEB formation protocol. The demonstration of the use of this forced aggregation system

in four hESC lines cultured using the same method (Denning *et al.*, 2006) answers important questions regarding the transferability of techniques as frequently differentiation methods are only tested on lines derived from one laboratory (Allegrucci and Young, 2007).

5.1.2 Spatial map of germ layer interaction during hEB differentiation

This is the first report of the spatial relationship between pluripotency and germ layer markers in hEBs. The pattern of differentiation observed in each of the hESC lines was broadly similar allowing the formation of a composite of the spatial relationship between pluripotency and germ layer marker expression in hEBs (Figure 5-1).
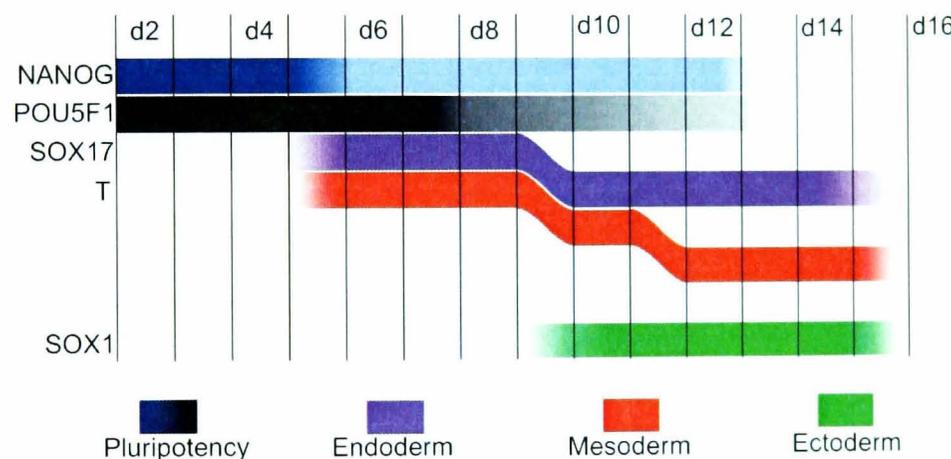
Figure 5-1: Composite of the spatial and temporal relationship between pluripotency and germ layer markers in hEBs

Lighter areas of the bars represent lower levels of expression. Adjoining bars represent areas of co-expression. Coloured bars which are adjacent to one-another represent co-localisation of markers at that time-point. Coloured bars that are not adjacent to one-another represent no co-localisation between markers.

The timing of the expression of pluripotency and mesoderm and endoderm marker expression closely correlates to a composite of data previously published (Ng *et al.*, 2005a, Vallier *et al.*, 2005, Kennedy *et al.*, 2007, Joannides *et al.*, 2007). The co-expression of NANOG, POU5F1, SOX17 and T seen at d6-d8 closely mimics the expression pattern seen *in vivo* in the mouse embryo as the posterior portion of the epiblast/primitive ectoderm becomes the primitive streak, although conformation of

this co-expression would require fluorescent double-labelling. The co-expression of POU5F1 and the mesoderm/endoderm marker, MIXL1, has been previously described in hESCs (Mossman et al., 2005). The co-expression of T and SOX17 at d10 before spatially separate expression at d12 tentatively suggests that these cells progress to mesoderm and endoderm from a bipotent cell type, mesendoderm. Mesendoderm has been suggested to exist in both vertebrate and non-vertebrate species (Rodaway and Patient, 2001), but has not been previously described in humans. The presence of mesendoderm could be further analysed by co-staining for T and SOX17 and subsequent FACS analysis as used by Mossman et al., (2005) for POU5F1 and MIXL1. The expression of SOX1 did not overlap with any of the other four markers at any time point in hEBs from any of the 4 hESC lines examined. Together with the known co-expression of POU5F1/NANOG/T/SOX17, this suggests that the SOX1 population arises from a distinct subset of cells that down-regulate POU5F1/NANOG early in differentiation. POU5F1 is expressed in primitive ectoderm until E7.5 of mouse development and SOX1 is detected from E8.0 onwards, which may explain why a POU5F1/SOX1 co-expressing population was not detected.

5.1.3   Germ layer marker expression in undifferentiated hESCs

T, SOX17 and SOX1 proteins were all detected in undifferentiated hESCs, both at low levels in all cells and at higher levels in scattered individual cells. The expression of germ layer marker mRNA in undifferentiated hESCs has been reported previously, albeit at low levels (Joannides et al., 2006). Studies of individual cells in early gastrula *Xenopus* embryos have shown that 'rogue' cells exist that express markers of one or more different germ layers than those predicted by the fate map (Wardle and Smith, 2006). This phenomenon is potentially a consequence of the

stochastic nature of gene expression (reviewed by Fiering *et al.*, 2000), which suggests that a gene is expressed in the absence of an enhancer and merely increased when an enhancer is linked to the gene. The exposure of hESCs to low levels of multiple signals (including signalling factors and their inhibitors) from the CM and the Matrigel; therefore may also enhance this stochastic gene expression. Low level expression of germ layer markers in hESCs may not represent irreversible commitment to a specific fate but may merely reflect establishment of the of the machinery permissive for differentiation should further external influences present themselves.

5.1.4 Inter-line variation in spatial and temporal marker expression and cardiomyocyte differentiation

Inter-line variation in mesoderm formation has been previously noted in hESCs (Mikkola *et al.*, 2006). Even after hEB cell number optimisation, BG01 hEBs consistently produced substantially fewer beating cardiomyocyte areas (1.6±1.0%) in comparison to HUES-7 (9.5±0.9%), NOTT1 (5.3±3.1%) and NOTT2 (6.6.±2.4%) as shown in Figure 3-13. BG01 hEBs also had a substantially different spatial and temporal profile of pluripotency down-regulation and germ layer (Figure 4-23). It is suggested that the complex conditions under which ESC lines have been derived has an effect on EB development (Weitzer, 2006). As these cells are grown under the same conditions and demonstrate similar pluripotency marker expression there may be an additional underlying cause of this difference in differentiation capacity. ESC isolation maybe prone to epigenetic events or other stochastic processes that predispose the differentiation process of an ESC line (Weitzer, 2006). It has been demonstrated that epigenetic changes can be induced by culture conditions and that these changes are inherited by differentiated cells (Allegrucci *et al.*, 2007). The

BG01 cells used in this study were also of a substantially later passage (p48-55) than any of the other three hESC lines (p20-31) and, although BG01 cells were karyotypically normal, this extended culture may have introduced epigenetic instability (Burridge *et al.*, 2007).

5.1.5 The synergistic role of tal1, lmo2 and gata1 in *Xenopus* haematopoiesis and potential for transfer to the hESC system

The co-injection of activin B or fgf4 mRNA along with tal1, gata1 and lmo2 mRNA into the *Xenopus* animal pole, and subsequent culture of animal cap explants demonstrated a highly successful system for the induction of mesoderm, haemangioblasts and primitive erythrocytes. Additionally, it was demonstrated that all three of tal1, gata1 and lmo2 mRNA are required for maximal differentiation to erythrocytes. Cells of the *Xenopus* animal cap are analogous to hESCs in that they are described as pluripotent (Heasman *et al.*, 1984). They also differ substantially from hESCs in that they survive in a simple saline medium, will differentiate to atypical epidermis without the addition of factors to direct differentiation and already have some three dimensional structure due to their origin from the blastocoel roof (Okabayashi and Asashima, 2003). Therefore, directed differentiation in *Xenopus* animal caps offers a substantially simplified version of the process required for directed differentiation in hESCs. In order to direct differentiation using transcription factors in hESCs a non-viral, transient delivery is desirable for clinical applications. Transient transfection has been reported in hESCs with over 50% efficiency (Anderson *et al.*, 2007), although either using three transcription factors in one plasmid or co-transfecting three plasmids has not been demonstrated and remains a technical challenge. Electroporation of *in vitro* transcribed mRNA has been demonstrated in hESCs with 80-90% efficiency (Van Driessche *et al.*, 2005) and,

although has not yet been demonstrated for the introduction of more than one mRNA, may prove a useful route for transcription factor-mediated directed differentiation.

5.1.6 Future prospects

The CDM-PVA+ medium for used for differentiation in this thesis was identical to that used by Vallier *et al.* (2005) for maintenance of hESCs in the undifferentiated state with the exception of replacing BSA with PVA. Use of defined media for both undifferentiated cell culture (without the use of feeders or serum) and differentiation (using a controlled number of cells and standard size of hEBs) would allow the fine tuning of conditions that promote lineage induction with minimised influence of other factors. Such a controlled system will leave just two main variables of hESC differentiation, i.e. the number of days of hEB culture and the growth factors the hEBs are treated with.

5.1.7 The advantages and drawbacks of hEBs

The main advantage of hEB formation is the generation of three-dimensional interactions that cannot be imitated in monolayer culture (Vallier and Pedersen, 2005). However, the three dimensional structure of hEBs also represents their major drawback, by reflecting that the extra-cellular environment inside of hEBs cannot be defined or controlled. As a consequence, the generation of pure populations of single cell types through hEB differentiation may not be possible. The potential for monolayer differentiation of hESCs has been described (Yao *et al.*, 2006) and further improvements in this type of system would present a significant step towards a simplified, scalable, clinically valuable system for hESC differentiation. Monolayer differentiation will necessitate improvements in our knowledge of factors that control

differentiation, potentially to mimic some of the environmental cues that are experienced in hEBs, and the possibility that three dimensional cell-cell contact may be required for differentiation represents a significant challenge.

5.1.8   Sequential treatment with growth factors: mimicking *in vivo* ontology

The involvement of growth factors in mESC and hESC cardiogenesis and haematopoiesis have been evaluated in several studies (see Table 3-2). As yet, the effect of individual factors added at different time-points and in different combinations has not been attempted. Therefore, after the establishment of this improved system for homogeneous hEB formation and high level mesoderm induction, the next step will be to trial factors known to promote the different steps of terminal lineage differentiation, potentially mimicking the sequence of events experienced *in vivo*.

5.1.9   Potential culture systems for differentiation along the mesodermal lineage

The hEB formation and differentiation system developed within this thesis could potentially be improved in different ways. Since this work was completed, further progress has been made by using a transgenic approach to positively select for cardiomyocytes expressing a bicistronic reporter (GFP and puromycin resistance) from the alpha myosin heavy chain that resulted in 91.5±4.3% cardiomyocytes (Anderson *et al.*, 2007). To further attempt to improve the yield of terminal lineage cells, one important step to be attempted would be to remove the mass culture stage after the initial hEB formation, by directly transferring hEBs to 96-well U bottom plates at d2-d4. This would remove factors associated with inter-hEB communication. This could be followed by a transgenic enrichment procedure or by

FACS to enrich for the desired lineage (Figure 5-2C). Removal of this mass culture step was attempted (results not shown) but resulted in a reduced cardiomyocyte production despite proving successful for blood formation (Ng *et al.*, 2005a). To further improve differentiation in the forced aggregation system, the use of hESCs grown in CDM, followed by introduction of either cardiomyocyte inducing transcription factors or haematopoiesis inducing transcription factors (such as tal1, lmo2 and gata2) either through transient transfection or mRNA electroporation followed could be used followed by sequential additional haematopoietic or cardiogenic inducing growth factors (Figure 5-2D). Careful attention to using the right combinations of transcription factors at the right time point will need to be made by referring to transcription factor networks (Loose and Patient, 2004, Swiers *et al.*, 2006). Finally, use of the above system of CDM along with transcription and growth factor induced directed differentiation could be used in combination with monolayer differentiation (Figure 5-2E). Without hEB formation this system could potentially provide an entire population of hESCs differentiated to mesoderm and subsequently to terminal mesodermal lineages. This high-yield differentiation, if used a hESC line derived under good manufacturing practice conditions could provide cells suitable for clinical use and allow simple scale up to clinically relevant levels.
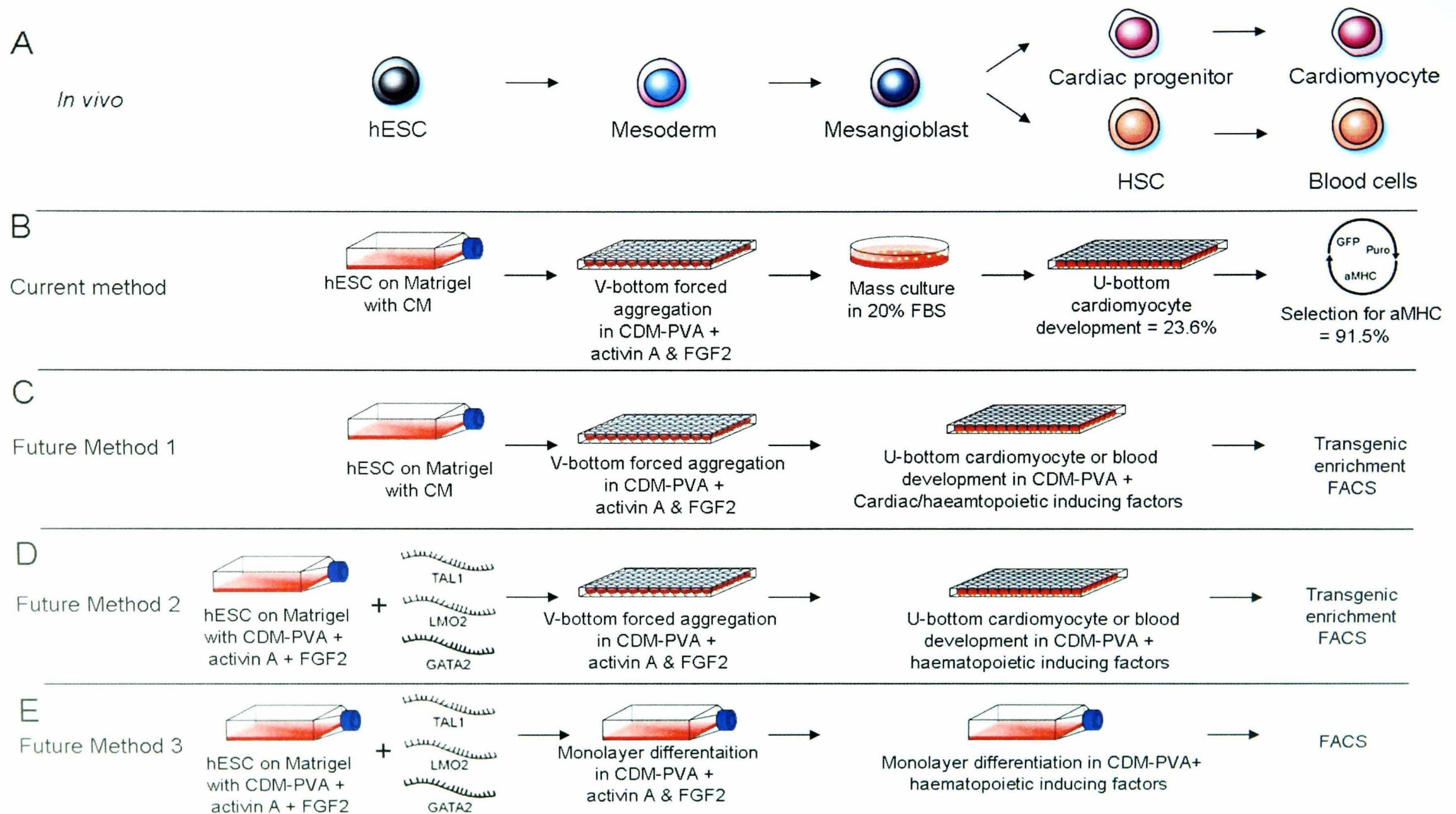
Figure 5-2: Potential future methods for differentiation along the mesodermal lineage

265

In conclusion, this work demonstrates that formation of forced aggregation hEBs enhances terminal lineage differentiation. However, forced aggregation hEBs do not differentiate according to the standard model of differentiation established in mEBs, but show a lack of a visceral endoderm layer and pluripotency down-regulation from the centre of the hEBs. Formation of hEBs in CDM supplemented with activin A and FGF2 further altered hEB formation, substantially increasing T expression at d2 of differentiation, whilst reducing the expression of markers of pluripotency, ectoderm and endoderm. This treatment prevented the formation of internal structures seen in hEBs formed in CM, but also further improved terminal lineage differentiation. Together these developments suggest that perhaps the future of hESC differentiation lies not in mimicking human development, but understanding it and perturbing hESC differentiation in a manner that directs to one cell type, without the normal interaction of other cell types.

6 REFERENCES

ABE, K., NIWA, H., IWASE, K., TAKIGUCHI, M., MORI, M., ABE, S. I., ABE, K. & YAMAMURA, K. I. (1996) Endoderm-specific gene expression in embryonic stem cells differentiated to embryoid bodies. *Exp Cell Res,* 229, 27-34.

ABEYTA, M. J., CLARK, A. T., RODRIGUEZ, R. T., BODNAR, M. S., PERA, R. A. & FIRPO, M. T. (2004) Unique gene expression signatures of independently-derived human embryonic stem cell lines. *Hum Mol Genet,* 13, 601-8.

ADEWUMI, O., AFLATOONIAN, B., AHRLUND-RICHTER, L., AMIT, M., ANDREWS, P. W., BEIGHTON, G., BELLO, P. A., BENVENISTY, N., BERRY, L. S., BEVAN, S., BLUM, B., BROOKING, J., CHEN, K. G., CHOO, A. B., CHURCHILL, G. A., CORBEL, M., DAMJANOV, I., DRAPER, J. S., DVORAK, P., EMANUELSSON, K., FLECK, R. A., FORD, A., GERTOW, K., GERTSENSTEIN, M., GOKHALE, P. J., HAMILTON, R. S., HAMPL, A., HEALY, L. E., HOVATTA, O., HYLLNER, J., IMREH, M. P., ITSKOVITZ-ELDOR, J., JACKSON, J., JOHNSON, J. L., JONES, M., KEE, K., KING, B. L., KNOWLES, B. B., LAKO, M., LEBRIN, F., MALLON, B. S., MANNING, D., MAYSHAR, Y., MCKAY, R. D., MICHALSKA, A. E., MIKKOLA, M., MILEIKOVSKY, M., MINGER, S. L., MOORE, H. D., MUMMERY, C. L., NAGY, A., NAKATSUJI, N., O'BRIEN, C. M., OH, S. K., OLSSON, C., OTONKOSKI, T., PARK, K. Y., PASSIER, R., PATEL, H., PATEL, M., PEDERSEN, R., PERA, M. F., PIEKARCZYK, M. S., PERA, R. A., REUBINOFF, B. E., ROBINS, A. J., ROSSANT, J., RUGG-GUNN, P., SCHULZ, T. C., SEMB, H., SHERRER, E. S., SIEMEN, H., STACEY, G. N., STOJKOVIC, M., SUEMORI, H., SZATKIEWICZ, J., TURETSKY, T., TUURI, T., VAN DEN BRINK, S., VINTERSTEN, K., VUORISTO, S., WARD, D., WEAVER, T. A., YOUNG, L. A. & ZHANG, W. (2007) Characterization of human embryonic stem cell lines by the International Stem Cell Initiative. *Nat Biotechnol,* 25, 803-16.

ADJAYE, J., HUNTRISS, J., HERWIG, R., BENKAHLA, A., BRINK, T. C., WIERLING, C., HULTSCHIG, C., GROTH, D., YASPO, M. L., PICTON, H. M., GOSDEN, R. G. & LEHRACH, H. (2005) Primary differentiation in the human blastocyst: comparative molecular portraits of inner cell mass and trophectoderm cells. *Stem Cells,* 23, 1514-25.

AGHAJANOVA, L., SKOTTMAN, H., STROMBERG, A. M., INZUNZA, J., LAHESMAA, R. & HOVATTA, O. (2006) Expression of leukemia inhibitory factor and its receptors is increased during differentiation of human embryonic stem cells. *Fertil Steril,* 86 Suppl 4, 1193-209.

AGULNICK, A. D., TAIRA, M., BREEN, J. J., TANAKA, T., DAWID, I. B. & WESTPHAL, H. (1996) Interactions of the LIM-domain-binding factor Ldb1 with LIM homeodomain proteins. *Nature,* 384, 270-2.

AHMAD, S., STEWART, R., YUNG, S., KOLLI, S., ARMSTRONG, L., STOJKOVIC, M., FIGUEIREDO, F. & LAKO, M. (2007) Differentiation of human embryonic stem cells into corneal epithelial-like cells by in vitro replication of the corneal epithelial stem cell niche. *Stem Cells,* 25, 1145-55.

ALBERIO, R., CAMPBELL, K. H. & JOHNSON, A. D. (2006) Reprogramming somatic cells into stem cells. *Reproduction,* 132, 709-20.

ALLEGRUCCI, C., DENNING, C. N., BURRIDGE, P., STEELE, W., SINCLAIR, K. D. & YOUNG, L. E. (2005) Human embryonic stem cells as a model for nutritional programming: An evaluation. *Reprod Toxicol,* 20, 353-67.

ALLEGRUCCI, C., WU, Y. Z., THURSTON, A., DENNING, C. N., PRIDDLE, H., MUMMERY, C. L., WARD-VAN OOSTWAARD, D., ANDREWS, P. W., STOJKOVIC, M., SMITH, N., PARKIN, T., JONES, M. E., WARREN, G., YU, L., BRENA, R. M., PLASS, C. & YOUNG, L. E. (2007) Restriction landmark genome scanning identifies culture-induced DNA methylation instability in the human embryonic stem cell epigenome. *Hum Mol Genet,* 16, 1253-68.

ALLEGRUCCI, C. & YOUNG, L. E. (2007) Differences between human embryonic stem cell lines. *Hum Reprod Update,* 13, 103-20.

AMIT, M., CARPENTER, M. K., INOKUMA, M. S., CHIU, C. P., HARRIS, C. P., WAKNITZ, M. A., ITSKOVITZ-ELDOR, J. & THOMSON, J. A. (2000) Clonally derived human embryonic stem cell lines maintain pluripotency and proliferative potential for prolonged periods of culture. *Dev Biol,* 227, 271-8.

AMIT, M. & ITSKOVITZ-ELDOR, J. (2002) Derivation and spontaneous differentiation of human embryonic stem cells. *J Anat,* 200, 225-32.

AMIT, M., SHARIKI, C., MARGULETS, V. & ITSKOVITZ-ELDOR, J. (2004) Feeder layer- and serum-free culture of human embryonic stem cells. *Biol Reprod,* 70, 837-45.

ANDERSON, D., SELF, T., MELLOR, I. R., GOH, G., HILL, S. J. & DENNING, C. (2007) Transgenic enrichment of cardiomyocytes from human embryonic stem cells. *Mol Ther,* 15, 2027-36.

ANDERSON, D. J., GAGE, F. H. & WEISSMAN, I. L. (2001) Can stem cells cross lineage boundaries? *Nat Med,* 7, 393-5.

ANDERSON, J. S., BANDI, S., KAUFMAN, D. S. & AKKINA, R. (2006) Derivation of normal macrophages from human embryonic stem (hES) cells for applications in HIV gene therapy. *Retrovirology,* 3, 24.

ANG, S. L., CONLON, R. A., JIN, O. & ROSSANT, J. (1994) Positive and negative signals from mesoderm regulate the expression of mouse Otx2 in ectoderm explants. *Development,* 120, 2979-89.

ANG, S. L. & CONSTAM, D. B. (2004) A gene network establishing polarity in the early mouse embryo. *Semin Cell Dev Biol,* 15, 555-61.

ANG, S. L., WIERDA, A., WONG, D., STEVENS, K. A., CASCIO, S., ROSSANT, J. & ZARET, K. S. (1993) The formation and maintenance of the definitive endoderm lineage in the mouse: involvement of HNF3/forkhead proteins. *Development,* 119, 1301-15.

APLAN, P. D., BEGLEY, C. G., BERTNESS, V., NUSSMEIER, M., EZQUERRA, A., COLIGAN, J. & KIRSCH, I. R. (1990) The SCL gene is formed from a transcriptionally complex locus. *Mol Cell Biol,* 10, 6426-35.

ARIIZUMI, T., SAWAMURA, K., UCHIYAMA, H. & ASASHIMA, M. (1991) Dose and time-dependent mesoderm induction and outgrowth formation by activin A in Xenopus laevis. *Int J Dev Biol,* 35, 407-14.

ARMSTRONG, L., HUGHES, O., YUNG, S., HYSLOP, L., STEWART, R., WAPPLER, I., PETERS, H., WALTER, T., STOJKOVIC, P., EVANS, J., STOJKOVIC, M. & LAKO, M. (2006) The role of PI3K/AKT, MAPK/ERK and NFkappabeta signalling in the maintenance of human embryonic stem

cell pluripotency and viability highlighted by transcriptional profiling and functional analysis. *Hum Mol Genet,* 15, 1894-913.

ARNOLD, S. J., STAPPERT, J., BAUER, A., KISPERT, A., HERRMANN, B. G. & KEMLER, R. (2000) Brachyury is a target gene of the Wnt/beta-catenin signaling pathway. *Mech Dev,* 91, 249-58.

ASSADY, S., MAOR, G., AMIT, M., ITSKOVITZ-ELDOR, J., SKORECKI, K. L. & TZUKERMAN, M. (2001) Insulin production by human embryonic stem cells. *Diabetes,* 50, 1691-7.

AVILION, A. A., NICOLIS, S. K., PEVNY, L. H., PEREZ, L., VIVIAN, N. & LOVELL-BADGE, R. (2003) Multipotent cell lineages in early mouse development depend on SOX2 function. *Genes Dev,* 17, 126-40.

BADER, A., GRUSS, A., HOLLRIGL, A., AL-DUBAI, H., CAPETANAKI, Y. & WEITZER, G. (2001) Paracrine promotion of cardiomyogenesis in embryoid bodies by LIF modulated endoderm. *Differentiation,* 68, 31-43.

BAHARVAND, H., ASHTIANI, S. K., TAEE, A., MASSUMI, M., VALOJERDI, M. R., YAZDI, P. E., MORADI, S. Z. & FARROKHI, A. (2006a) Generation of new human embryonic stem cell lines with diploid and triploid karyotypes. *Dev Growth Differ,* 48, 117-28.

BAHARVAND, H., ASHTIANI, S. K., VALOJERDI, M. R., SHAHVERDI, A., TAEE, A. & SABOUR, D. (2004) Establishment and in vitro differentiation of a new embryonic stem cell line from human blastocyst. *Differentiation,* 72, 224-9.

BAHARVAND, H., HASHEMI, S. M., KAZEMI ASHTIANI, S. & FARROKHI, A. (2006b) Differentiation of human embryonic stem cells into hepatocytes in 2D and 3D culture systems in vitro. *Int J Dev Biol,* 50, 645-52.

BAHARVAND, H., JAFARY, H., MASSUMI, M. & ASHTIANI, S. K. (2006c) Generation of insulin-secreting cells from human embryonic stem cells. *Dev Growth Differ,* 48, 323-32.

BANVILLE, D. & WILLIAMS, J. G. (1985) The pattern of expression of the Xenopus laevis tadpole alpha-globin genes and the amino acid sequence of the three major tadpole alpha-globin polypeptides. *Nucleic Acids Res,* 13, 5407-21.

BARBERI, T., BRADBURY, M., DINCER, Z., PANAGIOTAKOS, G., SOCCI, N. D. & STUDER, L. (2007) Derivation of engraftable skeletal myoblasts from human embryonic stem cells. *Nat Med,* 13, 642-8.

BARBERI, T., WILLIS, L. M., SOCCI, N. D. & STUDER, L. (2005) Derivation of multipotent mesenchymal precursors from human embryonic stem cells. *PLoS Med,* 2, e161.

BEATTIE, G. M., LOPEZ, A. D., BUCAY, N., HINTON, A., FIRPO, M. T., KING, C. C. & HAYEK, A. (2005) Activin A maintains pluripotency of human embryonic stem cells in the absence of feeder layers. *Stem Cells,* 23, 489-95.

BECK, S., LE GOOD, J. A., GUZMAN, M., BEN HAIM, N., ROY, K., BEERMANN, F. & CONSTAM, D. B. (2002) Extraembryonic proteases regulate Nodal signalling during gastrulation. *Nat Cell Biol,* 4, 981-5.

BECKER, S., CASANOVA, J. & GRABEL, L. (1992) Localization of endoderm-specific mRNAs in differentiating F9 embryoid bodies. *Mech Dev,* 37, 3-12.

BEDDINGTON, R. S. & ROBERTSON, E. J. (1998) Anterior patterning in mouse. *Trends Genet,* 14, 277-84.

BEDDINGTON, R. S. & ROBERTSON, E. J. (1999) Axis development and early asymmetry in mammals. *Cell,* 96, 195-209.

BEGLEY, C. G., APLAN, P. D., DAVEY, M. P., NAKAHARA, K., TCHORZ, K., KURTZBERG, J., HERSHFIELD, M. S., HAYNES, B. F., COHEN, D. I.. WALDMANN, T. A. & ET AL. (1989) Chromosomal translocation in a human leukemic stem-cell line disrupts the T-cell antigen receptor delta-chain diversity region and results in a previously unreported fusion transcript. *Proc Natl Acad Sci U S A*, 86, 2031-5.

BEGLEY, C. G., VISVADER, J., GREEN, A. R., APLAN, P. D., METCALF, D., KIRSCH, I. R. & GOUGH, N. M. (1991) Molecular cloning and chromosomal localization of the murine homolog of the human helix-loop-helix gene SCL. *Proc Natl Acad Sci U S A*, 88, 869-73.

BEHR, R., HENEWEER, C., VIEBAHN, C., DENKER, H. W. & THIE, M. (2005) Epithelial-mesenchymal transition in colonies of rhesus monkey embryonic stem cells: a model for processes involved in gastrulation. *Stem Cells*, 23, 805-16.

BELO, J. A., BOUWMEESTER, T., LEYNS, L., KERTESZ, N., GALLO, M., FOLLETTIE, M. & DE ROBERTIS, E. M. (1997) Cerberus-like is a secreted factor with neutralizing activity expressed in the anterior primitive endoderm of the mouse gastrula. *Mech Dev*, 68, 45-57.

BEN-HAIM, N., LU, C., GUZMAN-AYALA, M., PESCATORE, L., MESNARD, D., BISCHOFBERGER, M., NAEF, F., ROBERTSON, E. J. & CONSTAM, D. B. (2006) The nodal precursor acting via activin receptors induces mesoderm by maintaining a source of its convertases and BMP4. *Dev Cell*, 11, 313-23.

BEN-HUR, T., IDELSON, M., KHANER, H., PERA, M., REINHARTZ, E., ITZIK, A. & REUBINOFF, B. E. (2004) Transplantation of human embryonic stem cell-derived neural progenitors improves behavioral deficit in Parkinsonian rats. *Stem Cells*, 22, 1246-55.

BEN-NUN, I. F. & BENVENISTY, N. (2006) Human embryonic stem cells as a cellular model for human disorders. *Mol Cell Endocrinol*, 252, 154-9.

BENDALL, S. C., STEWART, M. H., MENENDEZ, P., GEORGE, D., VIJAYARAGAVAN, K., WERBOWETSKI-OGILVIE, T., RAMOS-MEJIA, V., ROULEAU, A., YANG, J., BOSSE, M., LAJOIE, G. & BHATIA, M. (2007) IGF and FGF cooperatively establish the regulatory stem cell niche of pluripotent human cells in vitro. *Nature*, 448, 1015-21.

BEPPU, H., KAWABATA, M., HAMAMOTO, T., CHYTIL, A., MINOWA, O., NODA, T. & MIYAZONO, K. (2000) BMP type II receptor is required for gastrulation and early development of mouse embryos. *Dev Biol*, 221, 249-58.

BETTIOL, E., SARTIANI, L., CHICHA, L., KRAUSE, K. H., CERBAI, E. & JACONI, M. E. (2007) Fetal bovine serum enables cardiac differentiation of human embryonic stem cells. *Differentiation*, 75, 669-81.

BHATTACHARYA, B., CAI, J., LUO, Y., MIURA, T., MEJIDO, J.. BRIMBLE, S. N., ZENG, X., SCHULZ, T. C., RAO, M. S. & PURI, R. K. (2005) Comparison of the gene expression profile of undifferentiated human embryonic stem cell lines and differentiating embryoid bodies. *BMC Dev Biol*, 5, 22.

BHATTACHARYA, B., MIURA, T., BRANDENBERGER, R., MEJIDO, J.. LUO. Y., YANG, A. X., JOSHI, B. H., GINIS, I., THIES, R. S.. AMIT. M.. LYONS, I., CONDIE, B. G., ITSKOVITZ-ELDOR, J.. RAO. M. S. & PURI.

R. K. (2004) Gene expression in human embryonic stem cell lines: unique molecular signature. *Blood,* 103, 2956-64.

BIANCHI, D. W., WILKINS-HAUG, L. E., ENDERS, A. C. & HAY, E. D. (1993) Origin of extraembryonic mesoderm in experimental animals: relevance to chorionic mosaicism in humans. *Am J Med Genet,* 46, 542-50.

BIELBY, R. C., BOCCACCINI, A. R., POLAK, J. M. & BUTTERY, L. D. (2004) In vitro differentiation and in vivo mineralization of osteogenic cells derived from human embryonic stem cells. *Tissue Eng,* 10, 1518-25.

BLUM, M., GAUNT, S. J., CHO, K. W., STEINBEISSER, H., BLUMBERG, B., BITTNER, D. & DE ROBERTIS, E. M. (1992) Gastrulation in the mouse: the role of the homeobox gene goosecoid. *Cell,* 69, 1097-106.

BOEHM, T., FORONI, L., KANEKO, Y., PERUTZ, M. F. & RABBITTS, T. H. (1991) The rhombotin family of cysteine-rich LIM-domain oncogenes: distinct members are involved in T-cell translocations to human chromosomes 11p15 and 11p13. *Proc Natl Acad Sci U S A,* 88, 4367-71.

BONGSO, A., FONG, C. Y., NG, S. C. & RATNAM, S. (1994) Isolation and culture of inner cell mass cells from human blastocysts. *Hum Reprod,* 9, 2110-7.

BOOTH, H. A. & HOLLAND, P. W. (2004) Eleven daughters of NANOG. *Genomics,* 84, 229-38.

BOWLES, K. M., VALLIER, L., SMITH, J. R., ALEXANDER, M. R. & PEDERSEN, R. A. (2006) HOXB4 overexpression promotes hematopoietic development by human embryonic stem cells. *Stem Cells,* 24, 1359-69.

BOYER, L. A., LEE, T. I., COLE, M. F., JOHNSTONE, S. E., LEVINE, S. S., ZUCKER, J. P., GUENTHER, M. G., KUMAR, R. M., MURRAY, H. L., JENNER, R. G., GIFFORD, D. K., MELTON, D. A., JAENISCH, R. & YOUNG, R. A. (2005) Core transcriptional regulatory circuitry in human embryonic stem cells. *Cell,* 122, 947-56.

BRADLEY, A., EVANS, M., KAUFMAN, M. H. & ROBERTSON, E. (1984) Formation of germ-line chimaeras from embryo-derived teratocarcinoma cell lines. *Nature,* 309, 255-6.

BRADLEY, J. A., BOLTON, E. M. & PEDERSEN, R. A. (2002) Stem cell medicine encounters the immune system. *Nat Rev Immunol,* 2, 859-71.

BRANDENBERGER, R., KHREBTUKOVA, I., THIES, R. S., MIURA, T., JINGLI, C., PURI, R., VASICEK, T., LEBKOWSKI, J. & RAO, M. (2004a) MPSS profiling of human embryonic stem cells. *BMC Dev Biol,* 4, 10.

BRANDENBERGER, R., WEI, H., ZHANG, S., LEI, S., MURAGE, J., FISK, G. J., LI, Y., XU, C., FANG, R., GUEGLER, K., RAO, M. S., MANDALAM, R., LEBKOWSKI, J. & STANTON, L. W. (2004b) Transcriptome characterization elucidates signaling networks that control human ES cell growth and differentiation. *Nat Biotechnol,* 22, 707-16.

BRENNAN, J., LU, C. C., NORRIS, D. P., RODRIGUEZ, T. A., BEDDINGTON, R. S. & ROBERTSON, E. J. (2001) Nodal signalling in the epiblast patterns the early mouse embryo. *Nature,* 411, 965-9.

BRIMBLE, S. N., SHERRER, E. S., UHL, E. W., WANG, E., KELLY, S., MERRILL, A. H., JR., ROBINS, A. J. & SCHULZ, T. C. (2007) The cell surface glycosphingolipids SSEA-3 and SSEA-4 are not essential for human ESC pluripotency. *Stem Cells,* 25, 54-62.

BURDON, T., CHAMBERS, I., STRACEY, C., NIWA, H. & SMITH, A. (1999a) Signaling mechanisms regulating self-renewal and differentiation of pluripotent embryonic stem cells. *Cells Tissues Organs,* 165, 131-43.

BURDON, T., SMITH, A. & SAVATIER, P. (2002) Signalling, cell cycle and pluripotency in embryonic stem cells. *Trends Cell Biol,* 12, 432-8.

BURDON, T., STRACEY, C., CHAMBERS, I., NICHOLS, J. & SMITH, A. (1999b) Suppression of SHP-2 and ERK signalling promotes self-renewal of mouse embryonic stem cells. *Dev Biol,* 210, 30-43.

BURDSAL, C. A., FLANNERY, M. L. & PEDERSEN, R. A. (1998) FGF-2 alters the fate of mouse epiblast from ectoderm to mesoderm in vitro. *Dev Biol,* 198, 231-44.

BURRIDGE, P. W., ANDERSON, D., PRIDDLE, H., BARBADILLO MUNOZ, M. D., CHAMBERLAIN, S., ALLEGRUCCI, C., YOUNG, L. E. & DENNING, C. (2007) Improved human embryonic stem cell embryoid body homogeneity and cardiomyocyte differentiation from a novel v-96 plate aggregation system highlights interline variability. *Stem Cells,* 25, 929-38.

BUYTAERT-HOEFEN, K. A., ALVAREZ, E. & FREED, C. R. (2004) Generation of tyrosine hydroxylase positive neurons from human embryonic stem cells after coculture with cellular substrates and exposure to GDNF. *Stem Cells,* 22, 669-74.

CAI, J., OLSON, J. M., RAO, M. S., STANLEY, M., TAYLOR, E. & NI, H. T. (2005) Development of antibodies to human embryonic stem cell antigens. *BMC Dev Biol,* 5, 26.

CALHOUN, J. D., RAO, R. R., WARRENFELTZ, S., REKAYA, R., DALTON, S., MCDONALD, J. & STICE, S. L. (2004) Transcriptional profiling of initial differentiation events in human embryonic stem cells. *Biochem Biophys Res Commun,* 323, 453-64.

CAMERON, C. M., HU, W. S. & KAUFMAN, D. S. (2006) Improved development of human embryonic stem cell-derived embryoid bodies by stirred vessel cultivation. *Biotechnol Bioeng,* 94, 938-48.

CARPENTER, M. K., INOKUMA, M. S., DENHAM, J., MUJTABA, T., CHIU, C. P. & RAO, M. S. (2001) Enrichment of neurons and neural precursors from human embryonic stem cells. *Exp Neurol,* 172, 383-97.

CARPENTER, M. K., ROSLER, E. & RAO, M. S. (2003) Characterization and differentiation of human embryonic stem cells. *Cloning Stem Cells,* 5, 79-88.

CARPENTER, M. K., ROSLER, E. S., FISK, G. J., BRANDENBERGER, R., ARES, X., MIURA, T., LUCERO, M. & RAO, M. S. (2004) Properties of four human embryonic stem cell lines maintained in a feeder-free culture system. *Dev Dyn,* 229, 243-58.

CASEY, E. S., O'REILLY, M. A., CONLON, F. L. & SMITH, J. C. (1998) The T-box transcription factor Brachyury regulates expression of eFGF through binding to a non-palindromic response element. *Development,* 125, 3887-94.

CERDAN, C., BENDALL, S. C., WANG, L., STEWART, M., WERBOWETSKI, T. & BHATIA, M. (2006) Complement targeting of nonhuman sialic acid does not mediate cell death of human embryonic stem cells. *Nat Med,* 12, 1113-4.

CERDAN, C., ROULEAU, A. & BHATIA, M. (2004) VEGF-A165 augments erythropoietic development from human embryonic stem cells. *Blood,* 103, 2504-12.

CHADWICK, K., WANG, L., LI, L., MENENDEZ, P., MURDOCH, B., ROULEAU, A. & BHATIA, M. (2003) Cytokines and BMP-4 promote hematopoietic differentiation of human embryonic stem cells. *Blood,* 102, 906-15.

CHAMBERS, I., COLBY, D., ROBERTSON, M., NICHOLS, J., LEE, S., TWEEDIE, S. & SMITH, A. (2003) Functional expression cloning of Nanog, a pluripotency sustaining factor in embryonic stem cells. *Cell,* 113, 643-55.

CHAMBERS, I., SILVA, J., COLBY, D., NICHOLS, J., NIJMEIJER, B., ROBERTSON, M., VRANA, J., JONES, K., GROTEWOLD, L. & SMITH, A. (2007) Nanog safeguards pluripotency and mediates germline development. *Nature,* 450, 1230-4.

CHAMBERS, I. & SMITH, A. (2004) Self-renewal of teratocarcinoma and embryonic stem cells. *Oncogene,* 23, 7150-60.

CHANG, K. H., NELSON, A. M., CAO, H., WANG, L., NAKAMOTO, B., WARE, C. B. & PAPAYANNOPOULOU, T. (2006) Definitive-like erythroid cells derived from human embryonic stem cells coexpress high levels of embryonic and fetal globins with little or no adult globin. *Blood,* 108, 1515-23.

CHAPMAN, D. L., COOPER-MORGAN, A., HARRELSON, Z. & PAPAIOANNOU, V. E. (2003) Critical role for Tbx6 in mesoderm specification in the mouse embryo. *Mech Dev,* 120, 837-47.

CHAZAUD, C. & ROSSANT, J. (2006) Disruption of early proximodistal patterning and AVE formation in Apc mutants. *Development,* 133, 3379-87.

CHAZAUD, C., YAMANAKA, Y., PAWSON, T. & ROSSANT, J. (2006) Early lineage segregation between epiblast and primitive endoderm in mouse blastocysts through the Grb2-MAPK pathway. *Dev Cell,* 10, 615-24.

CHEN, C., WARE, S. M., SATO, A., HOUSTON-HAWKINS, D. E., HABAS, R., MATZUK, M. M., SHEN, M. M. & BROWN, C. W. (2006a) The Vg1-related protein Gdf3 acts in a Nodal signaling pathway in the pre-gastrulation mouse embryo. *Development,* 133, 319-29.

CHEN, H. F., KUO, H. C., CHIEN, C. L., SHUN, C. T., YAO, Y. L., IP, P. L., CHUANG, C. Y., WANG, C. C., YANG, Y. S. & HO, H. N. (2007) Derivation, characterization and differentiation of human embryonic stem cells: comparing serum-containing versus serum-free media and evidence of germ cell differentiation. *Hum Reprod,* 22, 567-77.

CHEN, Y., LI, X., ESWARAKUMAR, V. P., SEGER, R. & LONAI, P. (2000) Fibroblast growth factor (FGF) signaling through PI 3-kinase and Akt/PKB is required for embryoid body differentiation. *Oncogene,* 19, 3750-6.

CHEN, Y. G., LUI, H. M., LIN, S. L., LEE, J. M. & YING, S. Y. (2002) Regulation of cell proliferation, apoptosis, and carcinogenesis by activin. *Exp Biol Med (Maywood),* 227, 75-87.

CHEN, Y. G., WANG, Q., LIN, S. L., CHANG, C. D., CHUANG, J. & YING, S. Y. (2006b) Activin signaling and its role in regulation of cell proliferation, apoptosis, and carcinogenesis. *Exp Biol Med (Maywood),* 231, 534-44.

CHENG, A. M., SAXTON, T. M., SAKAI, R., KULKARNI, S., MBAMALU, G., VOGEL, W., TORTORICE, C. G., CARDIFF, R. D., CROSS, J. C., MULLER, W. J. & PAWSON, T. (1998) Mammalian Grb2 regulates multiple steps in embryonic development and malignant transformation. *Cell,* 95, 793-803.

CHENG, L., HAMMOND, H., YE, Z., ZHAN, X. & DRAVID, G. (2003) Human adult marrow cells support prolonged expansion of human embryonic stem cells in culture. *Stem Cells,* 21, 131-42.

CHOO, A. B., PADMANABHAN, J., CHIN, A. C. & OH, S. K. (2004) Expansion of pluripotent human embryonic stem cells on human feeders. *Biotechnol Bioeng,* 88, 321-31.

CIAU-UITZ, A., WALMSLEY, M. & PATIENT, R. (2000) Distinct origins of adult and embryonic blood in Xenopus. *Cell,* 102, 787-96.

CIBELLI, J. B., GRANT, K. A., CHAPMAN, K. B., CUNNIFF, K., WORST, T., GREEN, H. L., WALKER, S. J., GUTIN, P. H., VILNER, L., TABAR, V., DOMINKO, T., KANE, J., WETTSTEIN, P. J., LANZA, R. P., STUDER, L., VRANA, K. E. & WEST, M. D. (2002) Parthenogenetic stem cells in nonhuman primates. *Science,* 295, 819.

CIRUNA, B. & ROSSANT, J. (2001) FGF signaling regulates mesoderm cell fate specification and morphogenetic movement at the primitive streak. *Dev Cell,* 1, 37-49.

CIRUNA, B. G. & ROSSANT, J. (1999) Expression of the T-box gene Eomesodermin during early mouse development. *Mech Dev,* 81, 199-203.

CLARK, A. T., BODNAR, M. S., FOX, M., RODRIQUEZ, R. T., ABEYTA, M. J., FIRPO, M. T. & PERA, R. A. (2004) Spontaneous differentiation of germ cells from human embryonic stem cells in vitro. *Hum Mol Genet,* 13, 727-39.

CLEMENTS, D., FRIDAY, R. V. & WOODLAND, H. R. (1999) Mode of action of VegT in mesoderm and endoderm formation. *Development,* 126, 4903-11.

COBO, F., STACEY, G. N., HUNT, C., CABRERA, C., NIETO, A., MONTES, R., CORTES, J. L., CATALINA, P., BARNIE, A. & CONCHA, A. (2005) Microbiological control in stem cell banks: approaches to standardisation. *Appl Microbiol Biotechnol,* 68, 456-66.

COLLIGNON, J., SOCKANATHAN, S., HACKER, A., COHEN-TANNOUDJI, M., NORRIS, D., RASTAN, S., STEVANOVIC, M., GOODFELLOW, P. N. & LOVELL-BADGE, R. (1996) A comparison of the properties of Sox-3 with Sry and two related genes, Sox-1 and Sox-2. *Development,* 122, 509-20.

CONLEY, B. J., ELLIS, S., GULLUYAN, L. & MOLLARD, R. (2007) BMPs regulate differentiation of a putative visceral endoderm layer within human embryonic stem-cell-derived embryoid bodies. *Biochem Cell Biol,* 85, 121-32.

CONLEY, B. J., TROUNSON, A. O. & MOLLARD, R. (2004a) Human embryonic stem cells form embryoid bodies containing visceral endoderm-like derivatives. *Fetal Diagn Ther,* 19, 218-23.

CONLEY, B. J., YOUNG, J. C., TROUNSON, A. O. & MOLLARD, R. (2004b) Derivation, propagation and differentiation of human embryonic stem cells. *Int J Biochem Cell Biol,* 36, 555-67.

CONLON, F. L., LYONS, K. M., TAKAESU, N., BARTH, K. S., KISPERT, A., HERRMANN, B. & ROBERTSON, E. J. (1994) A primary requirement for nodal in the formation and maintenance of the primitive streak in the mouse. *Development,* 120, 1919-28.

COUCOUVANIS, E. & MARTIN, G. R. (1995) Signals for death and survival: a two-step mechanism for cavitation in the vertebrate embryo. *Cell,* 83, 279-87.

COUCOUVANIS, E. & MARTIN, G. R. (1999) BMP signaling plays a role in visceral endoderm differentiation and cavitation in the early mouse embryo. *Development,* 126, 535-46.

COWAN, C. A., KLIMANSKAYA, I., MCMAHON, J., ATIENZA, J., WITMYER, J., ZUCKER, J. P., WANG, S., MORTON, C. C., MCMAHON, A. P.,

POWERS, D. & MELTON, D. A. (2004) Derivation of embryonic stem-cell lines from human blastocysts. *N Engl J Med,* 350, 1353-6.

CROSSLEY, P. H. & MARTIN, G. R. (1995) The mouse Fgf8 gene encodes a family of polypeptides and is expressed in regions that direct outgrowth and patterning in the developing embryo. *Development,* 121, 439-51.

CUI, L., JOHKURA, K., TAKEI, S., OGIWARA, N. & SASAKI, K. (2007) Structural differentiation, proliferation, and association of human embryonic stem cell-derived cardiomyocytes in vitro and in their extracardiac tissues. *J Struct Biol,* 158, 307-17.

D'AMOUR, K. A., AGULNICK, A. D., ELIAZER, S., KELLY, O. G., KROON, E. & BAETGE, E. E. (2005) Efficient differentiation of human embryonic stem cells to definitive endoderm. *Nat Biotechnol,* 23, 1534-41.

DAHERON, L., OPITZ, S. L., ZAEHRES, H., LENSCH, W. M., ANDREWS, P. W., ITSKOVITZ-ELDOR, J. & DALEY, G. Q. (2004) LIF/STAT3 signaling fails to maintain self-renewal of human embryonic stem cells. *Stem Cells,* 22, 770-8.

DALE, L., HOWES, G., PRICE, B. M. & SMITH, J. C. (1992) Bone morphogenetic protein 4: a ventralizing factor in early Xenopus development. *Development,* 115, 573-85.

DALEY, G. Q. (2002) Prospects for stem cell therapeutics: myths and medicines. *Curr Opin Genet Dev,* 12, 607-13.

DALEY, G. Q. (2003) From embryos to embryoid bodies: generating blood from embryonic stem cells. *Ann N Y Acad Sci,* 996, 122-31.

DALEY, G. Q., AHRLUND RICHTER, L., AUERBACH, J. M., BENVENISTY, N., CHARO, R. A., CHEN, G., DENG, H. K., GOLDSTEIN, L. S., HUDSON, K. L., HYUN, I., JUNN, S. C., LOVE, J., LEE, E. H., MCLAREN, A., MUMMERY, C. L., NAKATSUJI, N., RACOWSKY, C., ROOKE, H., ROSSANT, J., SCHOLER, H. R., SOLBAKK, J. H., TAYLOR, P., TROUNSON, A. O., WEISSMAN, I. L., WILMUT, I., YU, J. & ZOLOTH, L. (2007) Ethics. The ISSCR guidelines for human embryonic stem cell research. *Science,* 315, 603-4.

DANG, S. M., GERECHT-NIR, S., CHEN, J., ITSKOVITZ-ELDOR, J. & ZANDSTRA, P. W. (2004) Controlled, scalable embryonic stem cell differentiation culture. *Stem Cells,* 22, 275-82.

DANG, S. M., KYBA, M., PERLINGEIRO, R., DALEY, G. Q. & ZANDSTRA, P. W. (2002) Efficiency of embryoid body formation and hematopoietic development from embryonic stem cells in different culture systems. *Biotechnol Bioeng,* 78, 442-53.

DE BANK, P. A., HOU, Q., WARNER, R. M., WOOD, I. V., ALI, B. E., MACNEIL, S., KENDALL, D. A., KELLAM, B., SHAKESHEFF, K. M. & BUTTERY, L. D. (2007) Accelerated formation of multicellular 3-D structures by cell-to-cell cross-linking. *Biotechnol Bioeng,* 97, 1617-25.

DENNING, C., ALLEGRUCCI, C., PRIDDLE, H., BARBADILLO-MUNOZ, M. D., ANDERSON, D., SELF, T., SMITH, N. M., PARKIN, C. T. & YOUNG, L. E. (2006) Common culture conditions for maintenance and cardiomyocyte differentiation of the human embryonic stem cell lines, BG01 and HUES-7. *Int J Dev Biol,* 50, 27-37.

DESBAILLETS, I., ZIEGLER, U., GROSCURTH, P. & GASSMANN, M. (2000) Embryoid bodies: an in vitro model of mouse embryogenesis. *Exp Physiol,* 85, 645-51.

DOETSCHMAN, T. C., EISTETTER, H., KATZ, M., SCHMIDT, W. & KEMLER, R. (1985) The in vitro development of blastocyst-derived embryonic stem cell lines: formation of visceral yolk sac, blood islands and myocardium. *J Embryol Exp Morphol,* 87, 27-45.

DOHRMANN, C. E., HEMMATI-BRIVANLOU, A., THOMSEN, G. H., FIELDS, A., WOOLF, T. M. & MELTON, D. A. (1993) Expression of activin mRNA during early development in Xenopus laevis. *Dev Biol,* 157, 474-83.

DOWNS, K. M. & DAVIES, T. (1993) Staging of gastrulating mouse embryos by morphological landmarks in the dissecting microscope. *Development,* 118, 1255-66.

DRAPER, J. S., SMITH, K., GOKHALE, P., MOORE, H. D., MALTBY, E., JOHNSON, J., MEISNER, L., ZWAKA, T. P., THOMSON, J. A. & ANDREWS, P. W. (2004) Recurrent gain of chromosomes 17q and 12 in cultured human embryonic stem cells. *Nat Biotechnol,* 22, 53-4.

DRUKKER, M. & BENVENISTY, N. (2004) The immunogenicity of human embryonic stem-derived cells. *Trends Biotechnol,* 22, 136-41.

DUFORT, D., SCHWARTZ, L., HARPAL, K. & ROSSANT, J. (1998) The transcription factor HNF3beta is required in visceral endoderm for normal primitive streak morphogenesis. *Development,* 125, 3015-25.

DUNN, N. R., VINCENT, S. D., OXBURGH, L., ROBERTSON, E. J. & BIKOFF, E. K. (2004) Combinatorial activities of Smad2 and Smad3 regulate mesoderm formation and patterning in the mouse embryo. *Development,* 131, 1717-28.

DUSH, M. K. & MARTIN, G. R. (1992) Analysis of mouse Evx genes: Evx-1 displays graded expression in the primitive streak. *Dev Biol,* 151, 273-87.

DVASH, T., BEN-YOSEF, D. & EIGES, R. (2006) Human embryonic stem cells as a powerful tool for studying human embryogenesis. *Pediatr Res,* 60, 111-7.

DVASH, T. & BENVENISTY, N. (2004) Human embryonic stem cells as a model for early human development. *Best Pract Res Clin Obstet Gynaecol,* 18, 929-40.

DVASH, T., MAYSHAR, Y., DARR, H., MCELHANEY, M., BARKER, D., YANUKA, O., KOTKOW, K. J., RUBIN, L. L., BENVENISTY, N. & EIGES, R. (2004) Temporal gene expression during differentiation of human embryonic stem cells and embryoid bodies. *Hum Reprod,* 19, 2875-83.

DVASH, T., SHARON, N., YANUKA, O. & BENVENISTY, N. (2007) Molecular analysis of LEFTY-expressing cells in early human embryoid bodies. *Stem Cells,* 25, 465-72.

DVORAK, P. & HAMPL, A. (2005) Basic fibroblast growth factor and its receptors in human embryonic stem cells. *Folia Histochem Cytobiol,* 43, 203-8.

EAKIN, G. S. & BEHRINGER, R. R. (2004) Diversity of germ layer and axis formation among mammals. *Semin Cell Dev Biol,* 15, 619-29.

EBNER, R., CHEN, R. H., LAWLER, S., ZIONCHECK, T. & DERYNCK, R. (1993) Determination of type I receptor specificity by the type II receptors for TGF-beta or activin. *Science,* 262, 900-2.

EDWARDS, Y. H., PUTT, W., LEKOAPE, K. M., STOTT, D., FOX, M., HOPKINSON, D. A. & SOWDEN, J. (1996) The human homolog T of the mouse T(Brachyury) gene; gene structure, cDNA sequence, and assignment to chromosome 6q27. *Genome Res,* 6, 226-33.

EIGES, R., SCHULDINER, M., DRUKKER, M., YANUKA, O., ITSKOVITZ-ELDOR, J. & BENVENISTY, N. (2001) Establishment of human embryonic

stem cell-transfected clones carrying a marker for undifferentiated cells. *Curr Biol,* 11, 514-8.

ENVER, T., SONEJI, S., JOSHI, C., BROWN, J., IBORRA, F., ORNTOFT, T., THYKJAER, T., MALTBY, E., SMITH, K., DAWUD, R. A., JONES, M., MATIN, M., GOKHALE, P., DRAPER, J. & ANDREWS, P. W. (2005) Cellular differentiation hierarchies in normal and culture-adapted human embryonic stem cells. *Hum Mol Genet,* 14, 3129-40.

EVANS, M. J. & KAUFMAN, M. H. (1981) Establishment in culture of pluripotential cells from mouse embryos. *Nature,* 292, 154-6.

FANG, D., LEISHEAR, K., NGUYEN, T. K., FINKO, R., CAI, K., FUKUNAGA, M., LI, L., BRAFFORD, P. A., KULP, A. N., XU, X., SMALLEY, K. S. & HERLYN, M. (2006) Defining the conditions for the generation of melanocytes from human embryonic stem cells. *Stem Cells,* 24, 1668-77.

FELDMAN, B., POUEYMIROU, W., PAPAIOANNOU, V. E., DECHIARA, T. M. & GOLDFARB, M. (1995) Requirement of FGF-4 for postimplantation mouse development. *Science,* 267, 246-9.

FIERING, S., WHITELAW, E. & MARTIN, D. I. (2000) To be or not to be active: the stochastic nature of enhancer action. *Bioessays,* 22, 381-7.

FILOSA, S., RIVERA-PEREZ, J. A., GOMEZ, A. P., GANSMULLER, A., SASAKI, H., BEHRINGER, R. R. & ANG, S. L. (1997) Goosecoid and HNF-3beta genetically interact to regulate neural tube patterning during mouse embryogenesis. *Development,* 124, 2843-54.

FRIEL, R., VAN DER SAR, S. & MEE, P. J. (2005) Embryonic stem cells: understanding their history, cell biology and signalling. *Adv Drug Deliv Rev,* 57, 1894-903.

FUJIKURA, J., YAMATO, E., YONEMURA, S., HOSODA, K., MASUI, S., NAKAO, K., MIYAZAKI JI, J. & NIWA, H. (2002) Differentiation of embryonic stem cells is induced by GATA factors. *Genes Dev,* 16, 784-9.

FUNDEL, K. & ZIMMER, R. (2006) Gene and protein nomenclature in public databases. *BMC Bioinformatics,* 7, 372.

GALIC, Z., KITCHEN, S. G., KACENA, A., SUBRAMANIAN, A., BURKE, B., CORTADO, R. & ZACK, J. A. (2006) T lineage differentiation from human embryonic stem cells. *Proc Natl Acad Sci U S A,* 103, 11742-7.

GAUNT, S. J., BLUM, M. & DE ROBERTIS, E. M. (1993) Expression of the mouse goosecoid gene during mid-embryogenesis may mark mesenchymal cell lineages in the developing head, limbs and body wall. *Development,* 117, 769-78.

GEARING, D. P., GOUGH, N. M., KING, J. A., HILTON, D. J., NICOLA, N. A., SIMPSON, R. J., NICE, E. C., KELSO, A. & METCALF, D. (1987) Molecular cloning and expression of cDNA encoding a murine myeloid leukaemia inhibitory factor (LIF). *Embo J,* 6, 3995-4002.

GENBACEV, O., KRTOLICA, A., ZDRAVKOVIC, T., BRUNETTE, E., POWELL, S., NATH, A., CACERES, E., MCMASTER, M., MCDONAGH, S., LI, Y., MANDALAM, R., LEBKOWSKI, J. & FISHER, S. J. (2005) Serum-free derivation of human embryonic stem cell lines on human placental fibroblast feeders. *Fertil Steril,* 83, 1517-29.

GERAMI-NAINI, B., DOVZHENKO, O. V., DURNING, M., WEGNER, F. H., THOMSON, J. A. & GOLOS, T. G. (2004) Trophoblast differentiation in embryoid bodies derived from human embryonic stem cells. *Endocrinology,* 145, 1517-24.

GERECHT-NIR, S., COHEN, S. & ITSKOVITZ-ELDOR, J. (2004a) Bioreactor cultivation enhances the efficiency of human embryoid body (hEB) formation and differentiation. *Biotechnol Bioeng,* 86, 493-502.

GERECHT-NIR, S., COHEN, S., ZISKIND, A. & ITSKOVITZ-ELDOR, J. (2004b) Three-dimensional porous alginate scaffolds provide a conducive environment for generation of well-vascularized embryoid bodies from human embryonic stem cells. *Biotechnol Bioeng,* 88, 313-20.

GERECHT-NIR, S., DAZARD, J. E., GOLAN-MASHIACH, M., OSENBERG, S., BOTVINNIK, A., AMARIGLIO, N., DOMANY, E., RECHAVI, G., GIVOL, D. & ITSKOVITZ-ELDOR, J. (2005) Vascular gene expression and phenotypic correlation during differentiation of human embryonic stem cells. *Dev Dyn,* 232, 487-97.

GERECHT-NIR, S., OSENBERG, S., NEVO, O., ZISKIND, A., COLEMAN, R. & ITSKOVITZ-ELDOR, J. (2004c) Vascular development in early human embryos and in teratomas derived from human embryonic stem cells. *Biol Reprod,* 71, 2029-36.

GERECHT-NIR, S., ZISKIND, A., COHEN, S. & ITSKOVITZ-ELDOR, J. (2003) Human embryonic stem cells as an in vitro model for human vascular development and the induction of vascular differentiation. *Lab Invest,* 83, 1811-20.

GERING, M., RODAWAY, A. R., GOTTGENS, B., PATIENT, R. K. & GREEN, A. R. (1998) The SCL gene specifies haemangioblast development from early mesoderm. *Embo J,* 17, 4029-45.

GERING, M., YAMADA, Y., RABBITTS, T. H. & PATIENT, R. K. (2003) Lmo2 and Scl/Tal1 convert non-axial mesoderm into haemangioblasts which differentiate into endothelial cells in the absence of Gata1. *Development,* 130, 6187-99.

GERRARD, L., RODGERS, L. & CUI, W. (2005) Differentiation of human embryonic stem cells to neural lineages in adherent culture by blocking bone morphogenetic protein signaling. *Stem Cells,* 23, 1234-41.

GINIS, I., LUO, Y., MIURA, T., THIES, S., BRANDENBERGER, R., GERECHT-NIR, S., AMIT, M., HOKE, A., CARPENTER, M. K., ITSKOVITZ-ELDOR, J. & RAO, M. S. (2004) Differences between human and mouse embryonic stem cells. *Dev Biol,* 269, 360-80.

GLINKA, A., WU, W., DELIUS, H., MONAGHAN, A. P., BLUMENSTOCK, C. & NIEHRS, C. (1998) Dickkopf-1 is a member of a new family of secreted proteins and functions in head induction. *Nature,* 391, 357-62.

GOH, G., SELF, T., BARBADILLO MUNOZ, M. D., HALL, I. P., YOUNG, L. & DENNING, C. (2005) Molecular and phenotypic analyses of human embryonic stem cell-derived cardiomyocytes: opportunities and challenges for clinical translation. *Thromb Haemost,* 94, 728-37.

GOKHALE, P. J. & ANDREWS, P. W. (2008) New insights into the control of stem cell pluripotency. *Cell Stem Cell,* 2, 4-5.

GOLAN-MASHIACH, M., DAZARD, J. E., GERECHT-NIR, S., AMARIGLIO, N., FISHER, T., JACOB-HIRSCH, J., BIELORAI, B., OSENBERG, S., BARAD, O., GETZ, G., TOREN, A., RECHAVI, G., ITSKOVITZ-ELDOR, J., DOMANY, E. & GIVOL, D. (2005) Design principle of gene expression used by human stem cells: implication for pluripotency. *Faseb J,* 19, 147-9.

GOLDIN, S. N. & PAPAIOANNOU, V. E. (2003) Paracrine action of FGF4 during periimplantation development maintains trophectoderm and primitive endoderm. *Genesis,* 36, 40-7.

GRABEL, L. B. & CASANOVA, J. E. (1986) The outgrowth of parietal endoderm from mouse teratocarcinoma stem-cell embryoid bodies. *Differentiation,* 32, 67-73.

GREBER, B., LEHRACH, H. & ADJAYE, J. (2007) Fibroblast growth factor 2 modulates transforming growth factor beta signaling in mouse embryonic fibroblasts and human ESCs (hESCs) to support hESC self-renewal. *Stem Cells,* 25, 455-64.

GREEN, H., EASLEY, K. & IUCHI, S. (2003) Marker succession during the development of keratinocytes from cultured human embryonic stem cells. *Proc Natl Acad Sci U S A,* 100, 15625-30.

GRITSMAN, K., ZHANG, J., CHENG, S., HECKSCHER, E., TALBOT, W. S. & SCHIER, A. F. (1999) The EGF-CFC protein one-eyed pinhead is essential for nodal signaling. *Cell,* 97, 121-32.

GROPP, M., ITSYKSON, P., SINGER, O., BEN-HUR, T., REINHARTZ, E., GALUN, E. & REUBINOFF, B. E. (2003) Stable genetic modification of human embryonic stem cells by lentiviral vectors. *Mol Ther,* 7, 281-7.

GU, Z., NOMURA, M., SIMPSON, B. B., LEI, H., FEIJEN, A., VAN DEN EIJNDEN-VAN RAAIJ, J., DONAHOE, P. K. & LI, E. (1998) The type I activin receptor ActRIB is required for egg cylinder organization and gastrulation in the mouse. *Genes Dev,* 12, 844-57.

GUO, W., CHAN, A. P., LIANG, H., WIEDER, E. D., MOLLDREM, J. J., ETKIN, L. D. & NAGARAJAN, L. (2002) A human Mix-like homeobox gene MIXL shows functional similarity to Xenopus Mix.1. *Blood,* 100, 89-95.

GUZMAN-AYALA, M., BEN-HAIM, N., BECK, S. & CONSTAM, D. B. (2004) Nodal protein processing and fibroblast growth factor 4 synergize to maintain a trophoblast stem cell microenvironment. *Proc Natl Acad Sci U S A,* 101, 15656-60.

HADARI, Y. R., GOTOH, N., KOUHARA, H., LAX, I. & SCHLESSINGER, J. (2001) Critical role for the docking-protein FRS2 alpha in FGF receptor-mediated signal transduction pathways. *Proc Natl Acad Sci U S A,* 98, 8578-83.

HAMAZAKI, T., OKA, M., YAMANAKA, S. & TERADA, N. (2004) Aggregation of embryonic stem cells induces Nanog repression and primitive endoderm differentiation. *J Cell Sci,* 117, 5681-6.

HANCOCK, S. N., AGULNIK, S. I., SILVER, L. M. & PAPAIOANNOU, V. E. (1999) Mapping and expression analysis of the mouse ortholog of Xenopus Eomesodermin. *Mech Dev,* 81, 205-8.

HARLAND, R. & MISHER, L. (1988) Stability of RNA in developing Xenopus embryos and identification of a destabilizing sequence in TFIIIA messenger RNA. *Development,* 102, 837-52.

HARLAND, R. M. (1991) In situ hybridization: an improved whole-mount method for Xenopus embryos. *Methods Cell Biol,* 36, 685-95.

HART, A. H., HARTLEY, L., IBRAHIM, M. & ROBB, L. (2004) Identification, cloning and expression analysis of the pluripotency promoting Nanog genes in mouse and human. *Dev Dyn,* 230, 187-98.

HART, A. H., HARTLEY, L., SOURRIS, K., STADLER, E. S., LI, R., STANLEY, E. G., TAM, P. P., ELEFANTY, A. G. & ROBB, L. (2002) Mixl1 is required

for axial mesendoderm morphogenesis and patterning in the murine embryo. *Development,* 129, 3597-608.

HART, A. H., WILLSON, T. A., WONG, M., PARKER, K. & ROBB, L. (2005) Transcriptional regulation of the homeobox gene Mixl1 by TGF-beta and FoxH1. *Biochem Biophys Res Commun,* 333, 1361-9.

HAUB, O. & GOLDFARB, M. (1991) Expression of the fibroblast growth factor-5 gene in the mouse embryo. *Development,* 112, 397-406.

HAY, D. C., SUTHERLAND, L., CLARK, J. & BURDON, T. (2004) Oct-4 knockdown induces similar patterns of endoderm and trophoblast differentiation markers in human and mouse embryonic stem cells. *Stem Cells,* 22, 225-35.

HE, J. Q., MA, Y., LEE, Y., THOMSON, J. A. & KAMP, T. J. (2003) Human embryonic stem cells develop into multiple types of cardiac myocytes: action potential characterization. *Circ Res,* 93, 32-9.

HEASMAN, J. (2006) Patterning the early Xenopus embryo. *Development,* 133, 1205-17.

HEASMAN, J., WYLIE, C. C., HAUSEN, P. & SMITH, J. C. (1984) Fates and states of determination of single vegetal pole blastomeres of X. laevis. *Cell,* 37, 185-94.

HEINS, N., ENGLUND, M. C., SJOBLOM, C., DAHL, U., TONNING, A., BERGH, C., LINDAHL, A., HANSON, C. & SEMB, H. (2004) Derivation, characterization, and differentiation of human embryonic stem cells. *Stem Cells,* 22, 367-76.

HENDERSON, J. K., DRAPER, J. S., BAILLIE, H. S., FISHEL, S., THOMSON, J. A., MOORE, H. & ANDREWS, P. W. (2002) Preimplantation human embryos and embryonic stem cells show comparable expression of stage-specific embryonic antigens. *Stem Cells,* 20, 329-37.

HENG, B. C., HAIDER, H., SIM, E. K., CAO, T. & NG, S. C. (2004) Strategies for directing the differentiation of stem cells into the cardiomyogenic lineage in vitro. *Cardiovasc Res,* 62, 34-42.

HERR, W. & CLEARY, M. A. (1995) The POU domain: versatility in transcriptional regulation by a flexible two-in-one DNA-binding domain. *Genes Dev,* 9, 1679-93.

HERRMANN, B. G., LABEIT, S., POUSTKA, A., KING, T. R. & LEHRACH, H. (1990) Cloning of the T gene required in mesoderm formation in the mouse. *Nature,* 343, 617-22.

HIRST, C. E., NG, E. S., AZZOLA, L., VOSS, A. K., THOMAS, T., STANLEY, E. G. & ELEFANTY, A. G. (2006) Transcriptional profiling of mouse and human ES cells identifies SLAIN1, a novel stem cell gene. *Dev Biol,* 293, 90-103.

HOFFMAN, L. M., HALL, L., BATTEN, J. L., YOUNG, H., PARDASANI, D., BAETGE, E. E., LAWRENCE, J. & CARPENTER, M. K. (2005) X-inactivation status varies in human embryonic stem cell lines. *Stem Cells,* 23, 1468-78.

HONG-MEI, P. & GUI-AN, C. (2006) Serum-free medium cultivation to improve efficacy in establishment of human embryonic stem cell lines. *Hum Reprod,* 21, 217-22.

HOODLESS, P. A., PYE, M., CHAZAUD, C., LABBE, E., ATTISANO, L., ROSSANT, J. & WRANA, J. L. (2001) FoxH1 (Fast) functions to specify the anterior primitive streak in the mouse. *Genes Dev,* 15, 1257-71.

HOVATTA, O., MIKKOLA, M., GERTOW, K., STROMBERG, A. M., INZUNZA, J., HREINSSON, J., ROZELL, B., BLENNOW, E., ANDANG, M. & AHRLUND-RICHTER, L. (2003) A culture system using human foreskin fibroblasts as feeder cells allows production of human embryonic stem cells. *Hum Reprod*, 18, 1404-9.

HUANG, H., ZHAO, X., CHEN, L., XU, C., YAO, X., LU, Y., DAI, L. & ZHANG, M. (2006) Differentiation of human embryonic stem cells into smooth muscle cells in adherent monolayer culture. *Biochem Biophys Res Commun*, 351, 321-7.

HUBER, I., ITZHAKI, I., CASPI, O., ARBEL, G., TZUKERMAN, M., GEPSTEIN, A., HABIB, M., YANKELSON, L., KEHAT, I. & GEPSTEIN, L. (2007) Identification and selection of cardiomyocytes during human embryonic stem cell differentiation. *Faseb J*, 21, 2551-63.

HUBER, T. L., ZHOU, Y., MEAD, P. E. & ZON, L. I. (1998) Cooperative effects of growth factors involved in the induction of hematopoietic mesoderm. *Blood*, 92, 4128-37.

HUELSKEN, J., VOGEL, R., BRINKMANN, V., ERDMANN, B., BIRCHMEIER, C. & BIRCHMEIER, W. (2000) Requirement for beta-catenin in anterior-posterior axis formation in mice. *J Cell Biol*, 148, 567-78.

HUMPHREY, R. K., BEATTIE, G. M., LOPEZ, A. D., BUCAY, N., KING, C. C., FIRPO, M. T., ROSE-JOHN, S. & HAYEK, A. (2004) Maintenance of pluripotency in human embryonic stem cells is STAT3 independent. *Stem Cells*, 22, 522-30.

HYSLOP, L., STOJKOVIC, M., ARMSTRONG, L., WALTER, T., STOJKOVIC, P., PRZYBORSKI, S., HERBERT, M., MURDOCH, A., STRACHAN, T. & LAKO, M. (2005a) Downregulation of NANOG induces differentiation of human embryonic stem cells to extraembryonic lineages. *Stem Cells*, 23, 1035-43.

HYSLOP, L. A., ARMSTRONG, L., STOJKOVIC, M. & LAKO, M. (2005b) Human embryonic stem cells: biology and clinical implications. *Expert Rev Mol Med*, 7, 1-21.

IKEDA, W., NAKANISHI, H., MIYOSHI, J., MANDAI, K., ISHIZAKI, H., TANAKA, M., TOGAWA, A., TAKAHASHI, K., NISHIOKA, H., YOSHIDA, H., MIZOGUCHI, A., NISHIKAWA, S. & TAKAI, Y. (1999) Afadin: A key molecule essential for structural organization of cell-cell junctions of polarized epithelia during embryogenesis. *J Cell Biol*, 146, 1117-32.

ILLMENSEE, K. & MINTZ, B. (1976) Totipotency and normal differentiation of single teratocarcinoma cells cloned by injection into blastocysts. *Proc Natl Acad Sci U S A*, 73, 549-53.

IMREH, M. P., GERTOW, K., CEDERVALL, J., UNGER, C., HOLMBERG, K., SZOKE, K., CSOREGH, L., FRIED, G., DILBER, S., BLENNOW, E. & AHRLUND-RICHTER, L. (2006) In vitro culture conditions favoring selection of chromosomal abnormalities in human ES cells. *J Cell Biochem*, 99, 508-16.

INMAN, K. E. & DOWNS, K. M. (2006) Localization of Brachyury (T) in embryonic and extraembryonic tissues during mouse gastrulation. *Gene Expr Patterns*, 6, 783-93.

INZUNZA, J., GERTOW, K., STROMBERG, M. A., MATILAINEN, E., BLENNOW, E., SKOTTMAN, H., WOLBANK, S., AHRLUND-RICHTER,

L. & HOVATTA, O. (2005) Derivation of human embryonic stem cell lines in serum replacement medium using postnatal human fibroblasts as feeder cells. *Stem Cells,* 23, 544-9.

INZUNZA, J., SAHLEN, S., HOLMBERG, K., STROMBERG, A. M., TEERIJOKI. H., BLENNOW, E., HOVATTA, O. & MALMGREN, H. (2004) Comparative genomic hybridization and karyotyping of human embryonic stem cells reveals the occurrence of an isodicentric X chromosome after long-term cultivation. *Mol Hum Reprod,* 10, 461-6.

ISAACS, H. V., POWNALL, M. E. & SLACK, J. M. (1994) eFGF regulates Xbra expression during Xenopus gastrulation. *Embo J,* 13, 4469-81.

ISAACS, H. V., TANNAHILL, D. & SLACK, J. M. (1992) Expression of a novel FGF in the Xenopus embryo. A new candidate inducing factor for mesoderm formation and anteroposterior specification. *Development,* 114, 711-20.

ITSKOVITZ-ELDOR, J., SCHULDINER, M., KARSENTI, D., EDEN, A., YANUKA, O., AMIT, M., SOREQ, H. & BENVENISTY, N. (2000) Differentiation of human embryonic stem cells into embryoid bodies compromising the three embryonic germ layers. *Mol Med,* 6, 88-95.

IVANOVA, N. B., DIMOS, J. T., SCHANIEL, C., HACKNEY, J. A., MOORE, K. A. & LEMISCHKA, I. R. (2002) A stem cell molecular signature. *Science,* 298, 601-4.

JAMES, D., LEVINE, A. J., BESSER, D. & HEMMATI-BRIVANLOU, A. (2005) TGFbeta/activin/nodal signaling is necessary for the maintenance of pluripotency in human embryonic stem cells. *Development,* 132, 1273-82.

JIANG, W., SHI, Y., ZHAO, D., CHEN, S., YONG, J., ZHANG, J., QING, T., SUN, X., ZHANG, P., DING, M., LI, D. & DENG, H. (2007) In vitro derivation of functional insulin-producing cells from human embryonic stem cells. *Cell Res,* 17, 333-44.

JOANNIDES, A., FIORE-HERICHE, C., WESTMORE, K., CALDWELL, M., COMPSTON, A., ALLEN, N. & CHANDRAN, S. (2006) Automated mechanical passaging: a novel and efficient method for human embryonic stem cell expansion. *Stem Cells,* 24, 230-5.

JOANNIDES, A. J., FIORE-HERICHE, C., BATTERSBY, A. A., ATHAUDA-ARACHCHI, P., BOUHON, I. A., WILLIAMS, L., WESTMORE, K., KEMP, P. J., COMPSTON, A., ALLEN, N. D. & CHANDRAN, S. (2007) A scaleable and defined system for generating neural stem cells from human embryonic stem cells. *Stem Cells,* 25, 731-7.

JOHANSSON, B. M. & WILES, M. V. (1995) Evidence for involvement of activin A and bone morphogenetic protein 4 in mammalian mesoderm and hematopoietic development. *Mol Cell Biol,* 15, 141-51.

JOHNSON, B. V., RATHJEN, J. & RATHJEN, P. D. (2006) Transcriptional control of pluripotency: decisions in early development. *Curr Opin Genet Dev,* 16, 447-54.

JOHNSON, M. A., WEICK, J. P., PEARCE, R. A. & ZHANG, S. C. (2007) Functional neural development from human embryonic stem cells: accelerated synaptic activity via astrocyte coculture. *J Neurosci,* 27, 3069-77.

JONES, C. M., DALE, L., HOGAN, B. L., WRIGHT, C. V. & SMITH, J. C. (1996) Bone morphogenetic protein-4 (BMP-4) acts during gastrula stages to cause ventralization of Xenopus embryos. *Development,* 122, 1545-54.

JONES, C. M., LYONS, K. M., LAPAN, P. M., WRIGHT, C. V. & HOGAN, B. L. (1992) DVR-4 (bone morphogenetic protein-4) as a posterior-ventralizing factor in Xenopus mesoderm induction. *Development,* 115, 639-47.

JURATA, L. W., KENNY, D. A. & GILL, G. N. (1996) Nuclear LIM interactor, a rhombotin and LIM homeodomain interacting protein, is expressed early in neuronal development. *Proc Natl Acad Sci U S A,* 93, 11693-8.

KAMACHI, Y., UCHIKAWA, M. & KONDOH, H. (2000) Pairing SOX off: with partners in the regulation of embryonic development. *Trends Genet,* 16, 182-7.

KANAI-AZUMA, M., KANAI, Y., GAD, J. M., TAJIMA, Y., TAYA, C., KUROHMARU, M., SANAI, Y., YONEKAWA, H., YAZAKI, K., TAM, P. P. & HAYASHI, Y. (2002) Depletion of definitive gut endoderm in Sox17-null mutant mice. *Development,* 129, 2367-79.

KANAI, Y., KANAI-AZUMA, M., NOCE, T., SAIDO, T. C., SHIROISHI, T., HAYASHI, Y. & YAZAKI, K. (1996) Identification of two Sox17 messenger RNA isoforms, with and without the high mobility group box region, and their differential expression in mouse spermatogenesis. *J Cell Biol,* 133, 667-81.

KANG, H. B., KIM, J. S., KWON, H. J., NAM, K. H., YOUN, H. S., SOK, D. E. & LEE, Y. (2005) Basic fibroblast growth factor activates ERK and induces c-fos in human embryonic stem cell line MizhES1. *Stem Cells Dev,* 14, 395-401.

KARP, J. M., FERREIRA, L. S., KHADEMHOSSEINI, A., KWON, A. H., YEH, J. & LANGER, R. S. (2006) Cultivation of human embryonic stem cells without the embryoid body step enhances osteogenesis in vitro. *Stem Cells,* 24, 835-43.

KAU, C. L. & TURPEN, J. B. (1983) Dual contribution of embryonic ventral blood island and dorsal lateral plate mesoderm during ontogeny of hemopoietic cells in Xenopus laevis. *J Immunol,* 131, 2262-6.

KAUFMAN, D. S., HANSON, E. T., LEWIS, R. L., AUERBACH, R. & THOMSON, J. A. (2001) Hematopoietic colony-forming cells derived from human embryonic stem cells. *Proc Natl Acad Sci U S A,* 98, 10716-21.

KEHAT, I., GEPSTEIN, A., SPIRA, A., ITSKOVITZ-ELDOR, J. & GEPSTEIN, L. (2002) High-resolution electrophysiological assessment of human embryonic stem cell-derived cardiomyocytes: a novel in vitro model for the study of conduction. *Circ Res,* 91, 659-61.

KEHAT, I., KENYAGIN-KARSENTI, D., SNIR, M., SEGEV, H., AMIT, M., GEPSTEIN, A., LIVNE, E., BINAH, O., ITSKOVITZ-ELDOR, J. & GEPSTEIN, L. (2001) Human embryonic stem cells can differentiate into myocytes with structural and functional properties of cardiomyocytes. *J Clin Invest,* 108, 407-14.

KEHAT, I., KHIMOVICH, L., CASPI, O., GEPSTEIN, A., SHOFTI, R., ARBEL, G., HUBER, I., SATIN, J., ITSKOVITZ-ELDOR, J. & GEPSTEIN, L. (2004) Electromechanical integration of cardiomyocytes derived from human embryonic stem cells. *Nat Biotechnol,* 22, 1282-9.

KEHLER, J., TOLKUNOVA, E., KOSCHORZ, B., PESCE, M., GENTILE, L., BOIANI, M., LOMELI, H., NAGY, A., MCLAUGHLIN, K. J., SCHOLER, H. R. & TOMILIN, A. (2004) Oct4 is required for primordial germ cell survival. *EMBO Rep,* 5, 1078-83.

KELLER, G., KENNEDY, M., PAPAYANNOPOULOU, T. & WILES, M. V. (1993) Hematopoietic commitment during embryonic stem cell differentiation in culture. *Mol Cell Biol,* 13, 473-86.

KELLER, G. M. (1995) In vitro differentiation of embryonic stem cells. *Curr Opin Cell Biol,* 7, 862-9.

KELLER, R. (2005) Cell migration during gastrulation. *Curr Opin Cell Biol,* 17, 533-41.

KELLEY, C., YEE, K., HARLAND, R. & ZON, L. I. (1994) Ventral expression of GATA-1 and GATA-2 in the Xenopus embryo defines induction of hematopoietic mesoderm. *Dev Biol,* 165, 193-205.

KELLY, O. G., PINSON, K. I. & SKARNES, W. C. (2004) The Wnt co-receptors Lrp5 and Lrp6 are essential for gastrulation in mice. *Development,* 131, 2803-15.

KEMP, C., WILLEMS, E., ABDO, S., LAMBIV, L. & LEYNS, L. (2005) Expression of all Wnt genes and their secreted antagonists during mouse blastocyst and postimplantation development. *Dev Dyn,* 233, 1064-75.

KENNEDY, M., D'SOUZA, S. L., LYNCH-KATTMAN, M., SCHWANTZ, S. & KELLER, G. (2007) Development of the hemangioblast defines the onset of hematopoiesis in human ES cell differentiation cultures. *Blood,* 109, 2679-87.

KHOO, M. L., MCQUADE, L. R., SMITH, M. S., LEES, J. G., SIDHU, K. S. & TUCH, B. E. (2005) Growth and differentiation of embryoid bodies derived from human embryonic stem cells: effect of glucose and basic fibroblast growth factor. *Biol Reprod,* 73, 1147-56.

KIM, J., AULT, K. T., CHEN, H. D., XU, R. H., ROH, D. H., LIN, M. C., PARK, M. J. & KUNG, H. F. (1998) Transcriptional regulation of BMP-4 in the Xenopus embryo: analysis of genomic BMP-4 and its promoter. *Biochem Biophys Res Commun,* 250, 516-30.

KIM, J., CHU, J., SHEN, X., WANG, J. & ORKIN, S. H. (2008) An extended transcriptional network for pluripotency of embryonic stem cells. *Cell,* 132, 1049-61.

KIM, K., NG, K., RUGG-GUNN, P. J., SHIEH, J., KIRAK, O., JAENISCH, R., WAKAYAMA, T., MOORE, M. A., PEDERSEN, R. A. & DALEY, G. Q. (2007a) Recombination Signatures Distinguish Embryonic Stem Cells Derived by Parthenogenesis and Somatic Cell Nuclear Transfer. *Cell Stem Cell,* 1, 346-352.

KIM, N. W., PIATYSZEK, M. A., PROWSE, K. R., HARLEY, C. B., WEST, M. D., HO, P. L., COVIELLO, G. M., WRIGHT, W. E., WEINRICH, S. L. & SHAY, J. W. (1994) Specific association of human telomerase activity with immortal cells and cancer. *Science,* 266, 2011-5.

KIM, S. E., KIM, B. K., GIL, J. E., KIM, S. K. & KIM, J. H. (2007b) Comparative analysis of the developmental competence of three human embryonic stem cell lines in vitro. *Mol Cells,* 23, 49-56.

KIM, S. J., KIM, B. S., RYU, S. W., YOO, J. H., OH, J. H., SONG, C. H., KIM, S. H., CHOI, D. S., SEO, J. H., CHOI, C. W., SHIN, S. W., KIM, Y. H. & KIM, J. S. (2005) Hematopoietic Differentiation of Embryoid Bodies Derived from the Human Embryonic Stem Cell Line SNUhES3 in Co-culture with Human Bone Marrow Stromal Cells. *Yonsei Med J,* 46, 693-9.

KIMELMAN, D. (2006) Mesoderm induction: from caps to chips. *Nat Rev Genet,* 7, 360-72.

KIMELMAN, D. & GRIFFIN, K. J. (2000) Vertebrate mesendoderm induction and patterning. *Curr Opin Genet Dev,* 10, 350-6.

KIMURA, C., YOSHINAGA, K., TIAN, E., SUZUKI, M., AIZAWA, S. & MATSUO, I. (2000) Visceral endoderm mediates forebrain development by suppressing posteriorizing signals. *Dev Biol,* 225, 304-21.

KIMURA, N., NAKASHIMA, K., UENO, M., KIYAMA, H. & TAGA, T. (1999) A novel mammalian T-box-containing gene, Tbr2, expressed in mouse developing brain. *Brain Res Dev Brain Res,* 115, 183-93.

KINDER, S. J., TSANG, T. E., QUINLAN, G. A., HADJANTONAKIS, A. K., NAGY, A. & TAM, P. P. (1999) The orderly allocation of mesodermal cells to the extraembryonic structures and the anteroposterior axis during gastrulation of the mouse embryo. *Development,* 126, 4691-701.

KINDER, S. J., TSANG, T. E., WAKAMIYA, M., SASAKI, H., BEHRINGER, R. R., NAGY, A. & TAM, P. P. (2001) The organizer of the mouse gastrula is composed of a dynamic population of progenitor cells for the axial mesoderm. *Development,* 128, 3623-34.

KISPERT, A. & HERRMANN, B. G. (1994) Immunohistochemical analysis of the Brachyury protein in wild-type and mutant mouse embryos. *Dev Biol,* 161, 179-93.

KLIMANSKAYA, I., CHUNG, Y., BECKER, S., LU, S. J. & LANZA, R. (2006) Human embryonic stem cell lines derived from single blastomeres. *Nature,* 444, 481-5.

KLIMANSKAYA, I., CHUNG, Y., MEISNER, L., JOHNSON, J., WEST, M. D. & LANZA, R. (2005) Human embryonic stem cells derived without feeder cells. *Lancet,* 365, 1636-41.

KLIMANSKAYA, I., HIPP, J., REZAI, K. A., WEST, M., ATALA, A. & LANZA, R. (2004) Derivation and comparative assessment of retinal pigment epithelium from human embryonic stem cells using transcriptomics. *Cloning Stem Cells,* 6, 217-45.

KOFRON, M., DEMEL, T., XANTHOS, J., LOHR, J., SUN, B., SIVE, H., OSADA, S., WRIGHT, C., WYLIE, C. & HEASMAN, J. (1999) Mesoderm induction in Xenopus is a zygotic event regulated by maternal VegT via TGFbeta growth factors. *Development,* 126, 5759-70.

KONNO, T., AKITA, K., KURITA, K. & ITO, Y. (2005) Formation of embryoid bodies by mouse embryonic stem cells on plastic surfaces. *J Biosci Bioeng,* 100, 88-93.

KUBO, A., SHINOZAKI, K., SHANNON, J. M., KOUSKOFF, V., KENNEDY, M., WOO, S., FEHLING, H. J. & KELLER, G. (2004) Development of definitive endoderm from embryonic stem cells in culture. *Development,* 131, 1651-62.

KUO, C. T., MORRISEY, E. E., ANANDAPPA, R., SIGRIST, K., LU, M. M., PARMACEK, M. S., SOUDAIS, C. & LEIDEN, J. M. (1997) GATA4 transcription factor is required for ventral morphogenesis and heart tube formation. *Genes Dev,* 11, 1048-60.

LAFLAMME, M. A., CHEN, K. Y., NAUMOVA, A. V., MUSKHELI, V., FUGATE, J. A., DUPRAS, S. K., REINECKE, H., XU, C., HASSANIPOUR, M., POLICE, S., O'SULLIVAN, C., COLLINS, L., CHEN, Y., MINAMI, E., GILL, E. A., UENO, S., YUAN, C., GOLD, J. & MURRY, C. E. (2007) Cardiomyocytes derived from human embryonic stem cells in pro-survival factors enhance function of infarcted rat hearts. *Nat Biotechnol,* 25, 1015-24.

LAKE, J., RATHJEN, J., REMISZEWSKI, J. & RATHJEN, P. D. (2000) Reversible programming of pluripotent cell differentiation. *J Cell Sci,* 113 (Pt 3), 555-66.

LAKSHMIPATHY, U., PELACHO, B., SUDO, K., LINEHAN, J. L., COUCOUVANIS, E., KAUFMAN, D. S. & VERFAILLIE, C. M. (2004) Efficient transfection of embryonic and adult stem cells. *Stem Cells,* 22, 531-43.

LAKSHMIPATHY, U. & VERFAILLIE, C. (2005) Stem cell plasticity. *Blood Rev,* 19, 29-38.

LAMBA, D. A., KARL, M. O., WARE, C. B. & REH, T. A. (2006) Efficient generation of retinal progenitor cells from human embryonic stem cells. *Proc Natl Acad Sci U S A,* 103, 12769-74.

LAMOTHE, B., YAMADA, M., SCHAEPER, U., BIRCHMEIER, W., LAX, I. & SCHLESSINGER, J. (2004) The docking protein Gab1 is an essential component of an indirect mechanism for fibroblast growth factor stimulation of the phosphatidylinositol 3-kinase/Akt antiapoptotic pathway. *Mol Cell Biol,* 24, 5657-66.

LANZENDORF, S. E., BOYD, C. A., WRIGHT, D. L., MUASHER, S., OEHNINGER, S. & HODGEN, G. D. (2001) Use of human gametes obtained from anonymous donors for the production of human embryonic stem cell lines. *Fertil Steril,* 76, 132-7.

LARUE, L., OHSUGI, M., HIRCHENHAIN, J. & KEMLER, R. (1994) E-cadherin null mutant embryos fail to form a trophectoderm epithelium. *Proc Natl Acad Sci U S A,* 91, 8263-7.

LASLETT, A. L., GRIMMOND, S., GARDINER, B., STAMP, L., LIN, A., HAWES, S. M., WORMALD, S., NIKOLIC-PATERSON, D., HAYLOCK, D. & PERA, M. F. (2007) Transcriptional analysis of early lineage commitment in human embryonic stem cells. *BMC Dev Biol,* 7, 12.

LAVON, N., YANUKA, O. & BENVENISTY, N. (2004) Differentiation and isolation of hepatic-like cells from human embryonic stem cells. *Differentiation,* 72, 230-8.

LAVON, N., YANUKA, O. & BENVENISTY, N. (2006) The effect of overexpression of Pdx1 and Foxa2 on the differentiation of human embryonic stem cells into pancreatic cells. *Stem Cells,* 24, 1923-30.

LAWSON, K. A. & PEDERSEN, R. A. (1987) Cell fate, morphogenetic movement and population kinetics of embryonic endoderm at the time of germ layer formation in the mouse. *Development,* 101, 627-52.

LAWSON, K. A. & PEDERSEN, R. A. (1992) Clonal analysis of cell fate during gastrulation and early neurulation in the mouse. *Ciba Found Symp,* 165, 3-21; discussion 21-6.

LAX, I., WONG, A., LAMOTHE, B., LEE, A., FROST, A., HAWES, J. & SCHLESSINGER, J. (2002) The docking protein FRS2alpha controls a MAP kinase-mediated negative feedback mechanism for signaling by FGF receptors. *Mol Cell,* 10, 709-19.

LEAHY, A., XIONG, J. W., KUHNERT, F. & STUHLMANN, H. (1999) Use of developmental marker genes to define temporal and spatial patterns of differentiation during embryoid body formation. *J Exp Zool,* 284, 67-81.

LEBRUN, J. J., TAKABE, K., CHEN, Y. & VALE, W. (1999) Roles of pathway-specific and inhibitory Smads in activin receptor signaling. *Mol Endocrinol,* 13, 15-23.

LECUYER, E. & HOANG, T. (2004) SCL: From the origin of hematopoiesis to stem cells and leukemia. *Exp Hematol,* 32, 11-24.

LEE, J., KIM, H. K., RHO, J. Y., HAN, Y. M. & KIM, J. (2006) The human OCT-4 isoforms differ in their ability to confer self-renewal. *J Biol Chem,* 281, 33554-65.

LEE, J. B., LEE, J. E., PARK, J. H., KIM, S. J., KIM, M. K., ROH, S. I. & YOON. H. S. (2005) Establishment and maintenance of human embryonic stem cell lines on human feeder cells derived from uterine endometrium under serum-free condition. *Biol Reprod,* 72, 42-9.

LEMAIRE, P., DARRAS, S., CAILLOL, D. & KODJABACHIAN, L. (1998) A role for the vegetally expressed Xenopus gene Mix.1 in endoderm formation and in the restriction of mesoderm to the marginal zone. *Development,* 125, 2371-80.

LEMISCHKA, I. (2001) Stem cell dogmas in the genomics era. *Rev Clin Exp Hematol,* 5, 15-25.

LEROU, P. H. & DALEY, G. Q. (2005) Therapeutic potential of embryonic stem cells. *Blood Rev,* 19, 321-331.

LEVENBERG, S., GOLUB, J. S., AMIT, M., ITSKOVITZ-ELDOR, J. & LANGER, R. (2002) Endothelial cells derived from human embryonic stem cells. *Proc Natl Acad Sci U S A,* 99, 4391-6.

LEVENBERG, S., HUANG, N. F., LAVIK, E., ROGERS, A. B., ITSKOVITZ-ELDOR, J. & LANGER, R. (2003) Differentiation of human embryonic stem cells on three-dimensional polymer scaffolds. *Proc Natl Acad Sci U S A,* 100, 12741-6.

LEVENSTEIN, M. E., LUDWIG, T. E., XU, R. H., LLANAS, R. A., VANDENHEUVEL-KRAMER, K., MANNING, D. & THOMSON, J. A. (2006) Basic fibroblast growth factor support of human embryonic stem cell self-renewal. *Stem Cells,* 24, 568-74.

LEVINE, A. J., TOROSIAN, M., SAROKHAN, A. J. & TERESKY, A. K. (1974) Biochemical criteria for the in vitro differentiation of embryoid bodies produced by a transplantable teratoma of mice. The production of acetylcholine esterase and creatine phosphokinase by teratoma cells. *J Cell Physiol,* 84, 311-7.

LI, H., LIU, Y., SHIN, S., SUN, Y., LORING, J. F., MATTSON, M. P., RAO, M. S. & ZHAN, M. (2006a) Transcriptome coexpression map of human embryonic stem cells. *BMC Genomics,* 7, 103.

LI, J., WANG, G., WANG, C., ZHAO, Y., ZHANG, H., TAN, Z., SONG, Z., DING. M. & DENG, H. (2007) MEK/ERK signaling contributes to the maintenance of human embryonic stem cell self-renewal. *Differentiation,* 75, 299-307.

LI, L., ARMAN, E., EKBLOM, P., EDGAR, D., MURRAY, P. & LONAI, P. (2004a) Distinct GATA6- and laminin-dependent mechanisms regulate endodermal and ectodermal embryonic stem cell fates. *Development,* 131, 5277-86.

LI, L., BAROJA, M. L., MAJUMDAR, A., CHADWICK, K., ROULEAU, A.. GALLACHER, L., FERBER, I., LEBKOWSKI, J., MARTIN, T., MADRENAS, J. & BHATIA, M. (2004b) Human embryonic stem cells possess immune-privileged properties. *Stem Cells,* 22, 448-56.

LI, S., EDGAR, D., FASSLER, R., WADSWORTH, W. & YURCHENCO. P. D. (2003) The role of laminin in embryonic cell polarization and tissue organization. *Dev Cell,* 4, 613-24.

LI, S., HARRISON, D., CARBONETTO, S., FASSLER, R., SMYTH, N., EDGAR, D. & YURCHENCO, P. D. (2002) Matrix assembly, regulation, and survival functions of laminin and its receptors in embryonic stem cell differentiation. *J Cell Biol,* 157, 1279-90.

LI, X., CHEN, Y., SCHEELE, S., ARMAN, E., HAFFNER-KRAUSZ, R., EKBLOM, P. & LONAI, P. (2001a) Fibroblast growth factor signaling and basement membrane assembly are connected during epithelial morphogenesis of the embryoid body. *J Cell Biol,* 153, 811-22.

LI, X., TALTS, U., TALTS, J. F., ARMAN, E., EKBLOM, P. & LONAI, P. (2001b) Akt/PKB regulates laminin and collagen IV isotypes of the basement membrane. *Proc Natl Acad Sci U S A,* 98, 14416-21.

LI, X. J., DU, Z. W., ZARNOWSKA, E. D., PANKRATZ, M., HANSEN, L. O., PEARCE, R. A. & ZHANG, S. C. (2005) Specification of motoneurons from human embryonic stem cells. *Nat Biotechnol,* 23, 215-21.

LI, Y. J., CHUNG, E. H., RODRIGUEZ, R. T., FIRPO, M. T. & HEALY, K. E. (2006b) Hydrogels as artificial matrices for human embryonic stem cell self-renewal. *J Biomed Mater Res A,* 79, 1-5.

LIAN, Q., LYE, E., SUAN YEO, K., KHIA WAY TAN, E., SALTO-TELLEZ, M., LIU, T. M., PALANISAMY, N., EL OAKLEY, R. M., LEE, E. H., LIM, B. & LIM, S. K. (2007) Derivation of clinically compliant MSCs from CD105+, CD24- differentiated human ESCs. *Stem Cells,* 25, 425-36.

LICKERT, H., KUTSCH, S., KANZLER, B., TAMAI, Y., TAKETO, M. M. & KEMLER, R. (2002) Formation of multiple hearts in mice following deletion of beta-catenin in the embryonic endoderm. *Dev Cell,* 3, 171-81.

LIU, P., WAKAMIYA, M., SHEA, M. J., ALBRECHT, U., BEHRINGER, R. R. & BRADLEY, A. (1999) Requirement for Wnt3 in vertebrate axis formation. *Nat Genet,* 22, 361-5.

LIU, Y., SHIN, S., ZENG, X., ZHAN, M., GONZALEZ, R., MUELLER, F. J., SCHWARTZ, C. M., XUE, H., LI, H., BAKER, S. C., CHUDIN, E., BARKER, D. L., MCDANIEL, T. K., OESER, S., LORING, J. F., MATTSON, M. P. & RAO, M. S. (2006a) Genome wide profiling of human embryonic stem cells (hESCs), their derivatives and embryonal carcinoma cells to develop base profiles of U.S. Federal government approved hESC lines. *BMC Dev Biol,* 6, 20.

LIU, Y., SONG, Z., ZHAO, Y., QIN, H., CAI, J., ZHANG, H., YU, T., JIANG, S., WANG, G., DING, M. & DENG, H. (2006b) A novel chemical-defined medium with bFGF and N2B27 supplements supports undifferentiated growth in human embryonic stem cells. *Biochem Biophys Res Commun,* 346, 131-9.

LO, B., ZETTLER, P., CEDARS, M. I., GATES, E., KRIEGSTEIN, A. R., OBERMAN, M., REIJO PERA, R., WAGNER, R. M., WUERTH, M. T., WOLF, L. E. & YAMAMOTO, K. R. (2005) A new era in the ethics of human embryonic stem cell research. *Stem Cells,* 23, 1454-9.

LOEBEL, D. A., WATSON, C. M., DE YOUNG, R. A. & TAM, P. P. (2003) Lineage choice and differentiation in mouse embryos and embryonic stem cells. *Dev Biol,* 264, 1-14.

LOH, Y. H., WU, Q., CHEW, J. L., VEGA, V. B., ZHANG, W., CHEN, X., BOURQUE, G., GEORGE, J., LEONG, B., LIU, J., WONG, K. Y., SUNG, K. W., LEE, C. W., ZHAO, X. D., CHIU, K. P., LIPOVICH, L., KUZNETSOV, V. A., ROBSON, P., STANTON, L. W., WEI, C. L., RUAN,

Y., LIM, B. & NG, H. H. (2006) The Oct4 and Nanog transcription network regulates pluripotency in mouse embryonic stem cells. *Nat Genet,* 38, 431-40.

LOOSE, M. & PATIENT, R. (2004) A genetic regulatory network for Xenopus mesendoderm formation. *Dev Biol,* 271, 467-78.

LU, C. C., BRENNAN, J. & ROBERTSON, E. J. (2001) From fertilization to gastrulation: axis formation in the mouse embryo. *Curr Opin Genet Dev,* 11, 384-92.

LU, C. C. & ROBERTSON, E. J. (2004) Multiple roles for Nodal in the epiblast of the mouse embryo in the establishment of anterior-posterior patterning. *Dev Biol,* 273, 149-59.

LU, J., HOU, R., BOOTH, C. J., YANG, S. H. & SNYDER, M. (2006) Defined culture conditions of human embryonic stem cells. *Proc Natl Acad Sci U S A,* 103, 5688-93.

LU, S. J., LI, F., VIDA, L. & HONIG, G. R. (2004) CD34+CD38- hematopoietic precursors derived from human embryonic stem cells exhibit an embryonic gene expression pattern. *Blood,* 103, 4134-41.

LUDWIG, T. E., BERGENDAHL, V., LEVENSTEIN, M. E., YU, J., PROBASCO, M. D. & THOMSON, J. A. (2006a) Feeder-independent culture of human embryonic stem cells. *Nat Methods,* 3, 637-46.

LUDWIG, T. E., LEVENSTEIN, M. E., JONES, J. M., BERGGREN, W. T., MITCHEN, E. R., FRANE, J. L., CRANDALL, L. J., DAIGH, C. A., CONARD, K. R., PIEKARCZYK, M. S., LLANAS, R. A. & THOMSON, J. A. (2006b) Derivation of human embryonic stem cells in defined conditions. *Nat Biotechnol,* 24, 185-187.

MA, Y., RAMEZANI, A., LEWIS, R., HAWLEY, R. G. & THOMSON, J. A. (2003) High-level sustained transgene expression in human embryonic stem cells using lentiviral vectors. *Stem Cells,* 21, 111-7.

MAENO, M., ONG, R. C., SUZUKI, A., UENO, N. & KUNG, H. F. (1994) A truncated bone morphogenetic protein 4 receptor alters the fate of ventral mesoderm to dorsal mesoderm: roles of animal pole tissue in the development of ventral mesoderm. *Proc Natl Acad Sci U S A,* 91, 10260-4.

MAHERALI, N., SRIDHARAN, R., XIE, W., UTIKAL, J., EMINLI, S., ARNOLD, K., STADTFELD, M., YACHECHKO, R., TCHIEU, J., JAENISCH, R., PLATH, K. & HOCHEDLINGER, K. (2007) Directly Reprogrammed Fibroblasts Show Global Epigenetic Remodeling and Widespread Tissue Contribution. *Cell Stem Cell,* 1, 55-70.

MALAS, S., DUTHIE, S. M., MOHRI, F., LOVELL-BADGE, R. & EPISKOPOU, V. (1997) Cloning and mapping of the human SOX1: a highly conserved gene expressed in the developing brain. *Mamm Genome,* 8, 866-8.

MANDAL, A., TIPNIS, S., PAL, R., RAVINDRAN, G., BOSE, B., PATKI, A., RAO, M. S. & KHANNA, A. (2006) Characterization and in vitro differentiation potential of a new human embryonic stem cell line, ReliCellhES1. *Differentiation,* 74, 81-90.

MARSHALL, E. (2004) Getting the noise out of gene arrays. *Science,* 306, 630-1.

MARTIN-RENDON, E. & WATT, S. M. (2003) Exploitation of stem cell plasticity. *Transfus Med,* 13, 325-49.

MARTIN, G. R. (1981) Isolation of a pluripotent cell line from early mouse embryos cultured in medium conditioned by teratocarcinoma stem cells. *Proc Natl Acad Sci U S A,* 78, 7634-8.

MARTIN, G. R., WILEY, L. M. & DAMJANOV, I. (1977) The development of cystic embryoid bodies in vitro from clonal teratocarcinoma stem cells. *Dev Biol,* 61, 230-44.

MARTIN, M. J., MUOTRI, A., GAGE, F. & VARKI, A. (2005) Human embryonic stem cells express an immunogenic nonhuman sialic acid. *Nat Med,* 11, 228-32.

MATEIZEL, I., DE TEMMERMAN, N., ULLMANN, U., CAUFFMAN, G., SERMON, K., VAN DE VELDE, H., DE RYCKE, M., DEGREEF, E., DEVROEY, P., LIEBAERS, I. & VAN STEIRTEGHEM, A. (2006) Derivation of human embryonic stem cell lines from embryos obtained after IVF and after PGD for monogenic disorders. *Hum Reprod,* 21, 503-11.

MATIN, M. M., WALSH, J. R., GOKHALE, P. J., DRAPER, J. S., BAHRAMI, A. R., MORTON, I., MOORE, H. D. & ANDREWS, P. W. (2004) Specific knockdown of Oct4 and beta2-microglobulin expression by RNA interference in human embryonic stem cells and embryonic carcinoma cells. *Stem Cells,* 22, 659-68.

MATSUDA, T., NAKAMURA, T., NAKAO, K., ARAI, T., KATSUKI, M., HEIKE, T. & YOKOTA, T. (1999) STAT3 activation is sufficient to maintain an undifferentiated state of mouse embryonic stem cells. *Embo J,* 18, 4261-9.

MATSUI, Y., TOKSOZ, D., NISHIKAWA, S., NISHIKAWA, S., WILLIAMS, D., ZSEBO, K. & HOGAN, B. L. (1991) Effect of Steel factor and leukaemia inhibitory factor on murine primordial germ cells in culture. *Nature,* 353, 750-2.

MATSUURA, R., KOGO, H., OGAERI, T., MIWA, T., KUWAHARA, M., KANAI, Y., NAKAGAWA, T., KUROIWA, A., FUJIMOTO, T. & TORIHASHI, S. (2006) Crucial Transcription Factors in Endoderm and Embryonic Gut Development Are Expressed in Gut-Like Structures from Mouse ES Cells. *Stem Cells,* 24, 624-30.

MATZUK, M. M., KUMAR, T. R. & BRADLEY, A. (1995) Different phenotypes for mice deficient in either activins or activin receptor type II. *Nature,* 374, 356-60.

MAYE, P., BECKER, S., KASAMEYER, E., BYRD, N. & GRABEL, L. (2000) Indian hedgehog signaling in extraembryonic endoderm and ectoderm differentiation in ES embryoid bodies. *Mech Dev,* 94, 117-32.

MCCONNELL, J., PETRIE, L., STENNARD, F., RYAN, K. & NICHOLS, J. (2005) Eomesodermin is expressed in mouse oocytes and pre-implantation embryos. *Mol Reprod Dev,* 71, 399-404.

MCDOWELL, N. & GURDON, J. B. (1999) Activin as a morphogen in Xenopus mesoderm induction. *Semin Cell Dev Biol,* 10, 311-7.

MCLAREN, A. (2001) Ethical and social considerations of stem cell research. *Nature,* 414, 129-31.

MCLEAN, A. B., D'AMOUR, K. A., JONES, K. L., KRISHNAMOORTHY, M., KULIK, M. J., REYNOLDS, D. M., SHEPPARD, A. M., LIU, H., XU, Y., BAETGE, E. E. & DALTON, S. (2007) Activin a efficiently specifies definitive endoderm from human embryonic stem cells only when phosphatidylinositol 3-kinase signaling is suppressed. *Stem Cells,* 25, 29-38.

MEAD, P. E., DECONINCK, A. E., HUBER, T. L., ORKIN, S. H. & ZON, L. I. (2001) Primitive erythropoiesis in the Xenopus embryo: the synergistic role of LMO-2, SCL and GATA-binding proteins. *Development,* 128, 2301-8.

MEAD, P. E., KELLEY, C. M., HAHN, P. S., PIEDAD, O. & ZON, L. I. (1998)
SCL specifies hematopoietic mesoderm in Xenopus embryos. *Development,*
125, 2611-20.

MENENDEZ, P., WANG, L. & BHATIA, M. (2005) Genetic manipulation of
human embryonic stem cells: a system to study early human development and
potential therapeutic applications. *Curr Gene Ther,* 5, 375-85.

MENENDEZ, P., WANG, L., CHADWICK, K., LI, L. & BHATIA, M. (2004)
Retroviral transduction of hematopoietic cells differentiated from human
embryonic stem cell-derived CD45(neg)PFV hemogenic precursors. *Mol
Ther,* 10, 1109-20.

MENO, C., GRITSMAN, K., OHISHI, S., OHFUJI, Y., HECKSCHER, E.,
MOCHIDA, K., SHIMONO, A., KONDOH, H., TALBOT, W. S.,
ROBERTSON, E. J., SCHIER, A. F. & HAMADA, H. (1999) Mouse Lefty2
and zebrafish antivin are feedback inhibitors of nodal signaling during
vertebrate gastrulation. *Mol Cell,* 4, 287-98.

MESNARD, D., GUZMAN-AYALA, M. & CONSTAM, D. B. (2006) Nodal
specifies embryonic visceral endoderm and sustains pluripotent cells in the
epiblast before overt axial patterning. *Development,* 133, 2497-505.

METZ, A., KNOCHEL, S., BUCHLER, P., KOSTER, M. & KNOCHEL, W. (1998)
Structural and functional analysis of the BMP-4 promoter in early embryos of
Xenopus laevis. *Mech Dev,* 74, 29-39.

MEYER, D., STIEGLER, P., HINDELANG, C., MAGER, A. M. & REMY, P.
(1995) Whole-mount in situ hybridization reveals the expression of the Xl-Fli
gene in several lineages of migrating cells in Xenopus embryos. *Int J Dev
Biol,* 39, 909-19.

MIKI, K. (1999) Volume of liquid below the epithelium of an F9 cell as a signal for
differentiation into visceral endoderm. *J Cell Sci,* 112 Pt 18, 3071-80.

MIKKOLA, M., OLSSON, C., PALGI, J., USTINOV, J., PALOMAKI, T.,
HORELLI-KUITUNEN, N., KNUUTILA, S., LUNDIN, K., OTONKOSKI,
T. & TUURI, T. (2006) Distinct differentiation characteristics of individual
human embryonic stem cell lines. *BMC Dev Biol,* 6, 40.

MISHINA, Y., SUZUKI, A., UENO, N. & BEHRINGER, R. R. (1995) Bmpr
encodes a type I bone morphogenetic protein receptor that is essential for
gastrulation during mouse embryogenesis. *Genes Dev,* 9, 3027-37.

MITALIPOV, S. M., YEOMAN, R. R., NUSSER, K. D. & WOLF, D. P. (2002)
Rhesus monkey embryos produced by nuclear transfer from embryonic
blastomeres or somatic cells. *Biol Reprod,* 66, 1367-73.

MITALIPOVA, M., CALHOUN, J., SHIN, S., WININGER, D., SCHULZ, T.,
NOGGLE, S., VENABLE, A., LYONS, I., ROBINS, A. & STICE, S. (2003)
Human embryonic stem cell lines derived from discarded embryos. *Stem
Cells,* 21, 521-6.

MITSUI, K., TOKUZAWA, Y., ITOH, H., SEGAWA, K., MURAKAMI, M.,
TAKAHASHI, K., MARUYAMA, M., MAEDA, M. & YAMANAKA, S.
(2003) The homeoprotein Nanog is required for maintenance of pluripotency
in mouse epiblast and ES cells. *Cell,* 113, 631-42.

MIURA, T., LUO, Y., KHREBTUKOVA, I., BRANDENBERGER, R., ZHOU, D.,
THIES, R. S., VASICEK, T., YOUNG, H., LEBKOWSKI, J., CARPENTER,
M. K. & RAO, M. S. (2004) Monitoring early differentiation events in human
embryonic stem cells by massively parallel signature sequencing and
expressed sequence tag scan. *Stem Cells Dev,* 13, 694-715.

MIYANAGA, Y., SHIURBA, R. & ASASHIMA, M. (1999) Blood cell induction in Xenopus animal cap explants: effects of fibroblast growth factor, bone morphogenetic proteins, and activin. *Dev Genes Evol,* 209, 69-76.

MIYAZAWA, K., SHINOZAKI, M., HARA, T., FURUYA, T. & MIYAZONO, K. (2002) Two major Smad pathways in TGF-beta superfamily signalling. *Genes Cells,* 7, 1191-204.

MOHAMED, O. A., CLARKE, H. J. & DUFORT, D. (2004) Beta-catenin signaling marks the prospective site of primitive streak formation in the mouse embryo. *Dev Dyn,* 231, 416-24.

MOHN, D., CHEN, S. W., DIAS, D. C., WEINSTEIN, D. C., DYER, M. A., SAHR, K., DUCKER, C. E., ZAHRADKA, E., KELLER, G., ZARET, K. S., GUDAS, L. J. & BARON, M. H. (2003) Mouse Mix gene is activated early during differentiation of ES and F9 stem cells and induces endoderm in frog embryos. *Dev Dyn,* 226, 446-59.

MOLKENTIN, J. D., LIN, Q., DUNCAN, S. A. & OLSON, E. N. (1997) Requirement of the transcription factor GATA4 for heart tube formation and ventral morphogenesis. *Genes Dev,* 11, 1061-72.

MONAGHAN, A. P., KAESTNER, K. H., GRAU, E. & SCHUTZ, G. (1993) Postimplantation expression patterns indicate a role for the mouse forkhead/HNF-3 alpha, beta and gamma genes in determination of the definitive endoderm, chordamesoderm and neuroectoderm. *Development,* 119, 567-78.

MORKEL, M., HUELSKEN, J., WAKAMIYA, M., DING, J., VAN DE WETERING, M., CLEVERS, H., TAKETO, M. M., BEHRINGER, R. R., SHEN, M. M. & BIRCHMEIER, W. (2003) Beta-catenin regulates Cripto- and Wnt3-dependent gene expression programs in mouse axis and mesoderm formation. *Development,* 130, 6283-94.

MORRISEY, E. E., TANG, Z., SIGRIST, K., LU, M. M., JIANG, F., IP, H. S. & PARMACEK, M. S. (1998) GATA6 regulates HNF4 and is required for differentiation of visceral endoderm in the mouse embryo. *Genes Dev,* 12, 3579-90.

MORRISON, K., PAPAPETROU, C., ATTWOOD, J., HOL, F., LYNCH, S. A., SAMPATH, A., HAMEL, B., BURN, J., SOWDEN, J., STOTT, D., MARIMAN, E. & EDWARDS, Y. H. (1996) Genetic mapping of the human homologue (T) of mouse T(Brachyury) and a search for allele association between human T and spina bifida. *Hum Mol Genet,* 5, 669-74.

MOSSMAN, A. K., SOURRIS, K., NG, E., STANLEY, E. G. & ELEFANTY, A. G. (2005) Mixl1 and oct4 proteins are transiently co-expressed in differentiating mouse and human embryonic stem cells. *Stem Cells Dev,* 14, 656-63.

MOUNTFORD, P., NICHOLS, J., ZEVNIK, B., O'BRIEN, C. & SMITH, A. (1998) Maintenance of pluripotential embryonic stem cells by stem cell selection. *Reprod Fertil Dev,* 10, 527-33.

MUMMERY, C., WARD-VAN OOSTWAARD, D., DOEVENDANS, P., SPIJKER, R., VAN DEN BRINK, S., HASSINK, R., VAN DER HEYDEN, M., OPTHOF, T., PERA, M., DE LA RIVIERE, A. B., PASSIER, R. & TERTOOLEN, L. (2003) Differentiation of human embryonic stem cells to cardiomyocytes: role of coculture with visceral endoderm-like cells. *Circulation,* 107, 2733-40.

MUMMERY, C., WARD, D., VAN DEN BRINK, C. E., BIRD, S. D., DOEVENDANS, P. A., OPTHOF, T., BRUTEL DE LA RIVIERE, A.,

TERTOOLEN, L., VAN DER HEYDEN, M. & PERA, M. (2002) Cardiomyocyte differentiation of mouse and human embryonic stem cells. *J Anat,* 200, 233-42.

MURDOCH, B., GALLACHER, L., CHADWICK, K., FELLOWS, F. & BHATIA, M. (2002) Human embryonic-derived hematopoietic repopulating cells require distinct factors to sustain in vivo repopulating function. *Exp Hematol,* 30, 598-605.

MURRAY, P. & EDGAR, D. (2000) Regulation of programmed cell death by basement membranes in embryonic development. *J Cell Biol,* 150, 1215-21.

MURRAY, P. & EDGAR, D. (2001a) The regulation of embryonic stem cell differentiation by leukaemia inhibitory factor (LIF). *Differentiation,* 68, 227-34.

MURRAY, P. & EDGAR, D. (2001b) Regulation of laminin and COUP-TF expression in extraembryonic endodermal cells. *Mech Dev,* 101, 213-5.

MURRAY, P. & EDGAR, D. (2001c) Regulation of the differentiation and behaviour of extra-embryonic endodermal cells by basement membranes. *J Cell Sci,* 114, 931-9.

MURRAY, P. & EDGAR, D. (2004) The topographical regulation of embryonic stem cell differentiation. *Philos Trans R Soc Lond B Biol Sci,* 359, 1009-20.

NARAYAN, A. D., CHASE, J. L., LEWIS, R. L., TIAN, X., KAUFMAN, D. S., THOMSON, J. A. & ZANJANI, E. D. (2006) Human embryonic stem cell-derived hematopoietic cells are capable of engrafting primary as well as secondary fetal sheep recipients. *Blood,* 107, 2180-3.

NASONKIN, I. O. & KOLIATSOS, V. E. (2006) Nonhuman sialic acid Neu5Gc is very low in human embryonic stem cell-derived neural precursors differentiated with B27/N2 and noggin: Implications for transplantation. *Exp Neurol,* 201, 525-9.

NAT, R., NILBRATT, M., NARKILAHTI, S., WINBLAD, B., HOVATTA, O. & NORDBERG, A. (2007) Neurogenic neuroepithelial and radial glial cells generated from six human embryonic stem cell lines in serum-free suspension and adherent cultures. *Glia,* 55, 385-99.

NG, E. S., AZZOLA, L., SOURRIS, K., ROBB, L., STANLEY, E. G. & ELEFANTY, A. G. (2005a) The primitive streak gene Mixl1 is required for efficient haematopoiesis and BMP4-induced ventral mesoderm patterning in differentiating ES cells. *Development,* 132, 873-84.

NG, E. S., DAVIS, R. P., AZZOLA, L., STANLEY, E. G. & ELEFANTY, A. G. (2005b) Forced aggregation of defined numbers of human embryonic stem cells into embryoid bodies fosters robust, reproducible hematopoietic differentiation. *Blood,* 106, 1601-3.

NGUYEN, D. H., TANGVORANUNTAKUL, P. & VARKI, A. (2005) Effects of natural human antibodies against a nonhuman sialic acid that metabolically incorporates into activated and malignant immune cells. *J Immunol,* 175, 228-36.

NICHOLS, J., CHAMBERS, I., TAGA, T. & SMITH, A. (2001) Physiological rationale for responsiveness of mouse embryonic stem cells to gp130 cytokines. *Development,* 128, 2333-9.

NICHOLS, J., ZEVNIK, B., ANASTASSIADIS, K., NIWA, H., KLEWE-NEBENIUS, D., CHAMBERS, I., SCHOLER, H. & SMITH, A. (1998) Formation of pluripotent stem cells in the mammalian embryo depends on the POU transcription factor Oct4. *Cell,* 95, 379-91.

NIEUWKOOP, P. D. (1997) Short historical survey of pattern formation in the endo-mesoderm and the neural anlage in the vertebrates: the role of vertical and planar inductive actions. *Cell Mol Life Sci,* 53, 305-18.

NIEUWKOOP, P. D. & FABER, J. (1967) Normal Table of Xenopus laevis (Daudin).

NIR, S. G., DAVID, R., ZARUBA, M., FRANZ, W. M. & ITSKOVITZ-ELDOR, J. (2003) Human embryonic stem cells for cardiovascular repair. *Cardiovasc Res,* 58, 313-23.

NISHIGUCHI, S., WOOD, H., KONDOH, H., LOVELL-BADGE, R. & EPISKOPOU, V. (1998) Sox1 directly regulates the gamma-crystallin genes and is essential for lens development in mice. *Genes Dev,* 12, 776-81.

NISHIKAWA, S. I., NISHIKAWA, S., HIRASHIMA, M., MATSUYOSHI, N. & KODAMA, H. (1998) Progressive lineage analysis by cell sorting and culture identifies FLK1+VE-cadherin+ cells at a diverging point of endothelial and hemopoietic lineages. *Development,* 125, 1747-57.

NISTOR, G. I., TOTOIU, M. O., HAQUE, N., CARPENTER, M. K. & KEIRSTEAD, H. S. (2005) Human embryonic stem cells differentiate into oligodendrocytes in high purity and myelinate after spinal cord transplantation. *Glia,* 49, 385-96.

NISWANDER, L. & MARTIN, G. R. (1992) Fgf-4 expression during gastrulation, myogenesis, limb and tooth development in the mouse. *Development,* 114, 755-68.

NIWA, H., BURDON, T., CHAMBERS, I. & SMITH, A. (1998) Self-renewal of pluripotent embryonic stem cells is mediated via activation of STAT3. *Genes Dev,* 12, 2048-60.

NIWA, H., MIYAZAKI, J. & SMITH, A. G. (2000) Quantitative expression of Oct-3/4 defines differentiation, dedifferentiation or self-renewal of ES cells. *Nat Genet,* 24, 372-6.

NOAKSSON, K., ZORIC, N., ZENG, X., RAO, M. S., HYLLNER, J., SEMB, H., KUBISTA, M. & SARTIPY, P. (2005) Monitoring differentiation of human embryonic stem cells using real-time PCR. *Stem Cells,* 23, 1460-7.

NOLDEN, L., EDENHOFER, F., HAUPT, S., KOCH, P., WUNDERLICH, F. T., SIEMEN, H. & BRUSTLE, O. (2006) Site-specific recombination in human embryonic stem cells induced by cell-permeant Cre recombinase. *Nat Methods,* 3, 461-7.

NORSTROM, A., AKESSON, K., HARDARSON, T., HAMBERGER, L., BJORQUIST, P. & SARTIPY, P. (2006) Molecular and pharmacological properties of human embryonic stem cell-derived cardiomyocytes. *Exp Biol Med (Maywood),* 231, 1753-62.

OH, S. K., KIM, H. S., AHN, H. J., SEOL, H. W., KIM, Y. Y., PARK, Y. B., YOON, C. J., KIM, D. W., KIM, S. H. & MOON, S. Y. (2005) Derivation and characterization of new human embryonic stem cell lines: SNUhES1, SNUhES2, and SNUhES3. *Stem Cells,* 23, 211-9.

OKABAYASHI, K. & ASASHIMA, M. (2003) Tissue generation from amphibian animal caps. *Curr Opin Genet Dev,* 13, 502-7.

OKITA, K., ICHISAKA, T. & YAMANAKA, S. (2007) Generation of germline-competent induced pluripotent stem cells. *Nature,* 448, 313-7.

OLIVIER, E. N., RYBICKI, A. C. & BOUHASSIRA, E. E. (2006) Differentiation of human embryonic stem cells into bipotent mesenchymal stem cells. *Stem Cells,* 24, 1914-22.

ONUMA, Y., TAKAHASHI, S., YOKOTA, C. & ASASHIMA, M. (2002) Multiple nodal-related genes act coordinately in Xenopus embryogenesis. *Dev Biol,* 241, 94-105.

OSADA, H., GRUTZ, G., AXELSON, H., FORSTER, A. & RABBITTS, T. H. (1995) Association of erythroid transcription factors: complexes involving the LIM protein RBTN2 and the zinc-finger protein GATA1. *Proc Natl Acad Sci U S A,* 92, 9585-9.

PAIN, D., CHIRN, G. W., STRASSEL, C. & KEMP, D. M. (2005) Multiple retropseudogenes from pluripotent cell-specific gene expression indicates a potential signature for novel gene identification. *J Biol Chem,* 280, 6265-8.

PAL, R. & KHANNA, A. (2007) Similar pattern in cardiac differentiation of human embryonic stem cell lines, BG01V and ReliCell((R))hES1, under low serum concentration supplemented with bone morphogenetic protein-2. *Differentiation,* 75, 112-22.

PALMIERI, S. L., PETER, W., HESS, H. & SCHOLER, H. R. (1994) Oct-4 transcription factor is differentially expressed in the mouse embryo during establishment of the first two extraembryonic cell lineages involved in implantation. *Dev Biol,* 166, 259-67.

PAN, G. J., CHANG, Z. Y., SCHOLER, H. R. & PEI, D. (2002) Stem cell pluripotency and transcription factor Oct4. *Cell Res,* 12, 321-9.

PANKRATZ, M. T., LI, X. J., LAVAUTE, T. M., LYONS, E. A., CHEN, X. & ZHANG, S. C. (2007) Directed neural differentiation of human embryonic stem cells via an obligated primitive anterior stage. *Stem Cells,* 25, 1511-20.

PARK, J. H., KIM, S. J., OH, E. J., MOON, S. Y., ROH, S. I., KIM, C. G. & YOON, H. S. (2003) Establishment and maintenance of human embryonic stem cells on STO, a permanently growing cell line. *Biol Reprod,* 69, 2007-14.

PARK, S., LEE, K. S., LEE, Y. J., SHIN, H. A., CHO, H. Y., WANG, K. C., KIM, Y. S., LEE, H. T., CHUNG, K. S., KIM, E. Y. & LIM, J. (2004a) Generation of dopaminergic neurons in vitro from human embryonic stem cells treated with neurotrophic factors. *Neurosci Lett,* 359, 99-103.

PARK, S. P., LEE, Y. J., LEE, K. S., AH SHIN, H., CHO, H. Y., CHUNG, K. S., KIM, E. Y. & LIM, J. H. (2004b) Establishment of human embryonic stem cell lines from frozen-thawed blastocysts using STO cell feeder layers. *Hum Reprod,* 19, 676-84.

PASSIER, R., DENNING, C. & MUMMERY, C. (2006) Cardiomyocytes from human embryonic stem cells. *Handb Exp Pharmacol,* 101-22.

PASSIER, R. & MUMMERY, C. (2003) Origin and use of embryonic and adult stem cells in differentiation and tissue repair. *Cardiovasc Res,* 58, 324-35.

PEARCE, J. J. & EVANS, M. J. (1999) Mml, a mouse Mix-like gene expressed in the primitive streak. *Mech Dev,* 87, 189-92.

PERA, M. F., ANDRADE, J., HOUSSAMI, S., REUBINOFF, B., TROUNSON, A., STANLEY, E. G., WARD-VAN OOSTWAARD, D. & MUMMERY, C. (2004) Regulation of human embryonic stem cell differentiation by BMP-2 and its antagonist noggin. *J Cell Sci,* 117, 1269-80.

PEREA-GOMEZ, A., CAMUS, A., MOREAU, A., GRIEVE, K., MONERON, G., DUBOIS, A., CIBERT, C. & COLLIGNON, J. (2004) Initiation of gastrulation in the mouse embryo is preceded by an apparent shift in the orientation of the anterior-posterior axis. *Curr Biol,* 14, 197-207.

PEREA-GOMEZ, A., LAWSON, K. A., RHINN, M., ZAKIN, L., BRULET, P., MAZAN, S. & ANG, S. L. (2001) Otx2 is required for visceral endoderm

movement and for the restriction of posterior signals in the epiblast of the mouse embryo. *Development,* 128, 753-65.

PEREA-GOMEZ, A., SHAWLOT, W., SASAKI, H., BEHRINGER, R. R. & ANG, S. (1999) HNF3beta and Lim1 interact in the visceral endoderm to regulate primitive streak formation and anterior-posterior polarity in the mouse embryo. *Development,* 126, 4499-511.

PEREA-GOMEZ, A., VELLA, F. D., SHAWLOT, W., OULAD-ABDELGHANI, M., CHAZAUD, C., MENO, C., PFISTER, V., CHEN, L., ROBERTSON, E., HAMADA, H., BEHRINGER, R. R. & ANG, S. L. (2002) Nodal antagonists in the anterior visceral endoderm prevent the formation of multiple primitive streaks. *Dev Cell,* 3, 745-56.

PERRIER, A. L., TABAR, V., BARBERI, T., RUBIO, M. E., BRUSES, J., TOPF, N., HARRISON, N. L. & STUDER, L. (2004) Derivation of midbrain dopamine neurons from human embryonic stem cells. *Proc Natl Acad Sci U S A,* 101, 12543-8.

PESCE, M., WANG, X., WOLGEMUTH, D. J. & SCHOLER, H. (1998) Differential expression of the Oct-4 transcription factor during mouse germ cell differentiation. *Mech Dev,* 71, 89-98.

PEVNY, L., SIMON, M. C., ROBERTSON, E., KLEIN, W. H., TSAI, S. F., D'AGATI, V., ORKIN, S. H. & COSTANTINI, F. (1991) Erythroid differentiation in chimaeric mice blocked by a targeted mutation in the gene for transcription factor GATA-1. *Nature,* 349, 257-60.

PEVNY, L. H. & LOVELL-BADGE, R. (1997) Sox genes find their feet. *Curr Opin Genet Dev,* 7, 338-44.

PEVNY, L. H., SOCKANATHAN, S., PLACZEK, M. & LOVELL-BADGE, R. (1998) A role for SOX1 in neural determination. *Development,* 125, 1967-78.

PICCOLO, S., SASAI, Y., LU, B. & DE ROBERTIS, E. M. (1996) Dorsoventral patterning in Xenopus: inhibition of ventral signals by direct binding of chordin to BMP-4. *Cell,* 86, 589-98.

PICKERING, S. J., BRAUDE, P. R., PATEL, M., BURNS, C. J., TRUSSLER, J., BOLTON, V. & MINGER, S. (2003) Preimplantation genetic diagnosis as a novel source of embryos for stem cell research. *Reprod Biomed Online,* 7, 353-64.

PICKERING, S. J., MINGER, S. L., PATEL, M., TAYLOR, H., BLACK, C., BURNS, C. J., EKONOMOU, A. & BRAUDE, P. R. (2005) Generation of a human embryonic stem cell line encoding the cystic fibrosis mutation deltaF508, using preimplantation genetic diagnosis. *Reprod Biomed Online,* 10, 390-7.

PIEPENBURG, O., GRIMMER, D., WILLIAMS, P. H. & SMITH, J. C. (2004) Activin redux: specification of mesodermal pattern in Xenopus by graded concentrations of endogenous activin B. *Development,* 131, 4977-86.

POON, E., CLERMONT, F., FIRPO, M. T. & AKHURST, R. J. (2006) TGFbeta inhibition of yolk-sac-like differentiation of human embryonic stem-cell-derived embryoid bodies illustrates differences between early mouse and human development. *J Cell Sci,* 119, 759-68.

PORCHER, C., SWAT, W., ROCKWELL, K., FUJIWARA, Y., ALT, F. W. & ORKIN, S. H. (1996) The T cell leukemia oncoprotein SCL/tal-1 is essential for development of all hematopoietic lineages. *Cell,* 86, 47-57.

POUTON, C. W. & HAYNES, J. M. (2005) Pharmaceutical applications of embryonic stem cells. *Adv Drug Deliv Rev,* 57, 1918-34.

PRICE, P. J., GOLDSBOROUGH, M. D. & TILKINS, M. L. (1998) In International Patent Application WO 98/30679.

PRIDDLE, H., JONES, D. R., BURRIDGE, P. W. & PATIENT, R. (2006) Hematopoiesis from human embryonic stem cells: overcoming the immune barrier in stem cell therapies. *Stem Cells,* 24, 815-24.

QI, X., LI, T. G., HAO, J., HU, J., WANG, J., SIMMONS, H., MIURA, S., MISHINA, Y. & ZHAO, G. Q. (2004) BMP4 supports self-renewal of embryonic stem cells by inhibiting mitogen-activated protein kinase pathways. *Proc Natl Acad Sci U S A,* 101, 6027-32.

QIU, C., HANSON, E., OLIVIER, E., INADA, M., KAUFMAN, D. S., GUPTA, S. & BOUHASSIRA, E. E. (2005) Differentiation of human embryonic stem cells into hematopoietic cells by coculture with human fetal liver cells recapitulates the globin switch that occurs early in development. *Exp Hematol,* 33, 1450-1458.

QU, X., ZOU, Z., SUN, Q., LUBY-PHELPS, K., CHENG, P., HOGAN, R. N., GILPIN, C. & LEVINE, B. (2007) Autophagy gene-dependent clearance of apoptotic cells during embryonic development. *Cell,* 128, 931-46.

RAMALHO-SANTOS, M., YOON, S., MATSUZAKI, Y., MULLIGAN, R. C. & MELTON, D. A. (2002) "Stemness": transcriptional profiling of embryonic and adult stem cells. *Science,* 298, 597-600.

RAMBHATLA, L., CHIU, C. P., KUNDU, P., PENG, Y. & CARPENTER, M. K. (2003) Generation of hepatocyte-like cells from human embryonic stem cells. *Cell Transplant,* 12, 1-11.

RAO, M. (2004) Conserved and divergent paths that regulate self-renewal in mouse and human embryonic stem cells. *Dev Biol,* 275, 269-86.

RAO, R. R., CALHOUN, J. D., QIN, X., REKAYA, R., CLARK, J. K. & STICE, S. L. (2004) Comparative transcriptional profiling of two human embryonic stem cell lines. *Biotechnol Bioeng,* 88, 273-86.

RATHJEN, J., LAKE, J. A., BETTESS, M. D., WASHINGTON, J. M., CHAPMAN, G. & RATHJEN, P. D. (1999) Formation of a primitive ectoderm like cell population, EPL cells, from ES cells in response to biologically derived factors. *J Cell Sci,* 112 (Pt 5), 601-12.

REPPEL, M., BOETTINGER, C. & HESCHELER, J. (2004) Beta-adrenergic and muscarinic modulation of human embryonic stem cell-derived cardiomyocytes. *Cell Physiol Biochem,* 14, 187-96.

RESNICK, J. L., BIXLER, L. S., CHENG, L. & DONOVAN, P. J. (1992) Long-term proliferation of mouse primordial germ cells in culture. *Nature,* 359, 550-1.

REUBINOFF, B. E., ITSYKSON, P., TURETSKY, T., PERA, M. F., REINHARTZ, E., ITZIK, A. & BEN-HUR, T. (2001) Neural progenitors from human embryonic stem cells. *Nat Biotechnol,* 19, 1134-40.

REUBINOFF, B. E., PERA, M. F., FONG, C. Y., TROUNSON, A. & BONGSO, A. (2000) Embryonic stem cell lines from human blastocysts: somatic differentiation in vitro. *Nat Biotechnol,* 18, 399-404.

REVAZOVA, E. S., TUROVETS, N. A., KOCHETKOVA, O. D., KINDAROVA, L. B., KUZMICHEV, L. N., JANUS, J. D. & PRYZHKOVA, M. V. (2007) Patient-specific stem cell lines derived from human parthenogenetic blastocysts. *Cloning Stem Cells,* 9, 432-49.

REX, M., HILTON, E. & OLD, R. (2002) Multiple interactions between maternally-activated signalling pathways control Xenopus nodal-related genes. *Int J Dev Biol,* 46, 217-26.

REYA, T., MORRISON, S. J., CLARKE, M. F. & WEISSMAN, I. L. (2001) Stem cells, cancer, and cancer stem cells. *Nature,* 414, 105-11.

RICHARDS, M., FONG, C. Y., CHAN, W. K., WONG, P. C. & BONGSO, A. (2002) Human feeders support prolonged undifferentiated growth of human inner cell masses and embryonic stem cells. *Nat Biotechnol,* 20, 933-6.

RICHARDS, M., TAN, S., FONG, C. Y., BISWAS, A., CHAN, W. K. & BONGSO, A. (2003) Comparative evaluation of various human feeders for prolonged undifferentiated growth of human embryonic stem cells. *Stem Cells,* 21, 546-56.

RICHARDS, M., TAN, S. P., TAN, J. H., CHAN, W. K. & BONGSO, A. (2004) The transcriptome profile of human embryonic stem cells as defined by SAGE. *Stem Cells,* 22, 51-64.

RICHARDSON, L., TORRES-PADILLA, M. E. & ZERNICKA-GOETZ, M. (2006) Regionalised signalling within the extraembryonic ectoderm regulates anterior visceral endoderm positioning in the mouse embryo. *Mech Dev,* 123, 288-96.

RINGE, J., KAPS, C., BURMESTER, G. R. & SITTINGER, M. (2002) Stem cells for regenerative medicine: advances in the engineering of tissues and organs. *Naturwissenschaften,* 89, 338-51.

RIPPON, H. J. & BISHOP, A. E. (2004) Embryonic stem cells. *Cell Prolif,* 37, 23-34.

RIVERA-PEREZ, J. A. & MAGNUSON, T. (2005) Primitive streak formation in mice is preceded by localized activation of Brachyury and Wnt3. *Dev Biol,* 288, 363-71.

ROBB, L., HARTLEY, L., BEGLEY, C. G., BRODNICKI, T. C., COPELAND, N. G., GILBERT, D. J., JENKINS, N. A. & ELEFANTY, A. G. (2000) Cloning, expression analysis, and chromosomal localization of murine and human homologues of a Xenopus mix gene. *Dev Dyn,* 219, 497-504.

ROBB, L., RASKO, J. E., BATH, M. L., STRASSER, A. & BEGLEY, C. G. (1995) scl, a gene frequently activated in human T cell leukaemia, does not induce lymphomas in transgenic mice. *Oncogene,* 10, 205-9.

RODAWAY, A. & PATIENT, R. (2001) Mesendoderm. an ancient germ layer? *Cell,* 105, 169-72.

RODAWAY, A., TAKEDA, H., KOSHIDA, S., BROADBENT, J., PRICE, B., SMITH, J. C., PATIENT, R. & HOLDER, N. (1999) Induction of the mesendoderm in the zebrafish germ ring by yolk cell-derived TGF-beta family signals and discrimination of mesoderm and endoderm by FGF. *Development,* 126, 3067-78.

RODDA, D. J., CHEW, J. L., LIM, L. H., LOH, Y. H., WANG, B., NG, H. H. & ROBSON, P. (2005) Transcriptional regulation of nanog by OCT4 and SOX2. *J Biol Chem,* 280, 24731-7.

RODDA, S. J., KAVANAGH, S. J., RATHJEN, J. & RATHJEN, P. D. (2002) Embryonic stem cell differentiation and the analysis of mammalian development. *Int J Dev Biol,* 46, 449-58.

ROSNER, M. H., VIGANO, M. A., OZATO, K., TIMMONS, P. M., POIRIER, F., RIGBY, P. W. & STAUDT, L. M. (1990) A POU-domain transcription factor

in early stem cells and germ cells of the mammalian embryo. *Nature,* 345, 686-92.

ROSS, S. A., MCCAFFERY, P. J., DRAGER, U. C. & DE LUCA, L. M. (2000) Retinoids in embryonal development. *Physiol Rev,* 80, 1021-54.

ROSSANT, J., CHAZAUD, C. & YAMANAKA, Y. (2003) Lineage allocation and asymmetries in the early mouse embryo. *Philos Trans R Soc Lond B Biol Sci,* 358, 1341-8; discussion 1349.

ROYER-POKORA, B., RAGG, S., HECKL-OSTREICHER, B., HELD, M., LOOS, U., CALL, K., GLASER, T., HOUSMAN, D., SAUNDERS, G., ZABEL, B. & ET AL. (1991) Direct pulsed field gel electrophoresis of Wilms' tumors shows that DNA deletions in 11p13 are rare. *Genes Chromosomes Cancer,* 3, 89-100.

RUIZ I ALTABA, A., PREZIOSO, V. R., DARNELL, J. E. & JESSELL, T. M. (1993) Sequential expression of HNF-3 beta and HNF-3 alpha by embryonic organizing centers: the dorsal lip/node, notochord and floor plate. *Mech Dev,* 44, 91-108.

RUSS, A. P., WATTLER, S., COLLEDGE, W. H., APARICIO, S. A., CARLTON, M. B., PEARCE, J. J., BARTON, S. C., SURANI, M. A., RYAN, K., NEHLS, M. C., WILSON, V. & EVANS, M. J. (2000) Eomesodermin is required for mouse trophoblast development and mesoderm formation. *Nature,* 404, 95-9.

RUZINOVA, M. B. & BENEZRA, R. (2003) Id proteins in development, cell cycle and cancer. *Trends Cell Biol,* 13, 410-8.

SAHR, K., DIAS, D. C., SANCHEZ, R., CHEN, D., CHEN, S. W., GUDAS, L. J. & BARON, M. H. (2002) Structure, upstream promoter region, and functional domains of a mouse and human Mix paired-like homeobox gene. *Gene,* 291, 135-47.

SAITOU, M., BARTON, S. C. & SURANI, M. A. (2002) A molecular programme for the specification of germ cell fate in mice. *Nature,* 418, 293-300.

SALAMAT, M., MIOSGE, N. & HERKEN, R. (1995) Development of Reichert's membrane in the early mouse embryo. *Anat Embryol (Berl),* 192, 275-81.

SAMBROOK, J. & RUSSELL, D. W. (2001) Molecular Cloning: A Laboratory Manual (Third Edition).

SANADA, T., PARK, M. J., ARAKI, A., GOTOH, M., IZUTSU, Y. & MAENO, M. (2003) A BMP-4-dependent transcriptional control element in the 5' flanking region of Xenopus SCL gene. *Biochem Biophys Res Commun,* 310, 1160-7.

SASAKI, H. & HOGAN, B. L. (1993) Differential expression of multiple fork head related genes during gastrulation and axial pattern formation in the mouse embryo. *Development,* 118, 47-59.

SATIN, J., KEHAT, I., CASPI, O., HUBER, I., ARBEL, G., ITZHAKI, I., MAGYAR, J., SCHRODER, E. A., PERLMAN, I. & GEPSTEIN, L. (2004) Mechanism of spontaneous excitability in human embryonic stem cell derived cardiomyocytes. *J Physiol,* 559, 479-96.

SATO, N., SANJUAN, I. M., HEKE, M., UCHIDA, M., NAEF, F. & BRIVANLOU, A. H. (2003) Molecular signature of human embryonic stem cells and its comparison with the mouse. *Dev Biol,* 260, 404-13.

SAUER, H., HOFMANN, C., WARTENBERG, M., WOBUS, A. M. & HESCHELER, J. (1998) Spontaneous calcium oscillations in embryonic stem cell-derived primitive endodermal cells. *Exp Cell Res,* 238, 13-22.

SCHIER, A. F. & SHEN, M. M. (2000) Nodal signalling in vertebrate development. *Nature*, 403, 385-9.

SCHOLER, H. R., DRESSLER, G. R., BALLING, R., ROHDEWOHLD, H. & GRUSS, P. (1990a) Oct-4: a germline-specific transcription factor mapping to the mouse t-complex. *Embo J*, 9, 2185-95.

SCHOLER, H. R., RUPPERT, S., SUZUKI, N., CHOWDHURY, K. & GRUSS, P. (1990b) New type of POU domain in germ line-specific protein Oct-4. *Nature*, 344, 435-9.

SCHROEDER, M., NIEBRUEGGE, S., WERNER, A., WILLBOLD, E., BURG, M., RUEDIGER, M., FIELD, L. J., LEHMANN, J. & ZWEIGERDT, R. (2005) Differentiation and lineage selection of mouse embryonic stem cells in a stirred bench scale bioreactor with automated process control. *Biotechnol Bioeng*, 92, 920-33.

SCHULDINER, M., EIGES, R., EDEN, A., YANUKA, O., ITSKOVITZ-ELDOR, J., GOLDSTEIN, R. S. & BENVENISTY, N. (2001) Induced neuronal differentiation of human embryonic stem cells. *Brain Res*, 913, 201-5.

SCHULDINER, M., YANUKA, O., ITSKOVITZ-ELDOR, J., MELTON, D. A. & BENVENISTY, N. (2000) Effects of eight growth factors on the differentiation of cells derived from human embryonic stem cells. *Proc Natl Acad Sci U S A*, 97, 11307-12.

SCHULZ, T. C., NOGGLE, S. A., PALMARINI, G. M., WEILER, D. A., LYONS, I. G., PENSA, K. A., MEEDENIYA, A. C., DAVIDSON, B. P., LAMBERT, N. A. & CONDIE, B. G. (2004) Differentiation of human embryonic stem cells to dopaminergic neurons in serum-free suspension culture. *Stem Cells*, 22, 1218-38.

SCHULZ, T. C., PALMARINI, G. M., NOGGLE, S. A., WEILER, D. A., MITALIPOVA, M. M. & CONDIE, B. G. (2003) Directed neuronal differentiation of human embryonic stem cells. *BMC Neurosci*, 4, 27.

SEGEV, H., FISHMAN, B., ZISKIND, A., SHULMAN, M. & ITSKOVITZ-ELDOR, J. (2004) Differentiation of human embryonic stem cells into insulin-producing clusters. *Stem Cells*, 22, 265-74.

SEGEV, H., KENYAGIN-KARSENTI, D., FISHMAN, B., GERECHT-NIR, S., ZISKIND, A., AMIT, M., COLEMAN, R. & ITSKOVITZ-ELDOR, J. (2005) Molecular analysis of cardiomyocytes derived from human embryonic stem cells. *Dev Growth Differ*, 47, 295-306.

SERAFINI, M. & VERFAILLIE, C. M. (2006) Pluripotency in adult stem cells: state of the art. *Semin Reprod Med*, 24, 379-88.

SHAMBLOTT, M. J., AXELMAN, J., WANG, S., BUGG, E. M., LITTLEFIELD, J. W., DONOVAN, P. J., BLUMENTHAL, P. D., HUGGINS, G. R. & GEARHART, J. D. (1998) Derivation of pluripotent stem cells from cultured human primordial germ cells. *Proc Natl Acad Sci U S A*, 95, 13726-31.

SHINOHARA, M., KODAMA, A., MATOZAKI, T., FUKUHARA, A., TACHIBANA, K., NAKANISHI, H. & TAKAI, Y. (2001) Roles of cell-cell adhesion-dependent tyrosine phosphorylation of Gab-1. *J Biol Chem*, 276, 18941-6.

SHIRAHASHI, H., WU, J., YAMAMOTO, N., CATANA, A., WEGE, H., WAGER, B., OKITA, K. & ZERN, M. A. (2004) Differentiation of human and mouse embryonic stem cells along a hepatocyte lineage. *Cell Transplant*, 13, 197-211.

SHIVDASANI, R. A., MAYER, E. L. & ORKIN, S. H. (1995) Absence of blood formation in mice lacking the T-cell leukaemia oncoprotein tal-1/SCL. *Nature*, 373, 432-4.

SIEWEKE, M. H. & GRAF, T. (1998) A transcription factor party during blood cell differentiation. *Curr Opin Genet Dev*, 8, 545-51.

SIMON, C., ESCOBEDO, C., VALBUENA, D., GENBACEV, O., GALAN, A., KRTOLICA, A., ASENSI, A., SANCHEZ, E., ESPLUGUES, J., FISHER, S. & PELLICER, A. (2005) First derivation in Spain of human embryonic stem cell lines: use of long-term cryopreserved embryos and animal-free conditions. *Fertil Steril*, 83, 246-9.

SKOTTMAN, H., DILBER, M. S. & HOVATTA, O. (2006) The derivation of clinical-grade human embryonic stem cell lines. *FEBS Lett*, 580, 2875-8.

SKOTTMAN, H., MIKKOLA, M., LUNDIN, K., OLSSON, C., STROMBERG, A. M., TUURI, T., OTONKOSKI, T., HOVATTA, O. & LAHESMAA, R. (2005) Gene expression signatures of seven individual human embryonic stem cell lines. *Stem Cells*, 23, 1343-56.

SLACK, J. M. (1994) Inducing factors in Xenopus early embryos. *Curr Biol*, 4, 116-26.

SLUKVIN, II, VODYANIK, M. A., THOMSON, J. A., GUMENYUK, M. E. & CHOI, K. D. (2006) Directed differentiation of human embryonic stem cells into functional dendritic cells through the myeloid pathway. *J Immunol*, 176, 2924-32.

SMITH-ARICA, J. R., THOMSON, A. J., ANSELL, R., CHIORINI, J., DAVIDSON, B. & MCWHIR, J. (2003) Infection efficiency of human and mouse embryonic stem cells using adenoviral and adeno-associated viral vectors. *Cloning Stem Cells*, 5, 51-62.

SMITH, A. (2005) The battlefield of pluripotency. *Cell*, 123, 757-60.

SMITH, A. G., HEATH, J. K., DONALDSON, D. D., WONG, G. G., MOREAU, J., STAHL, M. & ROGERS, D. (1988) Inhibition of pluripotential embryonic stem cell differentiation by purified polypeptides. *Nature*, 336, 688-90.

SMITH, A. G. & HOOPER, M. L. (1987) Buffalo rat liver cells produce a diffusible activity which inhibits the differentiation of murine embryonal carcinoma and embryonic stem cells. *Dev Biol*, 121, 1-9.

SMYTH, N., VATANSEVER, H. S., MURRAY, P., MEYER, M., FRIE, C., PAULSSON, M. & EDGAR, D. (1999) Absence of basement membranes after targeting the LAMC1 gene results in embryonic lethality due to failure of endoderm differentiation. *J Cell Biol*, 144, 151-60.

SNIR, M., KEHAT, I., GEPSTEIN, A., COLEMAN, R., ITSKOVITZ-ELDOR, J., LIVNE, E. & GEPSTEIN, L. (2003) Assessment of the ultrastructural and proliferative properties of human embryonic stem cell-derived cardiomyocytes. *Am J Physiol Heart Circ Physiol*, 285, H2355-63.

SODERDAHL, T., KUPPERS-MUNTHER, B., HEINS, N., EDSBAGGE, J., BJORQUIST, P., COTGREAVE, I. & JERNSTROM, B. (2007) Glutathione transferases in hepatocyte-like cells derived from human embryonic stem cells. *Toxicol In Vitro*, 21, 929-37.

SOLTER, D. & KNOWLES, B. B. (1975) Immunosurgery of mouse blastocyst. *Proc Natl Acad Sci U S A*, 72, 5099-102.

SONG, J., OH, S. P., SCHREWE, H., NOMURA, M., LEI, H., OKANO, M., GRIDLEY, T. & LI, E. (1999) The type II activin receptors are essential for

egg cylinder growth, gastrulation, and rostral head development in mice. *Dev Biol,* 213, 157-69.

SOTTILE, V., THOMSON, A. & MCWHIR, J. (2003) In vitro osteogenic differentiation of human ES cells. *Cloning Stem Cells,* 5, 149-55.

SPAGNOLI, F. M. & HEMMATI-BRIVANLOU, A. (2006) Guiding embryonic stem cells towards differentiation: lessons from molecular embryology. *Curr Opin Genet Dev,* 16, 469-75.

SPERGER, J. M., CHEN, X., DRAPER, J. S., ANTOSIEWICZ, J. E., CHON, C. H., JONES, S. B., BROOKS, J. D., ANDREWS, P. W., BROWN, P. O. & THOMSON, J. A. (2003) Gene expression patterns in human embryonic stem cells and human pluripotent germ cell tumors. *Proc Natl Acad Sci U S A,* 100, 13350-5.

SPYROPOULOS, D. D. & CAPECCHI, M. R. (1994) Targeted disruption of the even-skipped gene, evx1, causes early postimplantation lethality of the mouse conceptus. *Genes Dev,* 8, 1949-61.

SRINIVAS, S., RODRIGUEZ, T., CLEMENTS, M., SMITH, J. C. & BEDDINGTON, R. S. (2004) Active cell migration drives the unilateral movements of the anterior visceral endoderm. *Development,* 131, 1157-64.

SRIVASTAVA, A. S., NEDELCU, E., ESMAELI-AZAD, B., MISHRA, R. & CARRIER, E. (2007) Thrombopoietin enhances generation of CD34+ cells from human embryonic stem cells. *Stem Cells,* 25, 1456-61.

STARY, M., PASTEINER, W., SUMMER, A., HRDINA, A., EGER, A. & WEITZER, G. (2005) Parietal endoderm secreted SPARC promotes early cardiomyogenesis in vitro. *Exp Cell Res,* 310, 331-43.

STEVANOVIC, M., LOVELL-BADGE, R., COLLIGNON, J. & GOODFELLOW, P. N. (1993) SOX3 is an X-linked gene related to SRY. *Hum Mol Genet,* 2, 2013-8.

STEVENS, L. C. & LITTLE, C. C. (1954) Spontaneous Testicular Teratomas in an Inbred Strain of Mice. *Proc Natl Acad Sci U S A,* 40, 1080-7.

STEWART, C. L., KASPAR, P., BRUNET, L. J., BHATT, H., GADI, I., KONTGEN, F. & ABBONDANZO, S. J. (1992) Blastocyst implantation depends on maternal expression of leukaemia inhibitory factor. *Nature,* 359, 76-9.

STEWART, R., STOJKOVIC, M. & LAKO, M. (2006) Mechanisms of self-renewal in human embryonic stem cells. *Eur J Cancer,* 42, 1257-72.

STOJKOVIC, M., LAKO, M., STOJKOVIC, P., STEWART, R., PRZYBORSKI, S., ARMSTRONG, L., EVANS, J., HERBERT, M., HYSLOP, L., AHMAD, S., MURDOCH, A. & STRACHAN, T. (2004a) Derivation of human embryonic stem cells from day-8 blastocysts recovered after three-step in vitro culture. *Stem Cells,* 22, 790-7.

STOJKOVIC, M., LAKO, M., STRACHAN, T. & MURDOCH, A. (2004b) Derivation, growth and applications of human embryonic stem cells. *Reproduction,* 128, 259-67.

STOJKOVIC, P., LAKO, M., PRZYBORSKI, S., STEWART, R., ARMSTRONG, L., EVANS, J., ZHANG, X. & STOJKOVIC, M. (2005) Human-serum matrix supports undifferentiated growth of human embryonic stem cells. *Stem Cells,* 23, 895-902.

STRELCHENKO, N., VERLINSKY, O., KUKHARENKO, V. & VERLINSKY, Y. (2004) Morula-derived human embryonic stem cells. *Reprod Biomed Online,* 9, 623-9.

STRUMPF, D., MAO, C. A., YAMANAKA, Y., RALSTON, A., CHAWENGSAKSOPHAK, K., BECK, F. & ROSSANT, J. (2005) Cdx2 is required for correct cell fate specification and differentiation of trophectoderm in the mouse blastocyst. *Development,* 132, 2093-102.

SUAREZ-FARINAS, M., NOGGLE, S., HEKE, M., HEMMATI-BRIVANLOU, A. & MAGNASCO, M. O. (2005) Comparing independent microarray studies: the case of human embryonic stem cells. *BMC Genomics,* 6, 99.

SUEMORI, H., TADA, T., TORII, R., HOSOI, Y., KOBAYASHI, K., IMAHIE, H., KONDO, Y., IRITANI, A. & NAKATSUJI, N. (2001) Establishment of embryonic stem cell lines from cynomolgus monkey blastocysts produced by IVF or ICSI. *Dev Dyn,* 222, 273-9.

SUN, X., MEYERS, E. N., LEWANDOSKI, M. & MARTIN, G. R. (1999) Targeted disruption of Fgf8 causes failure of cell migration in the gastrulating mouse embryo. *Genes Dev,* 13, 1834-46.

SUSS-TOBY, E., GERECHT-NIR, S., AMIT, M., MANOR, D. & ITSKOVITZ-ELDOR, J. (2004) Derivation of a diploid human embryonic stem cell line from a mononuclear zygote. *Hum Reprod,* 19, 670-5.

SUZUKI, A., RAYA, A., KAWAKAMI, Y., MORITA, M., MATSUI, T., NAKASHIMA, K., GAGE, F. H., RODRIGUEZ-ESTEBAN, C. & BELMONTE, J. C. (2006) Maintenance of embryonic stem cell pluripotency by Nanog-mediated reversal of mesoderm specification. *Nat Clin Pract Cardiovasc Med,* 3 Suppl 1, S114-22.

SWIERS, G., PATIENT, R. & LOOSE, M. (2006) Genetic regulatory networks programming hematopoietic stem cells and erythroid lineage specification. *Dev Biol,* 294, 525-40.

SYKES, M. (2001) Mixed chimerism and transplant tolerance. *Immunity,* 14, 417-24.

TADA, S., ERA, T., FURUSAWA, C., SAKURAI, H., NISHIKAWA, S., KINOSHITA, M., NAKAO, K., CHIBA, T. & NISHIKAWA, S. (2005) Characterization of mesendoderm: a diverging point of the definitive endoderm and mesoderm in embryonic stem cell differentiation culture. *Development,* 132, 4363-74.

TAKAHASHI, K. & YAMANAKA, S. (2006) Induction of pluripotent stem cells from mouse embryonic and adult fibroblast cultures by defined factors. *Cell,* 126, 663-76.

TAKAHASHI, S., YOKOTA, C., TAKANO, K., TANEGASHIMA, K., ONUMA, Y., GOTO, J. & ASASHIMA, M. (2000) Two novel nodal-related genes initiate early inductive events in Xenopus Nieuwkoop center. *Development,* 127, 5319-29.

TAKAOKA, K., YAMAMOTO, M. & HAMADA, H. (2007) Origin of body axes in the mouse embryo. *Curr Opin Genet Dev,* 17, 344-50.

TAKAOKA, K., YAMAMOTO, M., SHIRATORI, H., MENO, C., ROSSANT, J., SAIJOH, Y. & HAMADA, H. (2006) The mouse embryo autonomously acquires anterior-posterior polarity at implantation. *Dev Cell,* 10, 451-9.

TAKEDA, K., NOGUCHI, K., SHI, W., TANAKA, T., MATSUMOTO, M., YOSHIDA, N., KISHIMOTO, T. & AKIRA, S. (1997) Targeted disruption of the mouse Stat3 gene leads to early embryonic lethality. *Proc Natl Acad Sci U S A,* 94, 3801-4.

TAM, P. P. & BEDDINGTON, R. S. (1987) The formation of mesodermal tissues in the mouse embryo during gastrulation and early organogenesis. *Development,* 99, 109-26.

TAM, P. P. & BEHRINGER, R. R. (1997) Mouse gastrulation: the formation of a mammalian body plan. *Mech Dev,* 68, 3-25.

TAM, P. P., KHOO, P. L., LEWIS, S. L., BILDSOE, H., WONG, N., TSANG, T. E., GAD, J. M. & ROBB, L. (2007) Sequential allocation and global pattern of movement of the definitive endoderm in the mouse embryo during gastrulation. *Development,* 134, 251-60.

TAM, P. P., KHOO, P. L., WONG, N., TSANG, T. E. & BEHRINGER, R. R. (2004) Regionalization of cell fates and cell movement in the endoderm of the mouse gastrula and the impact of loss of Lhx1(Lim1) function. *Dev Biol,* 274, 171-87.

TAM, P. P. & LOEBEL, D. A. (2007) Gene function in mouse embryogenesis: get set for gastrulation. *Nat Rev Genet,* 8, 368-81.

TAM, P. P. & STEINER, K. A. (1999) Anterior patterning by synergistic activity of the early gastrula organizer and the anterior germ layer tissues of the mouse embryo. *Development,* 126, 5171-9.

TERADA, N., HAMAZAKI, T., OKA, M., HOKI, M., MASTALERZ, D. M., NAKANO, Y., MEYER, E. M., MOREL, L., PETERSEN, B. E. & SCOTT, E. W. (2002) Bone marrow cells adopt the phenotype of other cells by spontaneous cell fusion. *Nature,* 416, 542-5.

THOMAS, P. & BEDDINGTON, R. (1996) Anterior primitive endoderm may be responsible for patterning the anterior neural plate in the mouse embryo. *Curr Biol,* 6, 1487-96.

THOMAS, P. Q., BROWN, A. & BEDDINGTON, R. S. (1998) Hex: a homeobox gene revealing peri-implantation asymmetry in the mouse embryo and an early transient marker of endothelial cell precursors. *Development,* 125, 85-94.

THOMSON, J. A., ITSKOVITZ-ELDOR, J., SHAPIRO, S. S., WAKNITZ, M. A., SWIERGIEL, J. J., MARSHALL, V. S. & JONES, J. M. (1998) Embryonic stem cell lines derived from human blastocysts. *Science,* 282, 1145-7.

THOMSON, J. A., KALISHMAN, J., GOLOS, T. G., DURNING, M., HARRIS, C. P., BECKER, R. A. & HEARN, J. P. (1995) Isolation of a primate embryonic stem cell line. *Proc Natl Acad Sci U S A,* 92, 7844-8.

THOMSON, J. A., KALISHMAN, J., GOLOS, T. G., DURNING, M., HARRIS, C. P. & HEARN, J. P. (1996) Pluripotent cell lines derived from common marmoset (Callithrix jacchus) blastocysts. *Biol Reprod,* 55, 254-9.

THOMSON, J. A. & MARSHALL, V. S. (1998) Primate embryonic stem cells. *Curr Top Dev Biol,* 38, 133-65.

TIAN, X., MORRIS, J. K., LINEHAN, J. L. & KAUFMAN, D. S. (2004) Cytokine requirements differ for stroma and embryoid body-mediated hematopoiesis from human embryonic stem cells. *Exp Hematol,* 32, 1000-9.

TOH, W. S., YANG, Z., LIU, H., HENG, B. C., LEE, E. H. & CAO, T. (2007) Effects of culture conditions and bone morphogenetic protein 2 on extent of chondrogenesis from human embryonic stem cells. *Stem Cells,* 25, 950-60.

TRACEY, W. D., JR., PEPLING, M. E., HORB, M. E., THOMSEN, G. H. & GERGEN, J. P. (1998) A Xenopus homologue of aml-1 reveals unexpected patterning mechanisms leading to the formation of embryonic blood. *Development,* 125, 1371-80.

TROUNSON, A. (2006) The production and directed differentiation of human embryonic stem cells. *Endocr Rev,* 27, 208-19.

TSAI, D. F. (2005) Human embryonic stem cell research debates: a Confucian argument. *J Med Ethics,* 31, 635-640.

URBACH, A., SCHULDINER, M. & BENVENISTY, N. (2004) Modeling for Lesch-Nyhan disease by gene targeting in human embryonic stem cells. *Stem Cells,* 22, 635-41.

VALLIER, L., ALEXANDER, M. & PEDERSEN, R. (2007) Conditional gene expression in human embryonic stem cells. *Stem Cells,* 25, 1490-7.

VALLIER, L., ALEXANDER, M. & PEDERSEN, R. A. (2005) Activin/Nodal and FGF pathways cooperate to maintain pluripotency of human embryonic stem cells. *J Cell Sci,* 118, 4495-509.

VALLIER, L. & PEDERSEN, R. A. (2005) Human embryonic stem cells: an in vitro model to study mechanisms controlling pluripotency in early mammalian development. *Stem Cell Rev,* 1, 119-30.

VALLIER, L., REYNOLDS, D. & PEDERSEN, R. A. (2004a) Nodal inhibits differentiation of human embryonic stem cells along the neuroectodermal default pathway. *Dev Biol,* 275, 403-21.

VALLIER, L., RUGG-GUNN, P. J., BOUHON, I. A., ANDERSSON, F. K., SADLER, A. J. & PEDERSEN, R. A. (2004b) Enhancing and diminishing gene function in human embryonic stem cells. *Stem Cells,* 22, 2-11.

VAN DRIESSCHE, A., PONSAERTS, P., VAN BOCKSTAELE, D. R., VAN TENDELOO, V. F. & BERNEMAN, Z. N. (2005) Messenger RNA electroporation: an efficient tool in immunotherapy and stem cell research. *Folia Histochem Cytobiol,* 43, 213-6.

VAN HOOF, D., PASSIER, R., WARD-VAN OOSTWAARD, D., PINKSE, M. W., HECK, A. J., MUMMERY, C. L. & KRIJGSVELD, J. (2006) A quest for human and mouse embryonic stem cell-specific proteins. *Mol Cell Proteomics,* 5, 1261-73.

VARLET, I., COLLIGNON, J. & ROBERTSON, E. J. (1997) nodal expression in the primitive endoderm is required for specification of the anterior axis during mouse gastrulation. *Development,* 124, 1033-44.

VERFAILLIE, C. M., PERA, M. F. & LANSDORP, P. M. (2002) Stem cells: hype and reality. *Hematology (Am Soc Hematol Educ Program),* 369-91.

VERHEIJEN, M. H., WOLTHUIS, R. M., BOS, J. L. & DEFIZE, L. H. (1999) The Ras/Erk pathway induces primitive endoderm but prevents parietal endoderm differentiation of F9 embryonal carcinoma cells. *J Biol Chem,* 274, 1487-94.

VINCENT, S. D., DUNN, N. R., HAYASHI, S., NORRIS, D. P. & ROBERTSON, E. J. (2003) Cell fate decisions within the mouse organizer are governed by graded Nodal signals. *Genes Dev,* 17, 1646-62.

VISVADER, J. & BEGLEY, C. G. (1991) Helix-loop-helix genes translocated in lymphoid leukemia. *Trends Biochem Sci,* 16, 330-3.

VISVADER, J. E., FUJIWARA, Y. & ORKIN, S. H. (1998) Unsuspected role for the T-cell leukemia protein SCL/tal-1 in vascular development. *Genes Dev,* 12, 473-9.

VODYANIK, M. A., BORK, J. A., THOMSON, J. A. & SLUKVIN, II (2005) Human embryonic stem cell-derived CD34+ cells: efficient production in the coculture with OP9 stromal cells and analysis of lymphohematopoietic potential. *Blood,* 105, 617-26.

VODYANIK, M. A., THOMSON, J. A. & SLUKVIN, II (2006) Leukosialin (CD43) defines hematopoietic progenitors in human embryonic stem cell differentiation cultures. *Blood,* 108, 2095-105.

VRANA, K. E., HIPP, J. D., GOSS, A. M., MCCOOL, B. A., RIDDLE, D. R., WALKER, S. J., WETTSTEIN, P. J., STUDER, L. P., TABAR, V., CUNNIFF, K., CHAPMAN, K., VILNER, L., WEST, M. D., GRANT, K. A. & CIBELLI, J. B. (2003) Nonhuman primate parthenogenetic stem cells. *Proc Natl Acad Sci U S A,* 100 Suppl 1, 11911-6.

WADMAN, I. A., OSADA, H., GRUTZ, G. G., AGULNICK, A. D., WESTPHAL, H., FORSTER, A. & RABBITTS, T. H. (1997) The LIM-only protein Lmo2 is a bridging molecule assembling an erythroid, DNA-binding complex which includes the TAL1, E47, GATA-1 and Ldb1/NLI proteins. *Embo J,* 16, 3145-57.

WALMSLEY, M., CIAU-UITZ, A. & PATIENT, R. (2002) Adult and embryonic blood and endothelium derive from distinct precursor populations which are differentially programmed by BMP in Xenopus. *Development,* 129, 5683-95.

WANG, D., HAVILAND, D. L., BURNS, A. R., ZSIGMOND, E. & WETSEL, R. A. (2007a) A pure population of lung alveolar epithelial type II cells derived from human embryonic stem cells. *Proc Natl Acad Sci U S A,* 104, 4449-54.

WANG, G., ZHANG, H., ZHAO, Y., LI, J., CAI, J., WANG, P., MENG, S., FENG, J., MIAO, C., DING, M., LI, D. & DENG, H. (2005a) Noggin and bFGF cooperate to maintain the pluripotency of human embryonic stem cells in the absence of feeder layers. *Biochem Biophys Res Commun,* 330, 934-42.

WANG, J., RAO, S., CHU, J., SHEN, X., LEVASSEUR, D. N., THEUNISSEN, T. W. & ORKIN, S. H. (2006) A protein interaction network for pluripotency of embryonic stem cells. *Nature,* 444, 364-368.

WANG, L., LI, L., SHOJAEI, F., LEVAC, K., CERDAN, C., MENENDEZ, P., MARTIN, T., ROULEAU, A. & BHATIA, M. (2004) Endothelial and hematopoietic cell fate of human embryonic stem cells originates from primitive endothelium with hemangioblastic properties. *Immunity,* 21, 31-41.

WANG, L., MENENDEZ, P., CERDAN, C. & BHATIA, M. (2005b) Hematopoietic development from human embryonic stem cell lines. *Exp Hematol,* 33, 987-96.

WANG, L., MENENDEZ, P., SHOJAEI, F., LI, L., MAZURIER, F., DICK, J. E., CERDAN, C., LEVAC, K. & BHATIA, M. (2005c) Generation of hematopoietic repopulating cells from human embryonic stem cells independent of ectopic HOXB4 expression. *J Exp Med,* 201, 1603-14.

WANG, Q., FANG, Z. F., JIN, F., LU, Y., GAI, H. & SHENG, H. Z. (2005d) Derivation and growing human embryonic stem cells on feeders derived from themselves. *Stem Cells,* 23, 1221-7.

WANG, W. H. & SUN, X. F. (2005) Human embryonic stem cell lines are contaminated: what should we do? *Hum Reprod,* 20, 2987-9.

WANG, Z. Z., AU, P., CHEN, T., SHAO, Y., DAHERON, L. M., BAI, H., ARZIGIAN, M., FUKUMURA, D., JAIN, R. K. & SCADDEN, D. T. (2007b) Endothelial cells derived from human embryonic stem cells form durable blood vessels in vivo. *Nat Biotechnol,* 25, 317-8.

WARDLE, F. C. & SMITH, J. C. (2006) Transcriptional regulation of mesendoderm formation in Xenopus. *Semin Cell Dev Biol,* 17, 99-109.

WARE, C. B., NELSON, A. M. & BLAU, C. A. (2006) A comparison of NIH-approved human ESC lines. *Stem Cells,* 24, 2677-84.

WARGA, R. M. & NUSSLEIN-VOLHARD, C. (1999) Origin and development of the zebrafish endoderm. *Development,* 126, 827-38.

WARTENBERG, M., GUNTHER, J., HESCHELER, J. & SAUER, H. (1998) The
embryoid body as a novel in vitro assay system for antiangiogenic agents.
Lab Invest, 78, 1301-14.

WEI, C. L., MIURA, T., ROBSON, P., LIM, S. K., XU, X. Q., LEE, M. Y., GUPTA,
S., STANTON, L., LUO, Y., SCHMITT, J., THIES, S., WANG, W.,
KHREBTUKOVA, I., ZHOU, D., LIU, E. T., RUAN, Y. J., RAO, M. &
LIM, B. (2005) Transcriptome profiling of human and murine ESCs
identifies divergent paths required to maintain the stem cell state. *Stem Cells,*
23, 166-85.

WEISS, M. J., KELLER, G. & ORKIN, S. H. (1994) Novel insights into erythroid
development revealed through in vitro differentiation of GATA-1 embryonic
stem cells. *Genes Dev,* 8, 1184-97.

WEISS, M. J. & ORKIN, S. H. (1995) GATA transcription factors: key regulators of
hematopoiesis. *Exp Hematol,* 23, 99-107.

WEISSMAN, I. (2005) Stem cell research: paths to cancer therapies and regenerative
medicine. *Jama,* 294, 1359-66.

WEISSMAN, I. L. (2000) Stem cells: units of development, units of regeneration,
and units in evolution. *Cell,* 100, 157-68.

WEITZER, G. (2006) Embryonic stem cell-derived embryoid bodies: an in vitro
model of eutherian pregastrulation development and early gastrulation.
Handb Exp Pharmacol, 21-51.

WERNIG, M., MEISSNER, A., FOREMAN, R., BRAMBRINK, T., KU, M.,
HOCHEDLINGER, K., BERNSTEIN, B. E. & JAENISCH, R. (2007) In
vitro reprogramming of fibroblasts into a pluripotent ES-cell-like state.
Nature, 448, 318-24.

WILDER, P. J., KELLY, D., BRIGMAN, K., PETERSON, C. L., NOWLING, T.,
GAO, Q. S., MCCOMB, R. D., CAPECCHI, M. R. & RIZZINO, A. (1997)
Inactivation of the FGF-4 gene in embryonic stem cells alters the growth
and/or the survival of their early differentiated progeny. *Dev Biol,* 192, 614-
29.

WILES, M. V. & JOHANSSON, B. M. (1999) Embryonic stem cell development in
a chemically defined medium. *Exp Cell Res,* 247, 241-8.

WILKINSON, D. G., BHATT, S. & HERRMANN, B. G. (1990) Expression pattern
of the mouse T gene and its role in mesoderm formation. *Nature,* 343, 657-9.

WILLEMS, E., MATEIZEL, I., KEMP, C., CAUFFMAN, G., SERMON, K. &
LEYNS, L. (2006) Selection of reference genes in mouse embryos and in
differentiating human and mouse ES cells. *Int J Dev Biol,* 50, 627-35.

WILLEY, S., AYUSO-SACIDO, A., ZHANG, H., FRASER, S. T., SAHR, K. E.,
ADLAM, M. J., KYBA, M., DALEY, G. Q., KELLER, G. & BARON, M. H.
(2006) Acceleration of mesoderm development and expansion of
hematopoietic progenitors in differentiating ES cells by the mouse Mix-like
homeodomain transcription factor. *Blood,* 107, 3122-30.

WILLIAMS, R. L., HILTON, D. J., PEASE, S., WILLSON, T. A., STEWART, C.
L., GEARING, D. P., WAGNER, E. F., METCALF, D., NICOLA, N. A. &
GOUGH, N. M. (1988) Myeloid leukaemia inhibitory factor maintains the
developmental potential of embryonic stem cells. *Nature,* 336, 684-7.

WILSON, M. & KOOPMAN, P. (2002) Matching SOX: partner proteins and co-
factors of the SOX family of transcriptional regulators. *Curr Opin Genet Dev,*
12, 441-6.

WILSON, V. & CONLON, F. L. (2002) The T-box family. *Genome Biol,* 3, REVIEWS3008.

WILSON, V., RASHBASS, P. & BEDDINGTON, R. S. (1993) Chimeric analysis of T (Brachyury) gene function. *Development,* 117, 1321-31.

WINNIER, G., BLESSING, M., LABOSKY, P. A. & HOGAN, B. L. (1995) Bone morphogenetic protein-4 is required for mesoderm formation and patterning in the mouse. *Genes Dev,* 9, 2105-16.

WOBUS, A. M. & BOHELER, K. R. (2005) Embryonic stem cells: prospects for developmental biology and cell therapy. *Physiol Rev,* 85, 635-78.

WOBUS, A. M., WALLUKAT, G. & HESCHELER, J. (1991) Pluripotent mouse embryonic stem cells are able to differentiate into cardiomyocytes expressing chronotropic responses to adrenergic and cholinergic agents and Ca2+ channel blockers. *Differentiation,* 48, 173-82.

WOLL, P. S., MARTIN, C. H., MILLER, J. S. & KAUFMAN, D. S. (2005) Human embryonic stem cell-derived NK cells acquire functional receptors and cytolytic activity. *J Immunol,* 175, 5095-103.

WOOD, H. B. & EPISKOPOU, V. (1999) Comparative expression of the mouse Sox1, Sox2 and Sox3 genes from pre-gastrulation to early somite stages. *Mech Dev,* 86, 197-201.

WURMSER, A. E. & GAGE, F. H. (2002) Stem cells: cell fusion causes confusion. *Nature,* 416, 485-7.

XIAO, L., YUAN, X. & SHARKIS, S. J. (2006) Activin A maintains self-renewal and regulates fibroblast growth factor, Wnt, and bone morphogenic protein pathways in human embryonic stem cells. *Stem Cells,* 24, 1476-86.

XIONG, C., XIE, C. Q., ZHANG, L., ZHANG, J., XU, K., FU, M., THOMPSON, W. E., YANG, L. J. & CHEN, Y. E. (2005) Derivation of adipocytes from human embryonic stem cells. *Stem Cells Dev,* 14, 671-5.

XU, C., INOKUMA, M. S., DENHAM, J., GOLDS, K., KUNDU, P., GOLD, J. D. & CARPENTER, M. K. (2001) Feeder-free growth of undifferentiated human embryonic stem cells. *Nat Biotechnol,* 19, 971-4.

XU, C., POLICE, S., RAO, N. & CARPENTER, M. K. (2002a) Characterization and enrichment of cardiomyocytes derived from human embryonic stem cells. *Circ Res,* 91, 501-8.

XU, C., ROSLER, E., JIANG, J., LEBKOWSKI, J. S., GOLD, J. D., O'SULLIVAN, C., DELAVAN-BOORSMA, K., MOK, M., BRONSTEIN, A. & CARPENTER, M. K. (2005a) Basic fibroblast growth factor supports undifferentiated human embryonic stem cell growth without conditioned medium. *Stem Cells,* 23, 315-23.

XU, R. H., AULT, K. T., KIM, J., PARK, M. J., HWANG, Y. S., PENG, Y., SREDNI, D. & KUNG, H. (1999) Opposite effects of FGF and BMP-4 on embryonic blood formation: roles of PV.1 and GATA-2. *Dev Biol,* 208, 352-61.

XU, R. H., CHEN, X., LI, D. S., LI, R., ADDICKS, G. C., GLENNON, C., ZWAKA, T. P. & THOMSON, J. A. (2002b) BMP4 initiates human embryonic stem cell differentiation to trophoblast. *Nat Biotechnol,* 20, 1261-4.

XU, R. H., PECK, R. M., LI, D. S., FENG, X., LUDWIG, T. & THOMSON, J. A. (2005b) Basic FGF and suppression of BMP signaling sustain undifferentiated proliferation of human ES cells. *Nat Methods,* 2, 185-90.

XU, Z., HUANG, S., CHANG, L. S., AGULNICK, A. D. & BRANDT, S. J. (2003) Identification of a TAL1 target gene reveals a positive role for the LIM domain-binding protein Ldb1 in erythroid gene expression and differentiation. *Mol Cell Biol*, 23, 7585-99.

XUE, T., CHO, H. C., AKAR, F. G., TSANG, S. Y., JONES, S. P., MARBAN, E., TOMASELLI, G. F. & LI, R. A. (2005) Functional integration of electrically active cardiac derivatives from genetically engineered human embryonic stem cells with quiescent recipient ventricular cardiomyocytes: insights into the development of cell-based pacemakers. *Circulation*, 111, 11-20.

YAMADA, G., KIOUSSI, C., SCHUBERT, F. R., ETO, Y., CHOWDHURY, K., PITUELLO, F. & GRUSS, P. (1994) Regulated expression of Brachyury(T), Nkx1.1 and Pax genes in embryoid bodies. *Biochem Biophys Res Commun*, 199, 552-63.

YAMADA, Y., WARREN, A. J., DOBSON, C., FORSTER, A., PANNELL, R. & RABBITTS, T. H. (1998) The T cell leukemia LIM protein Lmo2 is necessary for adult mouse hematopoiesis. *Proc Natl Acad Sci U S A*, 95, 3890-5.

YAMAGUCHI, S., KIMURA, H., TADA, M., NAKATSUJI, N. & TADA, T. (2005) Nanog expression in mouse germ cell development. *Gene Expr Patterns*, 5, 639-46.

YAMAGUCHI, T. P., CONLON, R. A. & ROSSANT, J. (1992) Expression of the fibroblast growth factor receptor FGFR-1/flg during gastrulation and segmentation in the mouse embryo. *Dev Biol*, 152, 75-88.

YAMAGUCHI, T. P., TAKADA, S., YOSHIKAWA, Y., WU, N. & MCMAHON, A. P. (1999) T (Brachyury) is a direct target of Wnt3a during paraxial mesoderm specification. *Genes Dev*, 13, 3185-90.

YAMAMOTO, M., SAIJOH, Y., PEREA-GOMEZ, A., SHAWLOT, W., BEHRINGER, R. R., ANG, S. L., HAMADA, H. & MENO, C. (2004) Nodal antagonists regulate formation of the anteroposterior axis of the mouse embryo. *Nature*, 428, 387-92.

YAMANAKA, S. (2007) Strategies and New Developments in the Generation of Patient-Specific Pluripotent Stem Cells. *Cell Stem Cell*, 1, 39-49.

YAN, Y., YANG, D., ZARNOWSKA, E. D., DU, Z., WERBEL, B., VALLIERE, C., PEARCE, R. A., THOMSON, J. A. & ZHANG, S. C. (2005) Directed differentiation of dopaminergic neuronal subtypes from human embryonic stem cells. *Stem Cells*, 23, 781-90.

YAN, Y. T., LIU, J. J., LUO, Y., E, C., HALTIWANGER, R. S., ABATE-SHEN, C. & SHEN, M. M. (2002) Dual roles of Cripto as a ligand and coreceptor in the nodal signaling pathway. *Mol Cell Biol*, 22, 4439-49.

YAO, S., CHEN, S., CLARK, J., HAO, E., BEATTIE, G. M., HAYEK, A. & DING, S. (2006) Long-term self-renewal and directed differentiation of human embryonic stem cells in chemically defined conditions. *Proc Natl Acad Sci U S A*, 103, 6907-12.

YASUNAGA, M., TADA, S., TORIKAI-NISHIKAWA, S., NAKANO, Y., OKADA, M., JAKT, L. M., NISHIKAWA, S., CHIBA, T., ERA, T. & NISHIKAWA, S. (2005) Induction and monitoring of definitive and visceral endoderm differentiation of mouse ES cells. *Nat Biotechnol*, 23, 1542-50.

YATES, F. & DALEY, G. Q. (2006) Progress and prospects: gene transfer into embryonic stem cells. *Gene Ther*, 13, 1431-9.

YEO, C. & WHITMAN, M. (2001) Nodal signals to Smads through Cripto-dependent and Cripto-independent mechanisms. *Mol Cell*, 7, 949-57.

YEOM, Y. I., FUHRMANN, G., OVITT, C. E., BREHM, A., OHBO, K., GROSS. M., HUBNER, K. & SCHOLER, H. R. (1996) Germline regulatory element of Oct-4 specific for the totipotent cycle of embryonal cells. *Development*, 122, 881-94.

YING, Q. L., NICHOLS, J., CHAMBERS, I. & SMITH, A. (2003) BMP induction of Id proteins suppresses differentiation and sustains embryonic stem cell self-renewal in collaboration with STAT3. *Cell*, 115, 281-92.

YING, Q. L., NICHOLS, J., EVANS, E. P. & SMITH, A. G. (2002) Changing potency by spontaneous fusion. *Nature*, 416, 545-8.

YOON, B. S., YOO, S. J., LEE, J. E., YOU, S., LEE, H. T. & YOON, H. S. (2006) Enhanced differentiation of human embryonic stem cells into cardiomyocytes by combining hanging drop culture and 5-azacytidine treatment. *Differentiation*, 74, 149-59.

YOSHIKAWA, T., PIAO, Y., ZHONG, J., MATOBA, R., CARTER, M. G., WANG, Y., GOLDBERG, I. & KO, M. S. (2006) High-throughput screen for genes predominantly expressed in the ICM of mouse blastocysts by whole mount in situ hybridization. *Gene Expr Patterns*, 6, 213-24.

YOSHIMIZU, T., SUGIYAMA, N., DE FELICE, M., YEOM, Y. I., OHBO, K., MASUKO, K., OBINATA, M., ABE, K., SCHOLER, H. R. & MATSUI, Y. (1999) Germline-specific expression of the Oct-4/green fluorescent protein (GFP) transgene in mice. *Dev Growth Differ*, 41, 675-84.

ZAEHRES, H., LENSCH, M. W., DAHERON, L., STEWART, S. A., ITSKOVITZ-ELDOR, J. & DALEY, G. Q. (2005) High-efficiency RNA interference in human embryonic stem cells. *Stem Cells*, 23, 299-305.

ZAMBIDIS, E. T., PEAULT, B., PARK, T. S., BUNZ, F. & CIVIN, C. I. (2005) Hematopoietic differentiation of human embryonic stem cells progresses through sequential hematoendothelial, primitive, and definitive stages resembling human yolk sac development. *Blood*, 106, 860-70.

ZENG, X., CAI, J., CHEN, J., LUO, Y., YOU, Z. B., FOTTER, E., WANG, Y., HARVEY, B., MIURA, T., BACKMAN, C., CHEN, G. J., RAO, M. S. & FREED, W. J. (2004a) Dopaminergic differentiation of human embryonic stem cells. *Stem Cells*, 22, 925-40.

ZENG, X., MIURA, T., LUO, Y., BHATTACHARYA, B., CONDIE, B., CHEN, J., GINIS, I., LYONS, I., MEJIDO, J., PURI, R. K., RAO, M. S. & FREED, W. J. (2004b) Properties of pluripotent human embryonic stem cells BG01 and BG02. *Stem Cells*, 22, 292-312.

ZHAN, X., DRAVID, G., YE, Z., HAMMOND, H., SHAMBLOTT, M., GEARHART, J. & CHENG, L. (2004) Functional antigen-presenting leucocytes derived from human embryonic stem cells in vitro. *Lancet*, 364, 163-71.

ZHANG, C. & EVANS, T. (1996) BMP-like signals are required after the midblastula transition for blood cell development. *Dev Genet*, 18, 267-78.

ZHANG, H., SAEKI, K., KIMURA, A., SAEKI, K., NAKAHARA, M., DOSHI, M., KONDO, Y., NAKANO, T. & YUO, A. (2006) Efficient and repetitive production of hematopoietic and endothelial cells from feeder-free monolayer culture system of primate embryonic stem cells. *Biol Reprod*, 74, 295-306.

ZHANG, S. C., WERNIG, M., DUNCAN, I. D., BRUSTLE, O. & THOMSON. J. A. (2001) In vitro differentiation of transplantable neural precursors from human embryonic stem cells. *Nat Biotechnol,* 19, 1129-33.

ZHOU, Q., CHIPPERFIELD, H., MELTON, D. A. & WONG, W. H. (2007) A gene regulatory network in mouse embryonic stem cells. *Proc Natl Acad Sci U S A,* 104, 16438-43.

ZOLDAN, J. & LEVENBERG, S. (2006) Engineering three-dimensional tissue structures using stem cells. *Methods Enzymol,* 420, 381-91.

ZWAKA, T. P. & THOMSON, J. A. (2003) Homologous recombination in human embryonic stem cells. *Nat Biotechnol,* 21, 319-21.

ZWAKA, T. P. & THOMSON, J. A. (2005) Differentiation of human embryonic stem cells occurs through symmetric cell division. *Stem Cells,* 23, 146-9.

7 APPENDIX

7.1 BOND-MAX NEGATIVE CONTROLS

Figure 7-1: Supplementary images of negative controls for immunohistochemistry staining

Sections of whole E7.5 mouse embryos after immunohistochemistry for detection of the expression of T, SOX17 and MIXL1 and their respective negative Controls (with primary antibody omitted). Images of full embryos on are shown in A (using 10 x objective) and magnified areas of interest in B and C (20 x objective). Scale bar = 50 µm.
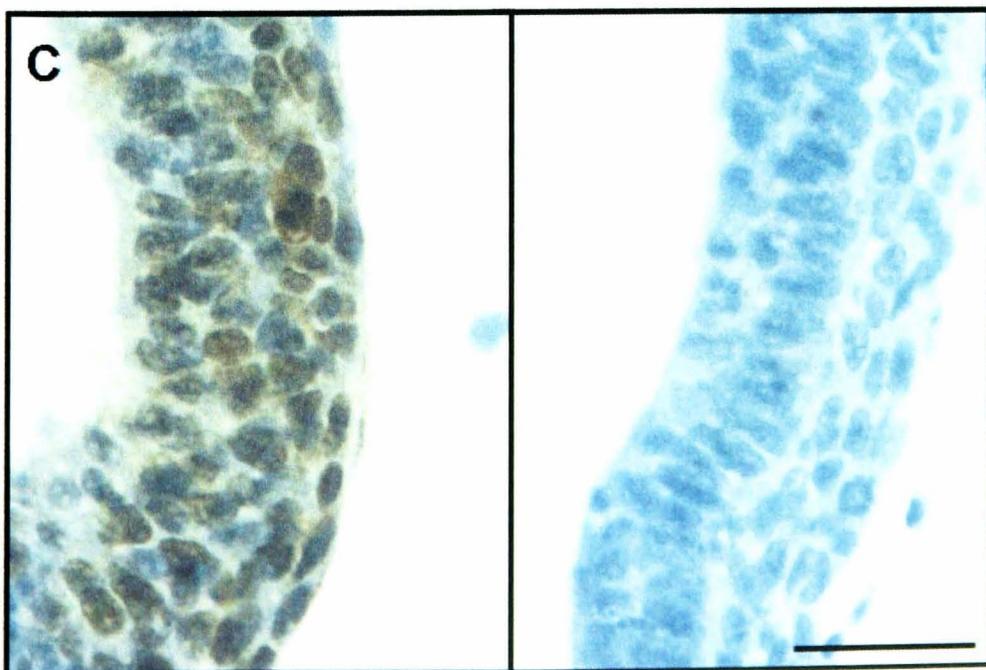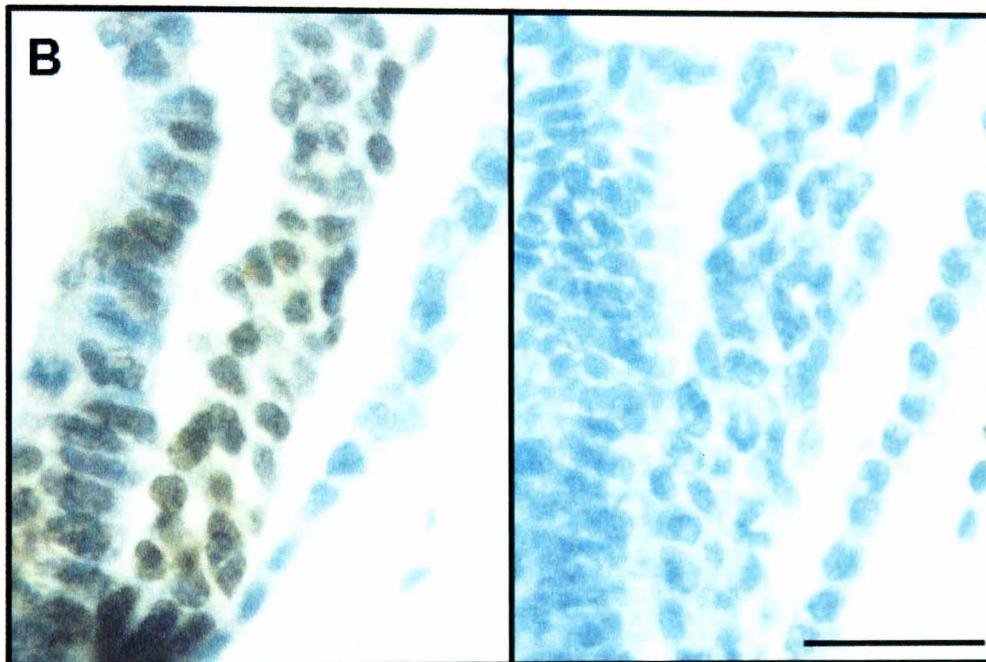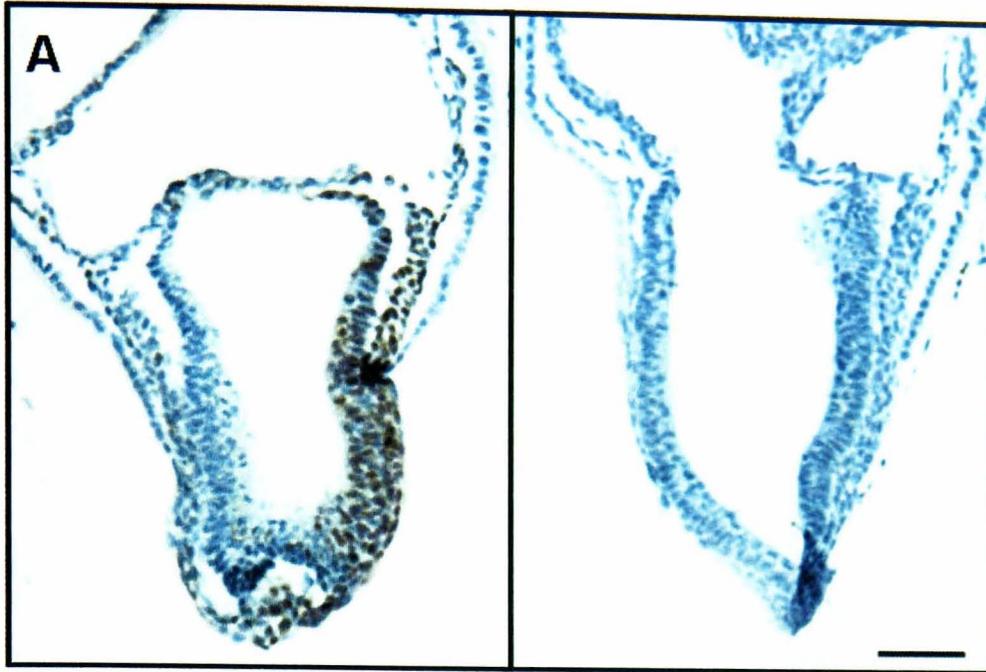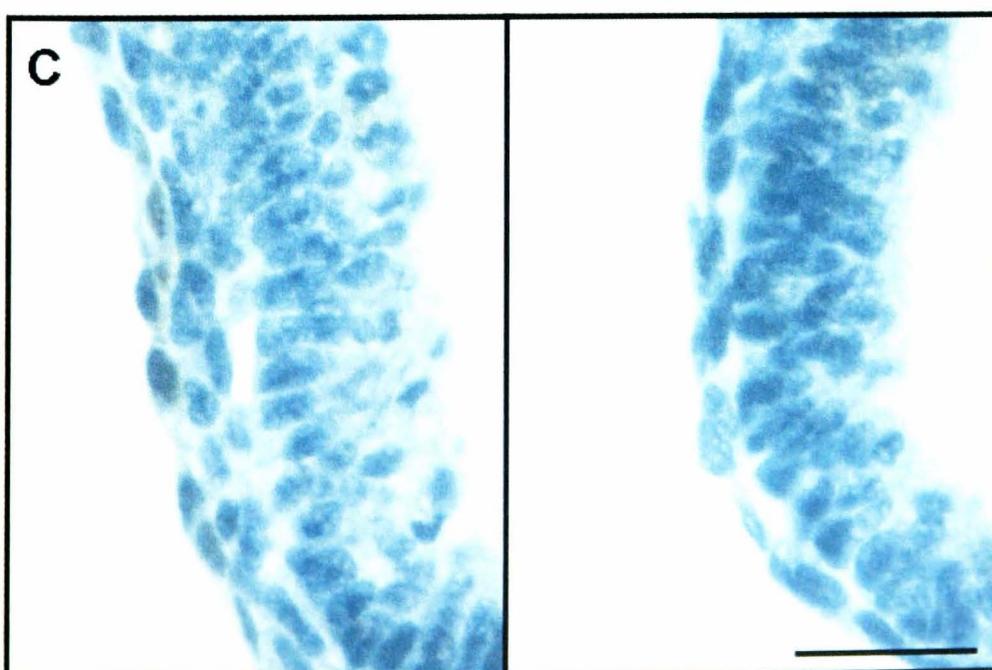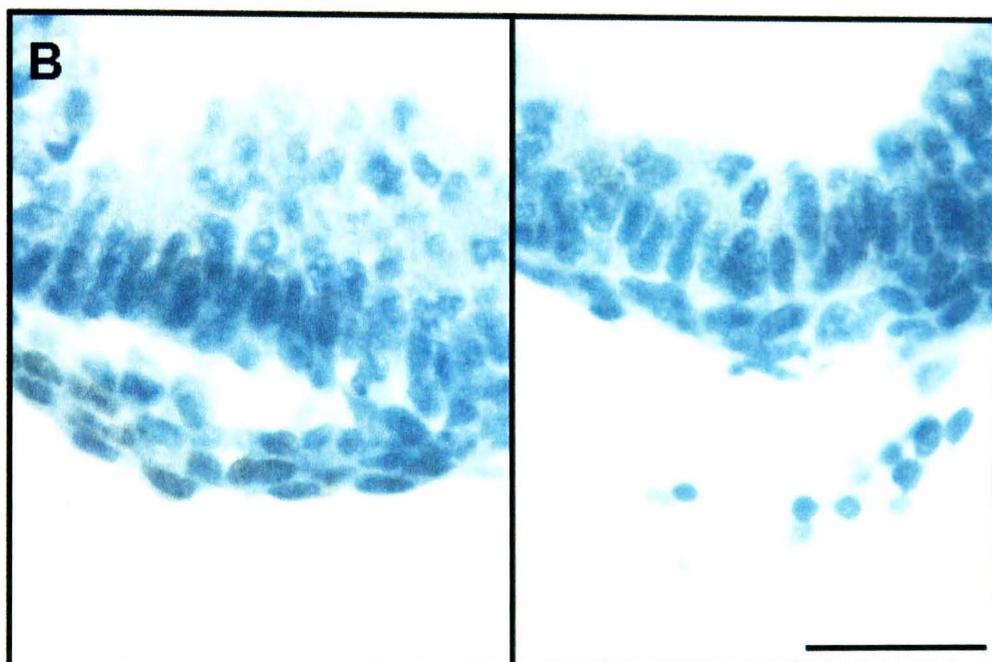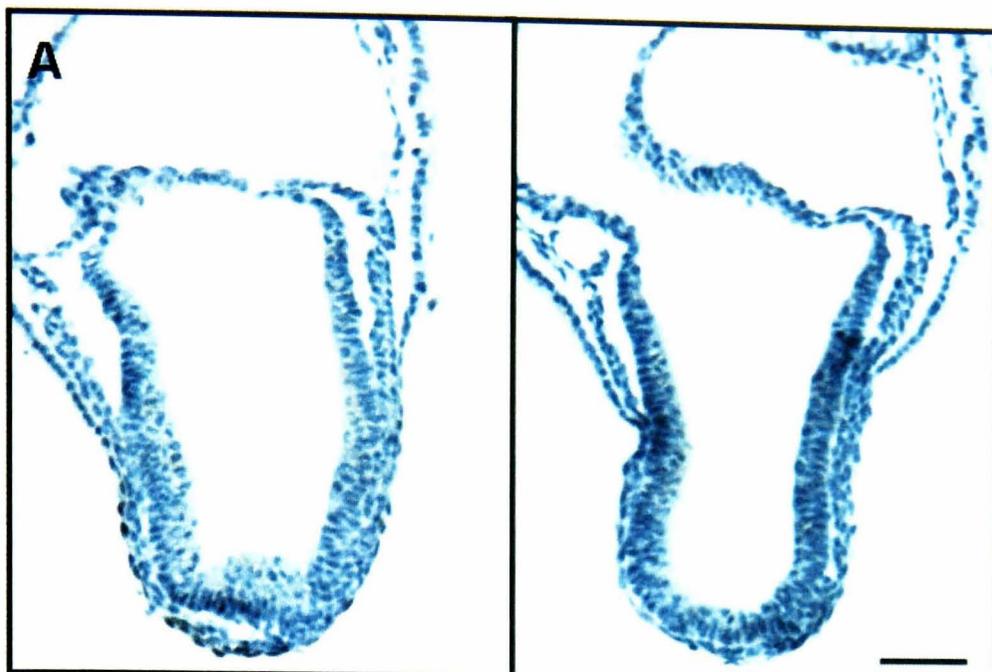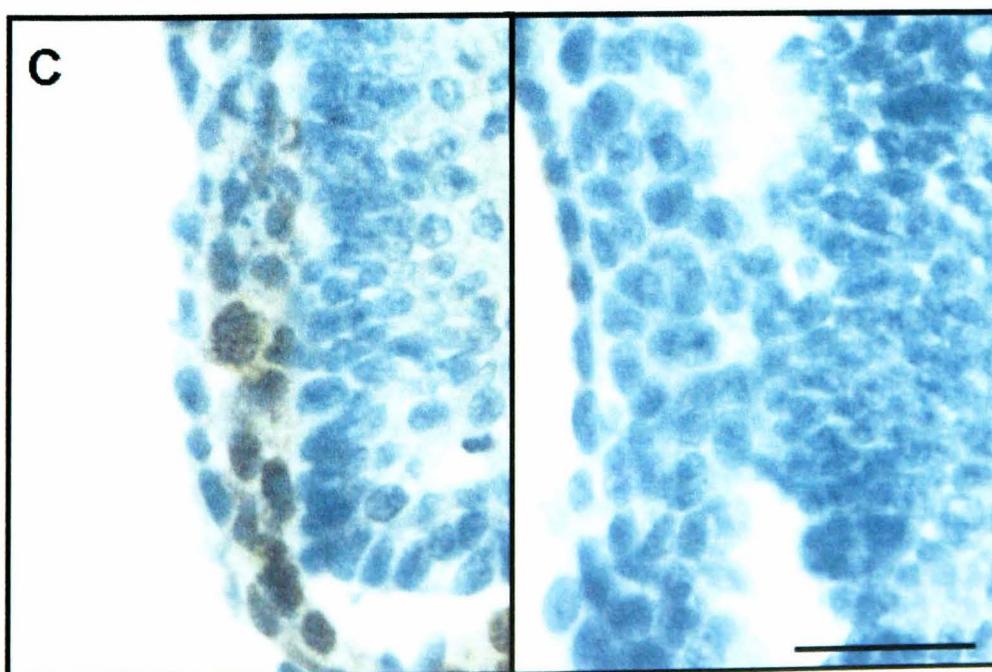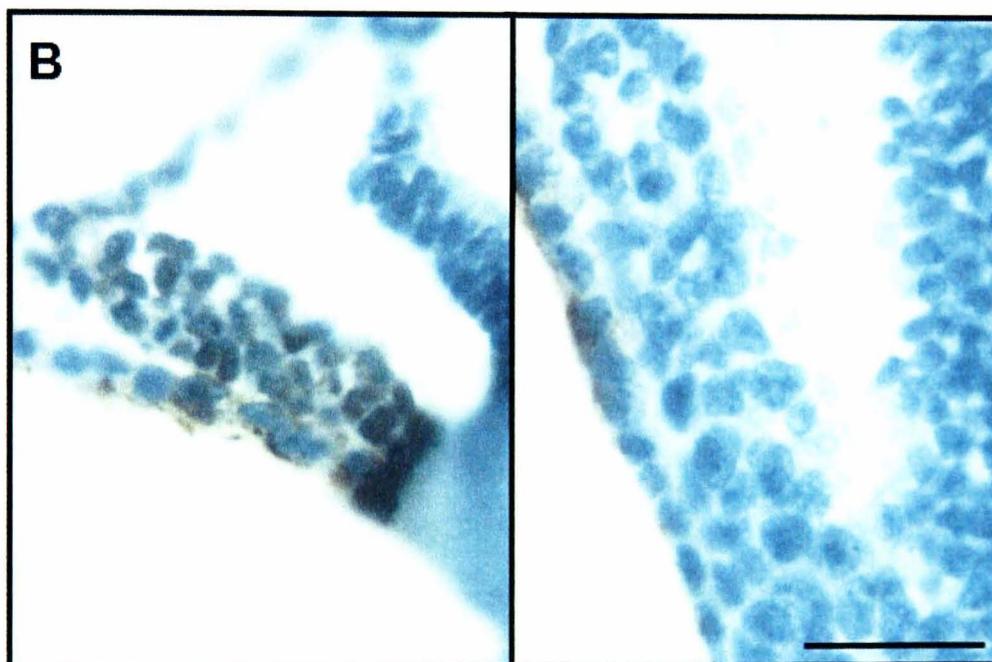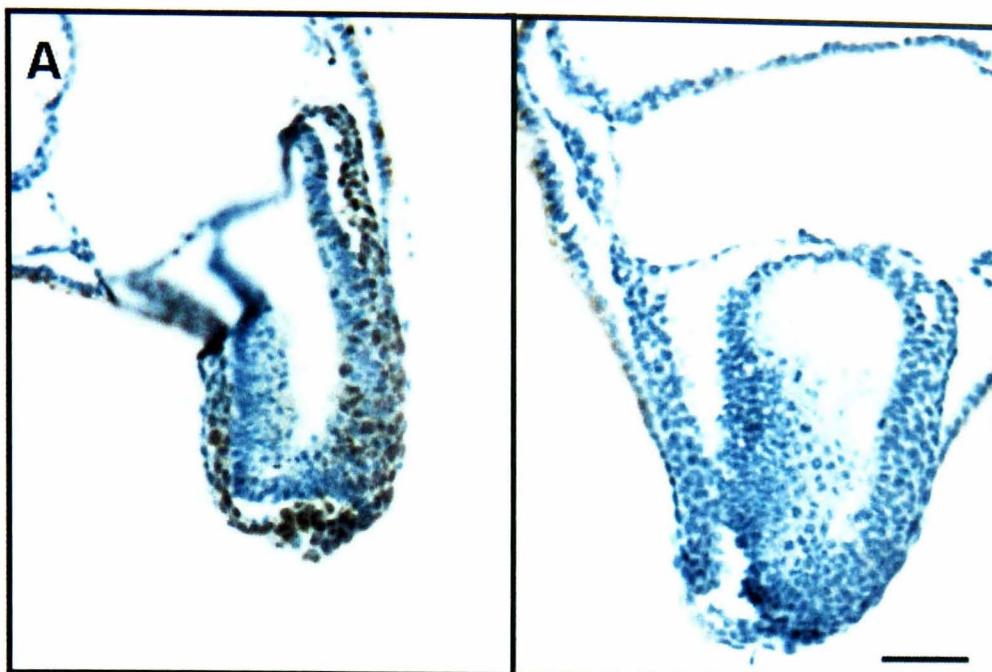
T　　　Control

A

B

C

SOX17   Control

314

MIXL1   Control

A

B

C

7.2 PUBLICATIONS

BURRIDGE, P.W., ANDERSON, D., PRIDDLE, H., BARBADILLO MUÑOZ, M.D., CHAMBERLAIN, S., ALLEGRUCCI, C., YOUNG, L.E., & DENNING, C. (2007) Improved human embryonic stem cell embryoid body homogeneity and cardiomyocyte differentiation from a novel V-96 plate aggregation system highlights interline variability. *Stem Cells*, 25, 929-38.

STEM CELLS®

EMBRYONIC STEM CELLS

Improved Human Embryonic Stem Cell Embryoid Body Homogeneity and Cardiomyocyte Differentiation from a Novel V-96 Plate Aggregation System Highlights Interline Variability

PAUL W. BURRIDGE,[a,b] DAVID ANDERSON,[b] HELEN PRIDDLE,[a,c] MARIA D. BARBADILLO MUÑOZ,[a,b] SARAH CHAMBERLAIN,[c] CINZIA ALLEGRUCCI,[a,b] LORRAINE E. YOUNG,[a,b] CHRIS DENNING[a,b]

[a]Wolfson Centre for Stem Cells, Tissue Engineering and Modelling, School of Human Development, [b]Institute of Genetics, and [c]Nottingham University Research and Treatment Unit, University of Nottingham, Queen's Medical Centre, Nottingham, United Kingdom

ABSTRACT

Although all human ESC (hESC) lines have similar morphology, express key pluripotency markers, and can differentiate toward primitive germ layers in vitro, the lineage-specific developmental potential may vary between individual lines. In the current study, four hESC lines were cultured in the same feeder-free conditions to provide a standardized platform for interline analysis. A high-throughput, forced-aggregation system involving centrifugation of defined numbers of hESCs in V-96 plates (V-96FA) was developed to examine formation, growth, and subsequent cardiomyocyte differentiation from >22,000 EBs. Homogeneity of EBs formed by V-96FA in mouse embryo fibroblast-conditioned medium was significantly improved compared with formation in mass culture ($p < .02$; Levene's test). V-96FA EB formation was successful in all four lines, although significant differences in EB growth were observed during the first 6 days of differentiation ($p = .044$ to .001;

one-way analysis of variance [ANOVA]). Cardiomyocyte differentiation potential also varied; $9.5\% \pm 0.9\%$, $6.6\% \pm 2.4\%$, $5.2\% \pm 3.1\%$, and $1.6\% \pm 1.0\%$ beating EBs were identified for HUES-7, NOTT2, NOTT1, and BG01, respectively ($p = .008$; one-way ANOVA). Formation of HUES-7 V-96FA EBs in defined medium containing activin A and basic fibroblast growth factor resulted in $23.6\% \pm 3.6\%$ beating EBs, representing a 13.1-fold increase relative to mass culture ($1.8\% \pm 0.7\%$), consistent with an observed 14.8-fold increase in MYH6 (αMHC) expression by real-time polymerase chain reaction. In contrast, no beating areas were derived from NOTT1-EBs and BG01-EBs formed in defined medium. Thus, the V-96FA system highlighted interline variability in EB growth and cardiomyocyte differentiation but, under the test conditions described, identified HUES-7 as a line that can respond to cardiomyogenic stimulation. STEM CELLS 2007;25:929–938

Disclosure of potential conflicts of interest is found at the end of this article.

INTRODUCTION

Numerous differentiated lineages have now been derived from hESCs [1], supporting the notion that these cells hold promise as tools for scientific research and as cell-based therapeutics. It has also been suggested that approximately 150 hESC lines will be required to match the majority of HLA isotypes in the U.K. population for transplantation [2]. However, considerably more hESC lines will be required if differentiation toward specific lineages is favored or restricted by the inherent or culture-induced properties of individual lines. It will therefore be important to evaluate lineage-specific differentiation potential by direct interline comparison, preferably under parallel, standardized conditions.

Comparison of hESC lines has begun through several organizations, including the International Stem Cell Initiative, the NIH Stem Cell Unit, and the American Type Culture Collection [3]. These initiatives are investigating variability in parameters

such as expression of surface markers and relative RNA levels in undifferentiated hESCs or at early stages of differentiation. Other interline comparisons indicate that there are differences in population doubling times [3], transcriptome [3], hematopoietic differentiation [4], and teratoma formation [5, 6]. However, the wide range of feeder cells, culture media, additives, and passage methods used between lines confounds interpretation of true interline differences. Consequently, it is challenging to draw conclusions as to whether variability is due to inherent genetic variation or environmental interference.

In an effort to limit the influence of culture-induced differences in interline comparison, we recently developed standardized conditions for culture and cardiomyocyte differentiation of two independently derived hESC lines, HUES-7 and BG01 [7]. These conditions have now been extended to NOTT1 and NOTT2, which we recently derived. However, the differentiation strategy we originally used [7] involved formation of embryoid bodies (EBs) from clumps of hESC colonies harvested using collagenase treatment, and

this resulted in a high degree of heterogeneity in EB size, morphology, and formation efficiency within each experiment. This confounds the ability to meaningfully test the efficacy of new factors/protocols on differentiation.

In this report, we have adapted an approach proposed by Ng et al. [8] to develop a high-throughput, forced-aggregation system that involves centrifugation of defined cell numbers in V-bottom 96-well plates (termed V-96FA). More than 22,000 EBs were generated either from 1,000, 3,000, or 10,000 trypsin-passaged HUES-7, BG01, NOTT1, and NOTT2 hESCs, which were routinely maintained in the same feeder-free conditions on Matrigel. V-96FA resulted in significantly greater reproducibility in EB size and gross morphology during early differentiation and, in some cases, in more beating areas at late stages of differentiation. Interestingly, significant interline variability was observed in EB size and cardiomyocyte differentiation. Moreover, although V-96FA formation of HUES-7 EBs in defined medium supplemented with activin A and basic fibroblast growth factor (bFGF) could dramatically enhance cardiomyogenesis, these conditions failed to produce beating outgrowths in the other lines tested. These data suggest that derivation of hESC lines with redundancy in HLA coverage will likely be required to ensure delivery of the full spectrum of clinically relevant lineages suitable for transplantation.

MATERIALS AND METHODS

Materials and General Culture

Culture reagents were purchased from Invitrogen (Paisley, U.K., http://www.invitrogen.com), and chemicals were from Sigma-Aldrich (Poole, U.K., http://www.sigmaaldrich.com) unless otherwise specified. Culture was carried out at 37°C in a humidified atmosphere containing 5% CO_2. Medium was changed daily for hESC cultures and every 3–4 days during differentiation.

hESC Culture

HUES-7p11 cells were kindly donated by Harvard University [9] and expanded using trypsin passaging on mouse embryo fibroblast (MEF) feeders for cryopreservation at p17, as recommended by the supplier. Aliquots of HUES-7 were thawed to Matrigel-coated flasks and cultured using trypsin passaging in feeder-free conditions in conditioned medium (CM); under these conditions, HUES-7 cells were routinely passaged by incubating with 0.05% trypsin for <1 minute at 37°C and then tapping the flasks to liberate single cells or preferably small clumps of cells. To prepare CM, MEFs (strain CD1, 13.5 days post coitum) were mitotically inactivated with mitomycin C (MMC) (10 μg/ml, 2.5 hours) and seeded at 6 × 10^4 cells per cm^2. The next day, inactivated MEFs in a T75 flask were incubated with 25 ml of Dulbecco's modified Eagle's medium-Ham's F-12 medium (DMEM-F12) supplemented with 15% KnockOut Serum Replacement, 100 μM β-mercaptoethanol (β-ME), 1% nonessential amino acids (NEAA), 2 mM GlutaMAX, and 4 ng/ml bFGF for 24 hours, at which time CM was harvested and made ready for use by supplementing with an additional 4 ng/ml bFGF. Each flask of inactivated MEFs was used to condition the medium for 7 consecutive days [7, 10].

BG01p24 cells were purchased from BresaGen (Athens, GA, http://www.bresagen.com) [11] and expanded using manual passaging on MEF feeders to p37, as recommended by the supplier. BG01 cells were transferred to feeder-free conditions in CM at p40 and cultured as for HUES-7. NOTT1 and NOTT2 were derived at the University of Nottingham with informed patient consent and in accordance with Human Fertilisation and Embryology Authority license R0141-2-a. Fresh IVF embryos (grade 2/3) were cultured for 5–6 days to the blastocyst stage in Vitrolife GIII sequential medium, as specified by the manufacturer. The zona pellucida was removed by treatment with acid Tyrode's, and the embryo was plated to MMC-inactivated MEFs (7.5 × 10^4 cells per cm^2). Cul-

tures were maintained in 80% KnockOut DMEM, 20% ES Screened Hyclone fetal bovine serum (Perbio, Tattenhall, U.K., http://www.perbio.com), 1× GlutaMAX, 1% NEAA, 100 μM β-ME, 4 ng/ml bFGF, and 10 ng/ml human recombinant leukemia inhibitory factor (Chemicon, Temecula, CA, http://www.chemicon.com). After 5 days, hESC outgrowths were isolated and expanded using manual passaging on MEF feeders. NOTT1p15 and NOTT2p18 were transferred to feeder-free trypsin/Matrigel culture in CM and cultured as for HUES-7. Both NOTT lines expressed OCT-4, SSEA-4, TRA-1-60, and TRA-1-81 but were negative for SSEA-1 (data not shown).

Karyotype Assessment

Exponentially growing cultures of at least 1 × 10^5 cells were treated with 100 ng/ml colcemid (Karyomax) for 45 minutes and harvested with 0.05% trypsin-EDTA. Pelleted cells (200g for 4 minutes) were resuspended in 0.6% sodium citrate and incubated at 37°C for 20 minutes. Cells were then centrifuged (300g for 4 minutes) and fixed by resuspension in 16.7% glacial acetic acid in methanol before washing with two additional changes of fixative. Chromosome spreads were prepared by dropping cells onto glass slides, which were air-dried and heated to 70°C overnight. Chromosomes were G banded with trypsin and stained with Leishman's. For each culture, 30 metaphase spreads were examined; full analysis involving band-by-band comparison between chromosome homologues was performed on three spreads, and the presence of gross abnormalities was visually examined in 27 spreads, in accordance with the International System for Human Cytogenetic Nomenclature international guidelines [12].

Feeder-free, trypsin-passaged cultures of HUES-7 were maintained from p18 to p37. Normal karyotype (46,XY) was observed at p18 and p31. However, by p37, only 22 (73%) cells of the 30 cells analyzed per culture (duplicate cultures) were 46,XY, up to seven (23%) cells were 47,XY,+12, and the remaining spreads showed nonclonal random gain or loss of chromosomes. Therefore, differentiation of HUES-7 was initiated from p20 to p28 cultures. Feeder-free, trypsin-passaged cultures of BG01 were maintained from p40 to p55 (46,XY at p40 and p52), NOTT1 from p15 to p33 (46,XX at p23 and p33), and NOTT2 from p18 to p28 (46,XY at p26).

Differentiation and Cardiomyocyte Analysis

Mass cultures of HUES-7 EBs and BG01 EBs were prepared as described previously [7]. Forced aggregation of EBs in untreated V-96-well plates (Nunc, Rochester, NY, http://www.nuncbrand.com), termed V-96FA, and subsequent evaluation of EB size and efficiency of cardiomyocyte differentiation is described in Figure 1A. V-96FA EBs were initiated from feeder-free, trypsin-passaged cultures of HUES-7 p20–28, BG01 p48–55, NOTT1 p26–31, and NOTT2 p24–28. The media tested for their ability to support V-96FA EB formation and growth were as follows: (a) CM, (b) unconditioned medium (UCM) was prepared as for CM but without MEF conditioning, (c) DMEM supplemented with 20% fetal bovine serum [FBS], 100 μM β-ME, 1% NEAA, and 2 mM GlutaMAX (D-FBS), (d) defined medium supplemented with bovine serum albumin (CDM-BSA), and (e) defined medium supplemented with polyvinyl alcohol (CDM-PVA) (both CDM-BSA and CDM-PVA as described by Vallier et al. [13] [L. Vallier, M. Alexander, R.A. Pedersen, personal communication]) and containing 1:1 mix of Iscove's modified Dulbecco's medium (F12 supplemented with 1× lipid, 450 μM monothioglycerol, 7 μg/ml insulin [Roche Diagnostics, Basel, Switzerland, http://www.roche-applied-science.com], and 15 μg/ml transferrin [Roche] plus 5 mg/ml bovine serum albumin fraction V [CDM-BSA] or 1 mg/ml polyvinyl alcohol). CDM-PVA was used either with or without 10 ng/ml activin A and 12 ng/ml bFGF (both from Peprotech, London, http://www.peprotech.com).

Numbers of viable cells present within HUES-7-derived EBs at d2, 4, and 6 of differentiation were measured using an MTT Cell Titre 96 nonradioactive cell proliferation assay (Promega, Southampton, U.K., http://www.promega.com) since this system has been previously used to define cell numbers in mouse EBs [14] HUES-7 EBs were transferred in 100 μl of medium to a flat-bottom 96-well plate on the appropriate day, and 15 μl of MTT dye solution
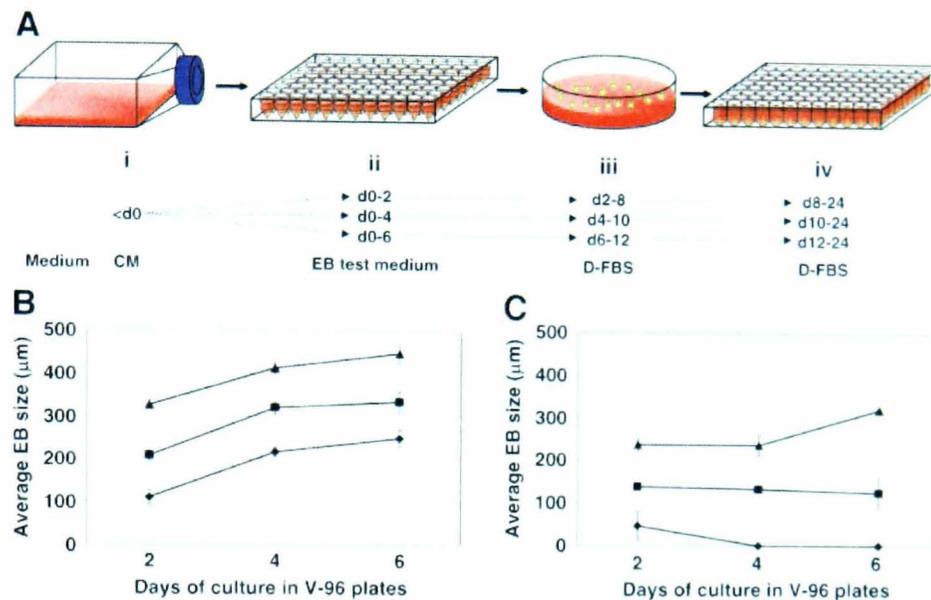
Figure 1. Developing the V-96FA system. **(A):** Schematic of the V-96FA procedure. (i): All human ESC (hESC) lines were cultured using trypsin passaging in feeder-free conditions on Matrigel in CM. (ii): On day 0 (d0) of differentiation, EB formation was initiated by seeding untreated V-96 plates in triplicate with either 1,000, 3,000, or 10,000 cells per well in different test media and centrifuging at 950g (~2,800 rpm) for 5 minutes at room temperature. To allow EBs to grow, V-96 plates were incubated for either 2, 4, or 6d (indicated by dotted arrows). (iii): On the specified day, growth was assessed by transferring all EBs from a V-96 plate to an untreated 90-mm dish in D-FBS and calculating the diameter of 20 randomly selected EBs per experiment by averaging the smallest and largest cross-sectional dimension of each body. (EBs were measured in 90-mm dishes, as optical distortion occurs in V-96 plates.) EBs were maintained in suspension for 6d to allow further differentiation, if necessary. EBs were detached from the culture dish by gentle pipetting. (iv): EBs were transferred to each well (one EB per well) of an untreated U-96-well plate. On d24 of differentiation, the percentage of beating EBs was calculated relative to 96 (i.e., the number of V-96 wells originally seeded with hESCs). CM **(B)** or defined medium supplemented with polyvinyl alcohol **(C)** V-96FA HUES-7 EBs were formed from 1,000 (diamonds), 3,000 (squares), or 10,000 (triangles) cells, and size was calculated on d2, 4, or 6 of differentiation. Abbreviations: CM, conditioned medium; d, day; D-FBS, Dulbecco's modified Eagle's medium supplemented with 20% fetal bovine serum.

was added. Plates were incubated for 2 hours at 37°C before adding 100 μl of stop solution and solubilizing overnight at 37°C. Absorbance was determined at 570 nm using a reference wavelength of 650 nm in a μQuant plate reader (BioTek, Winooski, VT, http://www.biotek.com). Cell numbers per EB were calculated from a standard curve using a known number of cells; all readings taken were in the linear range of the assay.

Real-time TaqMan polymerase chain reaction (PCR) was used to determine relative expression of myosin heavy chain 6 (*MYH6*, encodes αMHC). Reverse transcription was carried out using Superscript II (Invitrogen) with 400 ng of RNA according to the manufacturers' instructions. The resulting cDNA was diluted to a final volume of 100 μl. TaqMan PCR of samples was carried out using Applied Biosystems Assay on Demand (Foster City, CA, http://www.appliedbiosystems.com) primers/probe sets to *MYH6* (part number Hs00411908_m1) and *HPRT* (internal control; Hs99999909_m1) in conjunction with TaqMan Universal PCR Master Mix, No AmpErase UNG (Applied Biosystems) and 2 μl of cDNA in a total reaction volume of 20 μl. Cycle conditions were one cycle of 95°C for 5 minutes followed by 50 cycles of 95°C for 10 seconds, 60°C for 1 minute. Two independent PCRs, each in triplicate, were run, and relative quantification was performed using the Applied Biosystems 7500 Fast Real-time PCR System and software.

To confirm the presence of cardiomyocytes in beating areas derived from HUES-7 EBs in defined medium supplemented with polyvinyl alcohol, 10 ng/ml activin A, and 12 ng/ml bFGF (CDM-PVA+AF), nonquantitative RT-PCR and immunostaining were used. cDNA was prepared as above. PCR cycle parameters were as follows: one cycle of 94°C for 5 minutes; 35–40 cycles of 94°C for 30 seconds, 59°C for 30 seconds, and 68°C for 1 minute; and one cycle of 68°C for 10 minutes using High Fidelity PCR Master Mix (Roche). Sequences were as follows: *HPRT1* forward (F), 5'-TT-GACACTGG CAAAACAATG CAGA-3', and reverse (R), 5'-TGGCGATGTC AATAGGACTC CAGA-3', Gene ID 3251; *POU5F1* F, 5'-GAAGGTATTC AGCCAAAC-3', and R, 5'-CT-TAATCCAA AAACCCTGG-3', Gene ID 5460; *GATA4* F, 5'-AAAGAGGGGA TCCAAACCAG AAAA-3', and R, 5'-CA-

GATCCTCG GTGCTAGAAA CACA-3', Gene ID 2626; *NKX2.5* F, 5'-AGGACCCTAG AGCCGAAAA G-3', and R, 5'-GC-CGAAGTTC ACGAAGTTGT-3', Gene ID 1482; *TBX5* F, 5'-TGTGGCTAAA ATTCCACGAA-3', and R, 5'-TTCTGGAAGG AGACGAGCTG-3', Gene ID 6910; *MYH6* F, 5'-ATGACCGATG CCCAGATGGC TGA-3', and R, 5'-TCACTCCTCT TCTTGC-CCCGG TA-3', Gene ID 4624; *MYH7* F, 5'-AGCTGGCCCA GCGGCTGCAG G-3', and R, 5'-CTCCATCTTC TCGGCCTCCA GCT-3', Gene ID 4625; *MYL2* F, 5'-CCAACTCCAA CGTGT-TCTCC ATGT-3', and R, 5'-CATCAATTTC TTCATTTTTC ACGTTCA-3', Gene ID 4633; *SLC8A1* F, 5'-CCTTCTTCCT TGAGATTGGA GAGC-3', and R, 5'-TCCTCTTCCT CTTTGCT-GGT CAGT-3', Gene ID 6546; *NEB* F, 5'-ATGATGAATCA CGT-GCTGGCT AAA-3', and R, 5'-TGACTTTCTT CTGGGAATCC TTGG-3', Gene ID 4703.

Prior to immunostaining, beating areas were disaggregated as described previously [15, 16]. Briefly, beating areas were manually dissected, washed in phosphate-buffered saline (PBS), and then incubated for 30 minutes at room temperature in buffer 1 (120 mM NaCl, 5.4 mM KCl, 5 mM MgSO₄, 5 mM sodium pyruvate, 20 mM taurine, 10 mM HEPES, 20 mM glucose, pH 6.9), for 45 minutes at 37°C in buffer 2 (120 mM NaCl, 5.4 mM KCl, 5 mM MgSO₄, 5 mM sodium pyruvate, 20 mM taurine, 10 mM HEPES, 0.3 mM CaCl₂, 20 mM glucose, 1 mg/ml collagenase B, pH 6.9) and for 1 hour at room temperature in buffer 3 (85 mM KCl, 5 mM MgSO₄, 5 mM sodium pyruvate, 20 mM taurine, 1 mM EGTA, 5 mM creatine, 30 mM K₂HPO₄, 20 mM glucose, 1 mg/ml Na₂ATP, pH 7.2). Finally, cell clusters were dissociated by repeated pipetting through a P1000 tip, and the liberated cells were seeded to glass coverslips in D-FBS. Following attachment, cells were fixed with 4% paraformaldehyde (15 minutes at room temperature), permeabilized with Triton X-100 (0.1%; 8 minutes at room temperature), and then incubated with the mouse monoclonal anti-α-actinin (1:800) or anti-tropomyosin (1:50) for 1 hour at room temperature. Incubation with the secondary antibodies, Cy3 goat anti-mouse IgG (1:250), and fluorescein isothiocyanate goat anti-mouse IgG (1:100, both Jackson Immunoresearch Laboratories, West Grove, PA, http://www.jacksonimmuno.com), was performed for 1 hour at
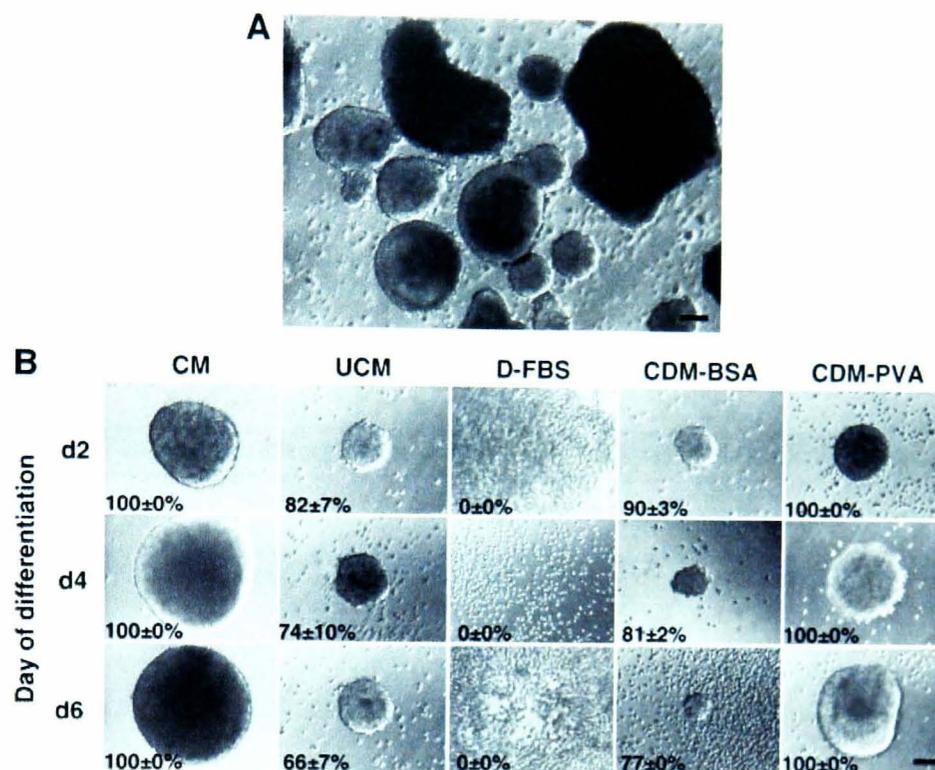
Figure 2. HUES-7-EB formation by mass culture or forced aggregation. Representative images are shown for mass culture EBs prepared by collagenase treatment + scraping of HUES-7 cells on mouse embryo fibroblast feeders and then culturing in suspension in CM until d6 of differentiation **(A)** and V-96FA EBs prepared from 10,000 feeder-free HUES-7 cells cultured in different media until d2, 4, or 6 of differentiation **(B)**. Media tested were as follows: CM, UCM, D-FBS, CDM-BSA, and CDM-PVA. Percentages were calculated from the number of wells in each V-96 plate that contained EBs (±SEM; two experiments). Scale bar = 100 μm. Abbreviations: CDM-BSA, defined medium supplemented with bovine serum albumin; CDM-PVA, defined medium supplemented with polyvinyl alcohol; CM, conditioned medium; d, day; D-FBS, Dulbecco's modified Eagle's medium supplemented with 20% fetal bovine serum (see Materials and Methods); UCM, unconditioned medium.

room temperature. Samples were mounted in Vectorshield Hardset containing 4,6-diamidino-2-phenylindole (Vector Laboratories, Peterborough, U.K., http://www.vectorlabs.com) and visualized on a Leica SP2 confocal microscope (Heerbrugg, Switzerland, http://www.leica.com).

H&E Staining

EBs were washed in twice in PBS, fixed in 4% paraformaldehyde in PBS for 15 minutes, and then washed twice in PBS. EBs were set into 1% agarose in double distilled H_2O and processed overnight using a Shandon Excelsior tissue processor (Thermo Scientific, Runcorn, U.K., http://www.thermo.com). Processed agarose blocks were embedded in paraffin wax (Tissue-Tek II embedding wax, Zoeterwoude, The Netherlands, http://www.tissue-tek.com) using a Tissue-Tek III thermal/dispensing/cryo-consol, sectioned using a microtome at 5 μm, and affixed to SuperFrost Plus slides (Menzel-Glaser, Braunschweig, Germany, http://www.menzel.de). Paraffin sections were dewaxed using xylene, rehydrated through an ethanol/H_2O gradient and stained with Harris' Hematoxylin (VWR, West Chester, PA, http://www.vwr.com) and Eosin Yellowish (VWR), before dehydrating and mounting using DePeX mounting medium (VWR). Samples were visualized using a Leica DMRB upright microscope and captured using Improvision 4.0.2 software.

RESULTS

Establishing a High-Throughput, Forced-Aggregation System

To establish a benchmark from which to gauge alternative strategies of EB formation, we first evaluated the degree of heterogeneity in size of EBs generated by a commonly used mass culture protocol [7]. HUES-7 or BG01 cells grown on

MEFs were harvested using collagenase plus scraping and incubated in suspension culture in CM for 6 days, as previously described [7]. Considerable variability in gross morphology was observed between EBs within each mass culture (Fig. 2A). Moreover, the diameter (calculated by averaging the smallest and largest cross sectional dimension of each body) for 20 randomly selected EBs per experiment ranged from 100 to 1,200 μm and from 175 to 1,150 μm for HUES-7 and BG01 (Table 1; supplemental online Fig. 1).

These observations prompted us to evaluate methods to generate EBs directly from trypsin-passaged hESCs cultured on Matrigel. This would enable each EB to be seeded from a defined number of hESCs maintained in feeder-free conditions and therefore potentially reduce variability in EB size, precisely specify the numbers of EBs generated in each experiment and eliminate MEF contamination. Incubation of hanging drop cultures seeded with between 300 and 10,000 HUES-7 or BG01 cells for up to 6 days failed to produce EBs (Table 1). As an alternative, we investigated EB formation using forced aggregation by centrifugation. Both hESC lines formed EBs efficiently when ultralow-attachment U-96 plates (ULA U-96) were seeded with 3,000 or 10,000 cells per well in CM, centrifuged at 950g for 5 minutes and incubated for 6 days (Table 1). However, these plates are prohibitively expensive for analysis of large numbers of EBs, and we sought to evaluate alternative plasticware.

Centrifugation of HUES-7 or BG01 cells in untreated (i.e., not treated for cell culture) U-96 plates resulted in erratic and/or poor EB formation (Table 1). In contrast, forced aggregation by centrifuging untreated V-96 plates (termed V-96FA) seeded with 3,000 or 10,000 hESCs/well in CM and then incubating for 6 days produced EBs at a similar efficiency and of similar size to those formed in ULA U-96 plates (Table 1). Furthermore, the

Table 1. Formation of EBs from HUES-7 and BG01 by mass culture or forced aggregation

	Undefined input cell number (mass culture): collagenase from MEFs	Defined input cell number (cells per hanging drop or cells per well)						
		Hanging drop (0.3–10,000)[a]	ULA (U-96)		Untreated (U-96)		Untreated (V-96)[b]	
			3,000	10,000	3,000	10,000	3,000	10,000
HUES-7								
% EB formation[c]	NA	0	82 ± 18	100 ± 0	0	56 ± 43	93 ± 6	100 ± 0
Average EB diameter (mm)	318 ± 27 (100–1,200)[d]	NA	389 ± 23	445 ± 15	NA	ND	377 ± 16 (250–450[d])	476 ± 15 (400–575[d])
BG01								
% EB formation	NA	0	91 ± 2	100 ± 0	0	0	90 ± 4	100 ± 0
Average EB diameter (mm)	333 ± 28 (175–1150[d])	NA	257 ± 16	401 ± 27	NA	NA	285 ± 11 (250–325[d])	387 ± 9 (325–450[d])

All EB size measurements were taken after incubation for 6 days in CM and represent averages (± SEM) from at least two independent experiments, with 20 EBs measured per experiment.
[a]Hanging drop cultures (30 μl) were seeded with 300, 1,000, 3,000, or 10,000 cells.
[b]Without centrifugation, formation efficiency was poor (data not shown).
[c]% EB formation was calculated as the number of wells containing EBs on day 6 of differentiation.
[d]Numbers in parentheses indicate the range of EB sizes (minimum to maximum) observed within the experimental groups; Levene's test for equality of variance indicated significant differences between HUES-7 EBs formed by mass culture EBs and by V-96FA from 3,000 ($p <$ .001) or 10,000 ($p <$ .001) cells or BG01 EBs formed by mass culture and by V-96FA from 3,000 ($p <$ .001) or 10,000 ($p =$ .02) cells. Abbreviations: CM, conditioned medium; MEF, mouse embryo fibroblast; NA, not applicable; ND, not done; ULA, ultralow-attachment U-bottomed 96-well plates.

diverse range of sizes observed between EBs formed in mass culture was significantly reduced by V-96FA (Table 1; supplemental online Fig. 1; $p <$ .02, Levene's test for equality of variances).

Evaluating the Effect of Media, Cell Number, and Day of Differentiation on V-96FA EBs

Successful formation of EBs in CM via the V-96FA system allowed the effectiveness of different media to be tested. As an initial screen, percentage EB formation was compared on d2, 4, or 6 after V-96FA with 10,000 HUES-7 cells in CM, UCM, or D-FBS, which contains 20% serum (Fig. 2B). CDM-BSA and CDM-PVA were also tested, since these semidefined and defined media, respectively, were recently reported to support undifferentiated proliferation of the hESC lines H9 and HSF-6 [13] (L. Vallier, M. Alexander, and R.A. Pedersen, personal communication). Consistent with our observations above, high efficiency formation (100%) in CM was observed on d2, 4, and 6 of differentiation (Fig. 2B). Efficiency was the same in CDM-PVA but lower in UCM (66%–82%), CDM-BSA (77%–90%), and D-FBS (0%). Therefore, subsequent experiments focused on formation, growth, and cardiomyocyte differentiation from EBs produced by V-96FA in CM and the defined medium, CDM-PVA.

The utility of the V-96FA system was developed further by investigating the kinetics of HUES-7 EB growth in relation to input cell number, days of differentiation, and medium formulation. Plates were seeded in triplicate with 1,000, 3,000, or 10,000 HUES-7 cells in CM or CDM-PVA. After centrifugation, one plate at each density was cultured until d2, 4, or 6 of differentiation, at which time average EB size was calculated (Fig. 1A). Analysis of EB size indicated a high degree of reproducibility between independent experiments using CM or CDM-PVA (Fig. 1B, 1C), which was confirmed by evaluating viable cell numbers per EB (supplemental online Fig. 2A, 2B). These observations were also consistent with histological examination using H&E staining, which showed greater homogeneity in size and tissue morphology of V-96FA EBs formed in either medium than their mass culture counterparts formed in CM (Fig. 3). For EBs formed in CM from all cell seeding densities, both increasing input cell number and day of differentiation contributed to increasing size (Fig. 1B). Similarly, EBs initiated from

10,000 cells in CDM-PVA increased in size from d2 to d6 of differentiation (Fig. 1C). However, the size of CDM-PVA EBs formed from 3,000 cells remained static, whereas those from 1,000 cells declined, with no EBs detectable by d6 of differentiation (Figs. 1C, 3). These observations indicated that V-96FA provided a reproducible platform with which to evaluate the effect of different media on EB formation and growth, thus enabling comparison between different hESC lines.

Formation of V-96FA EBs in CM was efficient from HUES-7, BG01, NOTT1, and NOTT2, with similar overall growth profiles observed between lines (Fig. 4), demonstrating that the system has the potential to be applied generically. However, statistical analysis indicated several interline differences in EB size (supplemental online Table 1). For example, on d4 of differentiation, the size of EBs seeded from 1,000 hESCs varied between the lines ($p =$ .002; one-way analysis of variance [ANOVA]), as did those from 3,000/d4 ($p =$ .001) and 10,000/d4 ($p =$ .001) or 10,000/d6 ($p =$ .042). Similar observations were made for CDM-PVA EBs from the three lines examined (HUES-7, BG01, and NOTT1; compare Fig. 1C with supplemental online Fig. 3A, 3B), with significant differences in size observed from 10,000/d2 ($p =$ .031), 3,000/d4 ($p =$ .038), and 10,000/d6 ($p =$ .007; supplemental online Table 1). Thus, clear differences in EB growth kinetics were observed between the lines.

Variable Cardiomyocyte Differentiation Between hESC Lines

The reproducibility of the V-96FA system and the ability to dictate EB size by altering input cell number and/or time in culture provided an opportunity to carry out systematic comparison of cardiomyocyte differentiation efficiency between the four hESC lines. As before, V-96FA EBs were formed from 1,000, 3,000, or 10,000 cells in CM and cultured until d2, 4, or 6 of differentiation. EBs were then switched to and maintained in D-FBS until d24 of differentiation (Fig. 1A). FBS was included during the extended differentiation period because absence of serum is reported to be detrimental to maintenance of primary cardiomyocytes [17].

For all four hESC lines, transfer of the V-96FA EBs produced from 1,000, 3,000, or 10,000 hESCs to D-FBS on d2 of differentiation yielded only limited numbers of beating EBs
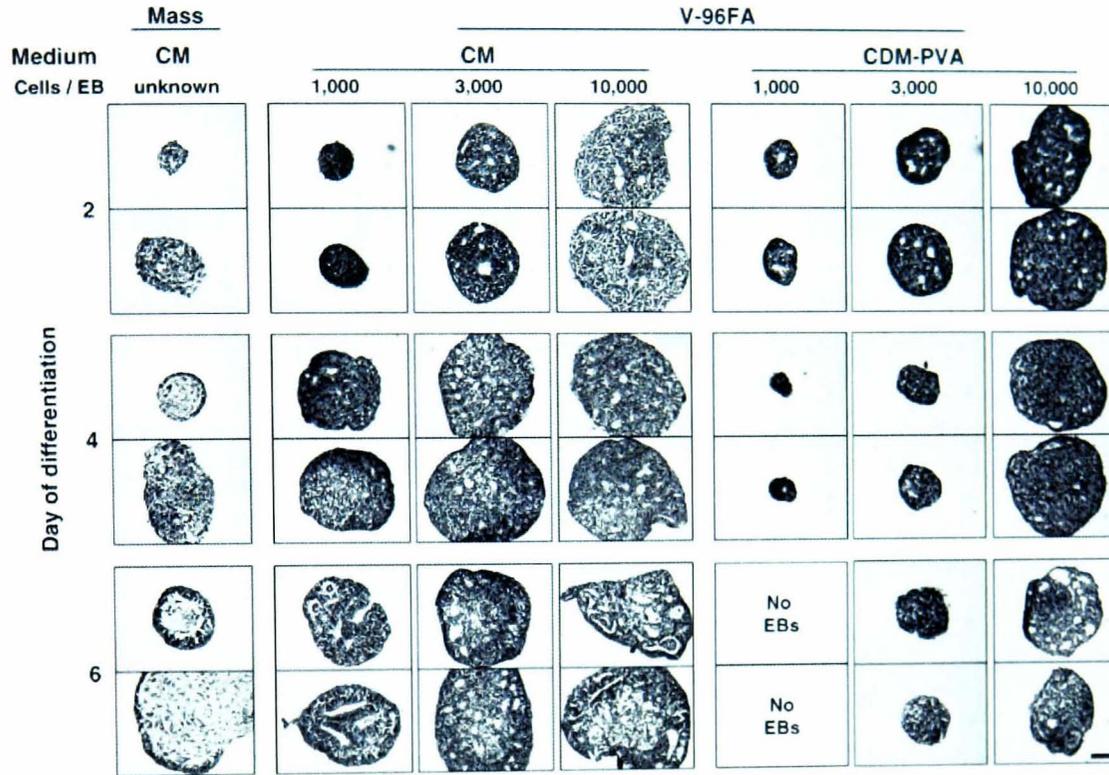
Figure 3. Sectioning and H&E staining of HUES-7-EBs. EBs were formed by mass culture of unknown numbers of cells per EB in CM or by V-96FA of 1,000, 3,000, and 10,000 cells per well in CM or CDM-PVA. EBs were incubated until d2, 4, or 6 of differentiation and then selected at random for processing. Representative images of sections from two separate EBs are shown. Scale bar = 100 μm. Abbreviations: CDM-PVA, defined medium supplemented with polyvinyl alcohol; CM, conditioned medium.
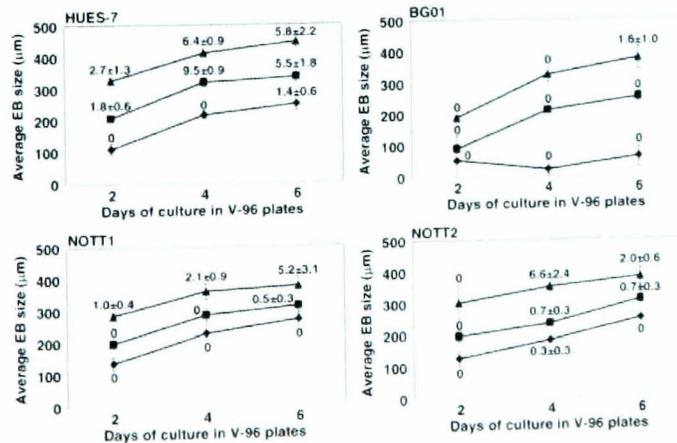

Figure 4. EB formation and cardiomyocyte differentiation between human ESC lines. EBs were formed by V-96FA from 1,000 (diamonds), 3,000 (squares), or 10,000 (triangles) cells in CM. On day (d)2, 4, or 6 of differentiation, EBs were transferred to Dulbecco's modified Eagle's medium supplemented with 20% fetal bovine serum, where they were measured and then cultured until d24, as described in Figure 1A. Each data point for EB size represents average (±SEM) of between 2 and 17 independent experiments (representing 40–340 EBs), and numbers represent average (±SEM) percentage of beating EBs scored from 2–21 independent experiments (representing 196–2,016 EBs).

(Fig. 4). Similarly, cardiomyocyte differentiation was consistently poor using 1,000 hESCs switched to D-FBS on d4 or 6. However, significant variability was observed between the lines in the percentage of beating areas produced by switching EBs formed from 3,000 cells/d4 ($p < .001$; one-way ANOVA), 10,000/d4 ($p = .003$), or 3,000/d6 ($p = .005$; Fig. 4; supplemental online Table 1). In the 3,000 and 10,000/d4 samples, these differences were also validated by showing good association between percentage of beating EBs and quantitative Taq-Man PCR of *MYH6* [18], which encodes αMHC (Fig. 5A).

Moreover, there was an interline difference in absolute efficiency of cardiomyogenesis (Fig. 4; HUES-7, 9.5% ± 0.9%; BG01, 1.6% ± 1.0%; NOTT1, 5.2% ± 3.1%; NOTT2, 6.6% ± 2.4%; $p = .008$, one-way ANOVA).

We also analyzed the percentage of beating areas identified on d24 of differentiation relative to EB size at time of transfer on d2, d4, or d6 from V-96 plates to D-FBS. Interestingly, of the five arbitrarily assigned EB size categories, all lines showed the highest percentages of beating EBs were obtained when size at transfer was 250–350 μm (Fig. 5B: HUES-7, 7.2% ± 0.9%; BG01, 1.1% ± 0.8%; NOTT1, 2.4% ± 1.1%; NOTT2, 3.1% ± 1.5%). However, interline differences were still evident in three categories (150–250 μm, $p = .016$; 250–350 μm, $p = .001$; 350–450 μm, $p = .025$; one-way ANOVA). Thus, together these data indicate that under the current test conditions, the cardiomyocyte differentiation potential of the four hESC lines varies significantly.

Growth Factor Induction of Cardiomyogenesis

Although cardiomyocyte differentiation was observed from EBs formed in CM for all the hESC lines, this medium is undefined and may contain factors that antagonize the effect of potentially cardiomyogenic agents. Therefore, CDM-PVA V-96FA EBs were generated with activin A and bFGF present or absent during the first 2–6d of differentiation, and the effect on subsequent cardiomyogenesis was evaluated; both growth factors have been proposed to support maintenance of undifferentiated hESCs [13] and during differentiation are involved in specification of cardiomyocyte/mesodermal fate [19, 20].

Size profiles of EBs were similar irrespective of whether CDM-PVA was supplemented with 10 ng/ml activin A and 12 ng/ml bFGF (CDM-PVA+AF), indicating that EB growth was not stimulated by addition of the factors (Fig. 6A, 6B; supplemental online Fig. 3). Formation of BG01 EBs or NOTT1 EBs in either medium failed to generate beating EBs. In contrast,
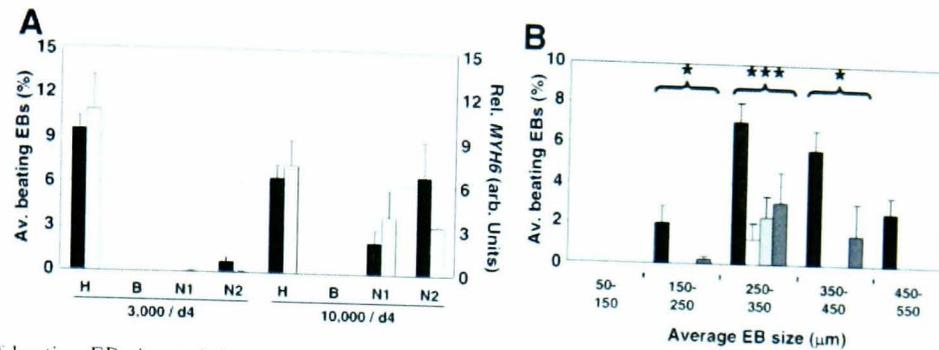
Figure 5. Analysis of beating EBs by real-time polymerase chain reaction (PCR) and by size category. **(A)**: The percentage of wells containing beating areas (black bars) was shown to associate well with *MYH6* expression, as determined by TaqMan PCR relative to *HPRT* (white bars). **(B)**: Average percentages of beating EBs (±SEM) were plotted versus arbitrarily assigned size categories that relate to EB size at time of transfer to Dulbecco's modified Eagle's medium supplemented with 20% fetal bovine serum. Black bars, HUES-7; white bars, BG01; light gray bars, NOTT1; dark gray bars, NOTT2. *, interline difference of $p < .05$; ***, $p = .001$ (one-way analysis of variance). Abbreviations: Av., average; B, BG01; d, day; H, HUES-7; N1, NOTT1; N2, NOTT2.
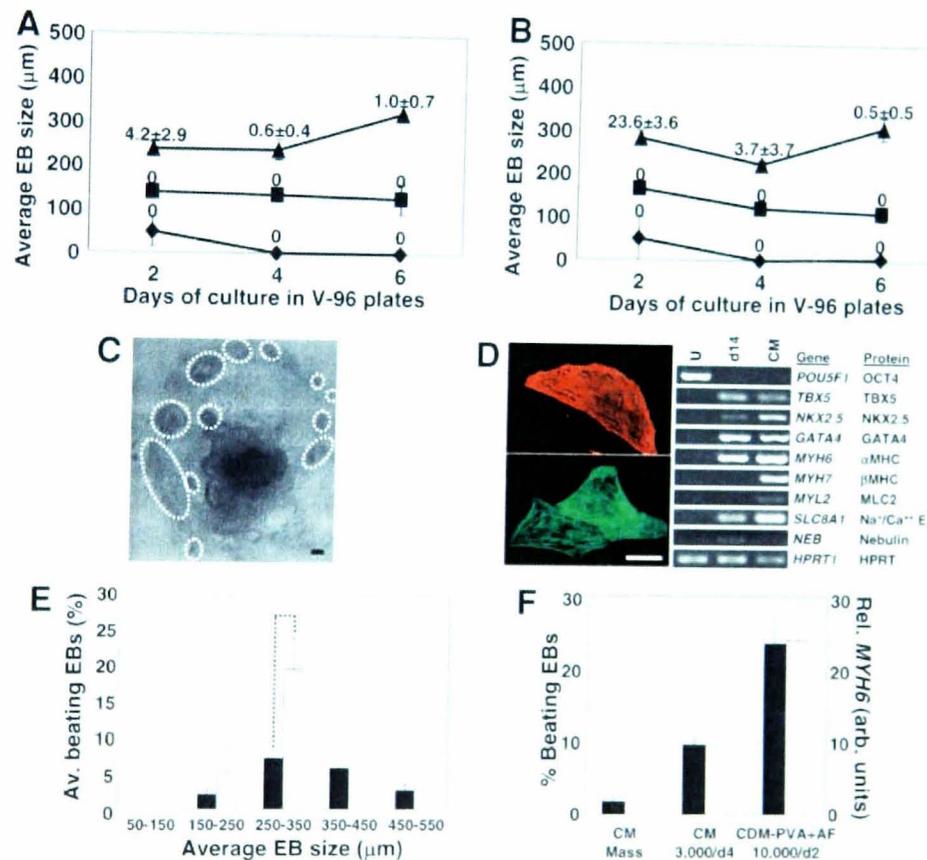

Figure 6. EB formation and cardiomyocyte differentiation from HUES-7 cells in defined media. EBs were formed by V-96FA from 1,000 (diamonds), 3,000 (squares), or 10,000 (triangles) cells in CDM-PVA **(A)** or CDM-PVA+AF **(B)**. On d2, 4, or 6 of differentiation, EBs were transferred to Dulbecco's modified Eagle's medium supplemented with 20% fetal bovine serum (D-FBS), where they were measured and cultured until d24, as described in Figure 1A. Each data point for EB size represents the average (±SEM) of 2–4 independent experiments (representing 40–80 EBs), whereas numbers represent average (+SEM) percentage of beating EBs observed from 2–9 independent experiments (representing 196–864 EBs). **(C)**: A representative image of the location and morphology of beating outgrowths (dotted ellipses) arising from EBs initially formed in CDM-PVA+AF. Scale bar = 100 μm. **(D)**: The presence of cardiomyocytes in the beating areas derived from CDM-PVA+AF EBs was confirmed by immunostaining to α-actinin (red) and tropomyosin (green; scale bar = 50 μm), as well as by reverse transcription polymerase chain reaction (PCR). **(E)**: Average percentages of beating EBs (±SEM) were plotted versus arbitrarily assigned size categories that relate to EB size at time of transfer to D-FBS. EBs were formed in CM (black bars) or CDM-PVA+AF (white bars). Dashed line signifies $p = .001$ (t test). **(F)**: Percentage of wells containing beating areas (black bars) relative to expression of *MYH6* (TaqMan PCR relative to *HPRT*; white bars) was determined for EBs that were initially formed by mass culture or by V-96FA from 3,000 cells in CM/d4 and 10,000 cells in CDM-PVA+AF/d2. Abbreviations: Arb., arbitrary; Av., average; CDM-PVA, defined medium supplemented with polyvinyl alcohol; CDM-PVA+AF, defined medium supplemented with polyvinyl alcohol, 10 ng/ml activin A, and 12 ng/ml basic fibroblast growth factor; CM, areas containing spontaneously contracting cells; d, day; d14, EBs at day 14 of differentiation; Rel., relative to expression of; U, undifferentiated HUES-7.

HUES-7 EBs formed in CDM-PVA with 10,000 cells and switched to D-FBS on d2 of differentiation produced 4.2% ± 2.9% beating areas by d24 of differentiation and this increased significantly to 23.6% ± 3.6% by formation in CDM-PVA+AF (Fig. 6A, 6B; $p = .01$, t test). The beating outgrowths from the

CDM-PVA+AF HUES-7 EBs had a readily identifiable cellular morphology, even before the onset of beating, and were most commonly located in a horseshoe shape at the EB perimeter (Fig. 6C). To confirm the presence of cardiomyocytes in these outgrowths, beating areas were manually dissected and then

disaggregated with collagenase to single cells or small clumps of cells. After replating, the cultures contained cells that continued to spontaneously contract and were immunoreactive to antibodies against α-actinin and tropomyosin (Fig. 6D). Analysis of the cultures by RT-PCR indicated the presence of transcripts for cardiac transcription factors (*GATA-4, TBX-5*, and *NKX2.5*) and structural/regulatory elements (*MYH6, MYH7, SLC8A1*, and *MYL2*) but not for *NEB*, which encodes the skeletal muscle protein nebulin (Fig. 6D) [18, 21]. Analysis by size category indicated that CDM-PVA+AF HUES-7 EBs of 250–350 μm at time of transfer to D-FBS produced the highest percentages (19.6% ± 4.5%) of beating EBs, a pattern similar to that seen for HUES-7 EBs formed in CM (Fig. 6E).

Formation of HUES-7 EBs in mass culture resulted in beating outgrowths arising from 1.8% ± 0.7% of total EBs analyzed on d24 of differentiation. This percentage increased to 9.5% ± 0.9% using V-96FA from 3,000 cells in CM with transfer to D-FBS on d4 and to 23.6% ± 3.6% using 10,000 cells in CDM-PVA+AF/d2. These data associated well with relative quantification by real-time PCR of *MYH6* transcripts (Fig. 6F), indicating that forced aggregation of HUES-7 in defined medium with addition of activin A and bFGF increased cardiomyogenesis by greater than 13-fold compared with mass culture in CM. Thus, the ability to form EBs in defined media makes the V-96FA system amenable to evaluating growth factor induction of cardiomyocyte differentiation.

DISCUSSION

Although formation of cell lineages representing the three germ layers via in vitro differentiation and expression of various pluripotency markers, such as SSEA-4, TRA-1–60, OCT4, or NANOG, forms a useful umbrella under which to group the 300 or so hESC lines derived to date, the phenotype of each line is likely influenced by both inherent genetics and environmental parameters [3]. Indeed, the culture environment can have a profound effect on the molecular signature of hESCs; changing the serum component of the culture medium to KnockOut Serum Replacement altered the expression profile of 1,417 genes in the hESC line HS237 [22]. Therefore, we used standardized conditions to provide a common platform to initiate differentiation of independently-derived hESC lines to test generic applicability of differentiation protocols.

Most differentiation protocols for human EB formation initiate suspension cultures by harvesting hESC colonies directly from feeders using manual dissection or collagenase. However, consistent with other reports [8, 23], we found that this strategy resulted in a high degree of heterogeneity in EB size and limited cardiomyocyte differentiation in all lines tested, likely a consequence of the variability in cell numbers that seed each EB. In mouse ESCs, this issue has been solved by seeding hanging drop cultures with a defined number of trypsin-passaged cells (typically 300–700). This results in reproducible production of mouse EBs that are 100–200 μm in diameter by d3 of differentiation and has enabled a reliable system that recapitulates the early stages of development [24]. Moreover, after extended differentiation, many of the murine EBs develop beating outgrowths [19]. Formation of human EBs in hanging drops has been reported from manually dissected hESC colony pieces [23]. However, the size of starting material remains heterogeneous, and the labor-intensive nature of the system is not amenable to high-throughput development. Our attempts to form EBs in hanging drops seeded with defined numbers of trypsinized in HUES-7 and BG01 cells were unsuccessful, consistent with a previous report using HES-1 and HES-2 [25].

As an alternative approach, Ng et al. [8] developed a forced aggregation system to form EBs from defined numbers of HES-2, -3, and -4 by centrifuging at 500g for 4 minutes at 4°C in ultralow-attachment U-96-well plates. Although data relating to EB size were not reported, efficient blood formation required a minimum of 500 cells per well, and input cell number was critical for directing efficient differentiation to specific hematopoietic lineages [8]. Although this strategy provided valuable proof of concept that forced aggregation was a viable technique, there are several potential limitations with the study. First, ULA U-96 plates are difficult to obtain and prohibitively expensive (~$20 USD per plate) for high-throughput development. Second, the three lines used were all derived at the same institution, and so the generic utility of the strategy between independently derived hESC lines was unknown. Finally, hESCs were cultured on MEFs, and mixed populations of the two cell types were used in the aggregation experiments; however, it has been suggested that contaminating MEFs have the potential to interfere with differentiation by both competing for cell-cell interactions and insulating communication between the ESCs [24].

We observed >90% EB formation using defined numbers of trypsin-passaged HUES-7 and BG01 cells maintained in feeder-free conditions in ULA U-96 plates, consistent with observations using HES-3 [8]. Importantly for high throughout development, aggregation was also efficient in untreated V-96 plates (~$1 USD per plate), and this method proved to be transferable to NOTT1 and NOTT2. In our laboratory, V-96FA has since been successful using defined numbers of trypsin-harvested H1 (routinely passaged with trypsin) and HUES-7 (routinely passaged with collagenase), both cultured in feeder-free conditions (unpublished observations).

Certain parameters influenced efficiency and reproducibility of EB formation. Rather than containing one discrete EB per well, multiple EBs were identified in a minority of wells when V-96 plates were centrifuged at 500g for 5 minutes. This issue was virtually eliminated when plates were subjected to 950g. Interestingly, EB formation occurred from HUES-7 and BG01 irrespective of the undifferentiated hESC culture density, whereas formation from NOTT1 (and H1) became erratic when density exceeded 2×10^5 cells per cm². The medium also influenced EB formation, with highest efficiencies occurring in CM and CDM-PVA, efficiency decreasing in UCM or CDM-BSA, and no formation in D-FBS. The underlying mechanisms responsible for the differences observed in EB formation between hESC lines or media are not known, but altered expression levels of key adhesion factors seems a likely target for future studies. Indeed, it has been demonstrated that over 60 cell adhesion-related genes were upregulated in the hESC line HS237 by switching the serum component of the medium to KnockOut Serum Replacement [22]. It is also notable that previous microarray studies have highlighted potential differences in expression profile of integrin subclasses in H1 and BG01 [10, 26]. However, from our data and that of Skottman et al. [22], it is plausible that differences in cell density or culture medium at time of cell harvesting could also account for some of the documented variability between hESC lines, and the potential influence of these factors will need to be considered when designing array studies to make future interline comparisons.

Since the standardized culture and V-96FA strategy described here functioned between all the lines investigated, we were able to make parallel, interline comparisons. Significant variability in EB formation, growth, and cardiomyocyte differentiation was observed between independently derived hESC entiation was observed between independently derived hESC lines but, notably, not between NOTT1 and NOTT2, which were both derived in our laboratory. Other studies, investigating gene expression, have also observed greater similarity between lines isolated within the same laboratory, implicating the derivation

and culture history of each line as a source of variability. For example, four lines from Finland (FES21, FES22, FES29, and FES30) were more similar to each other than to the three from Sweden (HS181, HS235, and HS237) [27], HSF1 and HSF6 were more similar to each other than to H9 [28], and BG01/BG01-MEDII were more similar to each other than to H1 [29]. Nevertheless, the greatest percentage of beating areas were obtained from NOTT1 by seeding EBs with 10,000 cells and culturing in V-96 plates until d4 before transfer to D-FBS, whereas 10,000/d6 was most effective for NOTT2, suggesting that inherent genetic and/or epigenetic differences are also important. This is consistent with observations of Yoon et al. [23], who observed spontaneous beating in 0% of EBs derived from Miz-hES-1, -4, and -6 but ~22% in Miz-hES2.

The variability in EB size and in cardiomyocyte differentiation observed between the hESC lines may also relate to passage number of the lines at time of differentiation. HUES-7 cells were provided at p12 by Harvard University [9], and we derived NOTT1/2. Consequently, differentiation could be carried out at p20–30. Conversely, only higher passage BG01 cells could be purchased from BresaGen [11], and p45–55 cells were used for the differentiation studies. Although the cells that were used for differentiation were assessed as karyotypically normal by G-banding analysis, there is mounting evidence to suggest that extended culture is associated with more subtle changes, such as gene amplification (e.g., the proto-oncogene MYC) and differential methylation [30]. Because this argues for using the lowest passage hESCs possible, we did not attempt to culture HUES-7, NOTT1, and NOTT2 to ~p50 for comparison with the passage BG01 cells and cannot rule out the possibility that high passage number has a negative effect on cardiomyocyte differentiation. However, it is notable that increasing passage number of H9.2 hESCs has been associated with increasing cardiomyogenic potential [31].

Cardiomyocyte differentiation of the four lines examined here appeared to be most efficient when EBs of 250–350 μm were transferred to D-FBS. This is consistent with several other studies that indicate EB size or input cell numbers are important for influencing lineage specification. Erythroid or myeloid lineages were formed most effectively from forced aggregation of 1,000 cells or 1,000–5,000 HES-3 hESCs, respectively. Moreover, a study investigating cardiomyocyte differentiation in hanging drops seeded with between 32 and 2,000 mouse AB2.2 ESCs found that EBs formed from 565 cells produced the highest percentage of beating areas [32]. In this case, primitive endoderm within the mouse EBs influenced the onset of cardiomyogenesis in a concentration-dependent manner [32]. In line with these observations, cardiomyocyte differentiation of mouse P19 embryonal carcinoma cells and human ESCs (HES-2, -3, and -4) has been induced by coculture with END-2, which has characteristics of visceral endoderm [33–35]. In addition, microarray studies monitoring cardiomyogenesis in HES-2 have shown that induction of genes of the primary mesoderm and endodermal lineages is followed by expression of those in cardiomyocyte progenitor cells and fetal cardiomyocytes [36]. Thus, detailed time course analysis of mesodermal- and endodermal-related proteins within developing human EBs may yield clues of how to promote cardiomyogenesis, which could be evaluated using V-96FA in defined media.

The V-96FA system also provides a much improved, homogeneous platform with which to test the effect of different media and/or factors on EB formation, growth, and differentiation between lines. Activin A and bFGF support proliferation of undifferentiated H9 and HSF6 hESCs [13] and have been implicated in cardiogenesis from mouse and human ESCs [19, 20]. Our observations with HUES-7 indicate that EB formation in defined CDM-PVA medium supplemented with both growth factors instigates up to a 2.5-fold increase in beating areas compared with forced aggregation in CM and a 13.1-fold increase compared with mass culture in CM. It will now not only be necessary to identify whether activin A, bFGF, or a combination of both factors has the greatest effect on cardiomyogenesis, but also to determine the most effective concentrations. Interestingly, formation in defined conditions did not produce beating EBs from BG01 or NOTT1, and it will therefore be important to use this system to test the interline efficacy of other potential cardiomyogenic agents, such as ascorbic acid [35], 5-azacytidine [18, 23], and BMP-4 [20]. An additional challenge will be to eliminate serum from the differentiation medium to develop a defined medium that both enables cardiomyogenesis from hESCs and sustains long-term cardiomyocyte function.

In conclusion, we have coupled standardized culture with a high-throughput, V-96FA procedure to facilitate accurate comparison of cardiomyocyte differentiation potential between independently derived hESC lines. Since this strategy will also be amenable for derivation of other differentiated lineages, it should provide a useful platform to rapidly identify whether particular lineages are favored by specific hESC lines. Relating such information to both the original derivation conditions of each line and the data emerging from organizations such as the International Stem Cell Initiative should expedite production of a new generation of hESC lines that are derived and cultured using universally agreed-upon conditions.

DISCLOSURE OF POTENTIAL CONFLICTS OF INTEREST

The authors indicate no potential conflicts of interest.

REFERENCES

1 Allegrucci C, Denning C, Burridge P et al. Human embryonic stem cells as a model for nutritional programming: An evaluation. Reproductive Toxicology 2005;20:353–367.

2 Taylor CJ, Bolton EM, Pocock S et al. Banking on human embryonic stem cells: Estimating the number of donor cell lines needed for HLA matching. Lancet 2005;366:2019–2025.

3 Allegrucci C, Young LE. Differences between human embryonic stem cell lines. Hum Reprod Update 2007;13:103–120.

4 Chang K, Nelson A, Ware C et al. Wide variation in haematopoietic induction potential among five human ES lines and synthesis of unique globin patterns by ES-derived erythroid cells. Abstract 204 from the 3rd

Annual Meeting of the International Society for Stem Cell Research; June 23–25, 2005; San Francisco

5 Otonkoski T, Mikkola M, Lundin K et al. Endocrine pancreatic differentiation in teratomas of transplanted human embryonic stem cells: Unique difference between five new hESC lines. Abstract 778 from the 3rd Annual Meeting of the International Society for Stem Cell Research; June 23–25, 2005; San Francisco.

6 Mikkola M, Olsson C, Palgi J et al. Distinct differentiation characteristics of individual human embryonic stem cell lines. BMC Dev Biol 2006;6:40–50.

7 Denning C, Allegrucci C, Priddle H et al. Common culture conditions for maintenance and cardiomyocyte differentiation of the human embryonic stem cell lines BG01 and HUES-7. Int J Dev Biol 2006;50:27–37.

8 Ng E, Davis R, Azzola L et al. Forced aggregation of defined numbers of human embryonic stem cells into embryoid bodies fosters robust, reproducible hematopoietic differentiation. Blood 2005;106:1601–1603.

9 Cowan CA, Klimanskaya I, McMahon J et al. Derivation of embryonic stem-cell lines from human blastocysts. N Engl J Med 2004; 350:1353–1356.

10 Xu C, Inokuma MS, Denham J et al. Feeder-free growth of undifferentiated human embryonic stem cells. Nat Biotechnol 2001;19:971–974.

11 Mitalipova M, Calhoun J, Shin S et al. Human embryonic stem cell lines derived from discarded embryos. STEM CELLS 2003;21:521–526.

12 Mitelman F, ed. ISCN: An International System for Human Cytogenetic Nomenclature. Basel: S Karger, 1995.

13 Vallier L, Alexander M, Pedersen RA. Activin/Nodal and FGF pathways cooperate to maintain pluripotency of human embryonic stem cells. J Cell Sci 2005;118:4495–4509.

14 Schroeder M, Niebruegge S, Werner A et al. Differentiation and lineage selection of mouse embryonic stem cells in a stirred bench scale bioreactor with automated process control. Biotechnol Bioeng 2005;92:920–933.

15 Maltsev VA, Wobus AM, Rohwedel J et al. Cardiomyocytes differentiated in vitro from embryonic stem cells developmentally express cardiac-specific genes and ionic currents. Circ Res 1994;75:233–244.

16 Moore JC, van Laake LW, Braam SR et al. Human embryonic stem cells: Genetic manipulation on the way to cardiac cell therapies. Reprod Toxicol 2005;20:377–391.

17 Heng BC, Haider HKh, Sim EK et al. Strategies for directing the differentiation of stem cells into the cardiomyogenic lineage in vitro. Cardiovasc Res 2004;62:34–42

18 Xu C, Police S, Rao N et al. Characterization and enrichment of cardiomyocytes derived from human embryonic stem cells. Circ Res 2002; 91:501–508.

19 Sachinidis A, Fleischmann B, Kolossov E et al. Cardiac specific differentiation of mouse embryonic stem cells. Cardiovasc Res 2003; 58:278–291.

20 Yao S, Chen S, Clark J et al. Long-term self renewal and directed differentiation of human embryonic stem cells in chemically defined conditions. Proc Natl Acad Sci U S A 2006;103:6907–6912.

21 Kehat I, Kenyagin-Karsenti D, Snir M et al. Human embryonic stem cells can differentiate into myocytes with structural and functional properties of cardiomyocytes. J Clin Invest 2001;108:407–414.

22 Skottman H, Stromberg AM, Matilainen E et al. Unique gene expression signature by human embryonic stem cells cultured under serum-free conditions correlates with their enhanced and prolonged growth in an undifferentiated stage. STEM CELLS 2006;24:151–167.

23 Yoon B, Yoo S, Lee J et al. Enhanced differentiation of human embryonic stem cells into cardiomyocytes by combing hanging drop culture and 5-azacytidine treatment. Differentiation 2006;74:149–159

24 Weitzer G. Embryonic stem cell-derived embryoid bodies: An in vitro model of eutherian pregastrulation development and early gastrulation. Handb Exp Pharmacol 2006;174:21–51.

25 Reubinoff BE, Pera MF, Fong CY et al. Embryonic stem cell lines from human blastocysts: Somatic differentiation in vitro. Nat Biotechnol 2000; 18:399–404.

26 Zeng X, Miura T, Luo Y et al. Properties of pluripotent human embryonic stem cells BG01 and BG02. STEM CELLS 2004;22:292–312.

27 Skottman H, Mikkola M, Lundin K et al. Gene expression signatures of seven individual human embryonic stem cell lines. STEM CELLS 2005; 23:1343–1356.

28 Abeyta MJ, Clark AT, Rodriguez RT et al. Unique gene expression signatures of independently-derived human embryonic stem cell lines. Hum Mol Genet 2004;13:601–608.

29 Rao RR, Calhoun JD, Qin X et al. Comparative transcriptional profiling of two human embryonic stem cell lines. Biotechnol Bioeng 2004;88: 273–286.

30 Maitra A, Arking DE, Shivapurkar N et al. Genomic alterations in cultured human embryonic stem cells. Nat Genet 2005;37:1099–1103.

31 Segev H, Kenyagin-Karsenti D, Fishman B et al. Molecular analysis of cardiomyocytes derived from human embryonic stem cells. Dev Growth Differ 2005;47:295–306.

32 Bader A, Gruss A, Hollrigl A et al. Paracrine promotion of cardiomyogenesis in embryoid bodies by LIF modulated endoderm. Differentiation 2001;68:31–43.

33 Mummery C, Ward-van Oostwaard D, Doevendans P et al. Differentiation of human embryonic stem cells to cardiomyocytes: Role of coculture with visceral endoderm-like cells. Circulation 2003;107:2733–2740

34 Mummery C, Ward D, van den Brink CE. Cardiomyocyte differentiation of mouse and human embryonic stem cells. J Anat 2002;200:233–242.

35 Passier R, van Oostwaard DW, Snapper J et al. Increased cardiomyocyte differentiation from human embryonic stem cells in serum-free cultures. STEM CELLS 2005;23:772–780

36 Beqqali A, Kloots J, Ward-van Oostwaard D et al. Genome-wide transcriptional profiling of human embryonic stem cells differentiating to cardiomyocytes. STEM CELLS 2006;27:1956–1967.

See www.StemCells.com for supplemental material available online.

7.3   LIST OF MANUFACTURERS

Table 7-1: List of manufacturers referred to in text

Reference in text	Full company name and location	Website
Ambion	Ambion, Austin, TX, USA (Supplied by Applied Biosystems)	http://www.ambion.com/
Applied Biosystems	Applied Biosystems, Warrington, UK	http://www.appliedbiosystems.com/
Beckman Coulter	Beckman Coulter (U.K.) Limited, High Wycombe, UK	http://www.beckmancoulter.com/
BD Biosciences	BD Biosciences, Oxford, UK (Supplied by SLS)	http://www.bdbiosciences.com
BioChain	BioChain, Hayward, CA, USA	http://www.biochain.com/
Blades Biologicals	Blades Biological Ltd. Edenbridge, Kent, UK	http://www.blades-bio.co.uk/
Chemicon	Chemicon Europe, Ltd., Chadlers Ford, Hampshire, UK	http://www.chemicon.com/
Eurogentec	Eurogentec Ltd., Southampton, Hampshire, UK	http://www.eurogentec.com/
Fisher	Fisher Scientific UK Ltd., Loughborough, Leicestershire, UK	http://www.fisher.co.uk/
GE Healthcare	GE Healthcare, Chalfont St Giles, Buckinghamshire, UK	http://www.gehealthcare.com/
Hyclone	Hyclone UK Ltd., Cramlington, Northumberland, UK	http://www.hyclone.com
Improvision	Improvision, Coventry, UK	http://www.improvision.com/
Intervet	Intervet UK Ltd., Milton Keynes, UK	http://www.intervet.co.uk/
Invitrogen	Invitrogen Ltd., Paisley, UK	http://www.invitrogen.com/
Jackson ImmunoResearch	Jackson ImmunoResearch Europe Ltd., Newmarket, UK	http://www.jireurope.com/
Labtech International	Labtech International Ltd., Ringmer, UK	http://www.labtech.co.uk
Leica	Leica Microsystems (UK) Ltd., Milton Keyes, UK	http://www.leica-microsystems.com/
Medical Systems Corps	Medical Systems Corps, Miami, FL, USA	http://www.medicalsystems.com/
Menzel-Gläser	Gerhard Menzel, Glasbearbeitungswerk GmbH & Co. KG, Braunschweig, Germany (supplied by SLS)	http://www.menzel.de/
NanoDrop Technologies	NanoDrop Technologies Inc., Wilmington, DE, USA (supplied by Labtech International)	http://www.nanodrop.com/

Nasco	NASCO, Fort Atkinson, WI, USA	http://www.enasco.com/
NEB	New England Biolabs (UK) Ltd., Hitchen, Hertfordshire, UK	http://www.neb.uk.com/
Nikon	Nikon UK Limited, Kingston upon Thames, Surrey, UK	http://www.nikon.co.uk/
NUNC	Nunc A/S, Roskilde, Denmark (supplied by Fisher/VWR)	http://www.nuncbrand.com/
Orange Scientific	Orange Scientific n.v./s.a. Braine-l'Alleud, Belgium (supplied by Fisher)	http://www.orangesci.com/
Promega	Promega, Southampton, UK	http://www.promega.com/uk/
PeproTech	PeproTech EC Ltd., London, UK	http://www.peprotechec.com/
QIAGEN	QIAGEN Ltd, Crawley, UK	http://www.qiagen.com/
R&D Systems	R&D Systems Europe Ltd., Abingdon, UK	http://www.rndsystems.com/
Raytek	Raytek Scientific Ltd., Sheffield, UK	http://www.raytek.co.uk/
Roche	Roche Diagnostics Ltd., Burgess Hill, UK	https://www.roche-applied-science.com/
Santa Cruz	Santa Cruz Biotechnology Inc., Heidelberg, Germany	http://www.scbt.com/
Sakura	Sakura Finetek Europe B.V., Zoeterwoulde, The Netherlands	http://www.sakuraeu.com/
Sigma	Sigma-Aldrich Company Ltd., Gillingham, Dorset, UK	http://www.sigmaaldrich.com/
SLS	Scientific Laboratory Supplies Ltd., Nottingham, UK	http://www.scientific-labs.net/
Sigma-Genosys	Sigma-Genosys, Cambridge, UK	http://www.sigmaaldrich.com/
Techne	Barloworld Scientific Ltd., Stone, UK	http://www.techne.com/
Thermo	Thermo Fisher Scientific (supplied by Fisher)	http://www.thermo.com/
UVItec	UVItec Ltd., Cambridge, UK	http://www.uvitec.co.uk/
Vector Laboratories	Vector Laboratories Ltd., Peterborough, UK	http://www.vectorlabs.com/uk
ViroGen	ViroGen Corporation, Watertown, MA, USA	http://www.virogen.com
Vision Biosystems	Vision BioSystems (Europe) Ltd., Newcastle, UK	http://www.vision-bio.com
VWR	VWR International Ltd., Lutterworth, UK	http://uk.vwr.com